DESIGN AND SYNTHESIS OF QUINAZOLINONES AND RELATED HETEROCYCLIC COMPOUNDS

THESIS

Submitted to the

JADAVPUR UNIVERSITY

For the degree of

DOCTOR OF PHILOSOPHY

In CHEMISTRY

By

SUDIPTA MONDAL

DR. MOHABUL ALAM MONDAL

(Research Guide)

SECTION OF ORGANIC CHEMISTRY
JADAVPUR UNIVERSITY
KOLKATA- 7000032
INDIA

DECEMBER 2023

Dedicated to my family...

যা দ ব পু র বি শ্ব বি দ্যা ল য়
ক ল কা তা - ৭০০ ০৩২, ভারত

JADAVPUR UNIVERSITY
KOLKATA-700 032, INDIA

FACULTY OF SCIENCE : DEPARTMENT OF CHEMISTRY : ORGANIC CHEMISTRY SECTION

CERTIFICATE FROM THE SUPERVISOR

This is to certify that the thesis entitled "**Design and synthesis of quinazolinones and related heterocyclic compounds**" Submitted by Smt. Sudipta Mondal who got her name registered on 07/10/2020 for the award of Ph. D. (Science) Degree of Jadavpur University, is absolutely based upon his own work under the supervision of Dr. Mohabul Alam Mondal and that neither this thesis nor any part of it has been submitted for either any degree / diploma or any other academic award anywhere before.

MA Mondal 21.12.2023

(Signature of the Supervisor
date with official seal)

DR MOHABUL ALAM MONDAL
Assistant Professor
Department of Chemistry
Jadavpur University
Kolkata-700032, India

দূরাভাষ : ৯১-০৩৩-২৪১৪-৬২২৩
দূরবার্তা : ৯১-০৩৩-২৪১৪-৬৪৮৪

Internet : http// www.jadavpur.edu

Phone : 91-033-2414-6223
Fax : 91-033-2414-6484

Candidate's Declaration

I hereby declare that the research work incorporated in the thesis entitled "**Design and synthesis of quinazolinones and related heterocyclic compounds**" submitted for the degree of ***Doctor of Philosophy*** in ***Chemistry*** to the ***Jadavpur University*** has been carried out by me at the Department of Chemistry, Jadavpur University, Kolkata, India, from **January 2019** to **December 2023** under the supervision of Dr. Mohabul Alam Mondal. This work has not been submitted in part or full by me for a degree or diploma to this or any other University or Institution.

Sudipta Mondal.
21/12/23

December, 2023

Sudipta Mondal

Research Student
Departmentof Chemistry
Jadavpur University
Kolkata- 700032, West Bengal

ACKNOWLEDGMENT

It is a moment of pleasure to recapture the several memorable moments, numerous people, who joined me in this long journey, whose continuous motivation, guidance, support, help, and blessing at the different stages helped to achieve this milestone of my life.

First and foremost, I would like to express my deep sense of gratefulness to my research guide Dr. Mohabul Alam Mondal for his constant guidance and support throughout my Ph.D. tenure. Without his enthusiastic motivation and expertise in organic synthesis achievement of this research work would have remained a dream. I am indebted him also for mentoring me and teaching me necessary things, and allowing me to work in a laboratory without any pressure. His inspiration and supportive conversations with no time boundaries have helped me to become a successful researcher. His continued motivation and suggestions in technical writing which are unprecedented in such a less period.

I am profoundly grateful for the cooperation and affection extended by all the respected teachers: Prof. Subrata Nath Koner, Dr. Tanurima Bhaumik, Dr. Samit Guha, Dr. Arunava Thakur, Dr. Amit Saha, Dr. Sanjay Bhar, Dr. Umesh Chandra Halder, Dr. Umasis Jana, Dr. Gourhari Maiti, Dr. Suman Das, Dr. Partha Roy and respected Rina Mam. I sincerely thanks to Dr. Partha Mahata for his great support in X-ray crystallographic data analysis.

I also thank our biology collaborator Dr. Sankhadeep Dutta (Cancer Virology, Chittaranjan National Cancer Institute, Kolkata) for studying anticancer activities and cell imaging.
I am grateful to the members of my Research Advisory Committee, Prof. Arindam Talukdar and Prof. Subrata Nath Koner for their valuable suggestions and cooperation during my research work.

Help from the NMR division, mass and other micro analysis groups is greatly acknowledged.

I would like to give my special thanks to my labmate Arunava Da for his helpful discussion and constant cooperation during this period. Working with him was an immense pleasure and indeed a learning experience.

I wholeheartedly thank all my colleagues Sunny, Manas, Debabrata, Sushanta, Sourav, Biswajit, Farhin, Adwitiya, Manisha, Rupsha, Rabi da, Anirban da, Sahanaz Di, and some juniors Soumya, Rwitabrita, Sourav, Susmita, Sayan, Pintu, Midda, Sneha for theircooperation and friendly attitude.

I would like to thanks to my close seniors Ipshita di, Rupa di, and Priyambada di for their excellent support and cheerful company, which made my stay at Kolkata a memorable one.

It is impossible to express my deep sense of gratitude to my parents. Without their scarify it is impossible to achieve this milestone. My special thanks to my sweetest brother Shubhadip for his continuous support, encouragement, care, and love.

I deeply acknowledge a very special person who entered in my life during my research journey and will continue the journey with me, my beloved life-partner Partha Sutradhar. His constant support, high level of patience, and unstopping flow of love always motivated me to reach my destination.

Now, I would like to thanks the Vice-Chancellor and Dean of faculty of Science, Jadavpur University and UGC for providing necessary facilities and financial support.

Last but not the least, I bow my head to Almighty who gave me enough strength to work hard and cross the toughest situations.

Sudipta Mondal

TABLE OF CONTENTS

Entries **Page No**

Chapter 3: Studies towards the synthesis of Luotonin/Rutaecarpine alkaloids analogues with application

APPENDICES

LIST OF TABLES

LIST OF FIGURES

LIST OF SCHEMES

SYNOPSIS

Since the last few decades, the development of biologically relevant *N*-heterocycles such as **Quinazolinones** and **Pyrimidinones** has retained their focus. As these *N*-heterocyclic moieties are found in various marketed drugs, material science, natural products, they have gained much importance for different research communities.

The thesis entitled "**Design and synthesis of quinazolinones and related heterocyclic compounds**" deals with the synthesis of selected *N*-heterocycles with detailed mechanistic investigation accompanied by finding some applications.

The first chapter of this thesis describes the synthesis of some functionalised **Quinazolin-4(*3H*) ones** in simplest route. From the literature scan it was noticed that there are numerous reports available for the synthesis of quinazolinones using 2-amino benzamide (anthranilamide) with monoaldehydes. But study of same phenomena with dialdehyde is less covered. So, firstly the synthesis of Isoindole fused quinazolin 4-ones involving *O*-Phthaladehyde (aromatic dialdehyde) and anthranilamide have been done in the presence of acid catalyst, by one pot method. Although the product was known, sufficient explanation or detailed mechanism was not available. Therefore, our study on mechanistic investigation revealed that there involved an intramolecular 1, 3- hydride transfer (HT) and it has been proved by deuterium exchange method. A handful number of compounds are synthesized using this condition. Crystallization of one compound was carried out in aq. methanol and the structure was solved by single-crystal X-ray diffraction study (**Scheme-AA**)

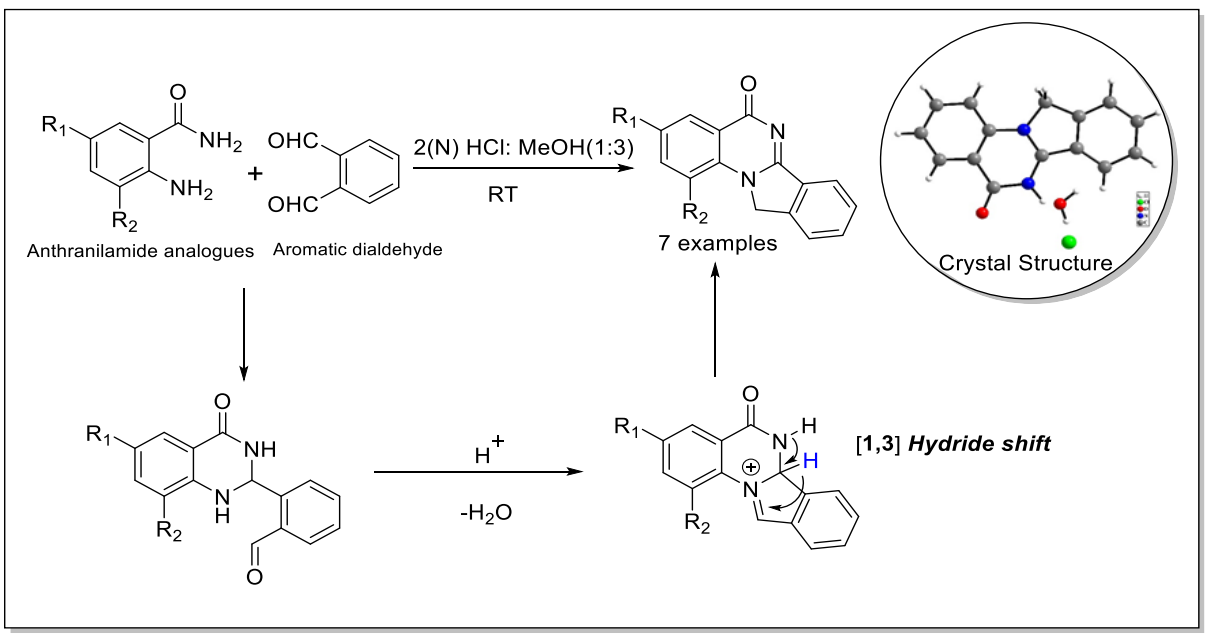

Scheme-AA: Isoindole fused quinazolinones formation with plausible mechanism

After doing the work with aromatic dialdehyde, it was extended to explore the reactivity of anthranilamide analogues with aliphatic dialdehydes. Firstly, we chose the glutaraldehyde (a five carbon dialdehyde) and carried the reaction with anthranilamide by same method (as mentioned for aromatic dialdehyde). After several attempts, we finally observed that anthranilamide and glutaraldehyde mixed in a 2:1 molar ratio with lower acid loading gave compound2-((4-(4-hydroxyquinazolin-2-yl)butyl)amino) benzamide (**12a**) as a white solid which was isolated by filtration (**Scheme-BB**). Using this method, we successfully synthesised two redox-neutral compounds and isolated some intermediates with proper characterization. The mechanistic investigation revealed an involvement of 1,5 hydride transfer, and the length of dialdehyde was a crucial factor for redox-neutral product formation.The hydride transfer was facile when the donor centre and the acceptor centre span five carbon atoms (gluteraldehyde). [1,2]; [1,3]; [1,4] HT were not observed when different anthranilamide analogues were treated with varying chain length of dialdehydes. Therefore, chain length of dialdehyde was a crucial factor for desired redox-neutral product formation. The intramolecular [1, 5] hydride transfer mechanism have also been proved by deuterated experiment.

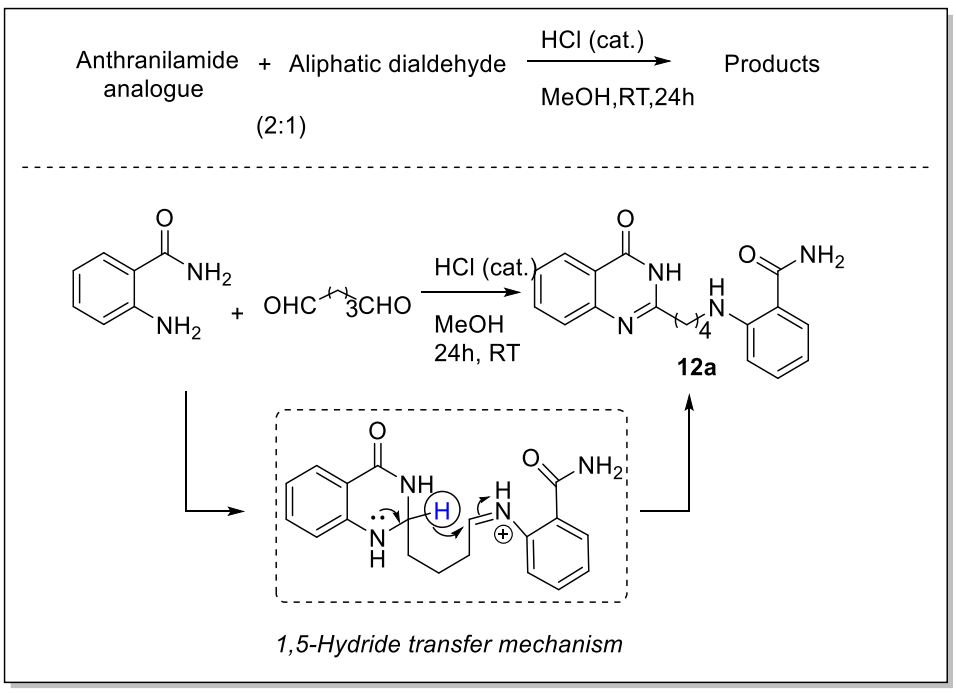

Scheme-BB: Optimized reaction condition with Anthranilamide and Gluteraldehyde

In second chapter, simplest starting DHPM, 5-acetyl-6-methyl-4-phenyl-3,4-dihydropyrimidin-2(1*H*)-one (**17c**) has been synthesized by acid-catalyzed multi-component synthesis, involving condensation of urea, β-keto ester, or β-diketo and aldehyde commonly known as Biginelli product. We wished to synthesize one suitable DHPM-based dye for a significant application. Firstly, we

synthesized a functionalized DHPM by modifying *C*6 methyl group under basic condition. As per our knowledge base promoted reaction of DHPMs is not straightforward because of the deep degradation through retro-Biginelli reaction, as suggested by Pietro Biginelli. Hence, we explored the relative reactivity of the ketomethyl and methyl group attached to the dihydropyrimidinone ring of **17c** (a Biginelli product) towards benzaldehyde in alkaline conditions. When **17c** was reacted with 2.5% aq. NaOH, at 100°C for 2 hours without adding external aldehyde, gave the product (E)-4-phenyl-6-styryl-3,4-dihydropyrimidin-2(1*H*)-one (**19d**) with less than 50% isolated yield. When the same reaction was carried out in the presence of externally added aldehyde, the yield of the reaction increased significantly (**Scheme-CC**). It has been revealed that the reaction goes through a retro-Biginelli path which was established by the cross-over experiment and LCMS analysis of one incomplete reaction mixture (identification of intermediates).

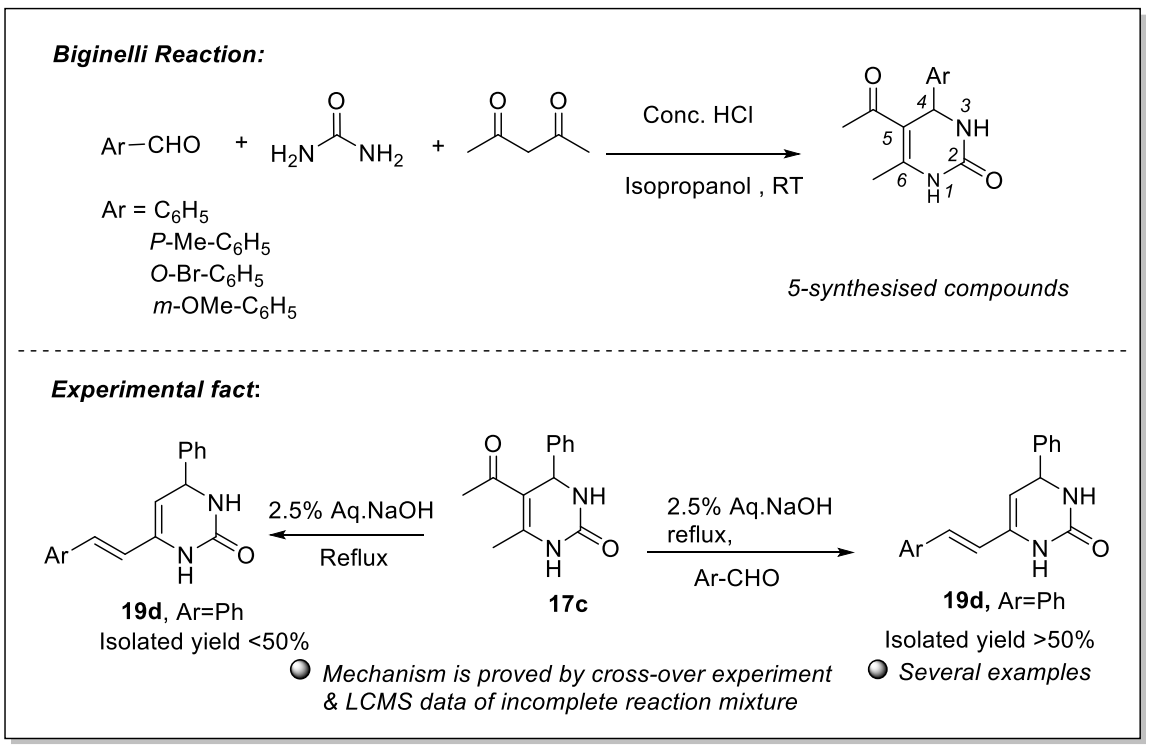

Scheme-CC: Preparartion of *C*6 modified DHPMs

Continuing our longstanding interest in functionalisation of DHPM, we have synthesized a new intramolecular Donor-π-Acceptor fluorescent probe through post-synthesis modification of the Biginelli product. The inherent instability of the ketomethyl-containing DHPMs was enhanced by attaching a cyanoethyl group selectively at the *N*3 atom and we have successfully developed a synthetic strategy for accessing a highly conjugated DHPM (fluorophore) by the post-synthesis modification of the Bigineili product (**Scheme-DD**). Significantly, we have showed that the synthesised compound **27a** was highly sensitive towards ds-DNA by different photophysical studies.

Hence, these types of compounds are useful for developing DNA-based drugs to modulate gene expression, monitor cellular processes involving DNA, visualise and quantify cellular DNA, to monitor the live activities of the nucleus of a cell. Most importantly, we explored the possibility of using of this compound as a cell-imaging agent on the SiHa cancer cell line and the result was compared with the nucleic acid specific dye acridine orange, a popular dye for the identification of live cell nucleus. Although, slight less cell permeability was observed as compared to acridine orange, but incorporation within the cell, along with the particular nucleus target ability of this compound has been established here.

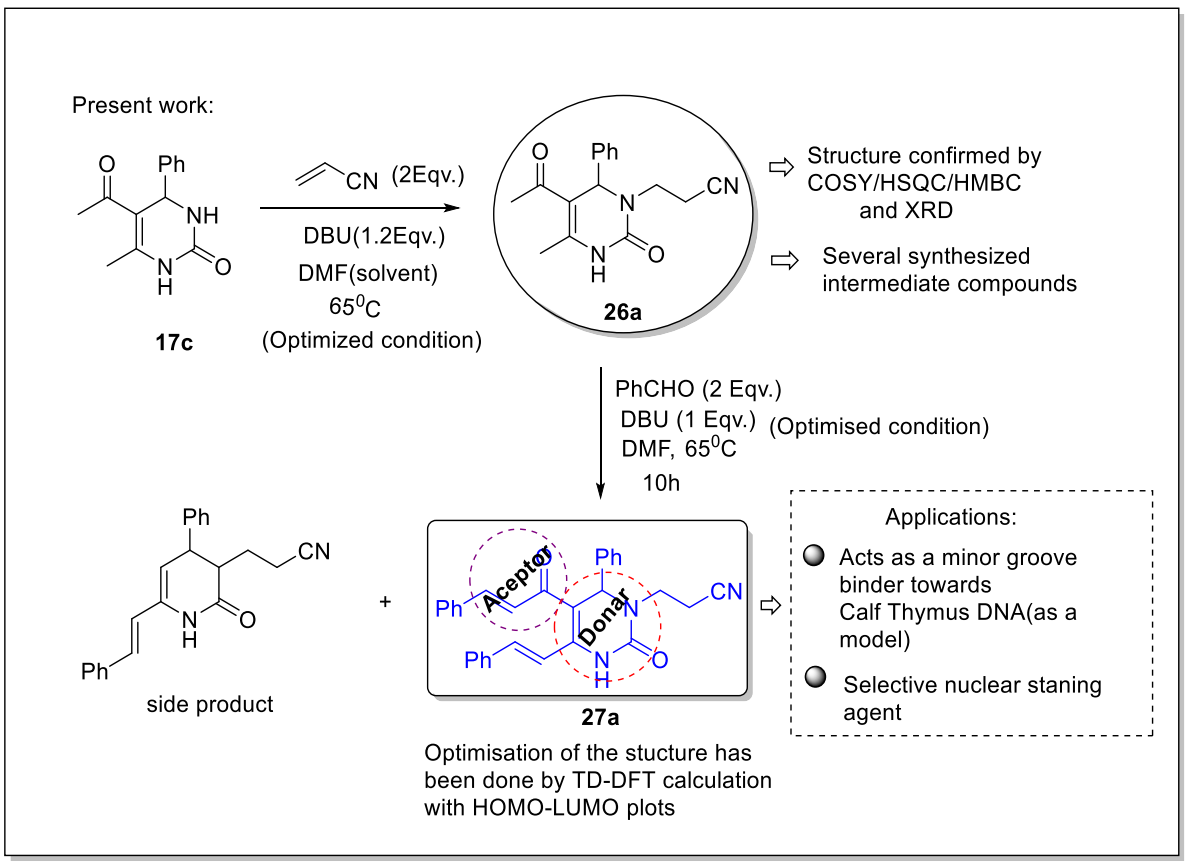

Scheme-DD: Synthesis of a donar-π -aceptor DHP fluorophore and study of its applications

In the third chapter, a new synthetic route has been proposed for the formation of Luotonin and Rutaecarpine (quinazolinone based alkaloids) analogues via intramolecular dehydrogenative cross coupling (CDC) and *C-H* oxidation in one pot manner. After several attempts it has been established that cat. $Pd(OAc)_2$ and 3 Eqv. AgOAc in the acetic acid solvent at 120°C is the optimal condition of the reaction. To check the scope of the reaction, the above reaction has been done with various starting materials having electronically different functional groups. Structures of two synthesized compound, having high crystalline nature, were solved by single-crystal XRD. The detailed synthetic

procedure and a systematic mechanistic study were carried out. Therefore, to see the application of synthesized compound firstly, we saw the DNA target ability with ct-DNA and found slight positive intercalation binding mode of compound **38h**. However, another compound **37d** remarkably showed an important biological importance towards application. Significantly, the results of the concentration dependent cell viability assay study with the compound **37d** on the SiHa carcinoma cell line revealed that it may have anti-cancer property. The observed IC_{50} value was 23 μM, which is a good indication of application. However, more detailed study is required to proof the anti-cancer activity in this regard and still under process.

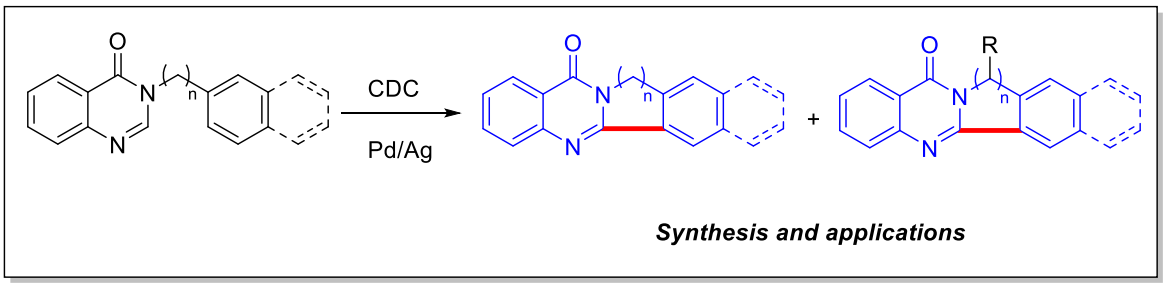

Scheme-EE: Synthesis of Luotonin/ Rutaecarpine analogues through CDC

List of Abbreviations/Symbols	Description
α	Alpha
β	Beta
δ	Delta
MW	Microwave
°C	Degree centigrade
Å	Angstrom
AcOH	Acetic acid
ACN	Acetonitrile
AgOAc	Silver acetate
Ar	Aryl
Aq.	Aqueous
Bn	Benzyl
Bu	Butyl
^{13}C	Carbon-13
Cat.	Catalyst
CD	Circular Dichroism
CDC	Cross-dehydrogentive coupling
$CDCl_3$	Deuterated chloroform
Conc.	Concentration
COSY	Correlation spectroscopy
ct	Calf-Thymus
D	Deuterium
d	Doublet
dd	Doublet of doublet
DBU	1,8-Diazabicyclo[5.4.0]undec-7-ene
DCM	Dichloromethane
DDQ	2,3-Dichloro-5,6-dicyanobenzoquinone
DEPT	Distortionless Enhancement by polarisation Transfer
DFT	Density Functional Theory
DHPM	Dihydropyrimidinone
DMF	*N*,*N*-Dimethylformamide
DMSO	Dimethyl sulphoxide
DNA	Deoxyribonucleic acid
ds	Double strand
ESI	Electron spray ionization mass spectrometry
EtOAc	Ethyl acetate
Et	Ethyl
EtOH	Ethanol
Eqv.	Equivalent
Eq.	Equation
g	Gram
h	Hours
HRMS	High resolution mass spectrometry
HMBC	Heteronuclear multiple bond correlation
HOMO	Highest occupied molecular orbital
HSQC	Heteronuclear single quantum coherence spectroscopy
HPLC	High-performance liquid chromatography

HT	Hydride Transfer
IR	Infrared
iPr	Isopropyl
Hz	Hertz
J	Coupling constant
LCMS	Liquid chromatography mass spectrometry
LUMO	Lowest occupied molecular orbital
mCPBA	meta-Chloroperbenzoxy acid
MCR	Multi-component reaction
Me	Methyl
MS	Mass spectrometry
m.p.	Melting point
Me	Methyl
MS	Mass spectrometry
m	Multiplet
mg	Milligram
MHz	Mega hertz
min	Minutes
mL	Milliliter
mmol	Millimole
m/z	Mass/Charge
N_2	Nitrogen gas
NBS	N-bromosuccinimide
nm	nanometer
NMR	Nuclear Magnetic Resonance
OD	Optical density
O_2	Oxygen gas
PDB	Protein Data Bank
$Pd(OAc)_2$	Palladium acetate
PivOH	Pivalic acid
Ph	Phenyl
ppm	Parts per million
Pr	Propyl
%	Percentage
p-TsOH	*p*-Toluenesulfonic acid
RNA	Ribonucleic acid
RT	Room temperature
s	Singlet
t	Triplet
TBHP	*tert*-Butyl hydroperoxide
TEA	Triethylamine
TFA	Trifluoroacetic acid
TfOH	Trifluoromethanesulfonic acid
THF	Tetrahydrofuran
TLC	Thin layer chromatography
TMS	Tetramethylsilane
TOF	Time of flight
UV	Ultraviolet
Vis	Visible

CHAPTER-1

Synthesis and modification of Quinazolin(4*H*)-one explored with hydride transfer protocol

1.1 INTRODUCTION

Organic chemistry is very much explored by heterocycles (called heterocyclic compounds). From the rough estimation, from 50 million of registered organic compounds, more than half are heterocycles, and the quantity is still increasing. Heterocycles are frequent in biologically active natural products and pharmaceuticals for their applications towards drug design.[1] Despite incidents like the "*thalidomide tragedy*",[2] their significance in drug discovery is constantly hiking for their selective binding aptitude to the drug targets. Besides their medicinal importance, they have a wide range of uses -in agrochemical, cosmetic, and veterinary[3] etc. Many compounds that have natural origin, such as alkaloids (morphine, reserpine, vinblastine); antibiotics (penicillin, cephalosporin) etc; contain heterocyclic components. In heterocycles, mostly nitrogen, oxygen, and sulphur are present in 5 or 6-membered rings. On account of the central role of heterocycles in chemistry and biology, a new boost in synthetic methodologies towards the synthesis of an enormous variety of functionalized heterocyclic compounds are witnessed by the scientific communities.

At the present time, human societies are suffering from different types of health-related problems and a few of them are pandemic in nature. These problems are often responsible for the loss of life on a massive scale in a short time. In this type of situation, the whole society puts their focus on research communities, mostly medicinal chemistry researchers, to get solutions either by the synthesis of new compounds which can be used as a potential drug against such diseases, or the production of already existing compounds in a short time. As the formation of new products for application is quite an arduous and lengthy process for clinical trials and getting permissions from concerned authorities, chemists generally focus on the alternative robust and economical synthetic pathways of already tested chemical compounds and these are mostly on heterocycles[4].

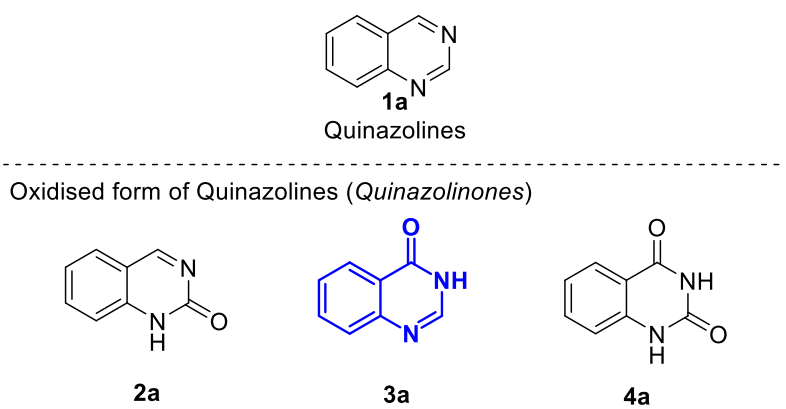

Figure-1.A: Basic stuctures of Quinazolinones

Heterocyclic compounds bearing nitrogen (*N*) atoms in their structures are taken into account as a vital class of heterocycles that are broadly employed in medicinal chemistry.[5]According to the position of *N*-atom(s) in the ring, they are familiar with different names e.g., Quinazolines,

Quinazolinones, Quinolins, Pyrimidines, Pyrimidinones, Indoles, Isoindoles, Pyrazoles, Triazoles, Imidazoles, etc. Among these heterocyclic compounds, Quinazolinones, Pyrimidinones, and Isoindoles, have gained a great significance in many research sectors, including synthetic organic and medicinal chemistry.Because of their diverse uses, the construction of heterocyclic compounds has become a centre of attention in organic synthesis.[6] Among the various *N*-heterocycles Quinazolinone, the oxidised form of Quinazoline (**1a**) is the most famed one. Quinazolinones are formed by fused benzene ring with 2- pyrimidinone, 4-pyrimidinone, and 2,4-pyrimidinone, which are popular with their name 2(1*H*) Quinazolinone (**2a**), 4(3*H*) Quinazolinone (**3a**), and 2,4 (1*H*,3*H*) Quinazoline dione(**4a**) respectively (**Figure-1.A**).

Among these moieties 4(3*H*) Quinazolinone (**3a**) is the most important as it is present in many bio-active natural products and gets attention for their diverse sorts of biological activities[7] like anti-bacterial, anti-tubercular, anti-fungal, anti-leukemic, anti-HIV, anti-leishmanial, anti-inflammatory, anti-hypertensive, anti-ulcer, anti-depressant analgesic, anti-proliferative, anti-cancer, anti-malarial, etc. So, being an important pharmacophore and a building block for many drugs / natural products (**Figure-1.B**) it is our particular area of interest and is considered to be a powerful structure for drug developments.[8]

The first documented preparation of a Quinazolinone i.e; 2-cyanoquinazolinone (**4c**) was given by Griess in 1869 from the reaction between 2-aminobenzoic acid (**4b**) and cyanogen[9]. But for the first time preparation of Quinazolinone was proposed by Niementowski[10]in 1895 from the condensation of anthranilic acid analogues with amides, proceeding through an ortho-amidobenzamide intermediate. On subsequent time different research groups[11] disclosed the formation of Quinazolinones with different fuctionalisations from several methods using alternative starting materials, reagents, conditions etc, with/without showing their mechanistic investigations.

The formation of simplest Quinazoline-4(*3H*)-one involves most commonly the condensation of aldehyde/ketone with anthranilamide or other 1,5-*N*-bisnucleophile (**4e**) (**Scheme-1.A**). Although adequatenumbers of literature are available involving the reactions of anthranilamide with monoaldehydes,[11b, 12] reports on dialdehydes are very limited. Only a few examples on dialdehydes are available i.e, reaction of **5a**, with terephthalaldehyde (**5c**) by Saha group[13], with glyoxal (**5d**) by Radfar group[11a], and with ortho-phthalaldehyde (**5b**) by Choghamarani's group[14] etc and the formation of products are the respective (**6b-d**) symmetric dimmers (bis-quinazolinones) in each case (**Scheme-1.B**).

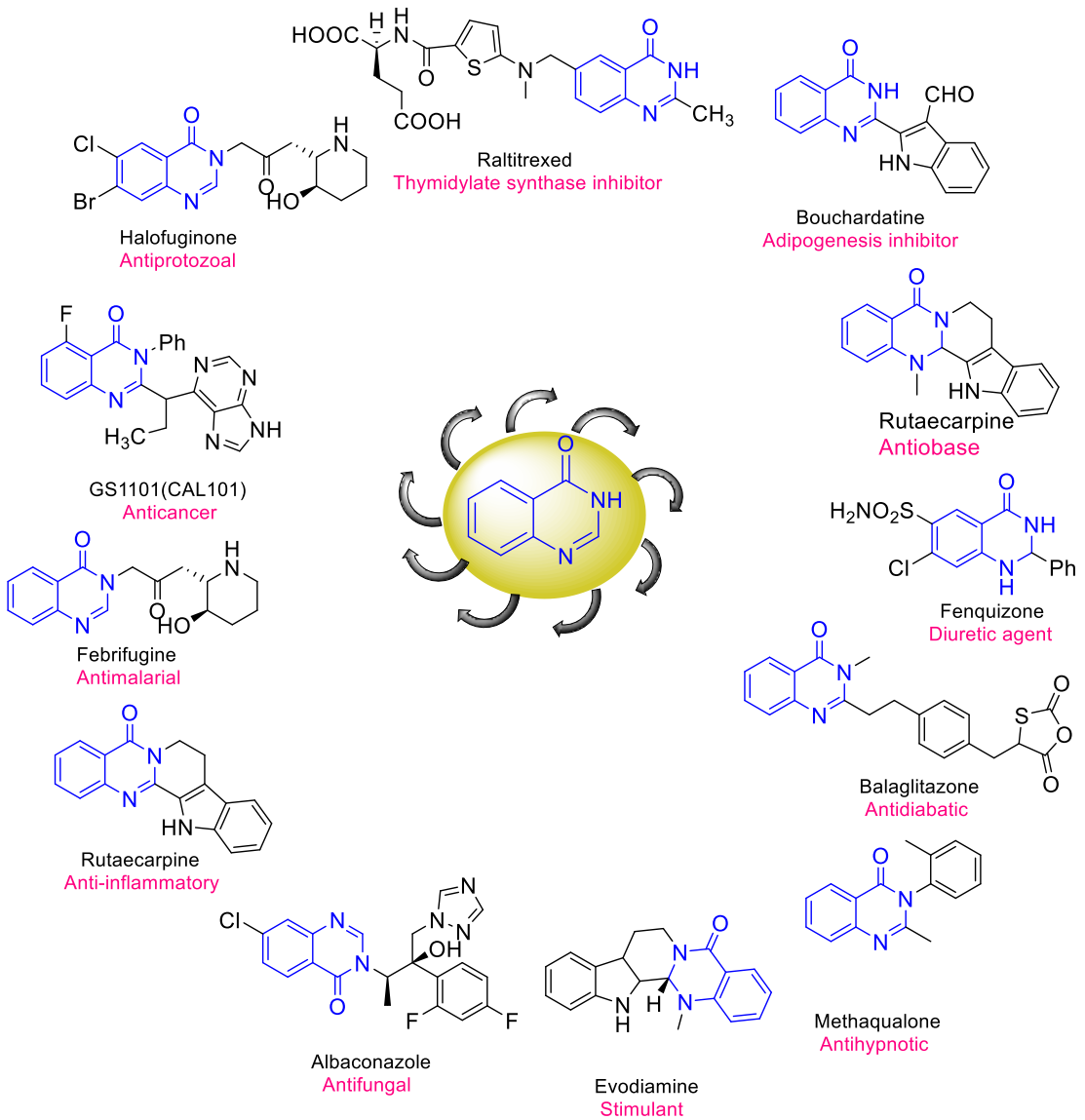

Figure-1.B: Pharmaceutically important Quinazolinone based drugs

From the thorough scan of literature on the chemical properties of the structure of Quinazolinones, it came to our notice that the hydrogen atoms present at position-2 (**3a**) (**Scheme-1.C**) has a tendency to shift (as hydride) towards a suitable electropositive centre. To the best of our knowledge, it is an interesting but less explored area that can be used for the functionalization of Quinazolinones or carry out several types of reactions using this hydride transfer (HT) protocol. Hydride transfer (HT) strategy in organic chemistry is always an ever-growing research area for its operational simplicity, high efficiency, and environmental sustainability. Mostly, [1,3] and [1,5] hydride transfers are common besides the use of [1,2], [1,4], and [1,6] hydride transfers[15] are quite uncommon in organic synthesis, but these are also possible with the special structural requirements. Depending upon the nature of the substrate and reaction condition, both intra as well as intermolecular hydride transfer may be possible. Intramolecular hydride transfer (HT) reaction is also known as redox-neutral[16] reaction and characteristics are that the migrated hydrogen does not exchange or combine with

solvent protons. It requires a proximal acceptor centre that has to be electron deficient in nature to accept the transferred hydride. Electron-deficient functional groups such as imine, carbonyl, *C=C* bond, α,β-unsaturated keto or ester are frequently used as an acceptor centre with the help of an activator. Another key factor for the fruitful application of the redox-neutral reaction is the assistance of a non-bonded electron pair or an anionic centre. So, hydrogen present at the methylene/methine group adjacent to heteroatoms (e.g; *N*, *O*, *S*) is facile for hydride donor and using this protocol a number of complex organic syntheses have been done[17-22].

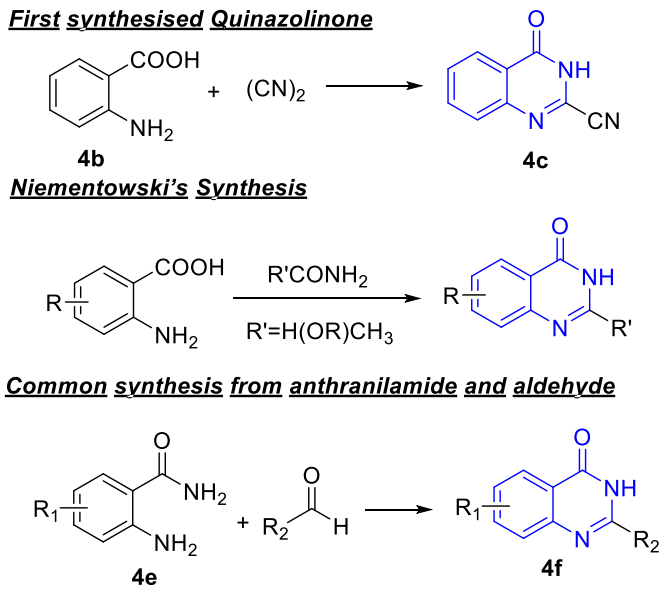

Scheme-1.A Preparation of quinazolin- 4(*3H*)-one

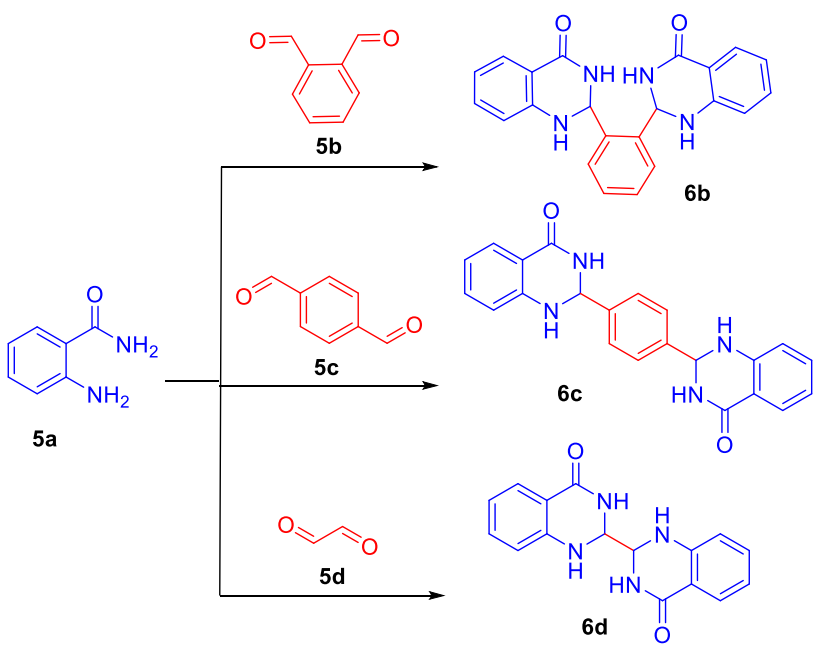

Scheme-1.B Reported synthesis of bis-quinazolinone from anthranilamide and dialdehyde

Jin-Ye Zhang's group has established the donor ability of hydride present in the 2-position of quinazolinone (**3a**), in an actual chemical reaction by thermo-kinetic parameters[17]. Playing with the

hydride, reductive amination of dihydrobenzothiazole as a hydride source has been done by Takahiko's group[18]. Besides, several groups like Ghosh *et al.*[19]and Chakraborty *et al.*[20] exhibited the intramolecular hydride transfer in dihydrobenzoimidazole for the synthesis of 1, 2-disubstituted benzimidazoles. In 1984 when Reinhoudt *et al.*[21]exhibited a method for the preparation of substituted tetrahydroquinolines using cyanoethene group as the hydride acceptor, then it could rapidly ring close via 6-endo-trig cyclization.[22]Using this concept, Youn's group displayed the Thiourea-catalytic synthesis of tetrahydroquinolines through a 1,5-hydride transfer with ring closure sequence[23] (**Scheme-1.C**).Thereupon, motivated by the redox- and step-economy, we reported an intramolecular hydride transfer to distal imines leading to the formation of highly functionalized Quinazolinones.

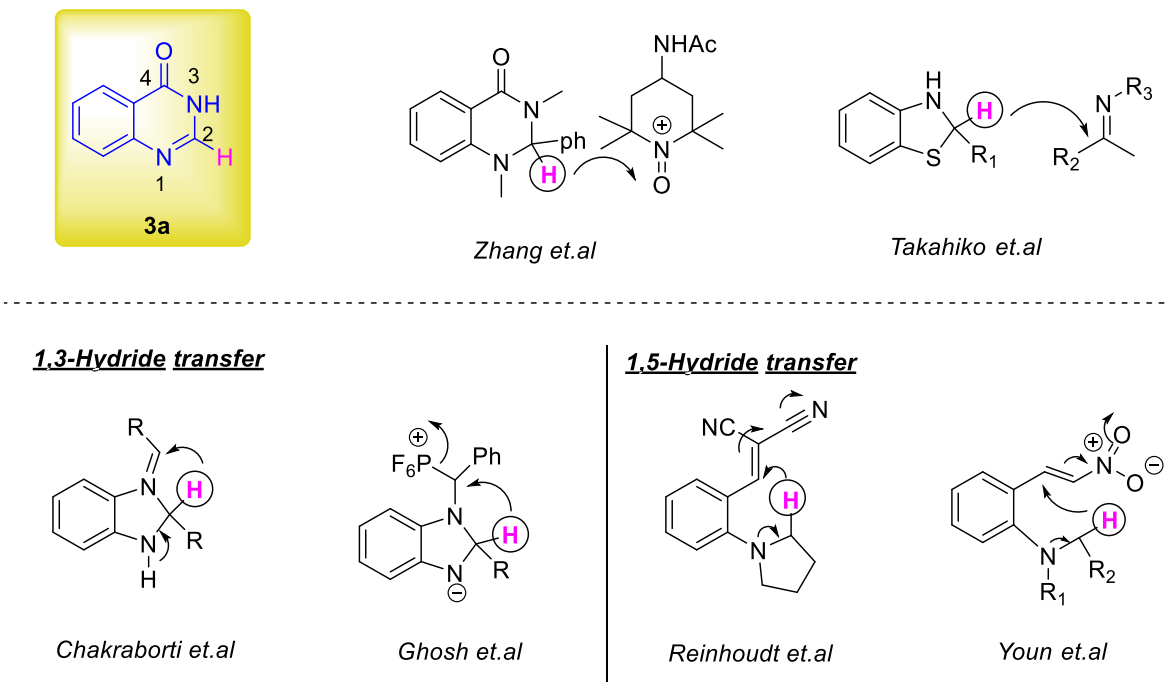

Scheme-1.C Available reports on hydride transfer from adjacent centre of heteroatoms

1.2 RESULT AND DISCUSSTION

At initial stage, we have started synthesis of the compound**5e** using the Reinhard et al.[24] mentioned condition.Equimolar mixture of 2-amino benzamide and ortho-phthalaldehyde in methanol and 2(*N*) aq. *HCl* (3:1) at room temperature gave the compound **5e** smoothly, from which white solid mass of hydrochloride salt (**5eHCl**) separated out. To get the analytical pure compound **5eHCl**, the solid mass was collected by filtration and washed well with 3:1 methanol water. Crystallization of the product was carried out in aq. methanol and the structure was solved by single crystal X-ray diffraction study (XRD).The Crystal structure displays that there is a tetra-cyclic skeleton accompanying with planar geometry and a water molecule present in the network of the lattice

through hydrogen bonding of amide hydrogen (**Figure-1.C**). It is interesting to observed that the position of the amide hydrogen atom in crystal structure of **5eHCl** in solid-state is different from in solution-state as amide proton is absent at ^{1}H-NMR in DMSO-d_6 solvent. Compound**5e** was obtained from **5eHCl**; washing with saturated $NaHCO_3$ solution and the structure of the compound **5e**was exactly matched with the ^{1}H-NMR with reported data.[25]

Table-1.A: Synthesis of isoindole fused quinazolin 4-ones

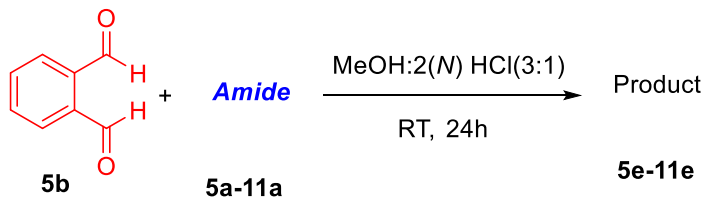

Entry	Amide	Products	Yield (%)
1	**5a**	**5e**	89
2	**7a**	**7e**	88
3	**8a**	**8e**	91
4	**9a**	**9e**	86
5	**10a**	**10e**	83
6	**11a**	**11e**	92

Reaction conditions: dialdehyde (2.50 mmol), amide (2.50mmol), in 30 mL MeOH and 10 mL HCl 2(*N*) at RT for 24h

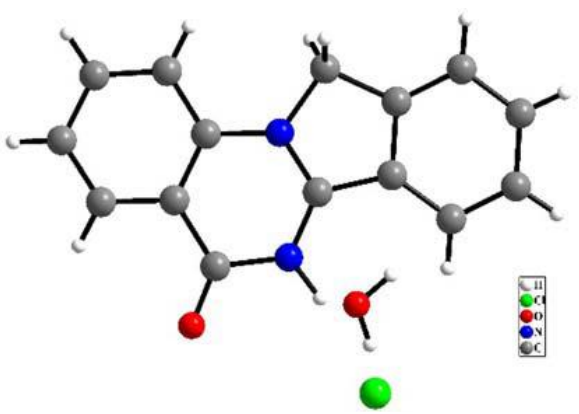

Figure-1.C Crystal structure of **5eHCl** (CCDC 1907967)

Use of other mild Lewis acid resulted product formation in low yield. Although, polar aprotic solvents DMF/DMSO can be used; but methanol or ethanol medium can give a benefit for product isolation without column purification. However, we used methanol for synthesizing the compounds mentioned here. Applying the above-mentioned condition (**Table-1.A**), scopes of the reaction was investigated with different 1,5-*N* bisnucleophiles (**5a-11a**) (**Figure-1.D**). Varieties of substituted

tetra-cyclic skeleton (**5e-11e**) have been synthesized here. Notably, from the substituted anthranilamides (**7a-11a**) compounds **7e-11e** (**Figure-1.D**) were isolated directly in the salt free form, from the reaction mixture simply by filtration. It is presumed that, presence of electron-withdrawing group in the amide part (**7a-11a**), make the tertiary amine centre less basic. Compounds **7e** to **9e** are absolutely new as they are not reported in the literature. The structures of product were confirmed by NMR and HRMS. Compound **10e** was isolated as a white solid from the equimolar mixture of 2-aminobenzenesulfonamide (**10a**) and **5b** under the above mentioned reaction condition (**Table-1.A**). Synthesis of this compound (**10e**) is reported in a multistep procedure without sufficient spectroscopic data[26].Compound **11e** was synthesized under the acid-catalysed condition with improved yield from the compound **11a** and *O*-phthalaldehyde (**5b**) using the reaction condition[27]. Owing to poor solubility in common organic solvents, collection of ^{13}C-NMR data of compound **8e**, **10e,** and **11e** were unable. Investigation on scopes of the substrates revealed that the electronic nature of the substituent present at the amide moiety does not influence significantly on yield.

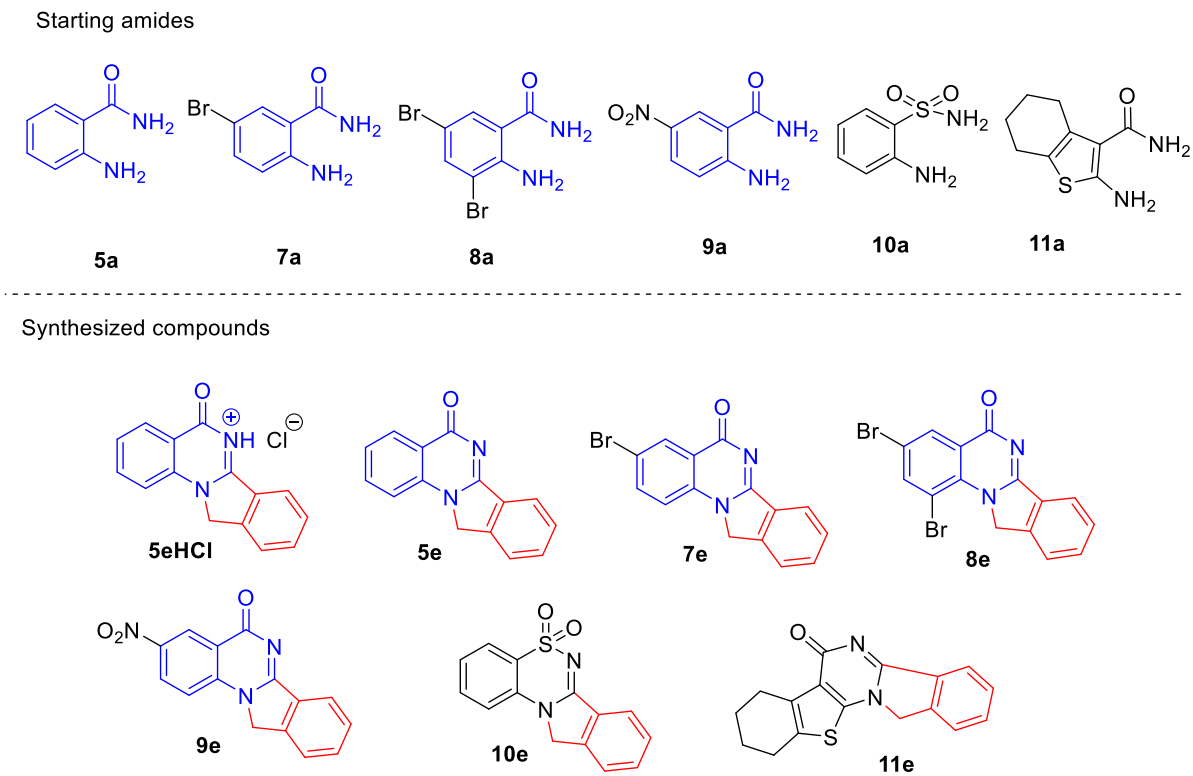

Figure-1.D:Structure of Amides and synthesized isoindole fused Quinazolin 4-ones (analogues)

Primarily, two types of mechanistic pathways; namely, intramolecular hydride transfer[27] (Path-A) and tautomerism[28] (Path-B) (**Scheme-1.D**) have been proposed for the reaction of **5b** with structurally identical 1,5-*N*- bisnucleophiles. Path-A involves intramolecular 1,3- hydride transfer (as proposed by Abdel-Latif et al.[27]) without participation of solvent proton in the key step.

Whereas, in the Path-B, multiple tautomeric sequences by which hydrogen atom transferring with the participation of solvent proton may lead to the compound **5eHCl** (as proposed by Ukhin et al.[28]). To confirm the mechanistic pathway for the formation of **5eHCl**, we have carried out the reaction of *O*-phthalaldehyde (**5b**) with 2-aminobenzamide (**5a**) in DCl/CD_3OD at room temperature (RT). And we observed that the exclusive formation of the product **5eDCl**, but not **5eD$_2$Cl** (**Scheme-1.D**). For further confirmation of structure **5eDCl**, it was treated with aq. $NaHCO_3$ and observed the formation of **5e**. The NMR and HRMS spectra of compound **5e** obtained from the above mentioned deuterated experiment show no deuterium incorporation in the structure of it. Formation of **5eDCl** and **5e** under deuterated solvent clearly shows that the rearrangement of initial intermediate **5g** into **5e** is 1,3-intramolecular hydride transfer (redox-neutral) as shown in Path-A in **Scheme 1.D**.

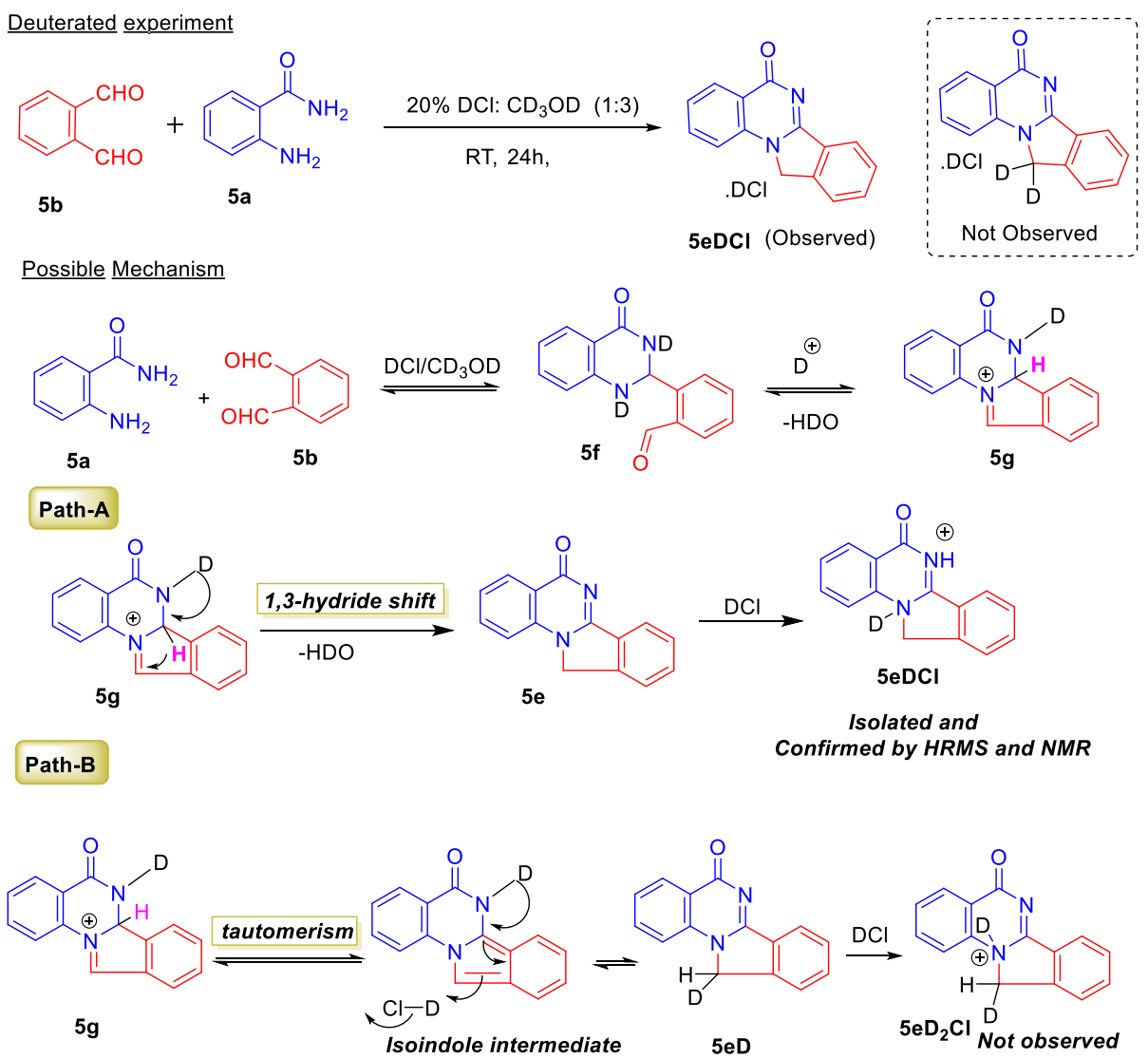

Scheme-1.D: Possible mechanism with deuterated experiment

The 1,3-hydride transfer is being facilitated by the electronically rich amide nitrogen donor centre. Acid catalyzed intramolecular hydride transfer from sp^3 carbon adjacent of nitrogen centre to closely

spaced electrophilic centre is well-known and an established phenomenon[29]. Based on the deuterated solvent experiment, the proposed mechanism for the formation of **5e** is assumed to be essentially same as proposed by Abdel-Latif et al.[27](Path-A; **Scheme-1.D**).The method involved initial formation of monomeric compound **5f**, followed by iminium ion (**5g**) formation. The subsequent intramolecular 1,3-hydride transfer gave compound **5eDCl**. After the treatment of **5eDCl** with aq. $NaHCO_3$ the resultant outcome was **5e**. Hence, rather getting dimeric dihydroquinazolinone[14], we synthesized Isoindole fused Quinazolin-4 ones out in the presence of an acid catalyst in one pot manner.

After the above observations we continue our exploration on the reactivity of anthranilamide with aliphatic dialdehydes. In case of aliphatic dialdehydes, primarily we observed a complex reaction mixture, confirmed by many interacting spots at TLC when compound **5a** and glutaraldehyde (**5h**) were subjected under the similar condition as **Table-1.A**. It was difficult to isolate any pure fraction from the reaction mixture. Fine-tuning of the reaction revealed that the outcome depends on the acid loading and stoichiometry (**Table-1.B**). However, 2:1 molar ratio of compound **5a** and **5h** mixed with lower acid loading gave the compound **12a** as a white solid. The solid was isolated by filtration and collected analytical and spectroscopic data without further purification.

Table-1.B: Optimization of reaction condition

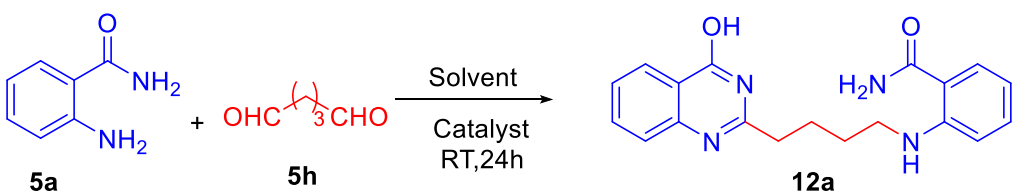

Entry	Solvent	Catalyst[a]	Yield[b](%)
1	MeOH	-	0
2	MeOH	HCl	87
3	EtOH	HCl	95
4	EtOH	$Y(NO_3)_3.6H_2O$	98
5	MeOH	$FeCl_3$	93
6	DMF	$FeCl_3$	85

[a] 20 mol%. [b] Isolated Yield of **12a**
The reaction carried out in 1 mmol scale of **5a** and **5h** with 2:1 molar ratio .

Notably, the compound **12a** is a redox-neutral product, where an oxidation and reduction process is going on without adding any external oxidative or reducing agents. In this case, an imine functionality acted as the hydride accepting counterpart and facilitated the intramolecular redox reaction. The reaction has been carried out with varieties of solvent and acid catalyst, and the results are shown in **Table-1.B**. Here also a protic-polar solvent has been used for the method because of

easy product isolation. A slightly different isolated yield was probably due to the different solubility of compound **12a** in the given solvents. For our subsequent studies, we used methanol as a solvent and HCl as an acid catalyst. Water stable Lewis acids such as $FeCl_3$, Y^{3+}, etc; were also used to catalyze the reaction. The structure of compound **12a**was confirmed by ^{1}H-NMR, ^{13}C-NMR, DEPT-135, and HRMS.

To see the influence of steric and electronic effects towards the formation of compound **12a**, we used differently substituted anthranilamide and its structural analogues. Experimental results are summarized in **Table 1.C**, and the structure of anthranilamide analogues are shown in **Figure-1.D** (**7a-10a**) and corresponding products are shown in **Figure-1.E**.5-Bromo anthranilamide[18] does not significantly influence the redox-neutral reaction, except at a bit slower rate. Moreover, when two bromine atoms or one nitro group were present at the amide side, the hydride shift was not observed and we have isolated intermediate products**14b**and **15b** respectively (Entry 3, 4; **Table-1.C**).In addition, the presence of a sulfonamide instead of carboxyl amide (Entry 5, **Table-1.C**) in the anthranilamide analogues part produced dimeric dihydroquinazolinone (**7d**) instead of a redox neutral product. Glyoxal, a two-carbon dialdehyde, gives a dimeric quinazolinone[19] **6d**.The reactivity of succinaldehyde[20] under the same reaction condition is complex. After a prolonged reaction time, we could isolate compound **16b** instead of redox-neutral product on the reaction of succinaldehyde with **5a**. Formation of **16b** occurs *via* initial condensation of aldehyde to form dihydroquinazolinone followed by the aerobic oxidation process [30].

Table-1.C Optimization with different aliphatic dialdehyde

Anthranilamide analogues + Aliphatic dialdehyde $\xrightarrow{[c]\text{Condition}}$ Products

Entry	Anthranilamide analogues	Aliphatic dialdehyde	Product[d]	Yield[e](%)
1	5a	Glutaraldehyde	12a	96
2	7a	Glutaraldehyde	13a	85
3	8a	Glutaraldehyde	14b	86
4	9a	Glutaraldehyde	15b	67
5	10a	Glutaraldehyde	7d	78
6	5a	Glyoxal	6d	85
7	5a	Succinaldehyde	16b	67

[c] 2:1 molar ratio of anthranilamide analogues and dialdehyde, 10 mL methanol, 1 drop 36% HCl are mixed and stirred for at RT, 24 h.
[d] Compound 16b isolated by column purification. Other compounds are isolated as a white solid by filtration.
[e] Isolated yield.

Initially, we thought that the tricyclic compound **14b** or **15b** could be an intermediate for the redox-neutral product formation. Accordingly, we tried to convert compound **14b** into corresponding redox-neutral-product under similar reaction conditions but failed even after a prolonged time and

under elevated temperature to get convincing evidence. Then, we shifted our attention to isolate tricyclic intermediate from **7a**. Accordingly, **7a** was treated with glutaraldehyde in the presence of a mild Lewis acid yttrium nitrate. We successfully isolated the intermediate **13b** under the mild reaction conditions, as mentioned in **Scheme-1.E**, and the compound **13b** on reaction with **7a** in the presence of MeOH/HCl converted to the redox-neutral product **13a** at the ambient temperature. When CD_3OD/DCl was used as a reaction medium compound **13b** converted into a redox-neutral product **7p–d2**. Structure of the product **7p–d2** has confirmed by comparing ^{1}H-NMR of **13a** and ^{1}H-^{1}H COSY spectra of **13a**. No deuterium incorporation was observed at the reduced site. This critical information led us to conclude that the hydride is being transferred from quinazolinone moiety to the reduced site without the participation of solvent protons.

Mechanistic investigation revealed that the length of dialdehyde is a crucial factor for redox neutral product formation. The hydride transfer is facile when the donor centre and acceptor centre spanning five carbon atoms. To our surprise, 1,2 HT was not observed (Entry 6; **Table-1.C**) when glyoxal, a two-carbon dialdehyde was treated with anthranilamide. Moreover, there is no evidence of deuterium incorporation at the reduction site in the CD_3OD/D^+ condition. However, deuterium incorporation was observed at the adjacent carbon of the reduced position of the product **7p–d2**.

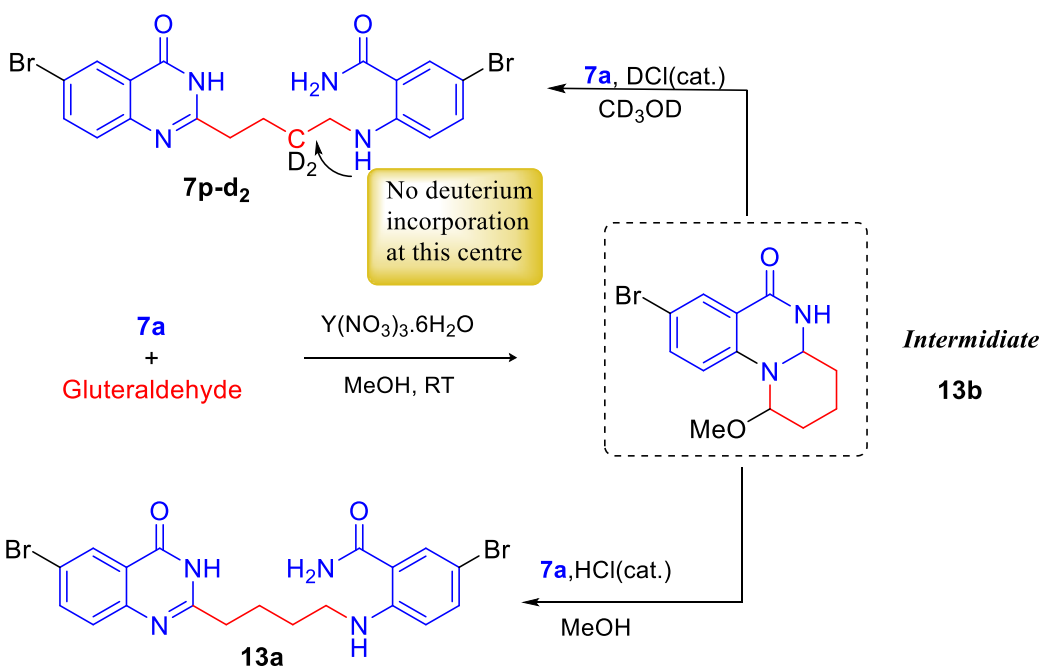

Scheme-1.E Identification of intermediate and deuterium exchange experiment

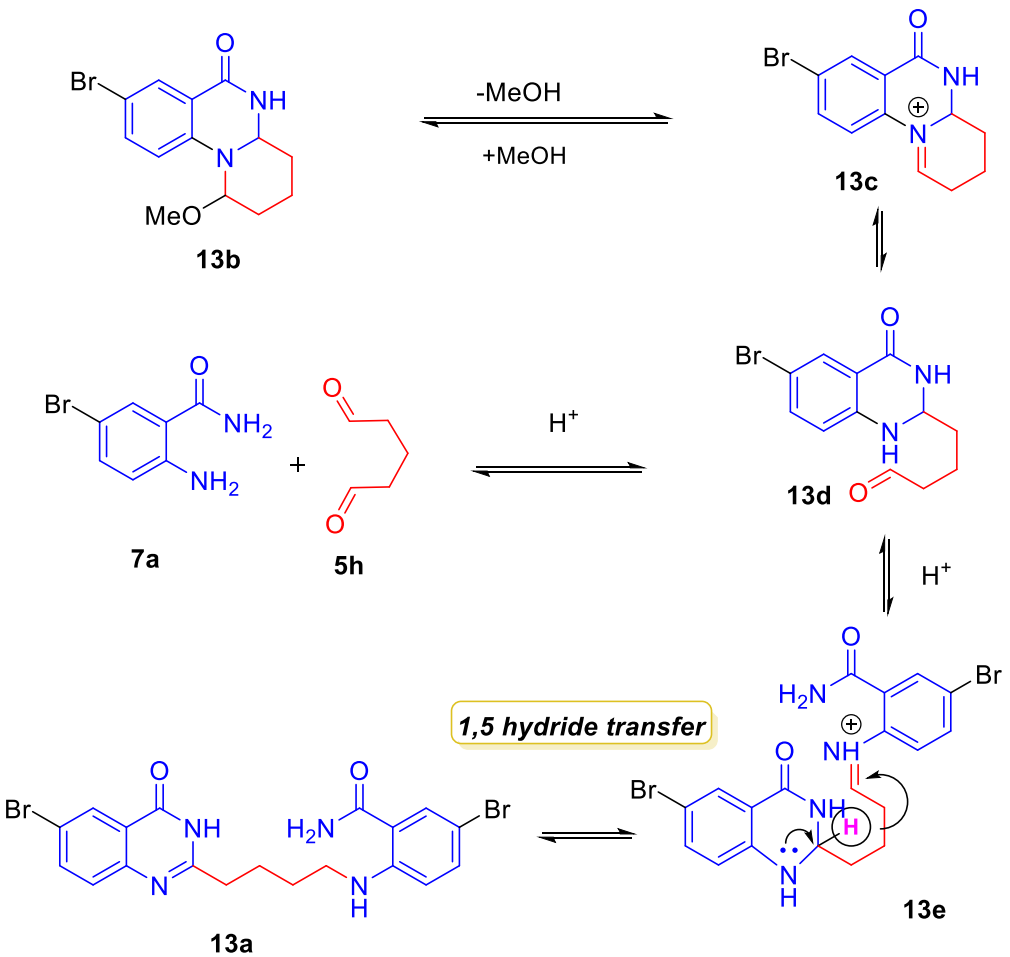

Scheme-1.F: Proposed mechanism

Based on these observations, we proposed an intramolecular hydride transfer mechanism, as shown in **Scheme-1.F**, and explained all the experimental results. When an equimolar mixture of 5-bromo anthranilamide (**7a**) and glutaraldehyde (**5h**) was used, intermediate **13b**, **13c** and **13d** remain in equilibrium. The bromo, nitro, and sulfonamide group in **8a**, **9a** and **10a** make the non-bonded electron on the nitrogen atom (donor site) less available for assisting hydride transfer. Therefore, the intermediate **13b** from compound **8a** and **9a** favours the formation **13c** instead of **13e**. Hence they do not give the desired redox-neutral product. The intermediate **13b** undergo H/D exchange under deuterated reaction condition. This phenomenon explains the formation of the product **7p–d**$_2$. This indicates the case of redox-neutral reaction passing through a concerted intramolecular hydride transfer pathway.

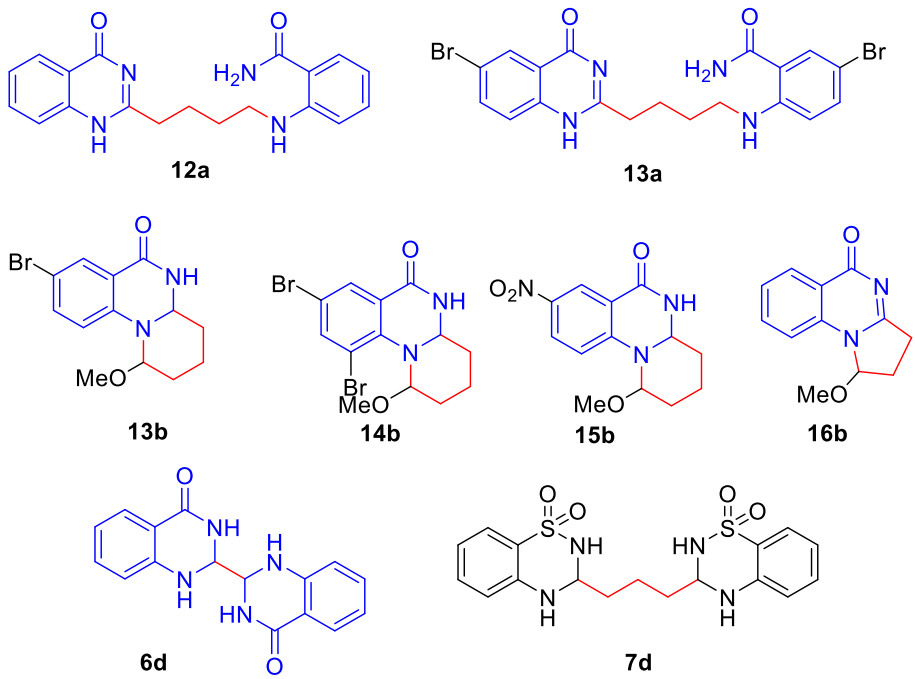

Figure-1.E: Structure of synthesised Quinazolinones

1.3 CONCLUSIONS

In summary, we have demonstrated two facile, 1,3 and 1,5- intramoleculer hydride transfer (redox-neutral) reaction in the presence of aq. acid. These methods allow quick access to functionalized quinazolinones. The presence of an electron withdrawing group at the donor side makes the reaction sluggish in case of aliphatic dialdehydes towards the formation of redox-neutral products. These two are also sensitive to the acid concentration and stoichiometry. Further scope of the reactions is being studied.

1.4 EXPERIMENTAL SECTION

1.4.1 General information: Melting points were determined in open capillary tubes by a LabX India digital melting point apparatus. All the commercially available reagents were used without further purification. All the reactions were carried out at open vessel and monitored by Thin layer chromatography (TLC) on 0.2 mm silica gel F_{254} plates and it was observed under UV light (254 nm). NMRs were recorded in Bruker 400 or 300 MHz spectrometer in DMSO-$d_6$solution. Chemical shifts are given in δ relative to TMS, the coupling constants *J* are given in Hz. High resolution mass spectra were recorded on ESI-TOF mass spectrometry. LCMS taken using ZORBAXEXT (4.6 ×50 mm, 5µ) column, NH_4OAc (10 mM):CAN::90:10 for liquid chromatogram. X-ray crystallographic data were collected from SMART (Bruker,2000), SHELXL-2018/3, version 2018/3', at 273K, θ range (deg) 2.618 to 27.135, radiation type λ (Mo Kα).

1.4.2 Representative procedure and spectral data:

Synthesis and analytical spectroscopic data of 5-oxo-11, 12-dihydro-5H-isoindolo[2,1-a]quinazolin-12-ium chloride (**5eHCl**):

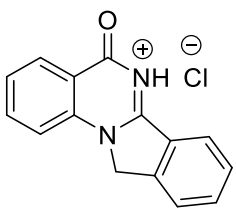

A mixture of anthranilamide (340 mg, 2.50 mmol), and *O*-phthalaldehyde (334.9 mg, 2.50 mmol) were taken in 100 mL round bottom flask. Then to this reaction mixture, 30 mL MeOH and 2(*N*) HCl (10 mL) were added. This reaction mixture was stirred at room temperature for 24 h. Then, the precipitate appeared was collected by filtration and washed with water to get pure **5eHCl** (411 mg).White solid, yield 70%, m.p. 256°C, ^{1}H-NMR (400 MHz, DMSO-d_6) δ 8.47 (d, *J* = 8Hz, 1H), 8.25(d, *J* = 8Hz, 1H), 8.06 (dt, *J* = 8Hz, 1H), 7.87–7.93(m, 3H), 7.77–7.68 (m, 2H), 5.71 (s, 2H). ESI-TOF MS: Calculated mass for $C_{15}H_{11}N_2O$ $[M+H]^+$ is 235.0871, observed m/z = 235.0328

Synthesis and analytical spectroscopic data of isoindolo[2,1-a]quinazolin-5(11H)-one **(5e)**

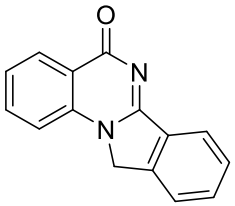

The solid mass of **5eHCl** (132 mg) was treatedwith saturated $NaHCO_3$ solution (5 mL) for 5 min andthen the suspension was filtered and washed with water,dried to get **5e** (102 mg) as white solid. yield 89%, m.p. 258°C, ^{1}H-NMR (400 MHz, DMSO-d_6) δ 8.14 (s, 1H),8.12 (d, *J* = 1.2 Hz,1H), 8.02 (d, *J* = 8Hz,1H),7.89–7.85 (dt, *J* = 8, 15 Hz,1H), 7.82–7.74 (m, 1H),7.66–7.63 (m, 2H), 7.51 (t, *J* = 15 Hz, 1H), 5.45 (s,2H). ESI-TOF MS: Calculated mass for $C_{15}H_{10}N_2NaO$ $[M+Na]^+$ = 257.0691, observed m/z = 257.1372

Synthesis and analytical spectroscopic data of 3-bromoisoindolo[2,1-a]quinazolin- 5(11H)-one**(7e)**

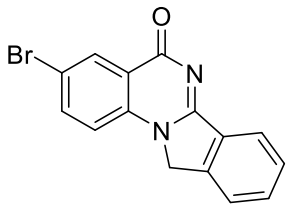

Same as described for **5eHCl**.White Solid, yield 88%, m.p. 257°C,^{1}H-NMR (400 MHz, DMSO-d_6+$CDCl_3$) δ 8.21 (s, 1H), 8.02 (d, J = 8Hz, 1H), 7.96–7.93 (m, 1H), 7.76–7.69 (m, 2H), 7.62–7.58 (m, 2H), 5.41 (s, 2H); ^{13}C-NMR (100 MHz, DMSO-d_6+$CDCl_3$) δ 161.2, 149.9, 139.6, 137.5, 133.6, 131.9, 131.6, 131.5, 129.5, 124.5, 123.1, 120.1, 119.7, 116.4, 52.0. ESI-TOF MS: Calculated mass for $C_{15}H_9BrNaN_2O$ $[M+Na]^+$ = 334.9796, observed m/z = 335.002

***Synthesis and analytical spectroscopic data of 1,3-dibromoisoindolo[2,1-a]quinazolin- 5(11H)-one* (8e)**

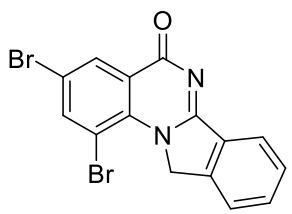

Same as described for **5eHCl**. White Solid, yield 91%, m.p. 259°C, ^{1}H-NMR (400 MHz, DMSO-d_6) δ 8.37 (d, J = 2Hz, 1H), 8.27 (d, J = 2Hz, 1H), 8.03 (d, J = 8Hz, 1H), 7.84–7.78 (m, 2H), 7.65 (d, J = 8Hz, 1H), 5.98 (s, 2H). ESI-TOF MS: Calculated mass for $C_{15}H_8Br_2N_2NaO$ $[M+Na]^+$ = 414.8881, observed m/z = 414.753

***Synthesis and analytical spectroscopic data of 3-nitroisoindolo[2,1-a]quinazolin-5(11H)-one* (9e)**

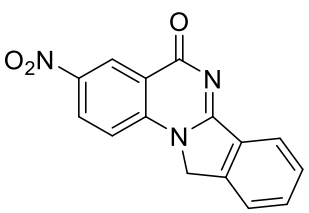

Same as described for **5eHCl**. Light yellow solid, yield 86%, m.p. 252°C, ^{1}H-NMR (400 MHz, DMSO-d_6) δ 8.79 (d, J = 2Hz, 1H), 8.64 (d, J = 2Hz, 1H), 8.03 (d, J = 7.2Hz, 1H), 7.83–7.79 (m, 3H), 7.65 (t, J = 7.2Hz, 1H), 5.48 (s, 2H); ^{13}C-NMR (100 MHz, DMSO-d_6+$CDCl_3$) δ 166.8, 148.5, 142.6, 141.4, 139.6, 131.8, 130.1, 127.2, 126.6, 122.2, 122.1, 121.9, 116.6, 115.8, 50.7. ESI-TOF-MS: Calculated mass for $C_{15}H_9N_3NaO_3$ $[M+Na]^+$ = 302.0542, observed m/z = 301.9480

***Synthesis and analytical spectroscopic data of 11H-benzo[5,6][1,2,4]thiadiazino[3,4- a]isoindole 5,5-dioxide* (10e)**

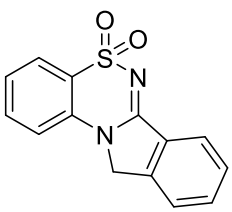

Same as described for **5eHCl**.White Solid, yield 83%, m.p. 295 °C, ^{1}H-NMR (400MHz, DMSO-d_6) δ 7.92 (dt, J = 8Hz, 12 Hz, 2H), 7.81–7.77 (m, 3H), 7.66-7.63 (m,1H), 7.55-7.52(m, 2H), 5.40 (s, 2H). ESI-TOF-MS calculatedmass for $C_{14}H_{10}N_2NaO_2S$ $[M+Na]^+$ 293.0361, observed m/ z = 293.1225

***Synthesis and analytical spectroscopic data of 7,8,9,10-tetrahydrobenzo[4',5']thieno [3',2':5,6]pyrimido[2,1-a]isoindol-6(13H)-one*(11e)**

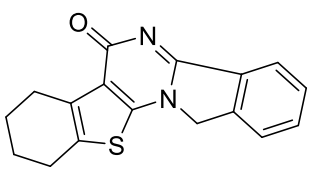

Same as described for **5eHCl**.White Solid, yield 92%, m.p. 254°C,^{1}H-NMR (400MHz, DMSO-d_6 + $CDCl_3$) δ 8.11 (s, 1H), 7.96 (d, J = 8Hz, 1H), 7.70–7.62 (m, 2H), 7.56 (t, J = 8Hz, 1H), 5.24 (s, 1H), 2.94 (m,

2H), 2.74 (m, 2H), 1.84–1.76 (m, 4H). ESI-TOF-MS Calculated mass for $C_{17}H_{14}N_2NaOS$ $[M+Na]^+$ =317.0725, observed m/z = 317.0002

***Synthesis and analytical spectroscopic data of 5-oxo-11,12-dihydro-5H-12l4-isoindolo[2,1-a]quinazolin-6-ium-12-d*(5eDCl)**

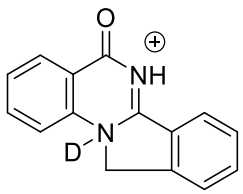

A mixture of anthranilamide (50 mg) and *O*-phthalaldehyde (49 mg) were taken in a 50 mL round bottom flask. Then 3 mL methanol-d_4, 0.5 mL D_2O and 0.5 mL DCl (20%) were added into this reaction mixture under argon atmosphere. The reaction mixture was stirred for 24 h to get white precipitation. The mixture was then diluted with 2 mL D_2O, filtered to collect white solid mass (61 mg, 71%). It was dried to get spectroscopic data without further purification. ^{1}H-NMR in DMSO-d_6 is essentially same with **5eHCl** except the position of residual H_2O present in the DMSO-$d_6$solvent. ^{1}H-NMR (400 MHz, DMSO-d_6) δ 8.43 (d, *J* = 8Hz, 1H), 8.26 (d, *J* = 8Hz, 1H), 8.07 (t, *J* = 8Hz, 1H), 7.94–7.88 (m, 3H), 7.78–7.69 (m, 2H), 5.72 (s, 2H). ESI-TOF-MS calculated mass for $C_{15}H_{10}DN_2O^+$ = 336.0929, observed m/z = 336.0995

Compound **5eDCl** was treated with saturated bicarbonate and the white solid obtained after base treatment was subjected to ^{1}H-NMR. It was exactly same as observed for **5e**.

***Synthesis and analytical spectroscopic data of 2-((4-(4-hydroxyquinazolin-2-yl)butyl)amino)benzamide* (12a)**

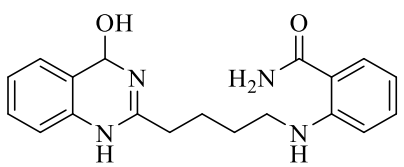

Method-I: A mixture of anthranilamide (250mg, 1.84mmol), glutaraldehyde (73mg, 0.734 mmol) and 2 drops of concentrated HCl (35%) in 10 mL methanol was stirred at room temperature for 24 hours. White precipitate starts appearing within 2-3 hours. Water (50 mL) was added into the reaction mixture. White precipitate was collected by filtration, washed with fresh water (3×20 mL) and air dried for analytical and spectroscopic data without further purification. Yield 87%. **Method-II**: Experimental procedure for synthesis of **12a** is the same as described in **Method-I** except for HCl. Here, we have used 20mol% $Y(NO_3)_3.6H_2O$ instead of HCl. White solid, yield 98%,^{1}H-NMR (400MHz, DMSO-d_6) δ 12.18 (s, 1H), 8.13-8.12 (m, 1H), 8.06 (d, *J* = 8 Hz, 1H), 7.77- 7.74 (m, 2H), 7.60-7.56 (m, 2H), 7.44 (t, *J* = 8 Hz, 1H), 7.22 (t, *J* = 8Hz, 1H), 7.20 (s, 1H), 6.64 (d, *J* = 8 Hz, 1H), 6.48 (t, *J* = 8 Hz, 1H), 3.15-3.10 (m, 2H), 2.64 (t, *J* = 8Hz, 2H), 1.83-1.80 (m, 2H), 1.62 (t, *J* = 8Hz, 2H). ^{13}C-NMR (100 MHz, DMSO-d_6) δ172.1, 162.2, 157.7, 150.3, 149.4, 134.7, 133.0, 129.5, 127.3, 126.4, 126.1, 121.3, 114.2, 114.1, 111.4, 42.2, 34.6, 28.6, 24.9. ESI-TOF-MS: Calculated mass for $C_{19}H_{20}N_4NaO_2$ $[M+Na]^+$ = 359.1484, observed m/z = 359.1621

***Synthesis and analytical spectroscopic data of 5-bromo-2-((4-(6-bromo-4-hydroxyquinazolin-2-yl)butyl)amino)benzamide*(13a)**

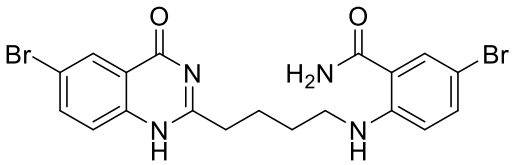

Experimental procedure was the same as described in **Method-I** for compound **12a**. Off white, yield 85%, ^{1}H-NMR (400 MHz, DMSO-d_6) δ 12.37 (bs, 1H), 8.13 (s, 2H), 7.89 (dd, *J* = 2Hz, 8 Hz, 2H), 7.73 (d, *J* = 2 Hz, 1H), 7.54 (d, *J* = 8 Hz, 1H), 7.33 (dd, *J* = 2 , 8 Hz, 1H), 7.23 (bs, 1H), 6.61 (d, *J* = 8 Hz, 1H), 3.11 (t, *J* = 6 Hz, 2H), 2.63 (m, *J* = 7 Hz, 2 H), 1.81-1.75 (m, 2H), 1.63-1.58 (m, 2H).^{13}C-NMR(100 MHz, DMSO-d_6) δ 170.3, 160.6, 158.0, 148.8, 147.6,137.0, 134.8, 131.0, 129.0, 127.7, 122.4, 118.2, 115.3, 113.2, 104.4, 41.7, 34.0, 27.8, 24.1. ESI-TOF-MS: Calculated mass for $C_{19}H_{18}Br_2N_4NaO_2$ $[M+Na]^+$ = 514.9694, observed m/z = 514.9941

***Synthesis and analytical spectroscopic data of 5-bromo-2-((4-(6-bromo-4-oxo-1,4-dihydroquinazolin-2-yl)butyl-2,2-d2)amino)benzamide* (7p-d2)**

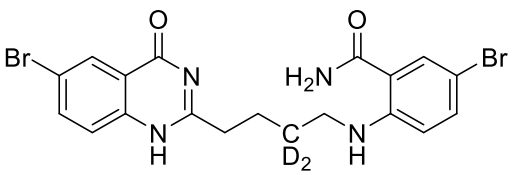

Experimental procedure is the same as described in **Method-I** for compound **12a** in CD_3ODsolvent and DCl as catalyst instead of MeOH/HCl. White solid, yield80%, ^{1}H-NMR (400 MHz, DMSO-d_6) δ12.35 (s, 1H), 8.13(d, *J*= 2.4, 8.8Hz, 2H),7.91-7.88(dd, *J*= 2.4, 8.8 Hz, 2H), 7.73(d, *J*= 2.4Hz, 1H), 7.54(d, *J*= 2.4Hz, 1H), 7.33 (dd, *J* = 2.4, 8.8 Hz, 1H), 7.22-7.17 (m, 1H), 6.61 (d, *J* = 8.8 Hz, 1H), 3.10 (s, 2H), 2.66-2.61(m, 2H), 1.80-1.76(m, 2H).

***Synthesis and analytical spectroscopic data of 2,2',3,3'-Tetrahydro-[2,2'-biquinazoline]-4,4'(1H,1'H)-dione* (6d)**

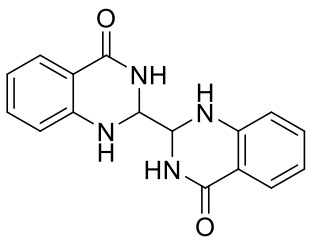

Experimental procedure is the same as described in **Method-II** for compound **12a**. White solid, yield 85%, ^{1}H-NMR (300 MHz, DMSO-d_6) δ 8.40 (bs, 2H), 7.72 (d, *J* = 7 Hz, 2H), 7.15 (t, *J* = 7 Hz, 2H), 6.96 (bs, 2H), 6.67 (t, *J* = 8 Hz, 4H), 4.82 (m, 2H). ^{13}C-NMR (100 MHz, DMSO-d_6) δ 144.1, 133.2, 124.1, 121.7, 116.7, 116.3, 66.0, 33.4, 31.1. ESI-TOF-MS: Calculated mass for $C_{16}H_{14}N_4NaO_2$ $[M+Na]^+$ = 317.1014, observed m/z = 317.1980

***Synthesis and analytical spectroscopic data of 3,3'-(propane-1,3-diyl)bis(3,4-dihydro-2H-benzo[e][1,2,4]thiadiazine 1,1-dioxide)* (7d)**

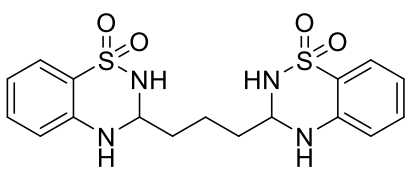

Experimental procedure is the same as described in **Method-I** for compound 1**2a**. White solid, yield 78%,^{1}H-NMR (400 MHz, DMSO-d_6) δ 7.47-7.42 (m, 4H), 7.31-7.26 (m, 2H), 7.06 (s, 2H), 6.81 (d, *J* = 8 Hz, 2H), 6.72(t, *J* = 8 Hz, 2H), 4.71(m, 2H), 1.81-1.64 (m, 6H). ^{13}C-NMR (100 MHz, DMSO-d_6) δ 144.1, 133.2, 124.1, 123.3, 116.7, 116.4, 66.1,

33.4, 32.5. ESI-TOF-MS:Calculated mass for $C_{17}H_{20}N_4NaO_4S_2$ $[M+Na]^+$ = 431.0824, observed m/z = 431.1061

***Synthesis and analytical spectroscopic data of 8-bromo-1-methoxy-1,2,3,4,4a,5-hexahydro-6H-pyrido[1,2-a]quinazolin-6-one* (13b)**

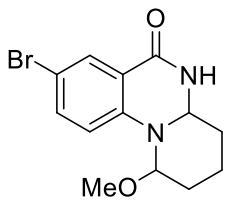

To a mixture of 5-bromoanthranilamide **7a** (250 mg, 1.16 mmol) and glutaraldehyde **5h** (0.250 mL, 1.16 mmol), $Y(NO_3)_3.H_2O$ (76 mg, 0.23 mmol) was added, and the mixture was stirred for 24 h at RT. The mixture was diluted with water and the white solid collected by filtration. Thus, the material isolated was used directly for analytical data without further purification. White solid, yield 84%, ^{1}H-NMR (400 MHz, DMSO-d_6 + $CDCl_3$) δ 8.30 (bs, 1H), 7.77 (bs, 1H), 7.54 (d, *J* = 8Hz, 1H), 6.89 (d, *J* = 8Hz, 1H), 5.08 (bs, 1H), 4.75-4.73 (m, 1H), 3.27 (s, 3H), 2.06 (m, 1H), 1.92 (m, 1H), 1.68-1.54 (m, 4H). ^{13}C-NMR (100 MHz, DMSO-d_6+ $CDCl_3$) δ 161.1, 146.2, 135.2, 129.8,119.1, 115.3, 110.2, 82.5, 63.1, 54.1, 30.7, 25.1, 15,5. ESI-TOF-MS: Calculated mass for $C_{13}H_{15}BrN_2NaO_2$ $[M+Na]^+$ =335.0194, obtained m/z = 334.9499

***Synthesis and analytical spectroscopic data of 8, 10-dibromo-1-methoxy-1,2,3,4,4a,5-hexahydro-6H-pyrido[1,2-a]quinazolin-6-one* (14b)**

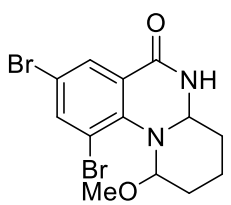

Experimental procedure is the same as described in **Method-I** for compound **12a** by using 2,5- dibromoanthranilamide (**8a**). White solid, yield86%, ^{1}H-NMR (400 MHz, DMSO-d_6) δ 7.78 (d, *J* = 2 Hz, 1H), 7.71 (d, *J* = 2 Hz, 1H), 6.54 (s, 1H), 5.68 (s, 1H), 5.08 (s, 1H), 4.99-4.97 (m, 1H), 3.23 (s, 3H), 1.94-1.92 (m, 1H), 1.80-1.54 (m, 5H). ^{13}C-NMR (100 MHz, DMSO-d_6) δ 161.4, 142.1, 138.3, 131.1, 116.6, 109.6, 108.1, 80.7, 64.0, 55.9, 33.6, 28.8, 17.0. LC-MS: Calculated mass for $C_{13}H_{15}Br_2N_2O_2$ $[M+H]^+$ = 388.9500, obtained m/z = 388.9

***Synthesis and analytical spectroscopic data of 1-Methoxy-8-nitro-1,2,3,4,4a,5-hexahydro-6H-pyrido[1,2-a]quinazolin-6-one*(15b)**

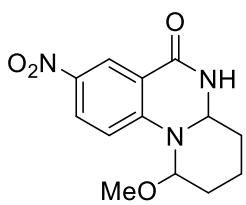

Experimental procedure is the same as described in **Method-I** for compound **12a**. Yellow solid, yield 67%, ^{1}H-NMR (400 MHz, DMSO-d_6) δ 8.59 (s, 1H), 8.49 (d, *J* = 2 Hz, 1H), 8.21 (dd, *J* = 2, 8 Hz, 1H),7.17 (d, *J* = 8 Hz, 1H), 5.37 (s, 1H), 4.92 (d, *J* = 8 Hz, 1H), 3.31 (s, 3H), 2.09-1.92 (m, 2H), 1.70-1.58 (m, 4H). ^{13}C-NMR (100 MHz, DMSO-d_6) δ 160.2, 151.9, 138.3, 128.4, 123.7, 115.9,113.7, 83.1, 63.5, 54.5, 31.6, 25.1, 15.9. ESI-TOF MS: Calculated for $C_{13}H_{15}N_3NaO_4$ $[M+Na]^+$ = 300.0960, obtained m/z = 300.0298

***Synthesis and analytical spectroscopic data of 1-methoxy-2,3-dihydropyrrolo[1,2-a]quinazolin-5(1H)-one* (16b)**

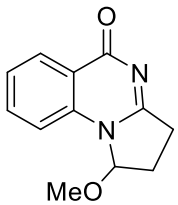

Experimental procedure is the same as described in **Method-I** for compound **12a**. Stock solution of succinaldehyde was prepared according to the reported procedure.[31]White solid, yield 67%,^{1}H-NMR (300MHz, $CDCl_3$) δ 8.29 (d, *J* = 6 Hz, 1H), 7.75-7.70 (m, 1H), 7.65-7.62 (m, 1H), 7.46-7.41 (m, 1H), 5.98 (s, 1H), 3.60 (s, 3H), 3.45-3.34(m, 1H), 3.03-2.94(m, 1H), 2.28-2.24 (m, 2H). ^{13}C-NMR (75 MHz, $CDCl_3$) δ 161.2, 159.4, 148.9, 134.5, 126.9, 126.8, 126.4, 120.8, 89.0, 58.3, 30.4, 28.5. ESI-TOF-MS: Calculated mass for $C_{12}H_{13}N_2O_2$ $[M+H]^+$= 217.0977, obtained m/z = 217.0977

1.4.3 Crystallographic Table:

Table 1.D *Crystallographic and structure refinement parameters for 3aHCl*

Emperical formula	$C_{15}H_{13}ClN_2O_2$
Formula weight	288.72
Crystal system	Orthorhombic
space group	Pca21
a/ Å	18.253(6)
b/Å	4.9135(17)
c/ Å	14.873(6)
V /*Å*^{3}	1334.0 (8)
Z	4
D_c/ g cm^{-3}	1.438
μ /mm^{-1}	2.980
T/K	273
θ range/°	2.618, 27.135
λ (Mo Kα) /*Å*	0.71073
R indices($I > 2\sigma(I)$)	R_1=0.0641, wR_2=0.1367
R indices (all data)	R_1=0.1038, wR_2=0.1575

$R_1 = \Sigma\ ||F_0|-|F_c|| / \Sigma\ |F_0|$; $wR_2 = [\Sigma[w(F_0^2 - F_c^2)^2] / \Sigma[w(F_0^2)^2]]^{1/2}$. $w = 1/[\sigma^2(F_0)^2 + (aP)^2 + bP]$, $P = [\max.(F_0^2,0) + 2(F_c)^2]/3$, where a= 0.0560 and b= 0.8626]

Copy of NMR

^{1}H-NMR of 5eHCl

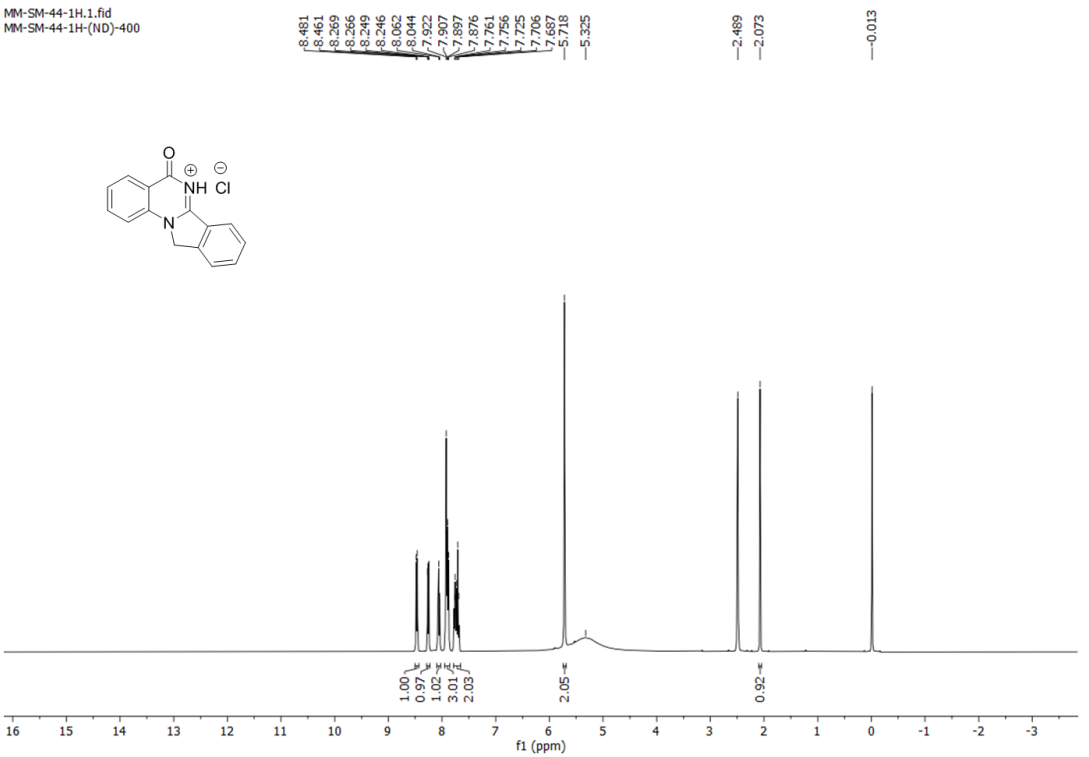

^{1}H-NMR 5e

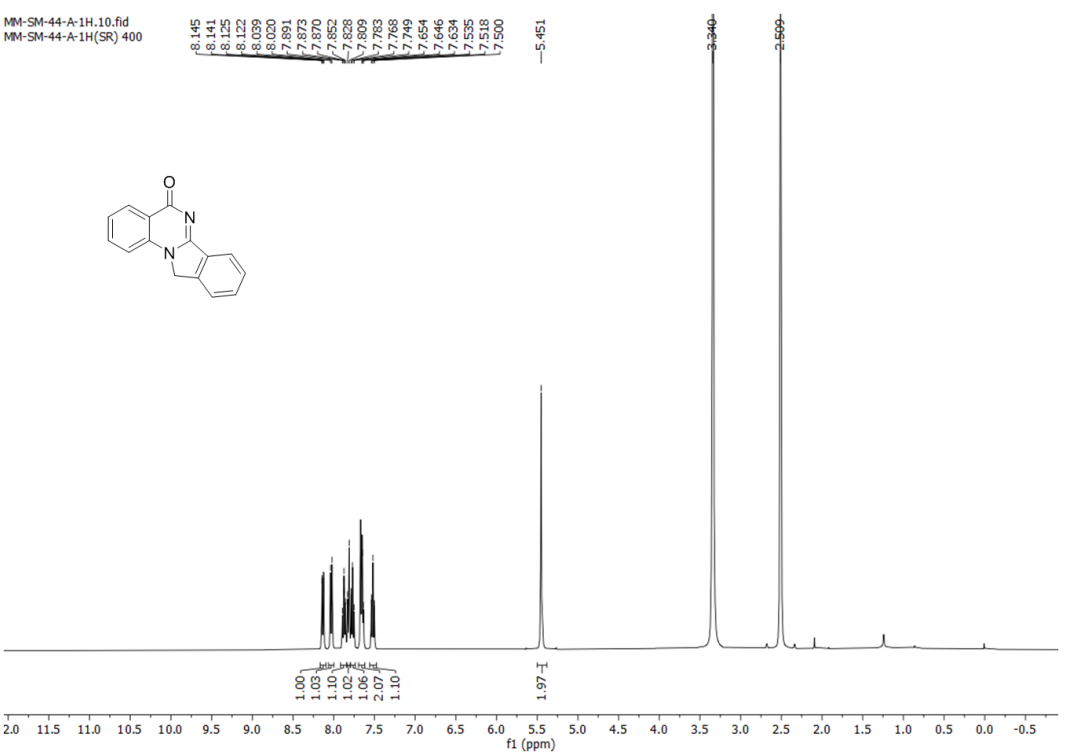

^{1}H-NMR of 9e

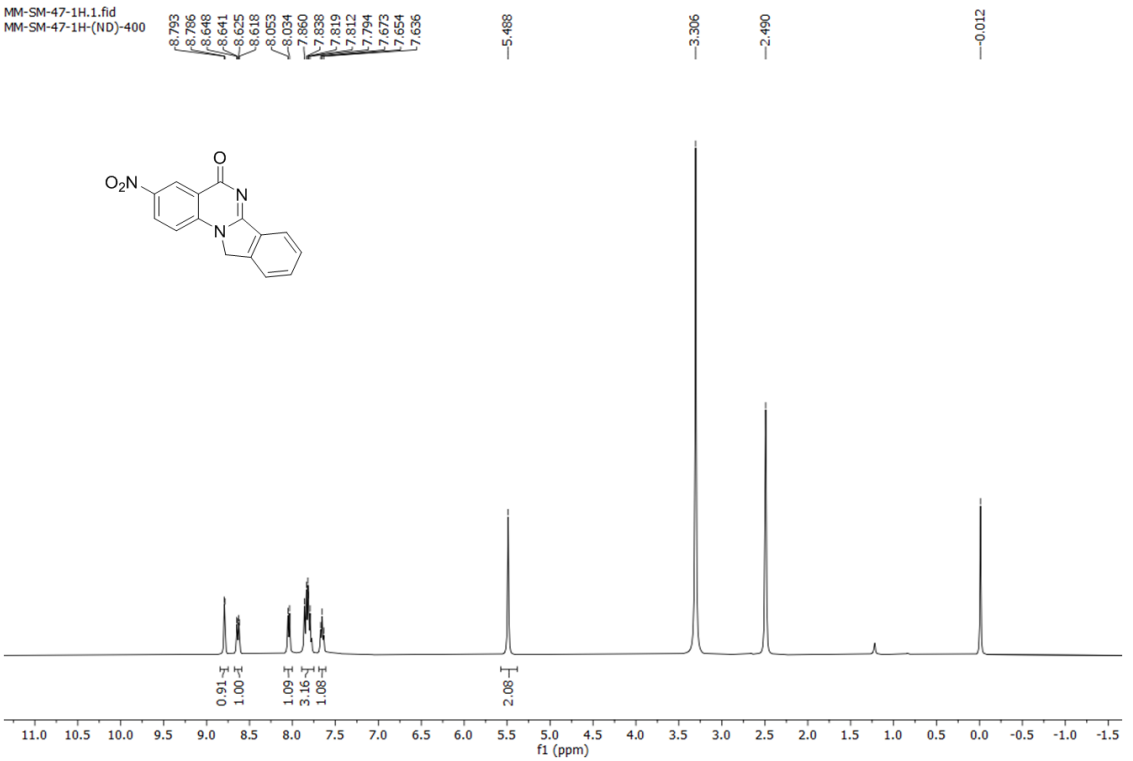

^{13}C-NMR of 9e

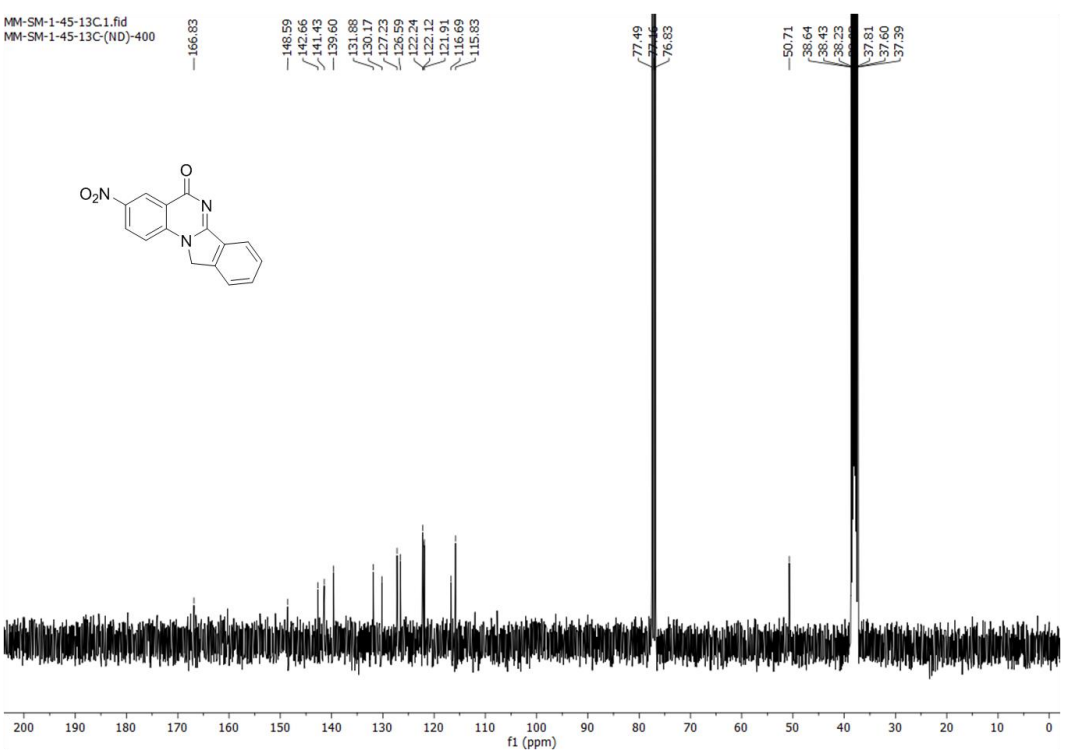

^{1}H-NMR of 7e

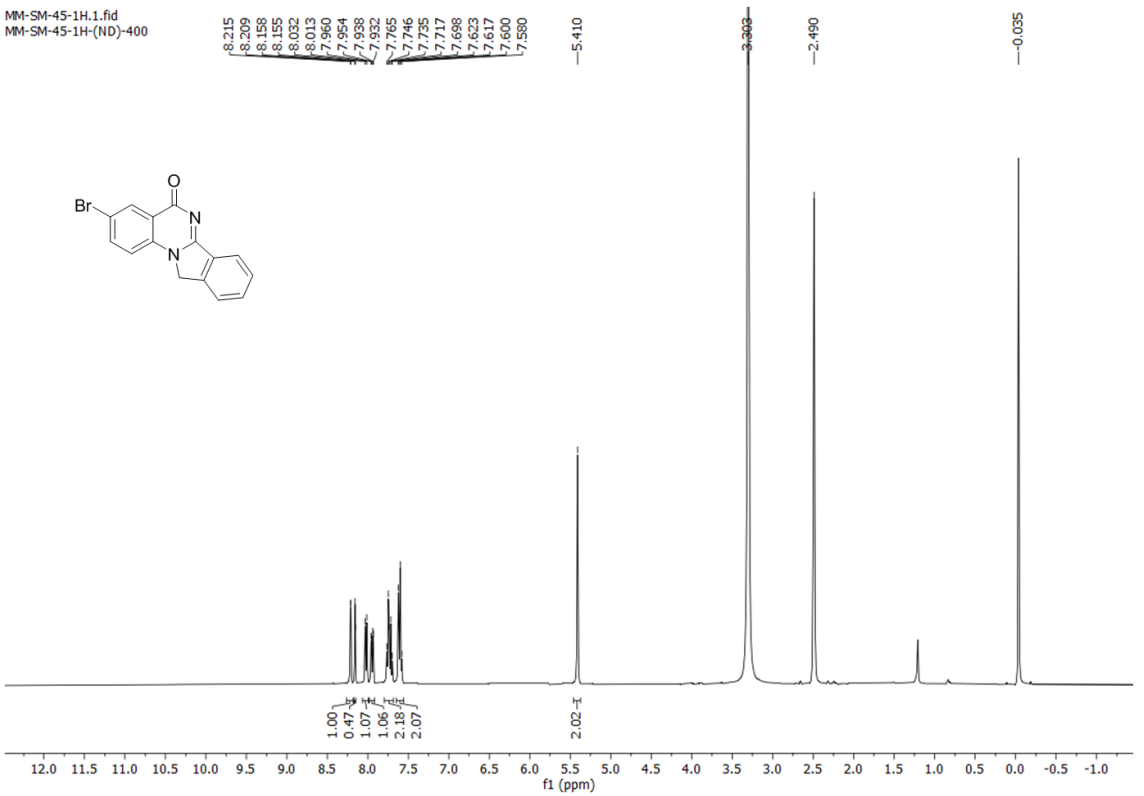

^{13}C-NMR 7e

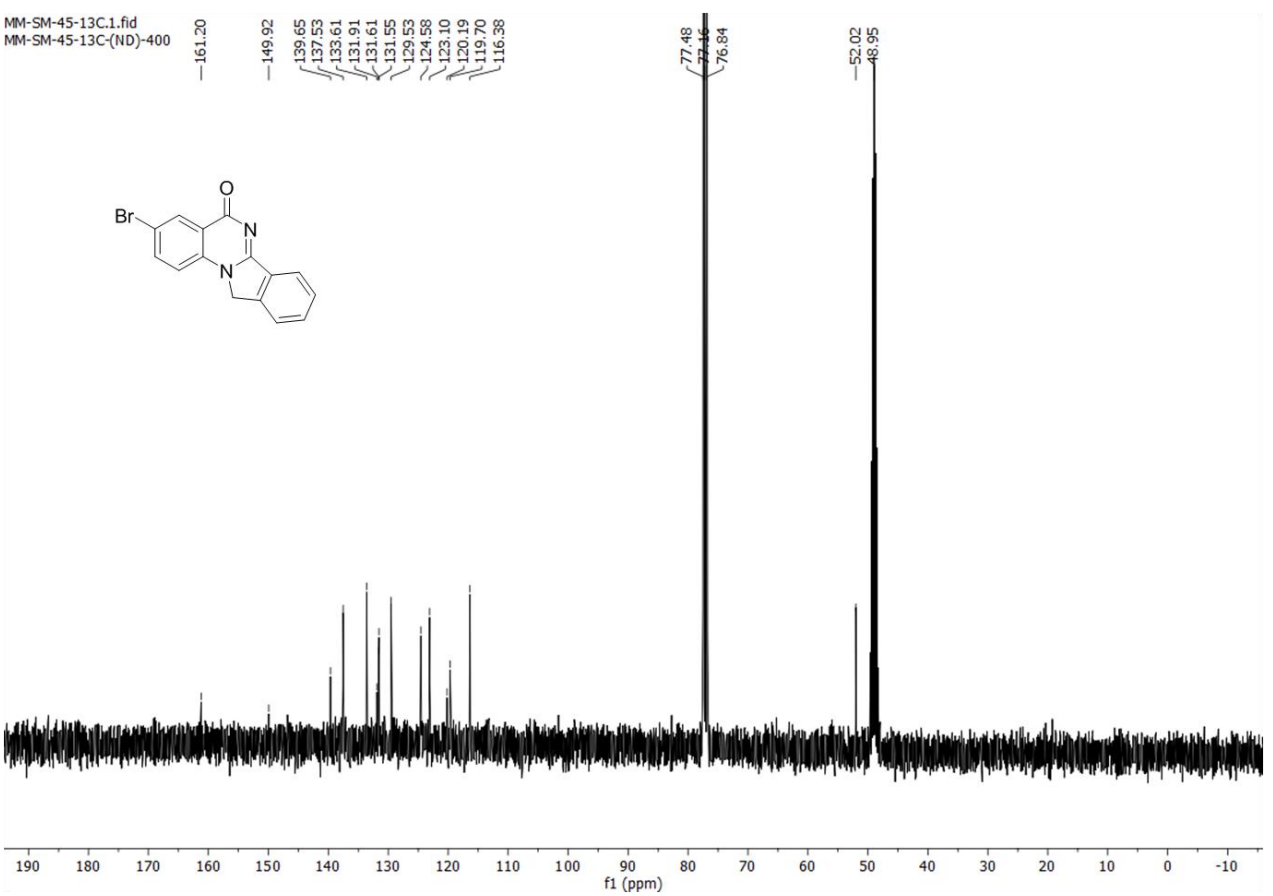

^{1}H-NMR of 8e

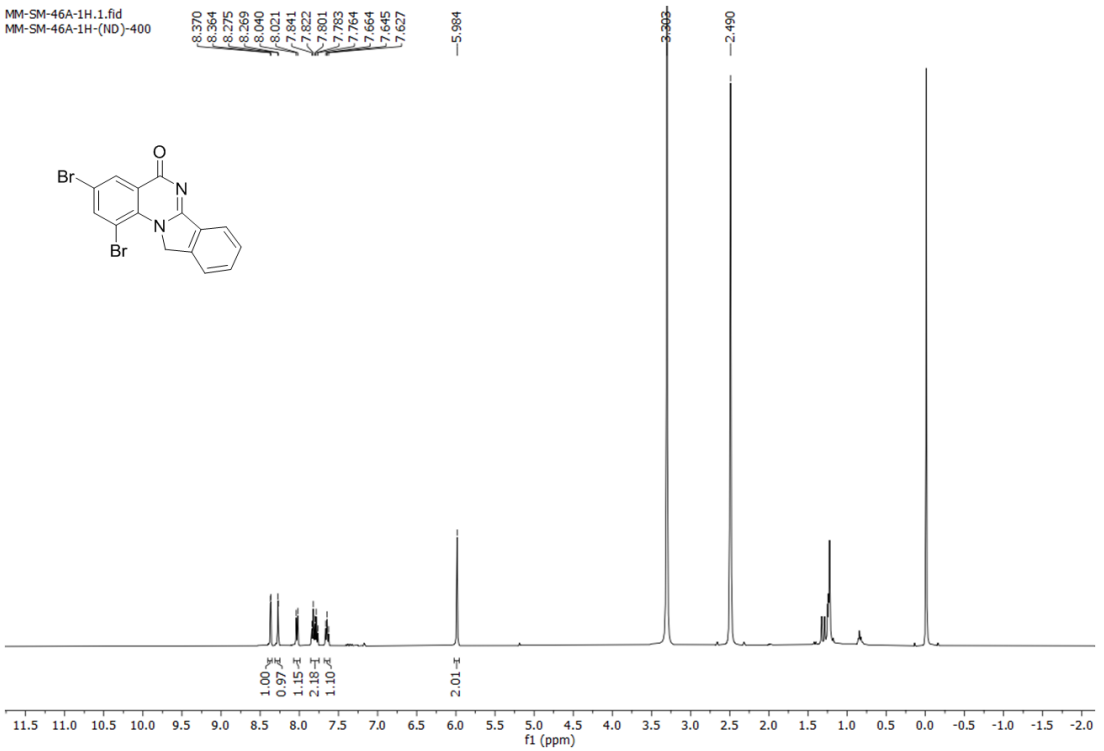

^{1}H-NMR of 10e

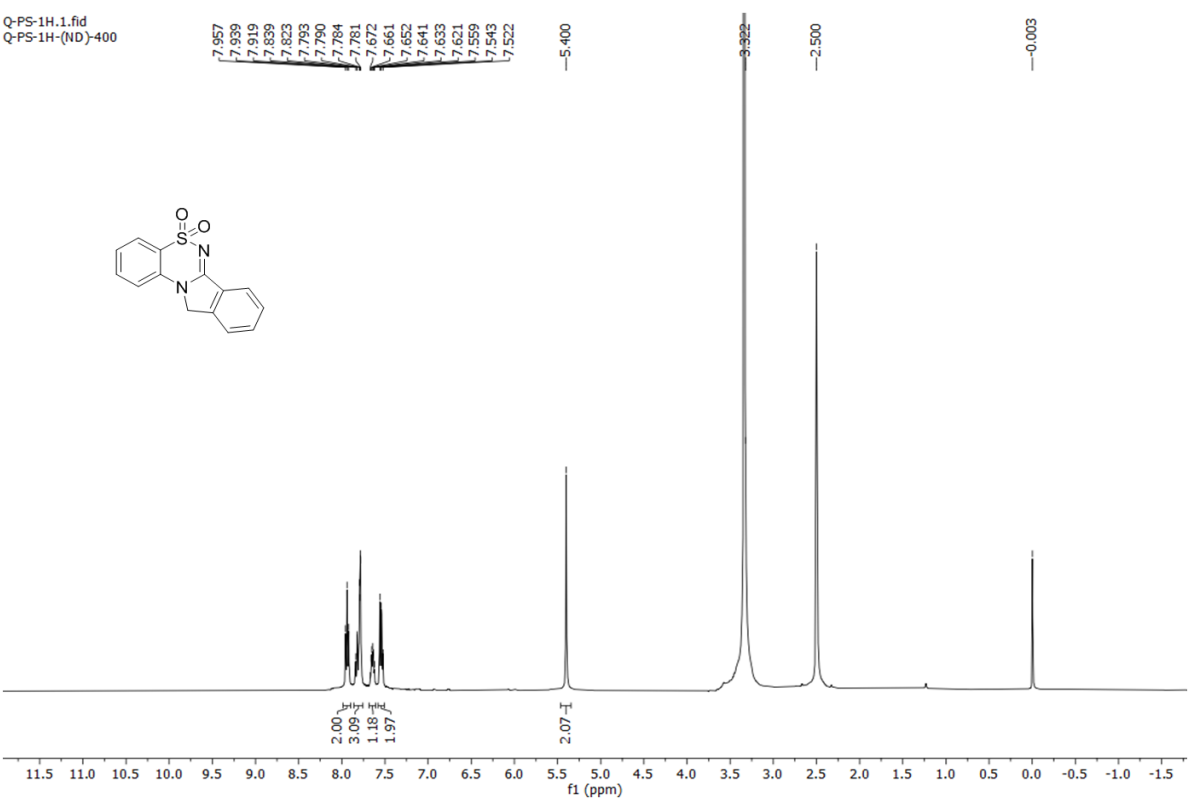

^{1}H-NMR of 11e

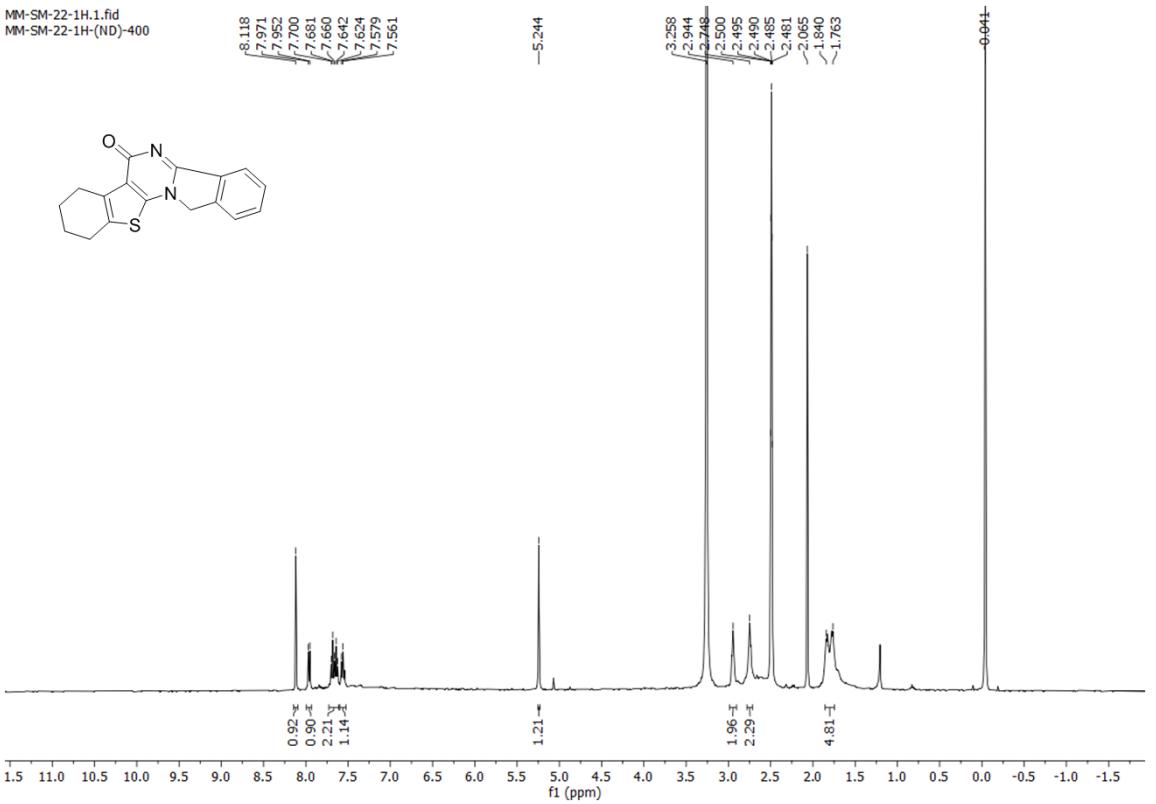

^{1}H-NMR of 5eDCl

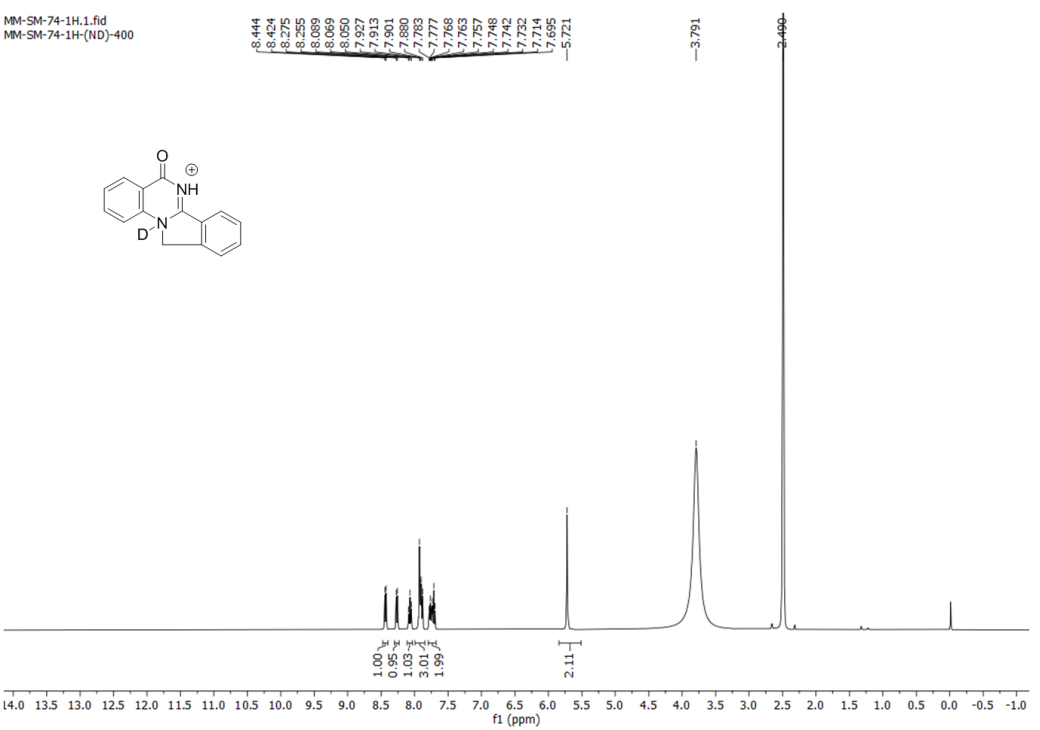

^{1}H-NMR of 12a

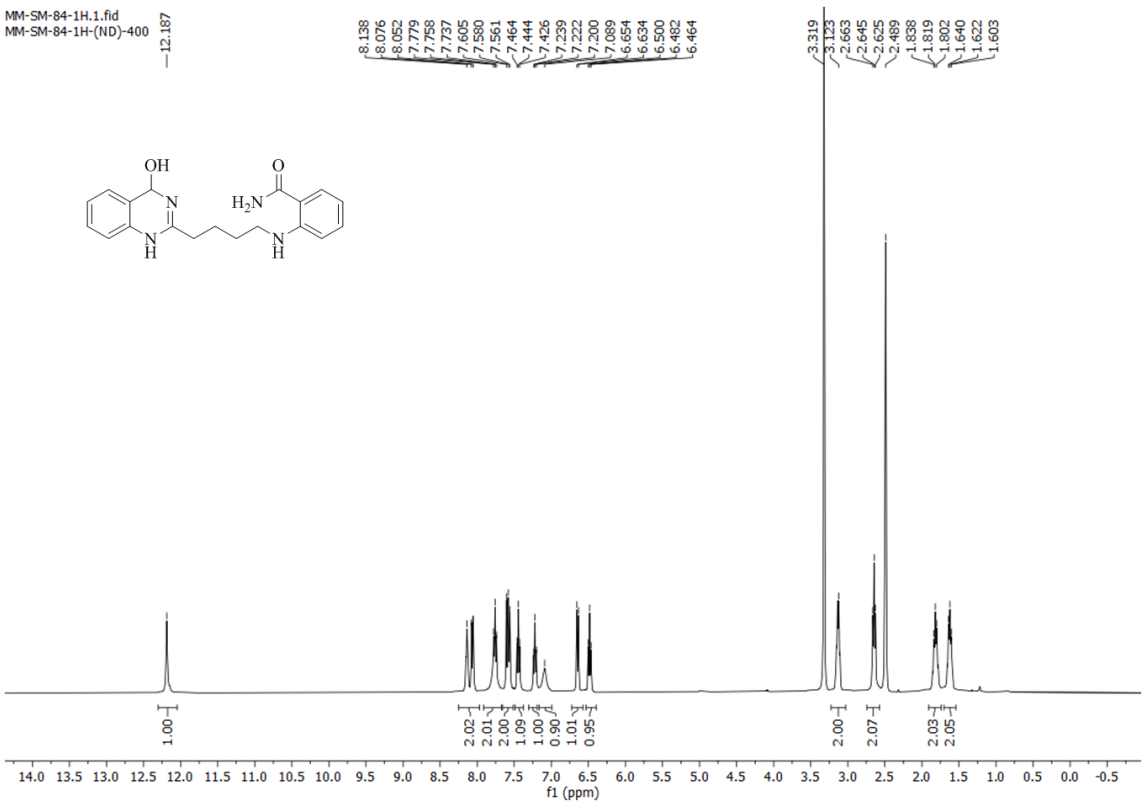

^{13}C-NMR of 12a

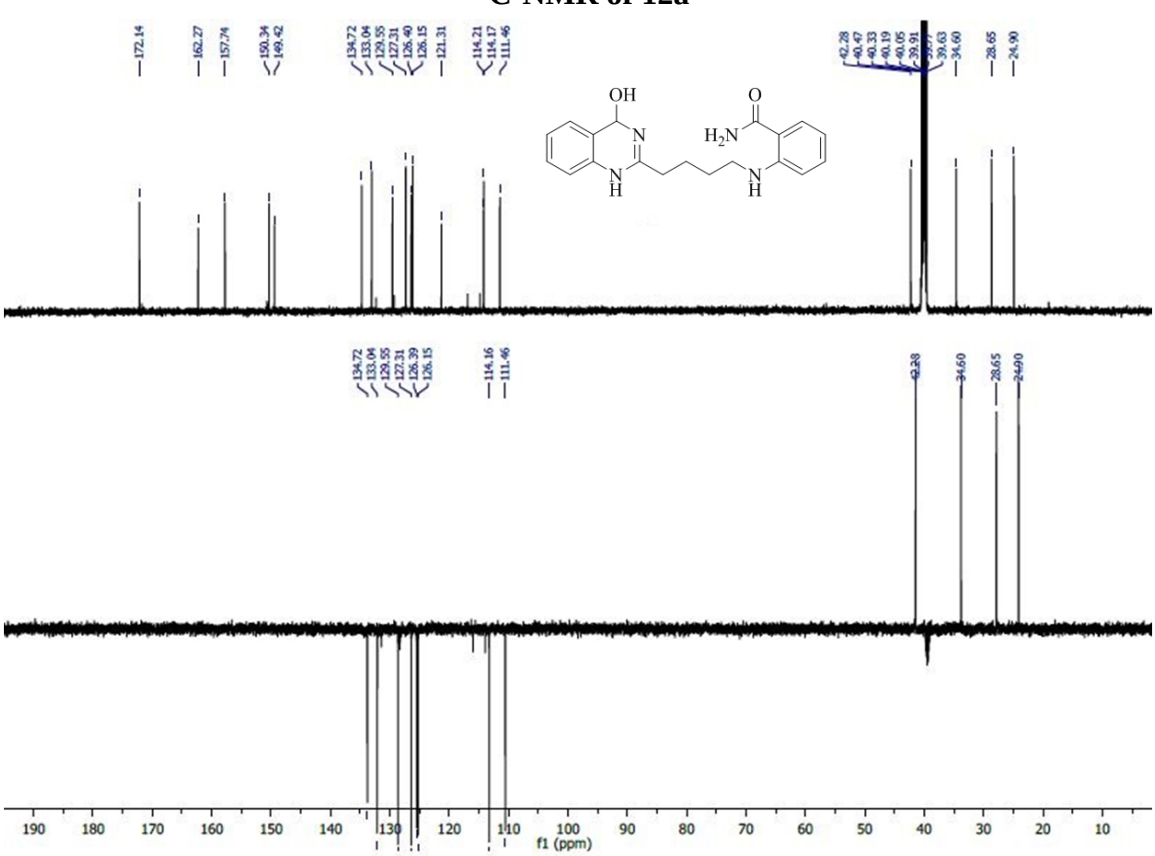

^{1}H-NMR of 13a

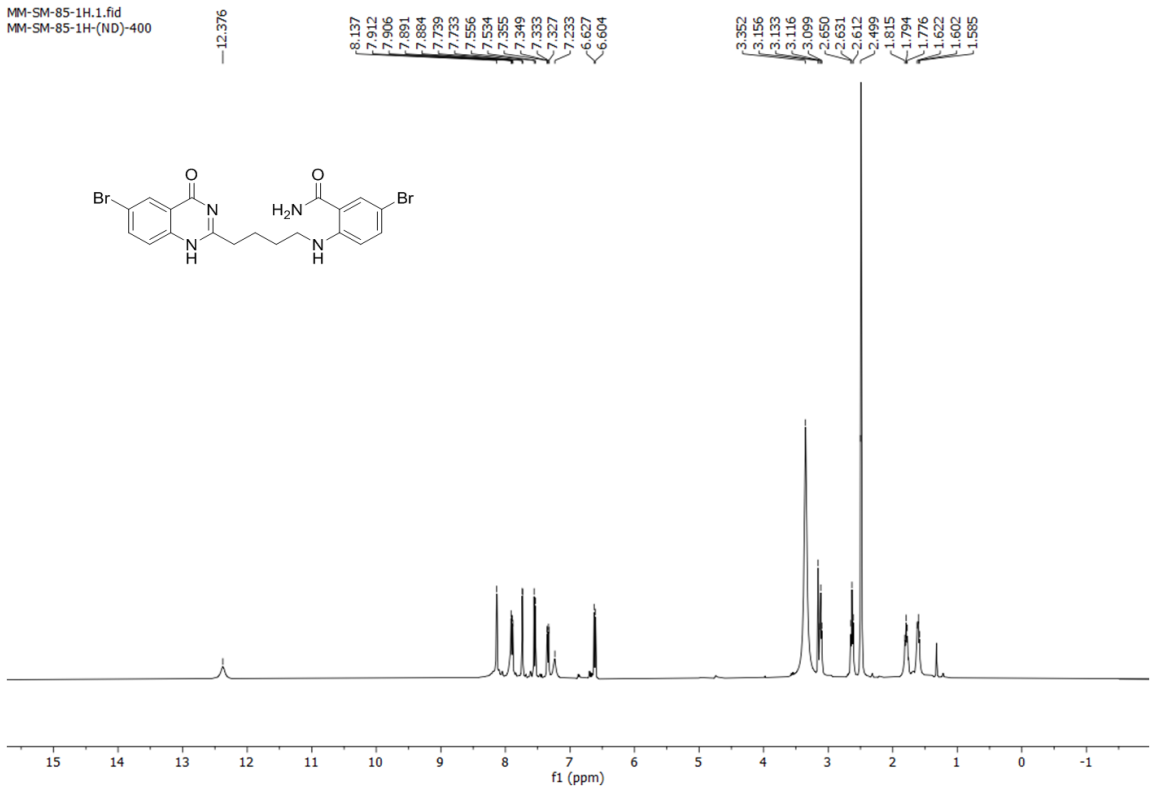

^{13}C-NMR of 13a

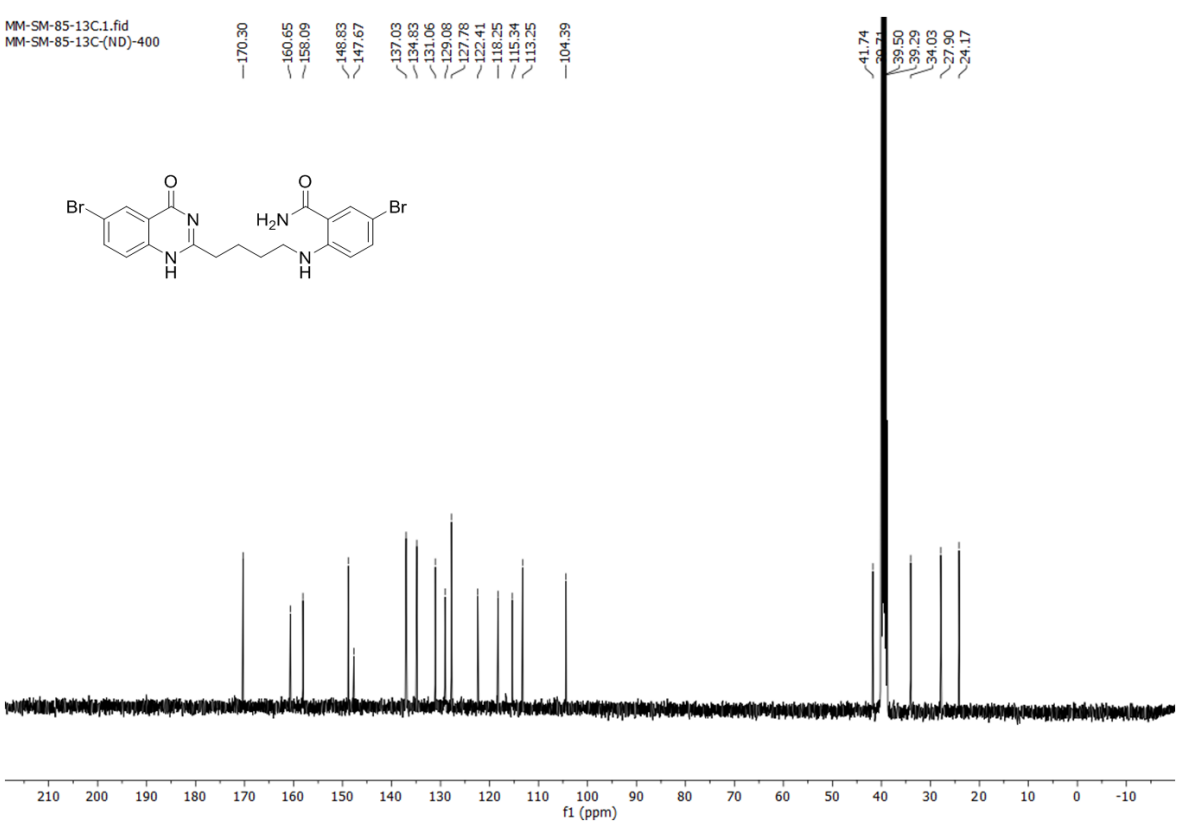

^{1}H-NMR of 7p-d2

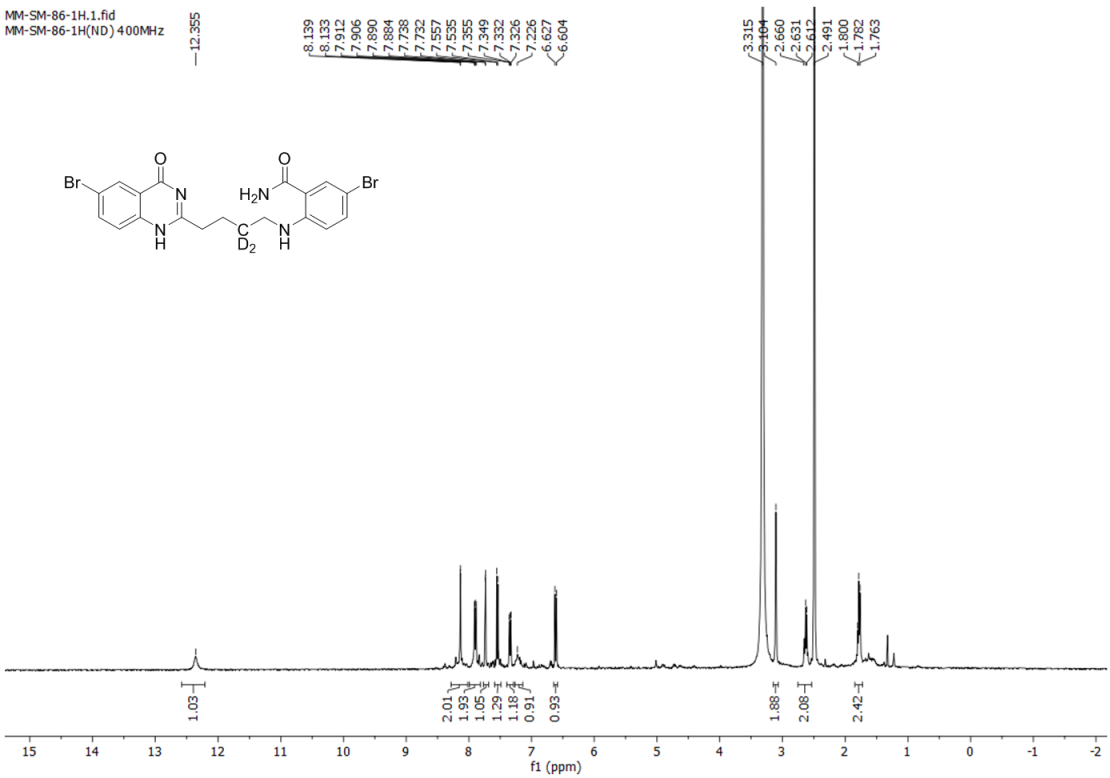

^{1}H-NMR of 6d

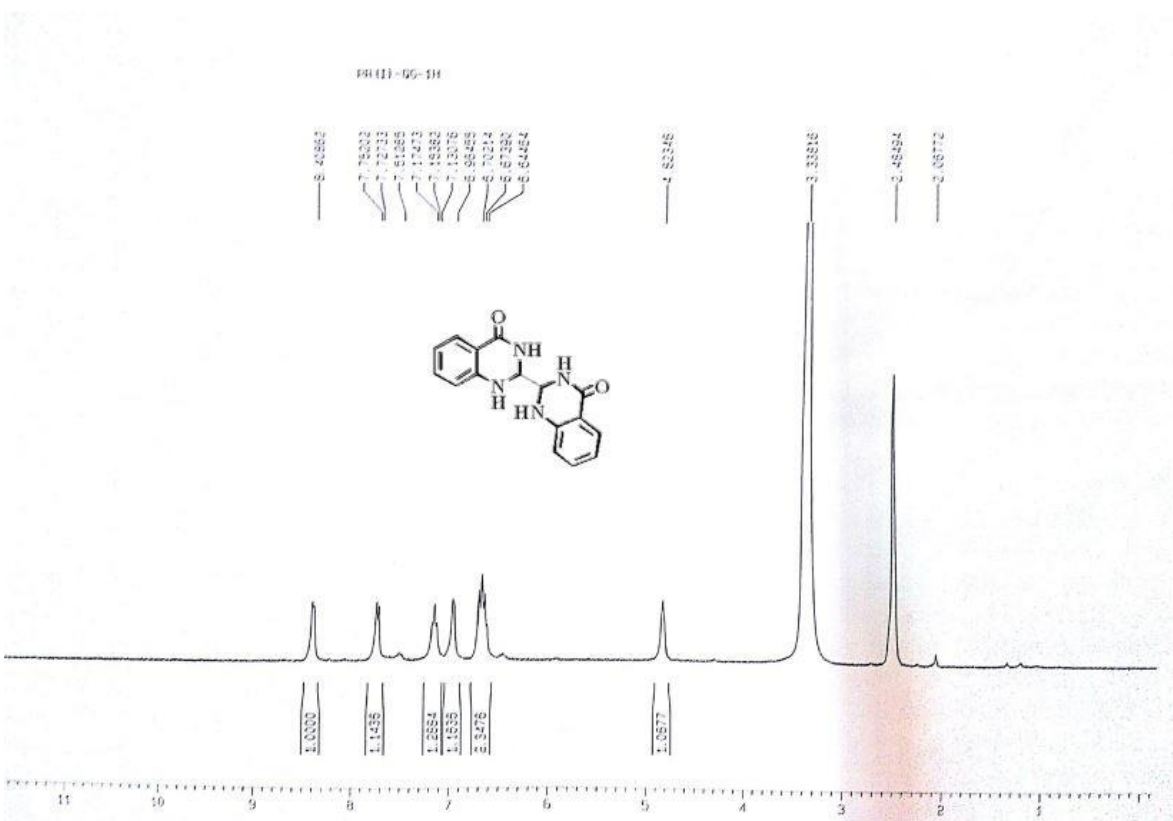

^{13}C-NMR of 6d

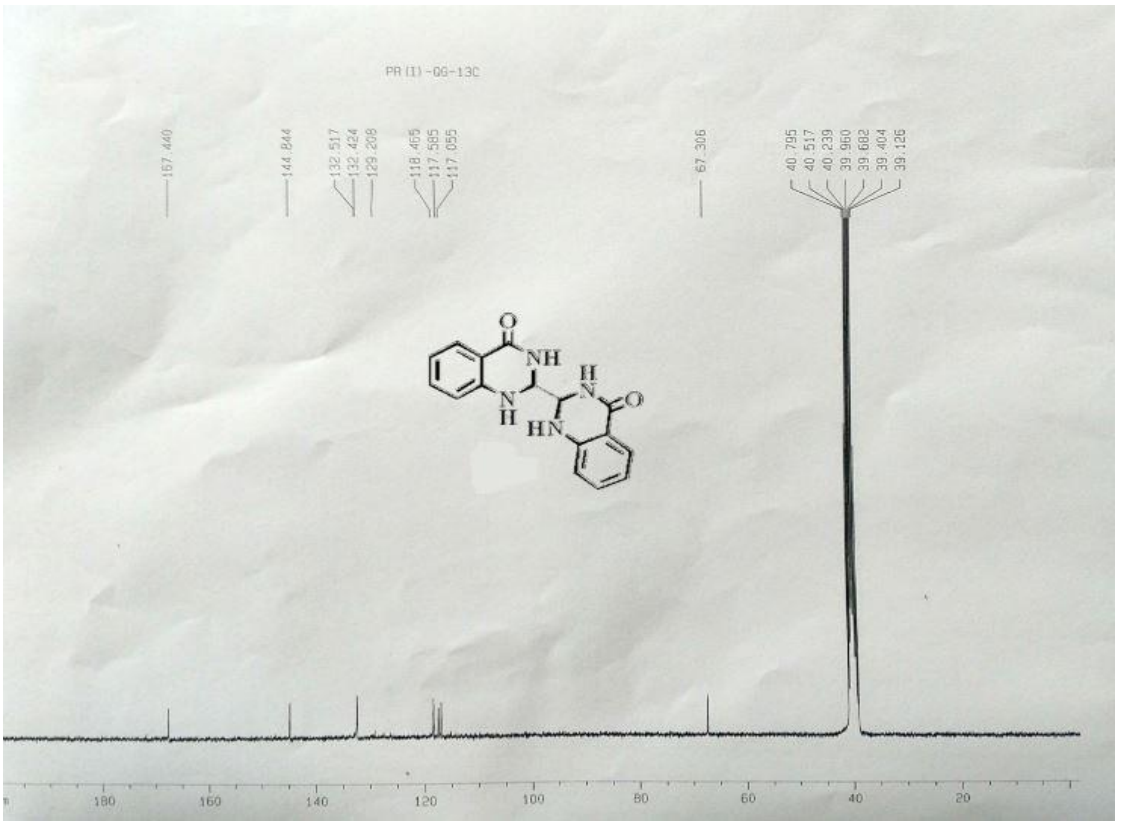

^{1}H-NMR of 7d

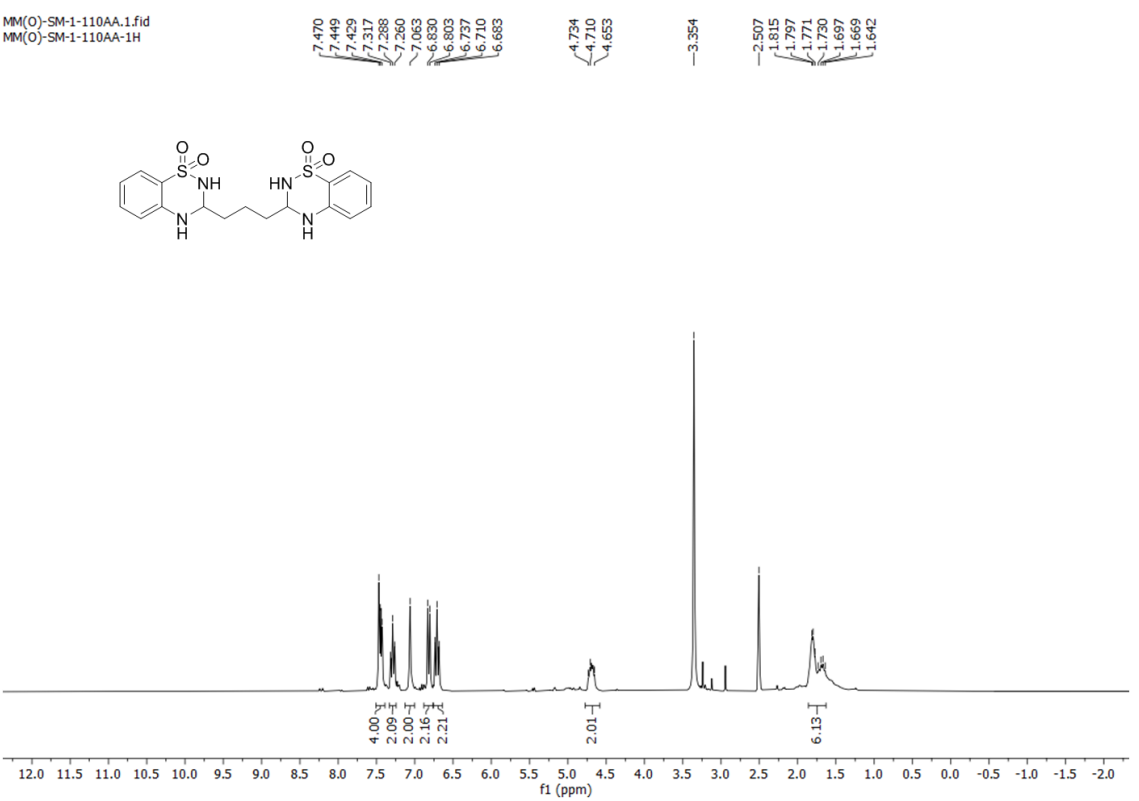

^{13}C-NMR of 7d

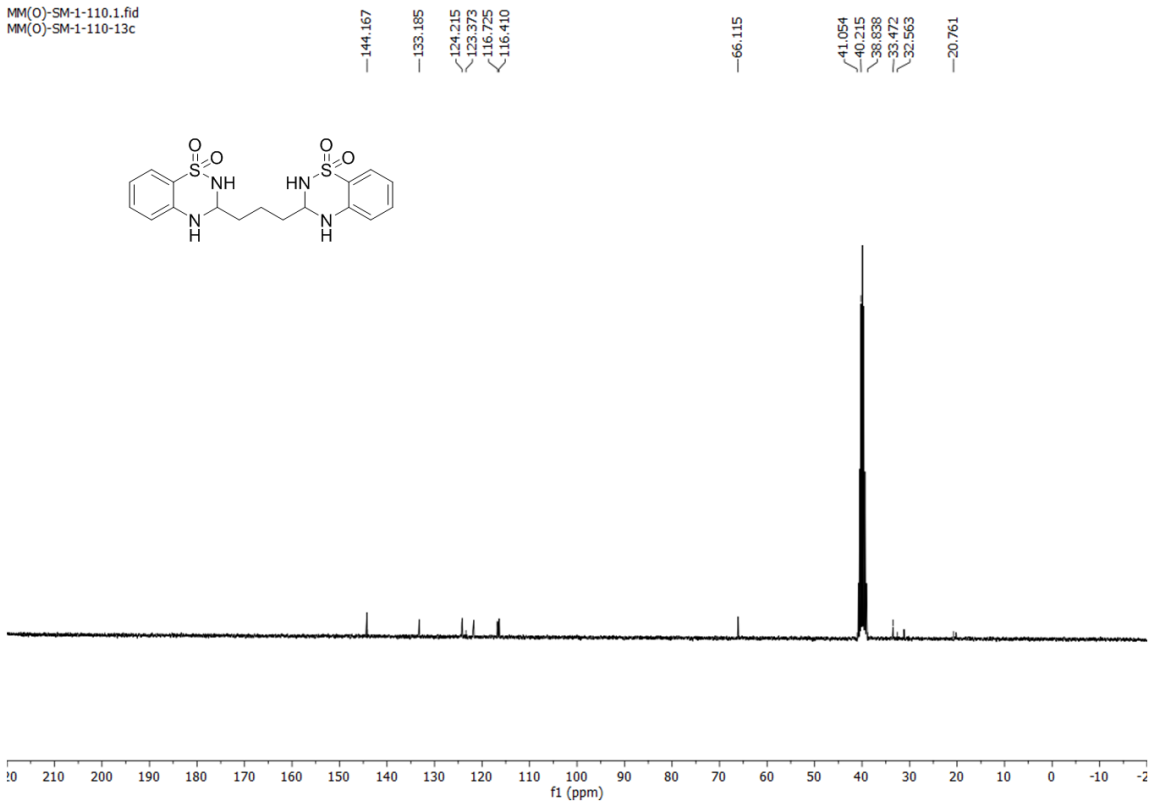

^{1}H-NMR of 13b

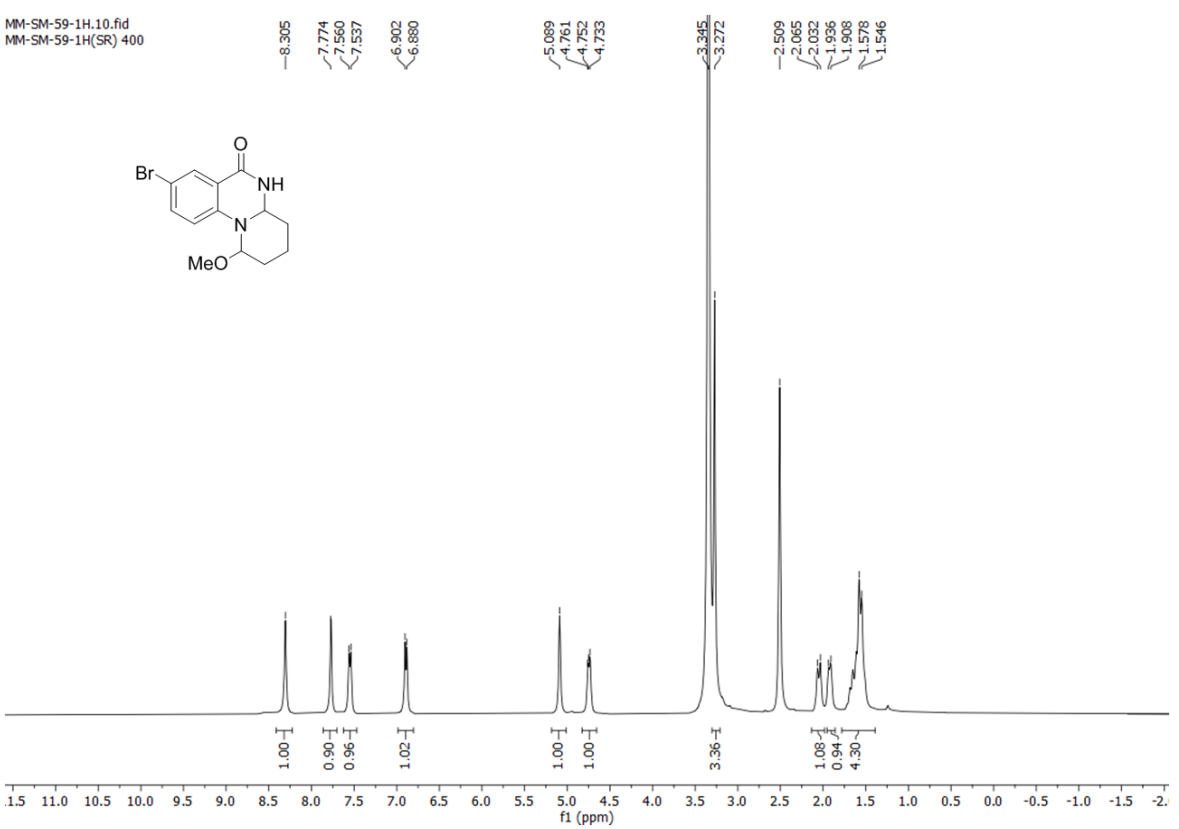

^{13}C-NMR of 13b

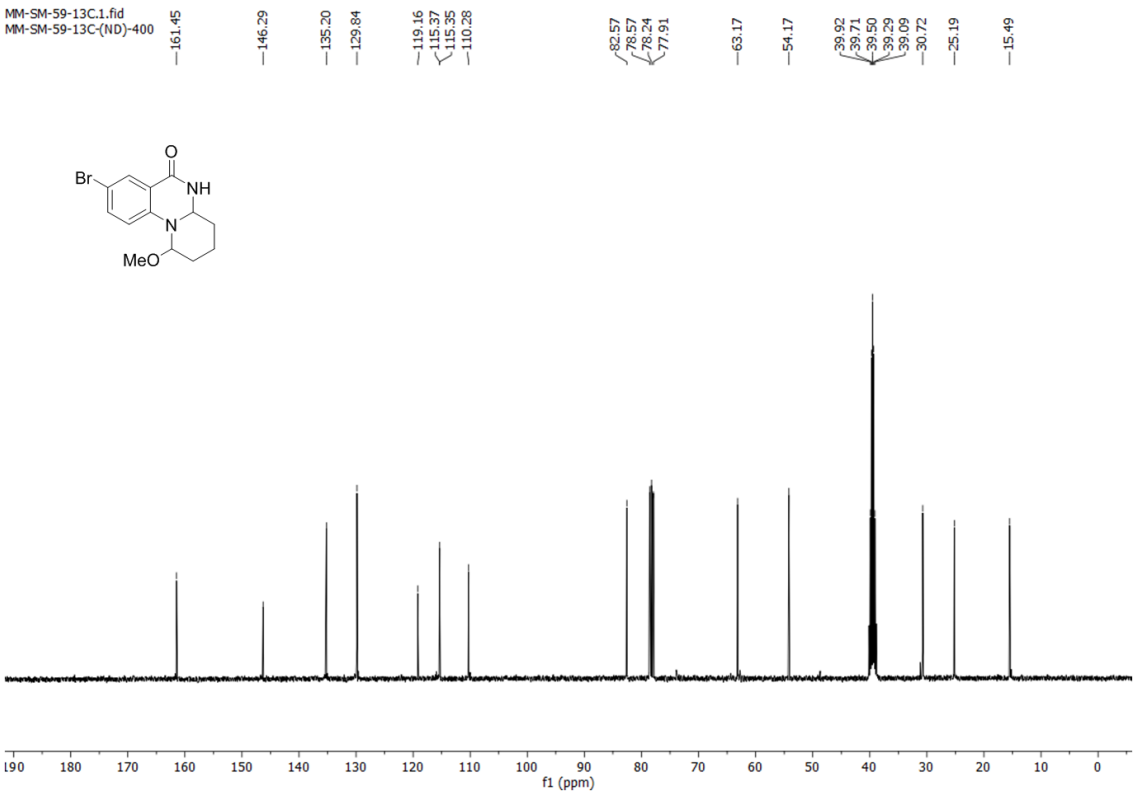

^{1}H-NMR of 14b

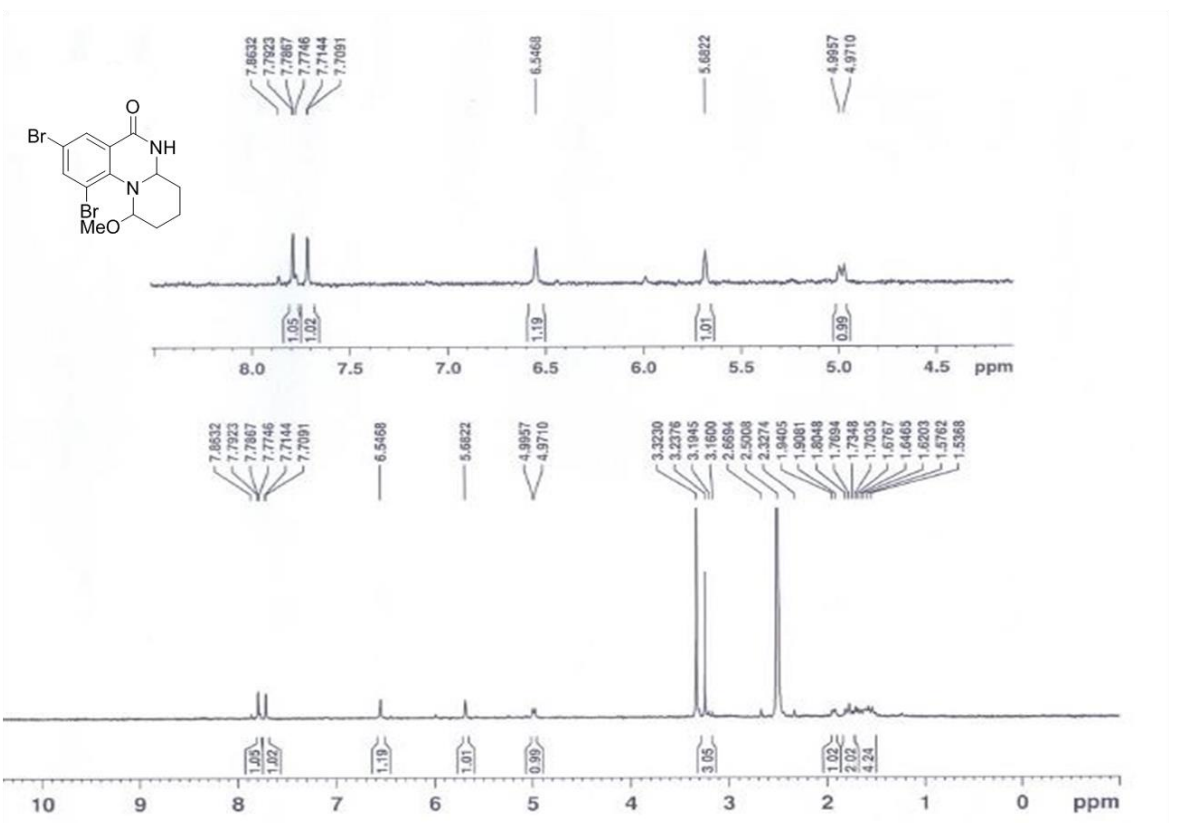

^{13}C-NMR of 14b

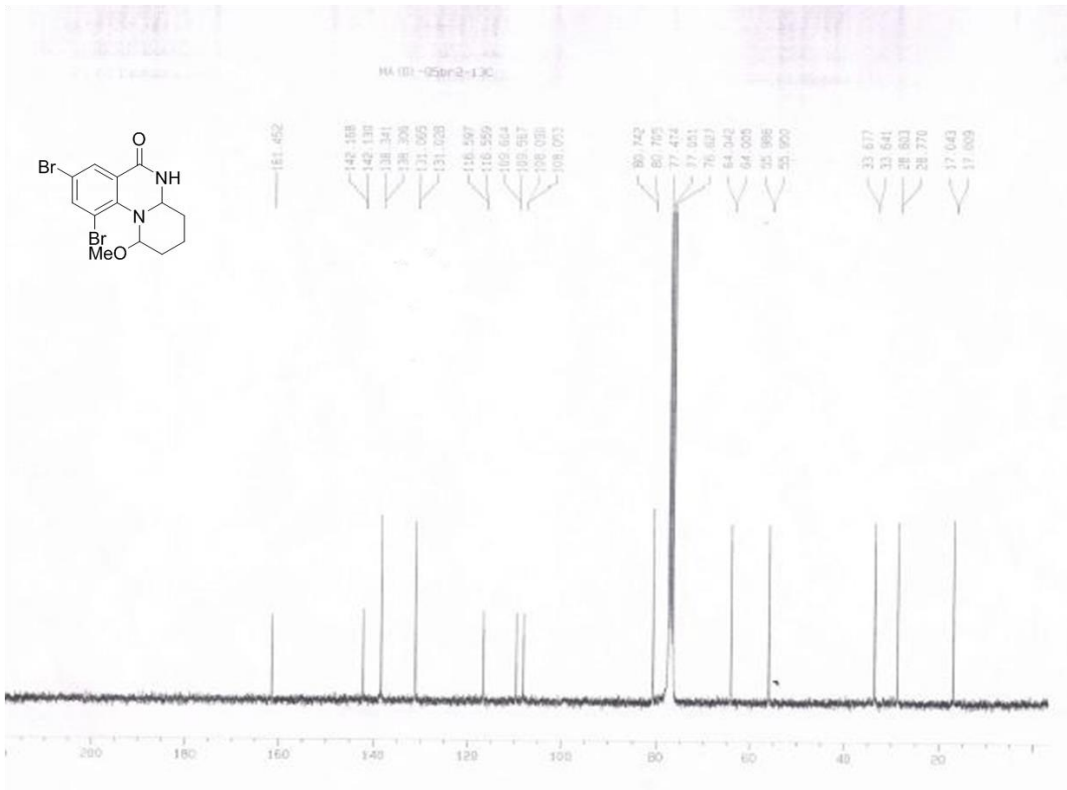

^{1}H-NMR of 15b

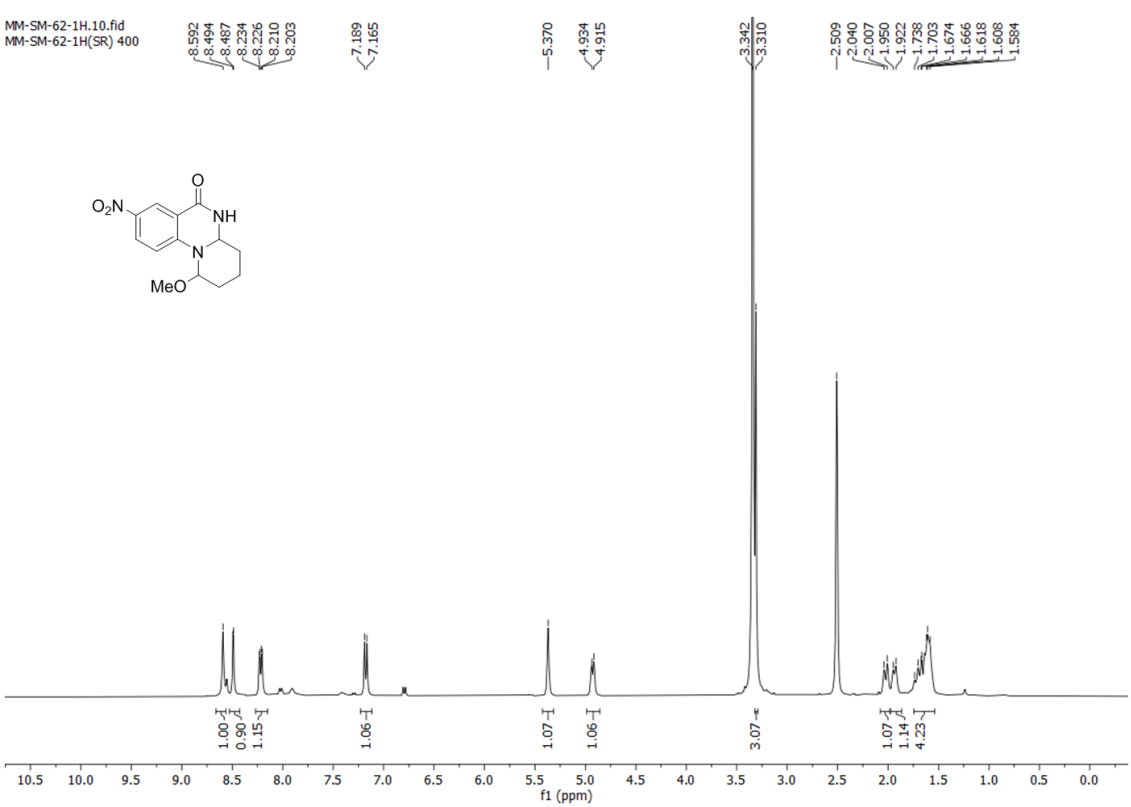

^{1}H-NMR of 15b

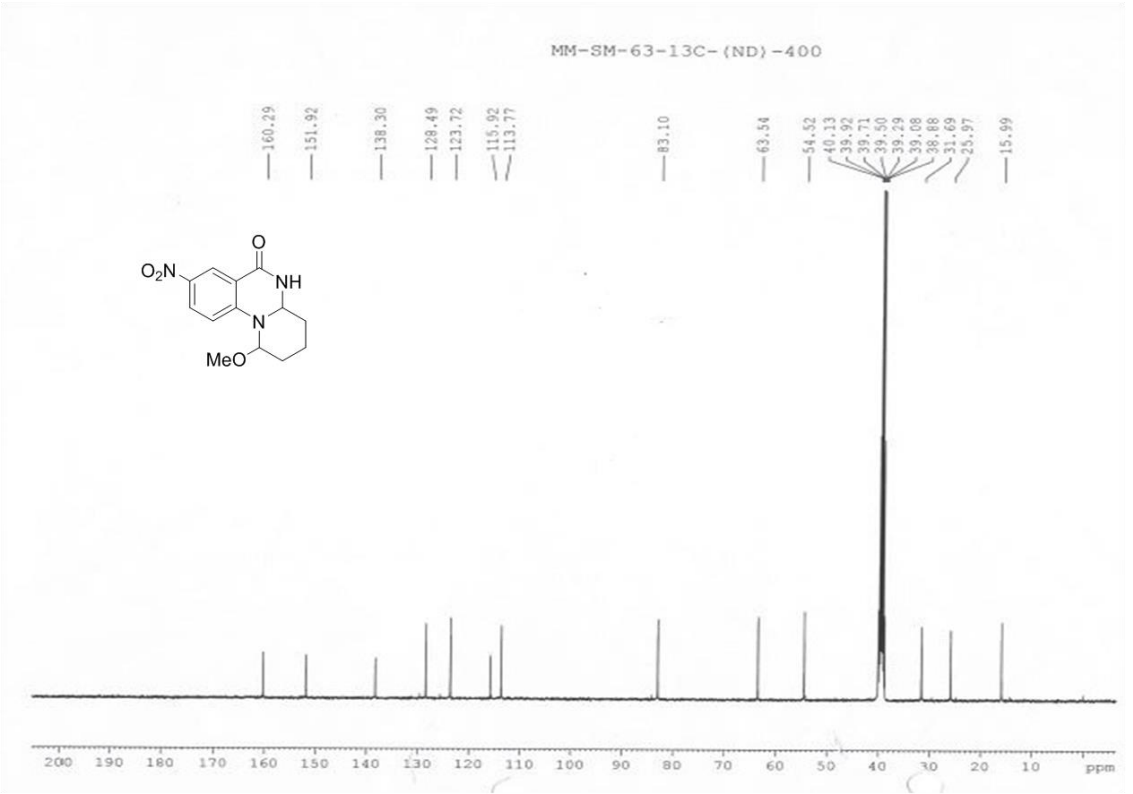

^{1}H-NMR of 16b

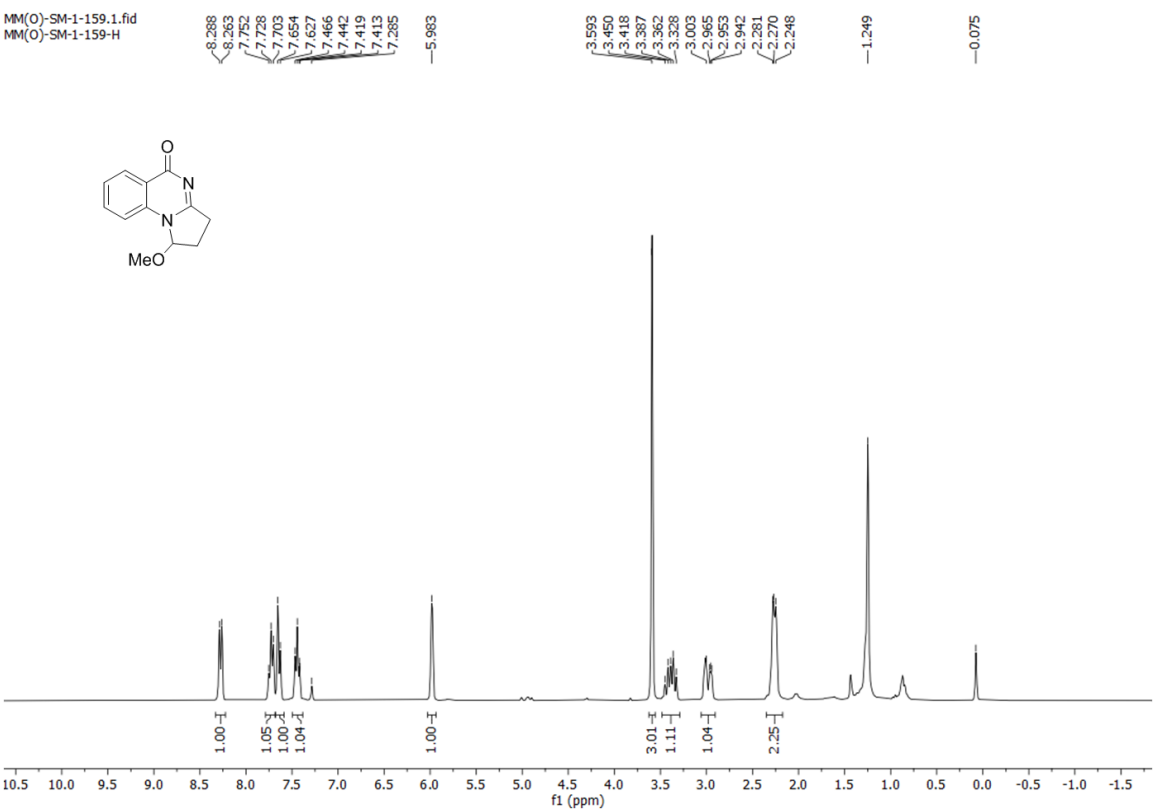

^{13}C-NMR of 16b

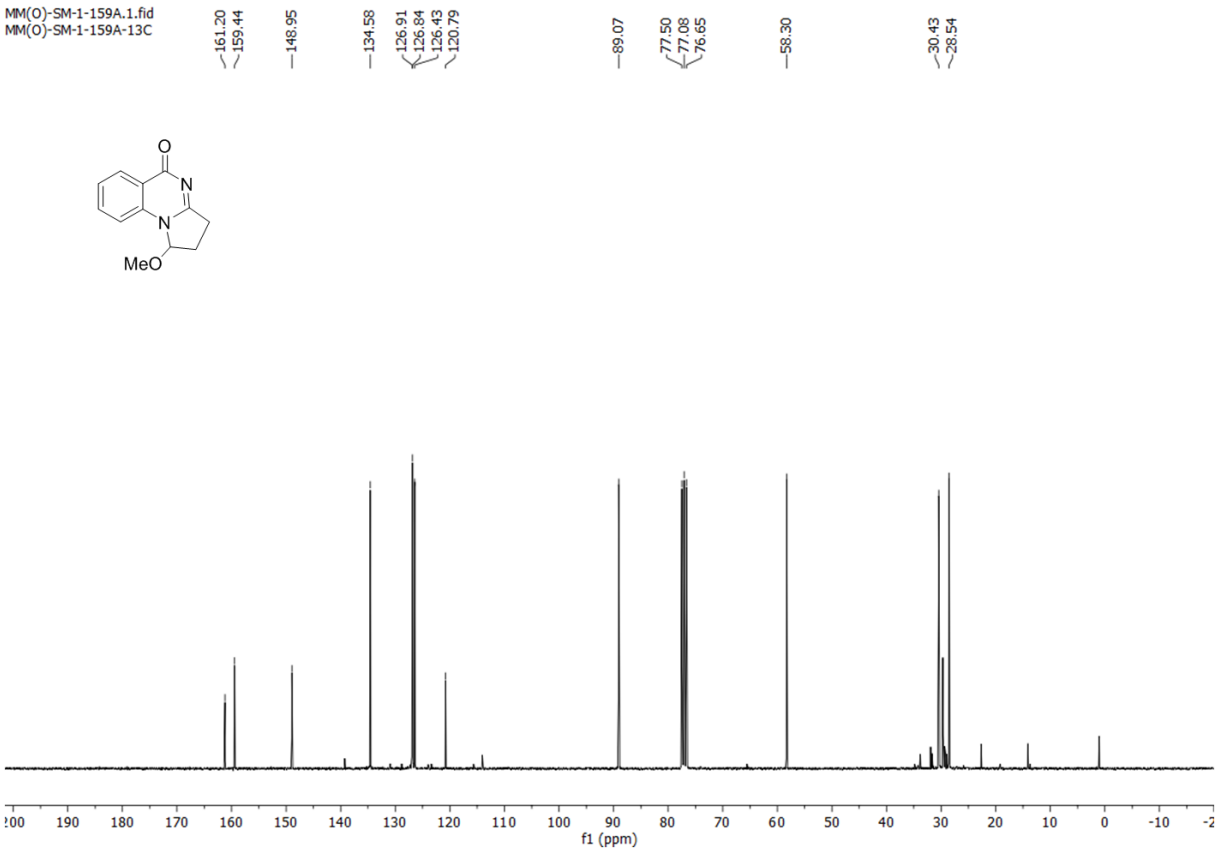

1.5 REFERENCES

[1] W. R. Pitt, D. M. Parry, B. G. Perry, C. R. Groom, *J. Med. Chem.* **2009**, *52*, 2952-2963.

[2] I. Ali, W. A. Wani, K. Saleem, A. Haque, *Curr. Drug Ther.* **2012**, *7*, 13-23.

[3] R. Sapra, D. Patel, D. Meshram, *J. Med. Chem. Sci.* **2020**, *3*, 71-78.

[4] J. Haribabu, V. Garisetti, R. E. Malekshah, S. Srividya, D. Gayathri, N. Bhuvanesh, R. V. Mangalaraja, C. Echeverria, R. Karvembu, *J. Mol. Struct.* **2022**, *1250*, 131782.

[5] a)N. B. Panchal, P. H. Patel, N. M. Chhipa, R. S. Parmar, **2020** b)L. Marín-Ocampo, L. A. Veloza, R. Abonia, J. C. Sepúlveda-Arias, *Eur. J. Med. Chem.* **2019**, *162*, 435-447.

[6] a)M. Campanati, A. Vaccari, O. Piccolo, *Catal. Today* **2000**, *60*, 289-295; b)R. H. Vekariya, K. D. Patel, N. P. Prajapati, H. D. Patel, *Synth. Commun.* **2018**, *48*, 1505-1533.

[7] a)K. Devi, M. Kachroo, *Der Pharma Chemica* **2014**, *6*, 353-359; b)F. Hassanzadeh, E. Jafari, G. H. Hakimelahi, M. R. Khajouei, M. Jalali, G. A. Khodarahmi, *Res. Pharm. Sci.* **2012**, *7*, 87-94; c)N. M. Raghavendra, T. Pp, G. Pm, *Electron J. Chem.* **2008**, *5*, 23-33; d)J. B. Jiang, D. P. Hesson, B. A. Dusak, D. L. Dexter, G. J. Kang, E. Hamel, *J. Med. Chem.* **1990**, *33*, 1721-1728.

[8] a)A. K. Nanda, S. Ganguli, R. Chakraborty, *Molecules* **2007**, *12*, 2413-2426; b)O. A. Fathalla, E. M. Kassem, N. M. Ibrahem, M. M. Kamel, *Acta Pol. Pharm.* **2008**, *65*, 11-20.

[9] P. Grieß, *Ber. Dtsch. Chem. Ges.* **1869**, *2*, 415-418.

[10] S. Von Niementowski, *J. Prakt. Chem.***1895**, 51, 564-572.

[11] a)I. Radfar, M. K. Miraki, L. Ghandi, N. Esfandiary, S. Abbasi, M. Karimi, A. Heydari, *Appl. Organomet. Chem.* **2018**, *32*, e4431; b)N. Y. Kim, C.-H. Cheon, *Tetrahedron Lett.* **2014**, *55*, 2340-2344.

[12] Z. Liu, L.-Y. Zeng, C. Li, F. Yang, F. Qiu, S. Liu, B. Xi,*Molecules***2018**, *23*, 2325.

[13] G. Yashwantrao, V. P. Jejurkar, R. Kshatriya, S. Saha, *ACS Sustain. Chem.& Eng.* **2019**, *7*, 13551-13558.

[14] F. Havasi, A. Ghorbani-Choghamarani, F. Nikpour, *Microporous Mesoporous Mater.* **2016**, *224*, 26-35.

[15] L. Wang, J. J. A. S. Xiao, *Catal*. **2014**, *356*, 1137-1171.

[16] B. Peng, N. Maulide, *Chem.Eur.J.***2013**, *19*, 13274-13287.

[17] J. Y. Zhang, X. Q. Zhu, *Molecules* **2022**, *27*.

[18] C. Zhu, T. Akiyama, *Synlett.* **2011**, *2011*, 1251-1254.

[19] P. Ghosh, A. Mandal, *Tetrahedron Lett.* **2012**, *53*, 6483–6488.

[20] D. Kumar, D. N. Kommi, R. Chebolu, S. K. Garg, R. Kumar, A. K. Chakraborti, *RSC Adv.***2013**, *3*, 91-98.

[21] W. Verboom, M. R. J. Hamzink, D. N. Reinhoudt, R. Visser, *Tetrahedron Lett.* **1984**, *25*, 4309-4312.

[22] a)J. E. Baldwin, J. Cutting, W. Dupont, L. Kruse, L. Silberman, R. C. Thomas, *J. Chem. Soc., Chem. Commun.* **1976**, 736-738; b)J. E. Baldwin, *J. Chem. Soc., Chem. Commun.* **1976**, 734-736.

[23] T. H. Youn, D. Y. Kim, *Synth. Commun.* **2017**, *47*, 2109-2114.

[24] R. Troschütz, O. Heinemann, *Arch. Pharm. Pharm. Med. Chem.***1995**, *328*, 759-764.

[25] a)X. Sun, Y. Hu, S.-z. Nie, Y.-y. Yan, X.-j. Zhang, M. Yan, **2013**, *355*, 2179-2184; b)M. Bakavoli, A. Davoodni, M. Rahimizadeh, M. M. Heravi, *Mendeleev Commun.* **2006**, *16*, 29-30.

[26] F. F. Abdel-Latif, K. M. El-Shaieb, A. G. El-Deen,*ZNB***2011**, *66*, 965-971.

[27] F. Abdel-Latif, K. El-Shaieb, A. El-Deen, *ZNB* **2012**, *66*, 965-971.

[28] L. Ukhin, L. Kuz'mina, T. Gribanova, L. Belousova, Z. Orlova, *Chem. Inform* **2009**, *40*.

[29] L. Wang, J. Xiao, *Top Curr. Chem. (Cham)* **2016**, *374*, 17.

[30] M. A. Mondal, S. Mondal, A. A. Khan,*J.Chem.Sci*. **2020**, *132*, 1-5.

[31] S. H. Bennett, G. Coulthard, V. K. Aggarwal, *Chem. Rec.***2020**, *20*, 936-947.

CHAPTER-2

Design, Synthesis, and Application of Dihydro-pyrimidinones (DHPs) based probes for DNA.

2.1 INTRODUCTION

Dihydropyrimidinones (DHPMs) are the most important *N*-heterocycles for their significant role in pharmacological and biological properties. It received significant attention for its wide range of pharmacological activities, such as calcium channel blockers, α-adrenergic antagonists, neuropeptide Y antagonists, mitotic kinesin Eg5 inhibitor, anti-hypertensive agents, anti-bacterial, anti-filarial, analgesic, anti-hyperglycemic, anti-cancer etc. One expected reason for their (DHPMs) biological activity is the presence of pyrimidine ring (thymine, cytosine, uracil etc.) as essential building blocks[1] of nucleotides (monomer of nucleic acids i.e; DNA & RNA). Besides, their antagonistic nature[2] from the natural pyrimidines, they are influential candidates for the synthesis of some effective drug. A number of drugs like molecule such as Monastrol, Idoxuridine, methyl thiouracil, 5-fluorouracil, emivirin, nitractin containing DHPMs are already been discovered and effectively used for the treatment of multiple diseases (**Figure-2.A**). Being a promising heterocyclic scaffold for drug development, the research area on the synthesis and biological evaluation of DHPMs has been extensively reviewed.[3]

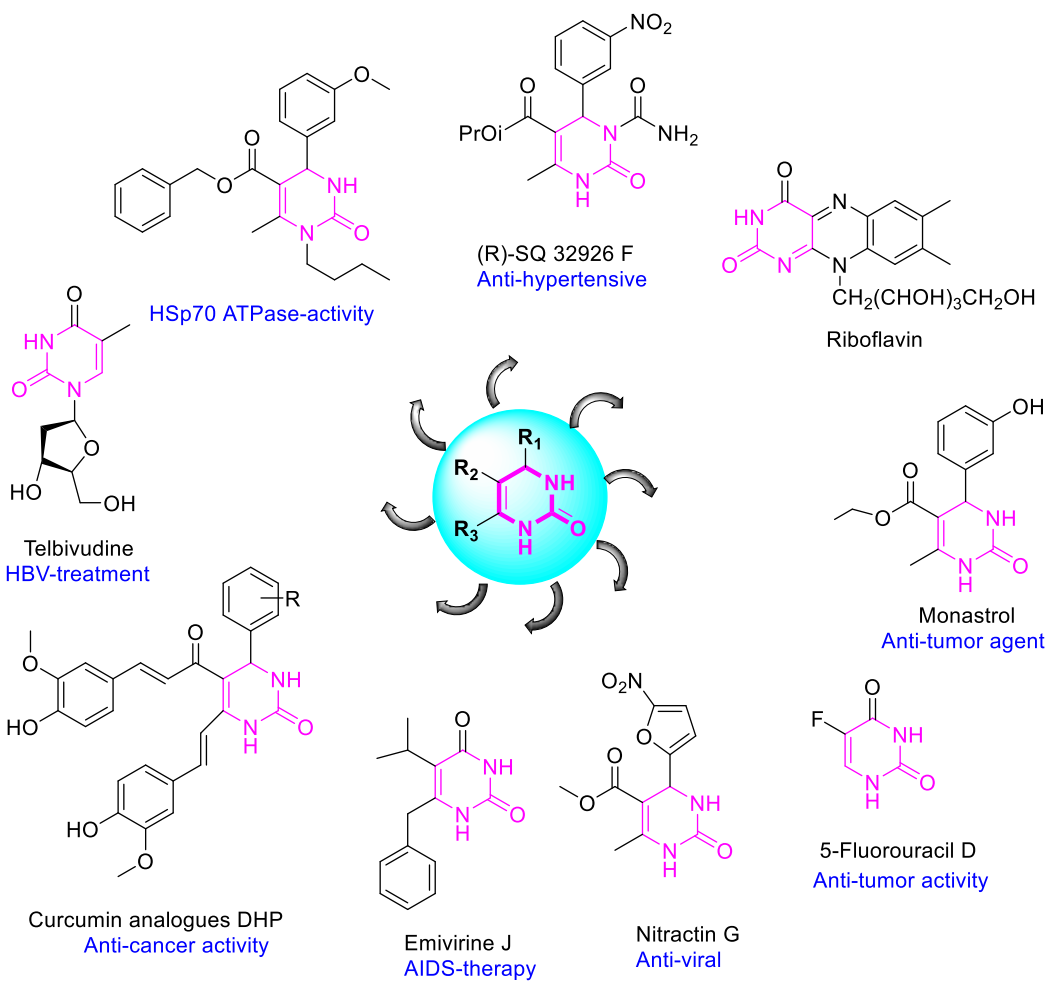

Figure-2.A Dihydropyrimidinone (DHPM) containing drugs

1893 was a landmark year for the discovery of DHPM heterocyclic moieties as the Biginelli adducts, named after the first report by the Italian chemist Pietro Biginelli[4]. At first he reported the acid-catalyzed cyclocondensation reaction of benzaldehyde, ethyl acetoacetate and urea using concentrated hydrochloric acid in ethanol at reflux temperature with the formation of **17a** (**Scheme-2.A**). Due to the interesting pharmacological properties of these heterocyclic moieties (DHPMs), they were synthesized using Multi-component reactions (MCRs). As the multi-component reactions are always promising in combinatorial chemistry for their convergent character, operational simplicity, and atom economy, the number of publications on the synthesis of novel DHPM analogs by the Biginelli reaction (MCR) is continuously growing.

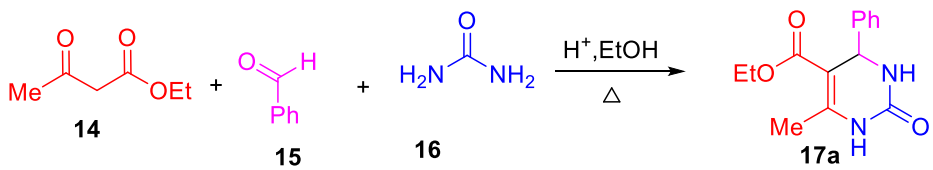

Scheme-2.A Original Biginelli Dihydropyrimidinone Synthesis (1893)

Based on this reaction, a lot of synthetic strategies have been outlined for the synthesis of different DHPMs by various research groups (**Scheme-2.B**). One pot synthesis of dihydropyrimidinones**17b** was published by Matthew et al.[5] using β-keto ester **14** and aldehyde **15** with urea **16**. Using 1-(piperidin-1-yl) butane-1,3- dione **14d**, benzaldehyde and excess thiourea in ethanol under mild acidic conditions Yadlapalli's group[6] provided the synthesis of novel DHPMs (**Scheme-2.B**) in good to excellent yield. A new class of 3,4-dihydropyrimidine-2(1H) one derivatives has been described by Shaabni et al.[7] as four-component reaction (MCR) with an aromatic/aliphatic amine **14c**, diketene **14b**, aromatic aldehyde and urea/thiourea using *p*-toluenesulfonic acid as catalyst in dichloromethane solvent at ambient temperature.

Functionalization of DHPMs is usually carried out either by modification of the conventional Biginelli components or post-synthesis modification of the Biginelli products[8].The first one has its limitations due to the difficulty of availability of the modified Biginelli reactants. Post-synthesis modification of the Biginelli product is the most popular method for complex DHPMs structures. For the post-synthesis modification by functionalization of DHPM, towards the drug design, firstly, it is essential to see the chemical reactivity nature of the core structure of it.

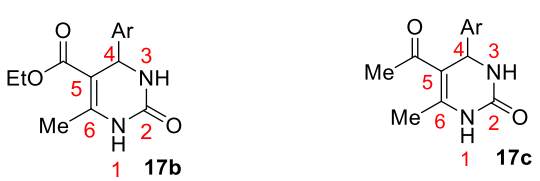

Figure-2.B Simplest Dihydropyrimidinone(DHPMs) core structure

From the literature survey, it has been found that usually the simplest DHPMs **17b** and **17c** have been synthesized by acid-catalyzed multi-component synthesis as they are stable under moderately strong acidic medium. The DHPM core (**Figure-2.B**) having some base sensitive groups such as free –*NH*, *C*5 ketomethyl, *C*6 methyl groups, base promoted reaction of **17b** and **17c** is not straight-forward[9]. Major reasons are presumably due to the degradation of this DHPM moiety through retro-Biginelli reaction, as suggested by Pietro Biginelli[4]. Timoshenko et al.[9] reported an elegant evidence of retro-Biginelli where the aldehyde residue in the Biginelli product 2-oxo-2-polyfluoroalkylethane-1-sulfone and-sulfamide exchanges with formaldehyde residue present in the hexamethylenetetramine via retro reaction (**Scheme-2.C**).

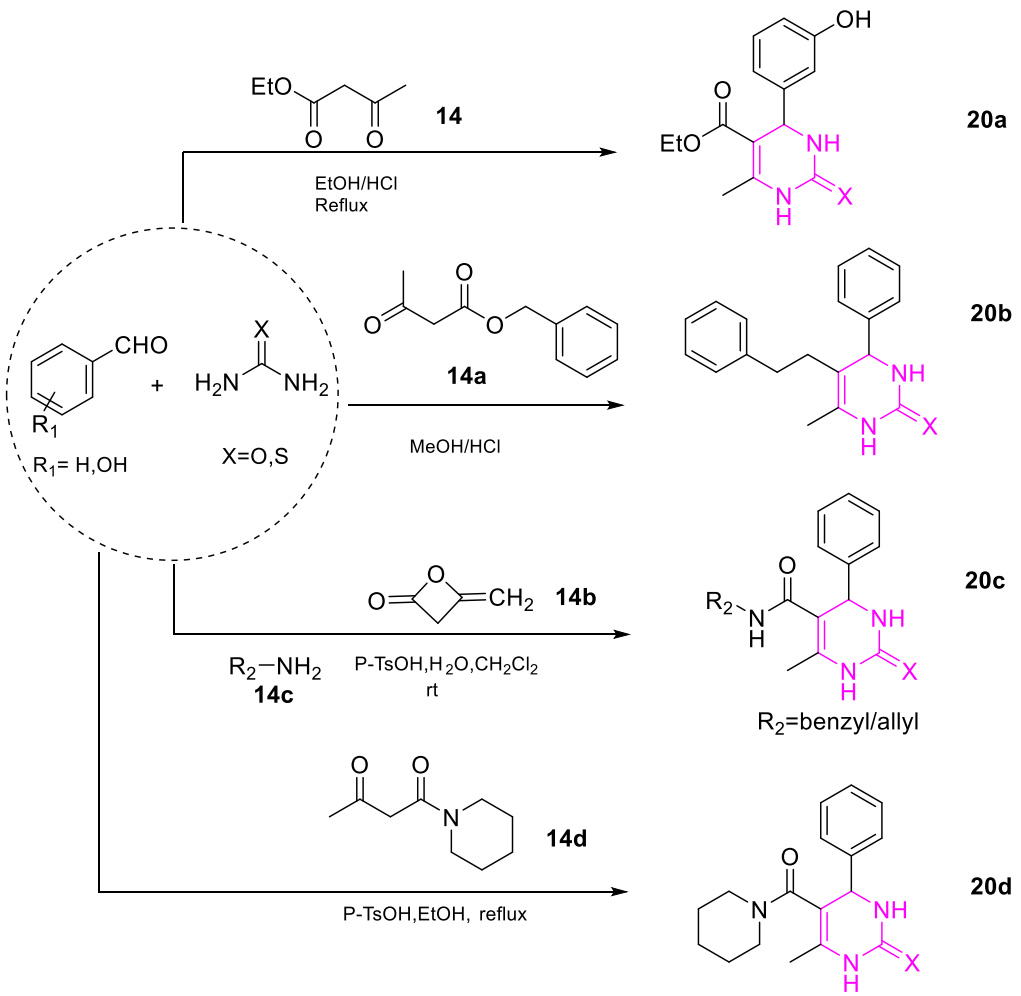

Scheme-2.B Various Multi-component approaches for synthesis of 3, 4-dihydropyrimidinones

Although the hydrolytic degradation of this moity is known as early in 1893, detailed mechanism and scope of the reaction are not available. Moreover, the behavior of DHPMs toward aq. base is not generalized and the exiting reports are conflicting[10]. Anatoly[11] reported the formationof compound **19** under the alkaline hydrolysis condition with Biginelli compound **17b**. The formation of compound **19** had been explained by two competitive reactions, namely hydrolytic decomposition to

aromatic aldehyde and decarboxylation.The decarboxylation product was then coupledwith the aldehyde generated in situ to form compound **19** (**Scheme-2.C**).

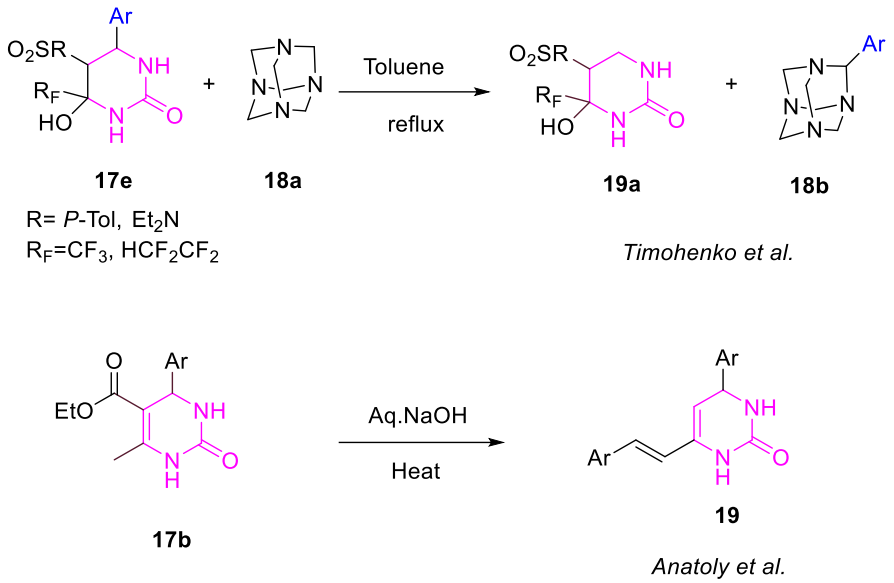

Scheme-2.C Evidence of retro-Biginelli and hydrolytic behaviour of DHPMs (Reported)

Herein, we reported the detailed mechanistic insights of ketomethyl containing DHPMs (Biginelli product, **17c**) in aq. alkaline condition with various scopes and found the inherent instability of this moiety as it degraded through retro-Biginelli reaction under this condition. Therefore, the stability has been increased by protecting the selective *N*3 atom protection as it was assumed that the free *NH* may be responsible for this type degradation. Finally, we established a convenient method for the synthesis of *C*5 and *C*6 alkylated DHPM as an important fluorescent probe through post-synthesis modification of the Biginelli product (**17c**) and found an important application on live cell imaging of a cancer cell by selective targeting the nuclear DNA of the particular cell.

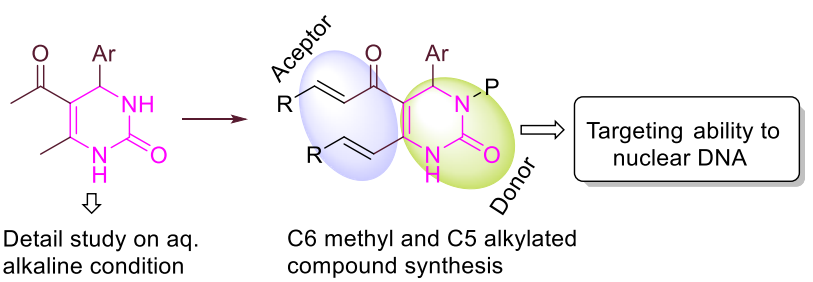

Scheme-2.D Our target synthesis

2.1.1 Nuclear DNA interaction towards drug development

The development of therapeutics by targeting genetic materials such as DNA is an important area of targeted drug development. Almost sixty years ago, few organic chemists developed the field of small molecule–DNA recognition and it was driven largely by biophysical chemists[12], who applied

some spectroscopic methods for specifying 'drug-DNA' interactions. It is evident that there is a clear role of the aberrant transcription factor signaling in the pathogenesis of various human diseases, which has stimulated the development of small molecule binders of DNA through which the DNA-transcription factor complex activity could be regulated[13]. Hence, the studies of small molecule-DNA binding to regulate transcriptions are considered as the method of developing more efficient anti-tumor agents [14]. Many existing drugs are known to exhibit therapeutic benefits by complexing cellular DNA. Noncovalent binding of a small molecule to the DNA leads to the reversible structural modification of DNA, as a result, the transcription factors are unable to locate the specific binding site. Small molecule fluorophores that bind to the DNA are used in flow cytometry[15] , measuring live cell DNA contents[16] , cell-cycle studies, quantification of DNA[17], and selective staining of nuclei, etc.[18] Therefore, designing new DNA-dyes[19] is a never-ending process to overcome difficulties in the existing methods.

Usually, the interaction of small molecules with DNA goes through either intercalation or groove-binding mode (**Figure-2.C**)although some compounds can bind to DNA via a combination of both binding modes and it has been comprehensively reviews[20].The intercalation of small molecules are the π–π stacking interactions available between the aromatic chromophore of the small molecule and the adjacent bases of ds-DNA, whereas groove biding mode of small molecules with DNA are the electrostatic potential, steric effects, hydrogen-bonding interactions and the degree of hydration. Usually the majority of small molecules prefer the minor groove binding mode[12] due to its narrower width affording better Van_der Waals contacts.

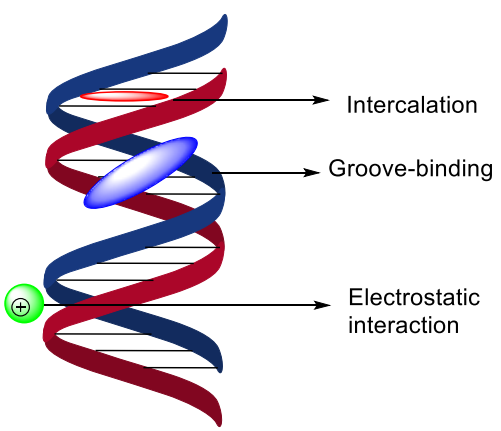

Figure-2.C Different interaction of small molecule (drug) with ds-DNA

However, many researchers explored their (DHPMs) structure activity relationship (SAR) as well as binding mode through molecular modeling studies as the appropriate substitutions are responsible for its effectiveness and toxicity so that the toxicity problems can be recognized and overcome. We have

যা দ ব পু র বি শ্ব বি দ্যা ল য়
ক ল কা তা - ৭০০ ০৩২, ভারত

JADAVPUR UNIVERSITY
KOLKATA-700 032, INDIA

FACULTY OF SCIENCE : DEPARTMENT OF CHEMISTRY : ORGANIC CHEMISTRY SECTION

CERTIFICATE FROM THE SUPERVISOR

This is to certify that the thesis entitled "**Design and synthesis of quinazolinones and related heterocyclic compounds**" Submitted by Smt. Sudipta Mondal who got her name registered on 07/10/2020 for the award of Ph. D. (Science) Degree of Jadavpur University, is absolutely based upon his own work under the supervision of Dr. Mohabul Alam Mondal and that neither this thesis nor any part of it has been submitted for either any degree / diploma or any other academic award anywhere before.

MA Mondal 21.12.2023

(Signature of the Supervisor
date with official seal)

DR MOHABUL ALAM MONDAL
Assistant Professor
Department of Chemistry
Jadavpur University
Kolkata-700032, India

দূরাভাষ : ৯১-০৩৩-২৪১৪-৬২২৩
দূরবার্তা : ৯১-০৩৩-২৪১৪-৬৪৮৪

Internet : http// www.jadavpur.edu

Phone : 91-033-2414-6223
Fax : 91-033-2414-6484

decided to synthesise a new intramolecular Donor-π-Acceptor fluorescent probe to create novel nuclear DNA targeting molecule through post-synthesis modification of the Biginelli product (**17c**) (**Scheme-2.D**).Docking studies are used to build a model of the binding pose with double-stranded (ds)-DNA. UV–Vis absorption, fluorescence, and circular dichroism (CD) spectroscopy were used to investigate the detailed DHPM binding interactions with double-stranded calf-thymus DNA (ct-DNA).

2.2 RESULT AND DISCUSSION

At the beginning of the work, we have explored the relative reactivity of the ketomethyl group and methyl group attached to the DHPM ring of **17d** toward benzaldehyde in alkaline conditions. Firstly, compound **17d** was treated with benzaldehyde in the presence of 30% aq. NaOH in EtOH (1:5) at room temperature for 48 hours. Results came out from this reaction is very complex as many interactive spots were observed on thin layer chromatography (TLC). The compound **19d** was isolated in 12% yield after repeated column chromatography of the reaction mixture. The concentration of base was tuned along with the solvent selection, to get a better result.

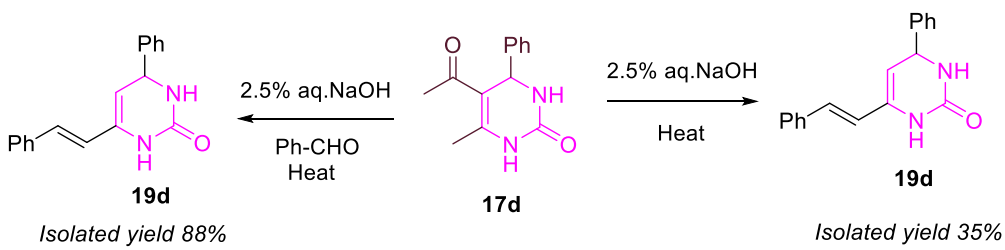

Scheme-2.E Isolated yield of compound 19d with/without added aldehyde

Notably, the treatment of 2.5% aq. NaOH on **17d** at 100°C for 2 hours, the compound **19d** was observed without adding any external aldehyde (**Table-2.A**, Entry 1). From the isolated yield (35%) of **19d**, there was an indication that at least two molecules of **17d** are involved in the formation of this product (**19d**). Using this method a similar result was observed from compound **17e**, forming compound **19e** in 32% isolated yield. We also synthesized compound **19f** in 41 % isolated yield from **17f**.The trans geometry of the newly formed double bond was supported by the ^{1}H-^{1}H spin coupling constant value (J = 16Hz) of the olefin protons. However, the substrate containing a nitro (**17g**) or hydroxyl (**17h**) group led to complete degradation of starting materials under this condition.

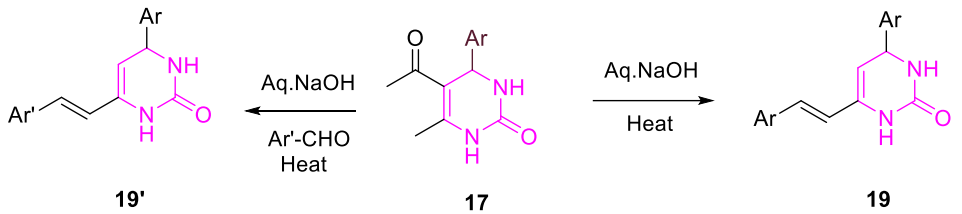

Entry	17: Ar	Aldehyde	19: Ar&Ar'	Yield(%)[f]
1	**17d**: Ph	-	**19d**: Ph & Ph	35
2	**17e**: *p*-Me-C_6H_4-	-	**19e**: *p*-Me-C_6H_4 & *p*-Me-C_6H_4-	32
3	**17f**: o-Br-C_6H_4-	-	**19f**: *o*-Br-C_6H_4-& *o*-Br-C_6H_4-	41
4	**17d**: Ph	PhCHO	**19d**: Ph & Ph	88
5	**17d**: Ph	m-MeO-C_6H_4CHO	**19g**: Ph & m-MeO-C_6H_4-	87
6	**17d**: Ph	*p*-Me-C_6H_4CHO	**19h**: Ph & p-Me-C_6H_4-	85
7	**17d**: Ph	*[g]	**19d**: Ph & Ph	20-30
8	**17g**: *p*-NO_2-C_6H_4-	-	Complete decomposition	-
9	**17h**: 2-OH, 3-OMe-C_6H_3-	-	Complete decmposition	-

[f]Isolated yield.
[g]2-nitrobenzaldehyde, 2-bromobenzaldehyde, 4-hydroxybenzaldehyde, 4-hydroxybenzaldehyde, *o*-phthalaldehyde, gluteraldehyde, glyoxal,*o*-vanillin were separately treated with **17d**. The Observed product is **19d** in all cases.

Table-2.A Formation of compound **19** with/without added external aldehyde

To understand the mechanistic insights of this reaction, compound **17d** was treated with externally added aldehydes. The Compound **19d** was isolated with improved yield when substrate **17d** was treated with added benzaldehyde (**Scheme-2.E**). Compound **19g** and **19h** are obtained from **17d** on the condensation of 3-methoxy benzaldehyde and 4-methyl benzaldehyde, respectively. Remarkably, it was observed that the formation of compound **19d** in each case when 2-nitrobenzaldehyde, 4-hydroxybenzaldehyde, 2-bromobenzaldehyde, *o*-vanillin, glyoxal, *O*-phthalaldehyde, glutaraldehyde is separately treated with **17d** instead of formation crossover products. These results are indicated that there involved at least two distinct and competitive reaction pathways by which **17d** was reacting in the presence of aqueous alkali. By doing a crossover experiment with the equimolar mixture of **17d** and **17e** with the optimal reaction condition, the intermolecular nature of the condensation has been established. From the crossover experiment the HPLC separation followed by HRMS led to the identification of two crossover products **19j**&**19h** (eluted at 4.14 minutes) along with two self-coupling products **19d** (3.62 minutes.) and **19e** (4.95 minutes) as shown in the HPLC chromatogram(**Scheme-2.F**).

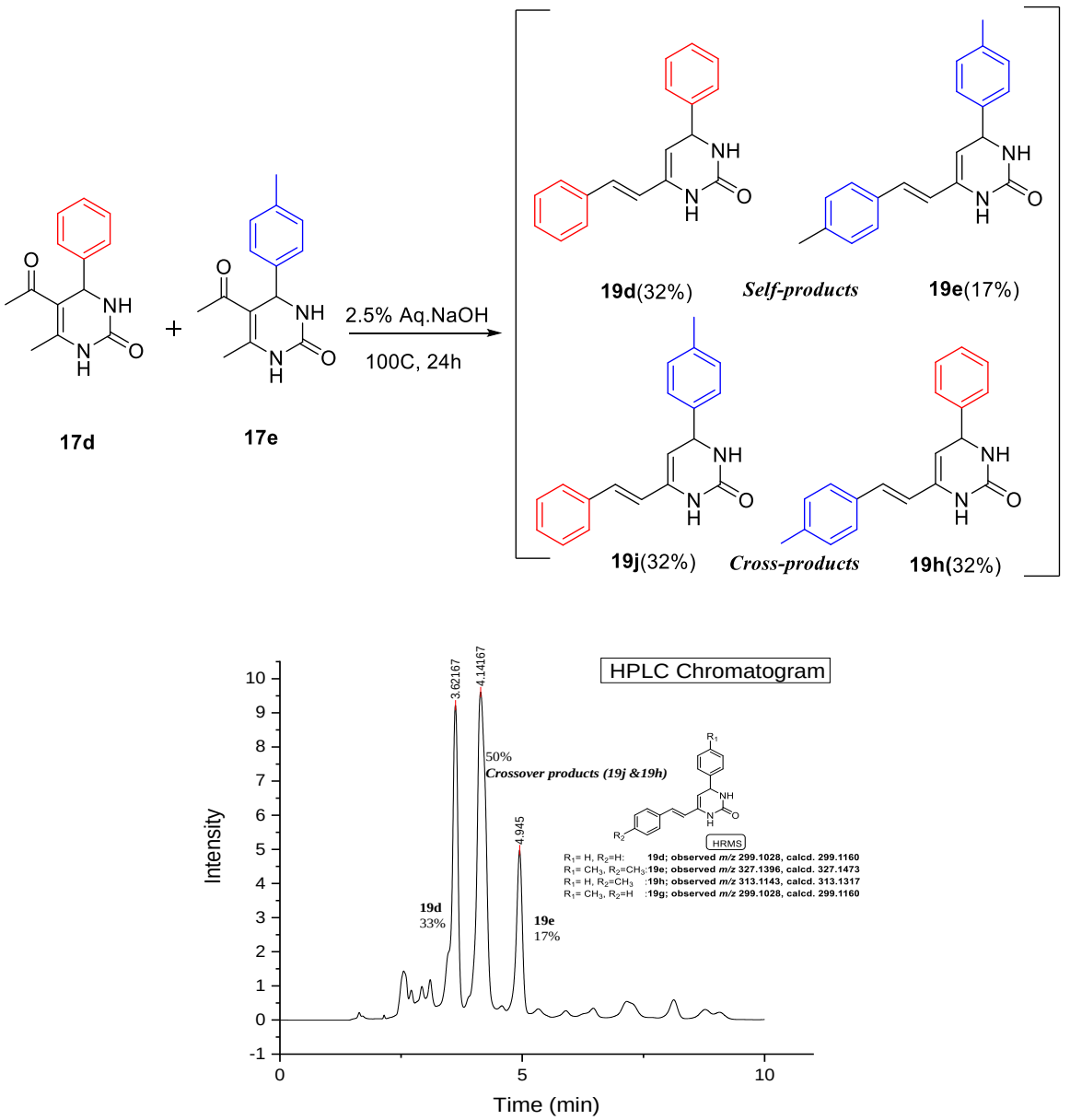

Scheme-2.F Crossover experiment with compound **17d** &**17e** and HPLC chromatogram

Liquid chromatography mass spectra (LCMS) data analysis of an incomplete reaction mixture, starting with **17d** in the above mentioned condition indicates that intermediate products are deacetylation product **21** and hydrates (**22**&**23**) (**Scheme-2.G)** of starting **17d** in the LCMS (**Figure 2.D**). Based on the evidences obtained from the crossover experiment and LCMS data of the incomplete reaction mixture, a plausible mechanism is shown in **Scheme-2.G**. The compound **17d** reacted in two distinct pathways, namely, deacetylation (Path-A)[21] and retro-Biginelli (Path-B).[22] The end product of Path-A is the deacetylation compound **21** which hydrates to product **22**, whereas the Path-B ends up with the formation of aldehyde. The final product formed by the aldol

condensation of **21** with aldehyde formed in situ. The relative rate of Path-A is assumed to be slightly higher than that of Path-B, as indicated by the yield (35%) of **19d** from **17d** and detection of the intermediate **21**. In the presence of externally added aldehyde (Entries 4, 5 & 6; **Table-2.A**), the reaction proceeds exclusively through the deacetylation path. Under this situation, the intermediate **21** is being trapped by added aldehyde and thereby shifting the equilibrium of the *C-C* bond cleavage step from intermediate **23** to **24** (Path-B) toward left. The presence of relatively less reactive aldehydes in this reaction both Path-A and B are operative (Entry 8; **Table-2.A**).It was assumed that the aldehydes mentioned in Entry 8 (**Table-2.A**) are undergoing Cannizaro[23]reaction instead of coupling with the intermediate **21**.

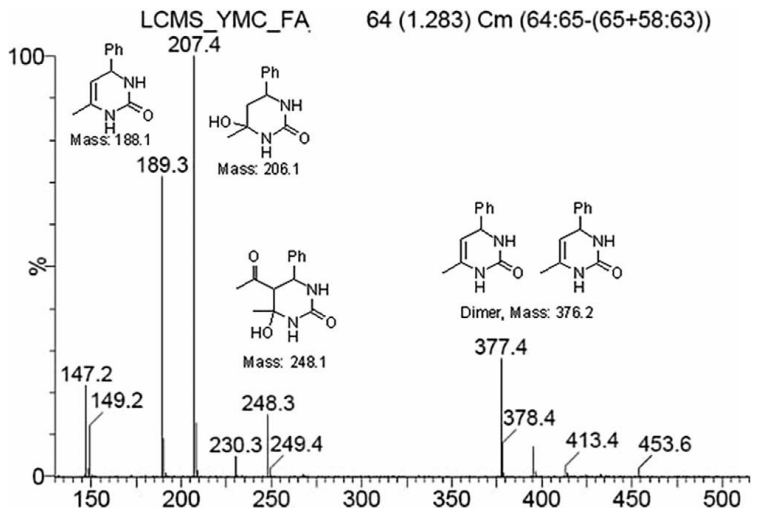

Figure-2.D LCMS of the major fraction of incomplete reaction mixture

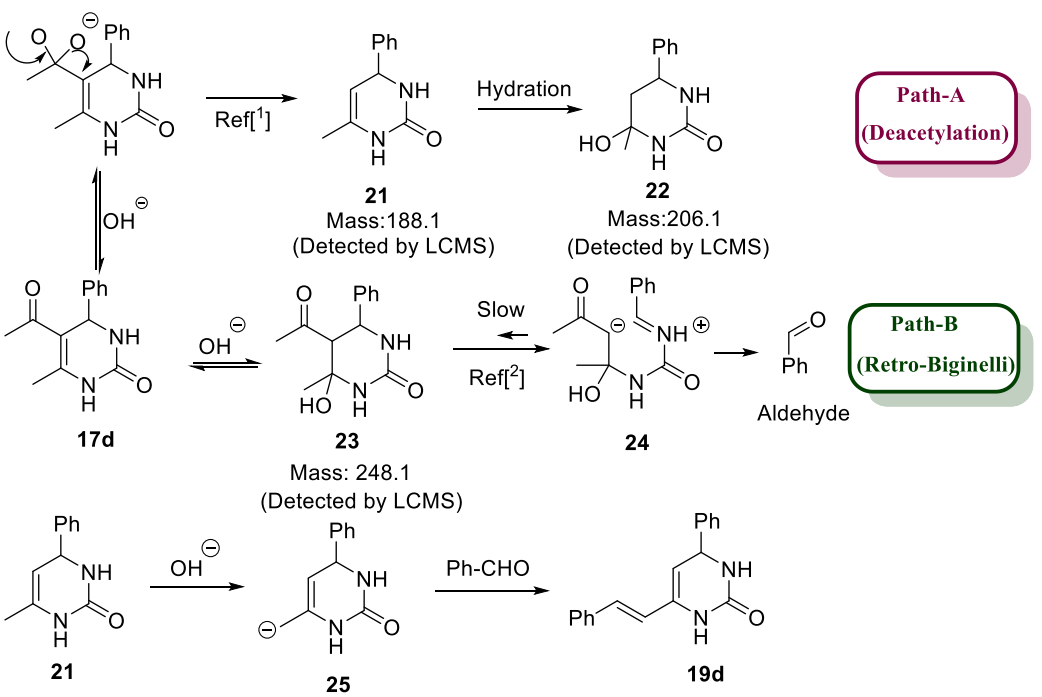

Scheme-2.G Plausible mechanism

Therefore, it has been proposed that under aq. alkaline condition 5-acetyl-6-methyl- 4-phenyl-3, 4-dihydropyrimidin-2(1H)-one (**17d**) undergoes two distinct reaction pathway namely; retro-Biginelli and deacetylation. Both the reaction pathways are in competitive mode. In the presence of externally added reactive aldehyde, only the deacetylation path was observed without degradation of DHPM moiety through the retro-Biginelli path, whereas in the presence of relatively less reactive aldehyde the substrate undergoes both the pathways in a competitive manner. Hence, we developed *C*6-alkylated DHPMs can be synthesized by this method.

From this above result, it is revealed that the basic hydrolytic degradation of DHPM moity could be avoided by permanently blocking the *N*1 and *N*3. There are many reports available for selective *N*3 alkylation of the DHPMs under basic conditions. Alkylation under basic conditions appears more challenging when -R is a base-sensitive group such as ketomethyl (**17d**)(**Scheme-2.H**). Direct alkylation at the *N*3 needs strong basic reaction conditions that suffers from several practical demeritssuch as polyalkylation, poor regio-selectivity (between *N*3 and *N*1)[24] and low yield because of the hydrolytic degradation[11] of the DHPM moiety. The complex reactivity pattern under basic condition of substrate **17d** is predominantly due to the hydrolysis of the DHPM moiety. Michael addition with reactive Michel acceptors such as acrylonitrile at the *N*3 position of DHPM is another pathway to add an alkyl group at *N*3 selectively, as it requires a relatively weak base. A limited number of methods available in the literature that used K_2CO_3 /PEG[25], and KF/Al_2O_3-DMF [26] as a base for the Michael addition of **17k**.

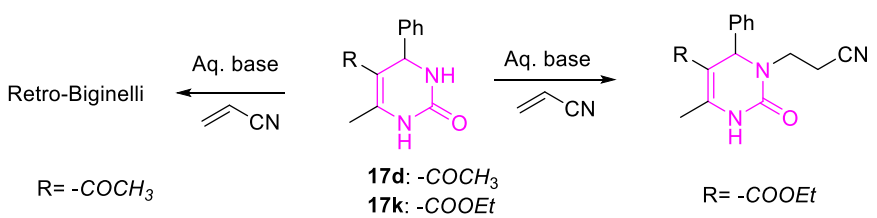

Scheme-2.H Different hydrolysis behavior of the DHPMs

However, a complex reaction mixture for substrate **17d** was observed when we attempted Michael addition with K_2CO_3 as a base in an alcoholic solution (**Table-2.B**). After several attempts, as shown in **Table-2.B**, we observed that a hindered non-aq. base such as DBU in DMF gives the best result on the Michel addition with acrylonitrile and the cyanoethyl group added exclusively at the *N*3 position in the presence of excess acrylonitrile (10 Eqv.). Slight excess acrylonitrile and two equivalent DBU is the optimum condition to observe exclusive *N*3 alkylation. The TLC analysis showed that the conversion was almost quantitative, and the slightly low isolated yield of **26a** (92%; **Table-2.B**; Entry 4) was due to the loss of the product during aq. workup to remove DMF and the reagents/byproducts from the mixture.

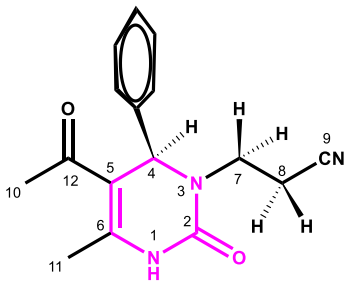

Structure of **26a**

13C Assignment

194.36: *C*12
153.15: *C*2
145.21: C6
140.88: $C_{Ar,q}$
129.05: $C_{Ar,d}$
128.58: $C_{Ar,q}$
127.07: $C_{Ar,d}$
117.62: C9
112.39: C5
61.64: C4
42.14: C7
19.52: C11
16.48: C8

Observed HMBC correlations

1) C_4 & H_{7a}, H_{7b}, H_{8a}, H_{8b}
2) C_2 & H_{11}, H_{7a}, H_{7b}

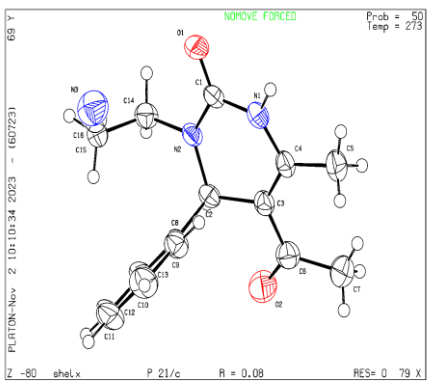

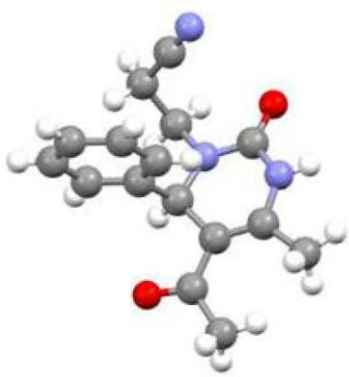

Figure-2.E Labeled NMR peak assignment and the single crystal XRD structure of **26a**

(For detail crystal parameters see the experimental section of this chapter)

The position of attachment of the alkyl group in **26a** was confirmed unambiguously by NMR (^{1}H, ^{13}C, COSY, HSQC) study. The presence of the cyanoethyl group in the structure of **26a** has been confirmed by a weak and sharp peak at 2247 cm^{-1} in IR spectra. Because of the chirality at *C*4, the *H*7a and *H*7b become diastereomeric in nature and exhibit different chemical shifts in ^{1}H-NMR (chemically different). Based on the ^{1}H, ^{13}C, ^{1}H-^{1}H-COSY, HSQC, and HMBC-NMR, all the labeled peaks observed in NMR are assigned at structure **26a** (**Figure-2.E**). All the compounds (**26a-d**) having crystalline nature, compound **26a** was subjected to the X-ray diffraction study, and the crystal structure obtained is shown in **Figure-2.E**. The crystallographic data has been submitted to the Cambridge Crystallographic Data Center (**CCDC:** 2219665). From the crystal structure it is notable that *N*1, *C*2, *N*3, *C*5, and *C*6 are occupied in a plane, and the phenyl ring is perpendicular to the plane of the heterocyclic ring. The significant difference in chemical shift of *H*7a, *H*7b and *H*8a, *H*8b is due to their different location of the anisotropy created by the phenyl ring along with the chirality effect of *C*4. To check the generality and regioselectivity of this reaction, weprepared the other three substrates (**26b-26d**) using the same protocol and found them to be equally efficient as observed for **26a** (**Scheme-2.I**).

Table-2.B Optimization of the reaction condition

Entry	Base	Solvent	Temperature(^{0}C)	Yield
1	20% NaOH	Water	100	Complex reaction
2	K_2CO_3	Ethanol	70	Complex reaction
3	TEA	$CHCl_3$	60	Starting Intact
4	DBU	DMF	60	92%

Hence, the developed method could be used as a general method for regioselective cyanoethylation at the *N*3 of Beginelli product **17d**. Alkylation at the *N*3 is especially important, as most of the biologically important DHPMs are *N*3 substituted or derived from it [3b, 27]. It has been observed that the attachment of cyanoethyl group at the *N*3 significantly reduces the base susceptibility of the DHPM moiety. This crucial observation led us to further functionalize at *C*10 and *C*11 groups to make highly functionalized dihydropyrimidinoneas shown in **Scheme-2.J**. Considering the nucleophilic nature of *C*10 and *C*11, the compound **26a** was treated with two equivalent benzaldehyde in the presence of non- nucleophilic base DBU in DMF and observed the formation of **27a** along with the deacylation product **28a**. The result indicated that *N*3 alkylation enhanced the stability of the DHPMs under the basic condition as direct treatment of **17d** resulted in structural degradation instead of forming an analogous product of **27a** in the presence of DBU. The cynoethylation and subsequent aldol-type condensation could also be carried out in one pot without isolation of intermediate **26a**.

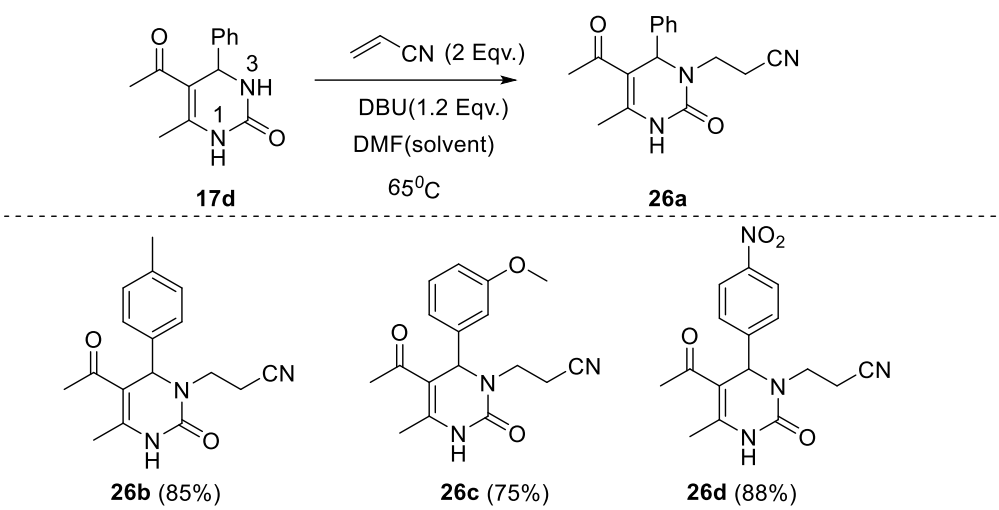

Scheme-2.I Synthesis of *N*3-cyanoethylated compounds **26a-d**

A plausible mechanism has been proposed based on the dual nature (nucleophile and Brönsted base) of DBU[28]. Products **27a** and **28a** are formed by a multistep reaction. Initially, the compound **26a** undergoes DBU-mediated aldol condensation at the *C*6 methyl group of **26a** to form the intermediate

product **30**, which undergoes either DBU mediated deacetylation to form the compound **28a** or aldol condensation with benzaldehyde to form **27a**. It is essential to mention that aldol condensation might be catalyzed by DBU or intermediate **29a**. The possibility of deacylation of **27a** by DBU is ruled out, as the treatment of compound **27a** with DBU did not produce **28a** under the same reaction condition. Moreover, we did not observe deacetylation of **26a** in the presence of DBU. The proposed initial aldol at the *C*6 methyl of **26a** is based on the above report on a similar moiety (**Scheme-2.E**).

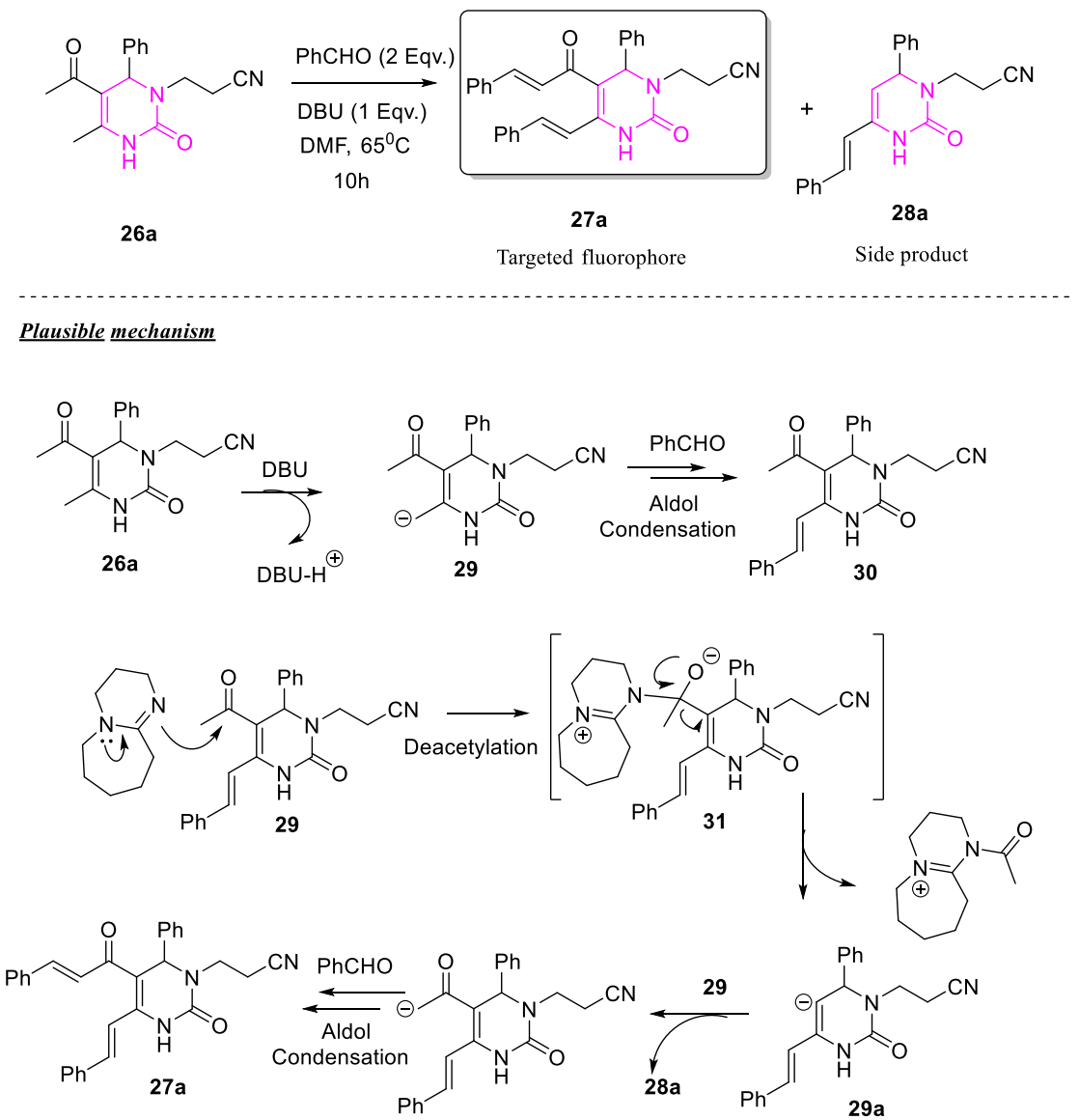

Scheme-2.J Functionalization at the carbon centre by base-catalyzed Aldol-type reaction and a plausible mechanism

The aromatic rings attached at *C*11 and *C*10 of **27a** are in extended conjugation through ethylenic double bonds, and therefore **27a** shows absorption in the visible range. Considering the medicinal importance of the DHPMs, the synthesized compound **27a** was subjected to the DNA binding study by UV–Vis and fluorescence spectroscopy. The presence of a cyanoethyl group might improve pharmacological properties such as water solubility, binding with target biomolecules etc. The

binding parameters were calculated based on the spectroscopic data to determine the possibility of **27a**being used as a DNA modulation agent.

2.2.1Interaction study with Calf-thymus DNA (ct-DNA)

In order to find the general affinity of **27a** towards double stranded DNA (ds-DNA), we studied the titration of **27a** with ct-DNA by UV–Vis spectrophotometer. The intrinsic UV–Vis spectrum of **27a** in Tris-HCl (TE) buffer at pH 7.2 shows a strong, unstructured absorption band at 294 nm and another moderately strong band at 386 nm. We observed that the intensity of both bands was gradually decreasing with the increasing concentration of ct-DNA (0 to 1μM). The observed hypochromic effect was 43.5% at λ= 386 nm. Moreover, a clear bathochromic shift (Δλ= 12 nm) band was observed from 386 nm to 398 nm (**Figure-2.F**(A)). The combined hypochromic effect and the bathochromic shift were presumably due to the non-covalent interaction of the **27a** with ds-DNA and ruled out the possibilities of the external mode of binding[29]. Additionally, a clear isobestic point at 286 nm indicates the formation of an adduct with DNA. To calculate the binding constant, we have used the measured OD value at 386 nm at the different concentrations of ct-DNA. The plot of A_0 /(A-A_0) vs. 1/[DNA] showed a linear relationship. The binding constant K_b was calculated from the slope and intercept (**Figure- 2.F**(B)) according to the Benesi–Hildebrand Equation(1)[30].

$$\frac{A_0}{A-A_0} = \frac{\varepsilon_0}{\varepsilon_0-\varepsilon} + \frac{1}{K_b}.\frac{\varepsilon_0}{\varepsilon_0-\varepsilon}.1/[DNA] \qquad (1)$$

The measured binding constant was considerably (3.65 ×10^6 M^{-1}) high (**Figure-2.F**(B)). To get further insight into the binding mode, we compared the simulated UV spectrum of **27a** (**Figure-2.F**(C))with that of the experimental one. The Gaussian 16 package using the methodRB3LYP/6–31+*G*(d) level of theory and the command td = (nstates = 20)b3lyp/6–31+*g* (d)scrf = (ief pcm, solvent = water) geom = connectivity scf = xqc, the UV spectrum had been calculated. The calculated and experimental UV–Vis spectrum were in good agreement. The HOMO of **27a** was located mainly at the DHPM heterocyclic unit, whereas, the LUMO was found primarily in the conjugated olefinic area (**Figure-2.I**). Hence, it had been observed a clear separation of the HOMO and LUMO orbitals. The experimental UV titration showed that the absorption spectrum was sensitive to the concentration of the ds-DNA and exhibited a strong hypochromic effect and bathochromic shift. This spectral change in presence of the ct-DNA might be due to the interaction of the electronic state HOMO of **27a** with the heteroatomic units exposed in the narrow and shallow minor groove of the ds-DNA, resulted lowering the band gap of the chromophore **27a**.The combined UV–Vis spectra and calculated results suggest that the **27a** is binding at the minor groove of ct-DNA.

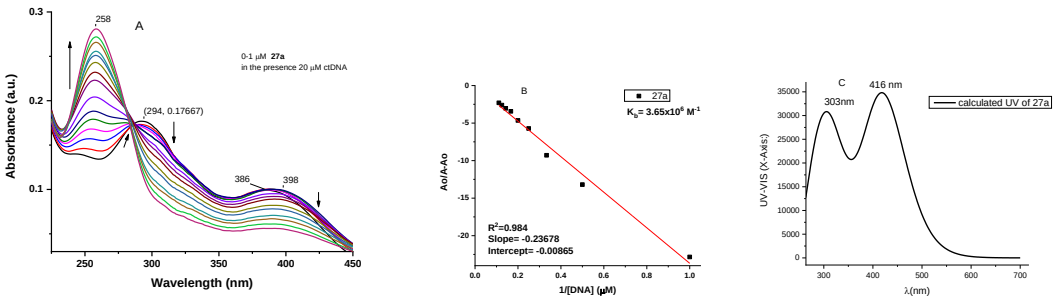

Figure-2.F (A) UV–Vis spectra for **27a** (20 μM) in the absence and presence of ct-DNA. The UV titration was carried out by increasing the concentration of ct-DNA from 0.1 to 1 μM. The arrow direction indicates the change in absorption peak intensity by increasing DNA concentration. (B) Linear plot obtained from A_0 /(A –A_0) vs. 1/[DNA], where A_0 and A are the absorptions in the presence and absence of DNA at 395 nm. Measured K_b = 3.65 ×10^6 M^{-1}. (C) Simulated UV–Vis spectrum obtained from TD-DFT calculation.

To understand binding interactions at the molecular level, we used the self-docking strategy (use of the crystallographic structure of DNA as a rigid framework with **27a** by AutoDock Vina, an open-source program for molecular docking[31].We used the duplex structure of dodecamer D(CGCGAATTCGCG)$_2$ [PDB ID: 289D] that targeted a small molecule minor groove binder[32]. The water molecules and the ligands in the crystal structure are not included in the calculation, and only the polar hydrogen atoms are considered. The charge is balanced at the macromolecule before the docking experiment. The crystallographic structure of the DNA without intercalation gap was used as a rigid framework for the docking study. A grid dimension of 60 ×60×80 cubic angstrom was used to cover the entire DNA structure for docking. The Insilcocalculated binding energy was −7.2 Kcal/mol and hence predicted binding constant K_b (1.9 ×10^5 M^{-1}) was found to be very close to the experimental value obtained from the UV–Vis and fluorescence spectroscopy. The noncovalent interaction predicted by the model is shown in **Figure-2.G**.

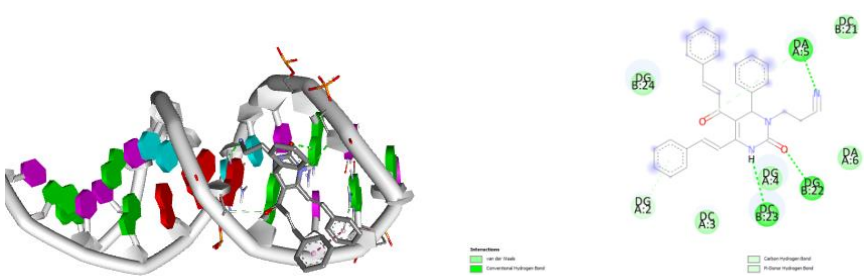

Figure-2.G. Binding model constructed by AutoDock Vina and the interaction details of **27a** with ds-DNA.

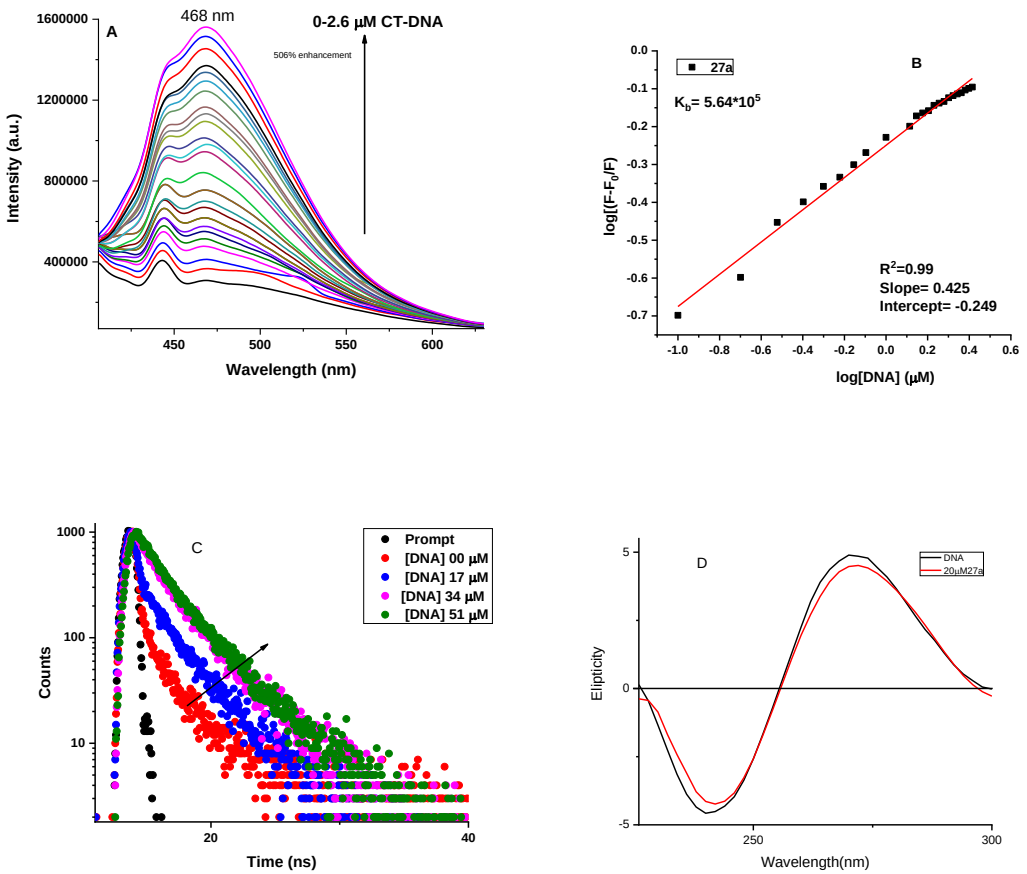

Figure-2.H (A) Fluorescence titration spectra of **27a** (20 µM) in the presence of DNA at a different concentration (0.1–1 µM), at pH 7.2 in 10 mM Tris–HCl buffer at 25 °C. The first reading (black line) is the Fl spectrum of **27a** in the absence of DNA. The arrow's direction indicates an intensity enhancement (5 times) (B) The linear plot of log[($F - F_0$)/ F] vs. log[DNA]. The emission band at 475 has been used to monitor the change in fluorescence intensity and at the excitation wavelength 385 nm and calculation of K_E = 5.64 ×10^5 M^{-1}. (C) Time-resolved fluorescence spectra of **27a** at different concentrations of ct-DNA (00 µM, 17 µM, 34 µM, 51 µM). (D) CD spectra (black) of 30 µM ct-DNA in 2 mM Tris–HCl buffer (pH 7.2) and presence of 20 µM of **27a** .

The effect of ds-DNA on the fluorescence emission spectra of a chromophore is one of the most common techniques to understand the interactions of small molecule as potential drugs. Depending upon the type of interaction with the small molecules with ds-DNA, the fluorescence emission intensity may decrease or increase with a change in the spectral shape. In this study, we observed a substantial enhancement of fluorescence emission intensity of **27a** in the presence of ct-DNA (**Figure-2.H** (A)).

The inherent fluorescence emission spectra of the **27a** in TE buffer at pH 7.2 show a weak band at about 470 nm excited at 385 nm. However, increasing the concentration of ct-DNA from 0.1 to 2.6 µM at a similar condition resulted in a strong enhancement of fluorescence emission intensity with no apparent change in the peak shape. The double logarithm Eq. (4)[33]was used to calculate the

enhancement constant K_E, where F, F_0 represents the fluorescence emission intensity in the presence and absence of ct-DNA respectively. The n corresponds to the binding site dimension number

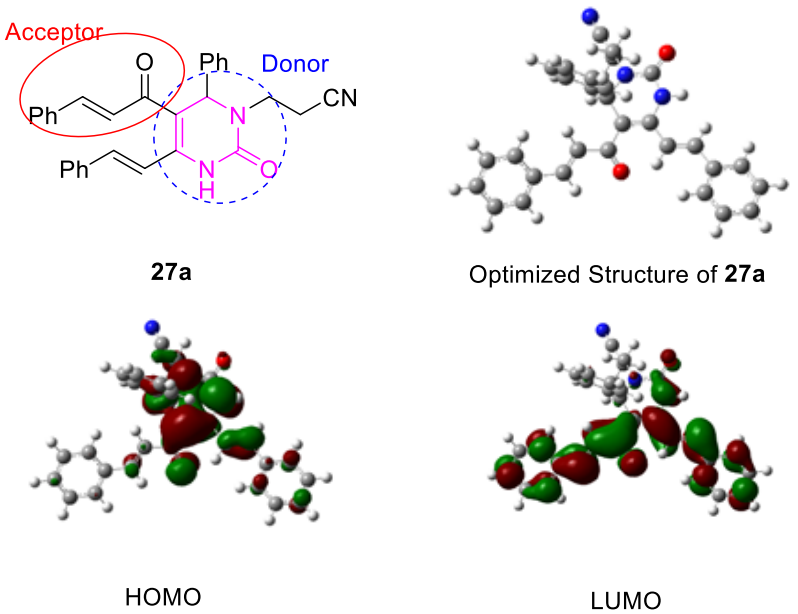

Figure-2.I Optimized structure of **27a** , HOMO, and LUMO plots obtained from TD-DFT calculation.

TheEq. (3) is derived from the classical Stern-Volmer Eq. (2). The increase in fluorescence intensity is supposed to the reduction in the collisional quenching of fluorophore as shielding by the DNA groove and no dynamic effect associated with DNA bound fluorophore. For enhancement $F_0<F$ as a result, the Eq. (3) can be rewrite as the Eq. (4)[34].

$$[DNA]^n K_q = \frac{[F]_0}{[F]} - \qquad (2)$$

Where Kq is the quenching constant and n is the number of equivalent binding site. Taking log on both side, the Eq. (2) can be written as:

$$\log Kq + n\log[DNA] = \log\frac{F_0 - F}{F}. \qquad (3)$$

$$\log\frac{F_0 - F}{F} = \log K_E + n\log[DNA] \qquad (4)$$

If a dynamic process is part of the enhancing mechanism, the above equation can be written as follows:

$$K_E = \tau_0 K_B \qquad (5)$$

Where, K_E is the dynamic enhancement constant (Similar to a dynamic quenching constant), K_B is the bimolecular enhancement constant (like to a bimolecular quenching constant) and $\tau 0$ is the lifetime of the compound **27a** in the absence of the DNA. The dynamic enhancement constant (K_E) of **27a**

was calculated as K_E = 5.64×10^5 M^{-1} and the measured fluorescence lifetime $\tau 0$was calculated as 2.76 ns (*Vide* experimental section). Therefore, the bimolecular enhancement constant K_B= 2.04 ×10^{14} M^{-1}s $^{-1}$, which was greater than the largest possible value (~1 ×10^{10} M^{-1}S^{-1}).[35]It suggests that a static process involves complex formation in the ground state of the **27a** when it interacts with DNA, not initiated by a dynamic process[36].The heterocyclic unit (donor) and the conjugated carbonyl (acceptor) effectively created an intramolecular donor-π-acceptor system[37]. Because of the conformational flexible nature of the acceptor part, the inherent fluorescence emission is very low. When it bound to the minor groove of the ds-DNA, the vibrational and conformational flexibility reduces to a great extent, hence reducing the non-radiative relaxation process after binding with the DNA double helix.This model was also supported by the time-resolved fluorescence spectroscopy (**Figure-2.H**(C)), and it showed a minor change in the fluorescence lifetime on increasing concentration of ds-DNA.We observed only about 3 ns enhancement of the half-life ($t_{1/2}$) of the excited state of **27a** between free and bound state respectively.The donor-acceptor character of the **27a** was also supported by the HOMO LUMO plot by the Time-dependent density functional (TD-DFT) theory calculation (**Figure-2.I**).

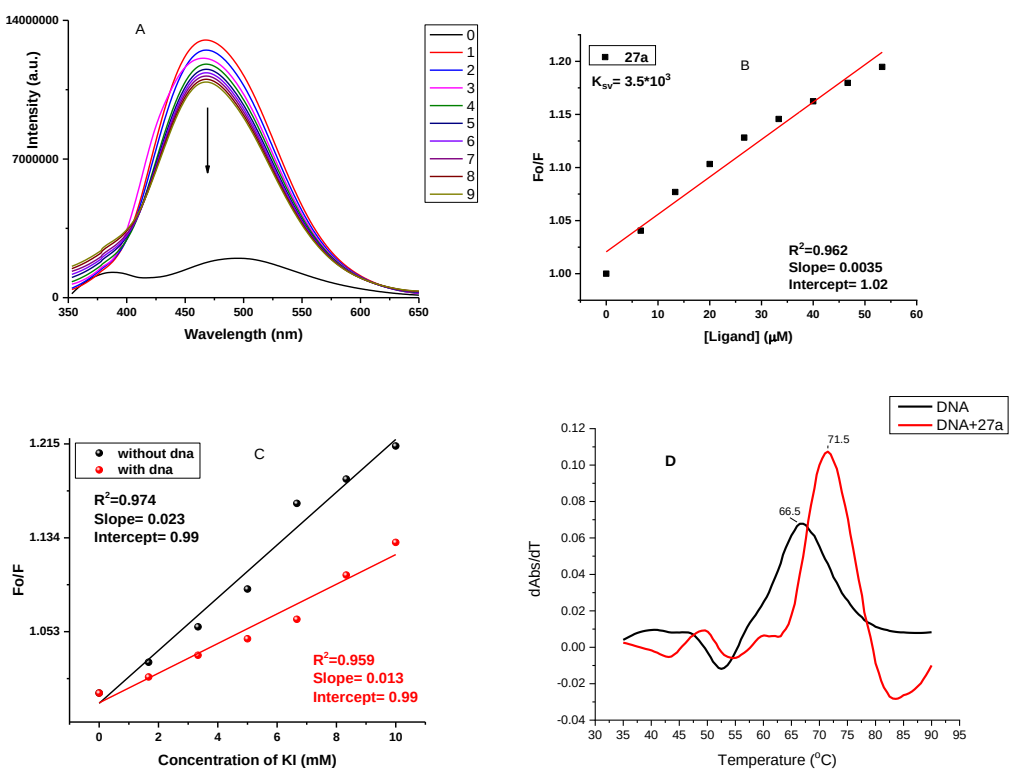

Figure-2.J (A) Hochest 33258 displacement assay. (B) Displacement equilibrium constant calculation. (C) The relative quenching effect of iodine on fluorescence emission of **27a** in the presence and absence of ct-DNA. (D) DNA melting

temperature plot of ct-DNA (4 μM) in 10 mM Tris–HCl buffer (pH 7.2) (black line) and in the presence of 4 μM of compound **27a** (red line). The plot shows the first derivative of OD w.r.t. temperature vs. temperature.

Acridine Orange (20x) **27a compound (20x)** **Merged (20x)**

Figure-2.K Confocal images (20 × magnification) showed that the compound **27a** targeted into the nucleus of the cell. Photograph of the stained cells under 20 × magnification with acridine orange, compound **27a** and merged respectively.

The minor groove binding nature was also suggested by the effect of iodide on the fluorescence emission quenching of **27a** in the presence and absence of ds-DNA. Iodide is known to promote intersystem crossing (ISC) during a collision with fluorophore molecules and, thus, a dynamic quencher. We measured the quenching constant in the presence and absence of ct-DNA by using the Stern–Volmer equation, $F_0/F = 1 + K_{SV}[Q]$, where F_0 and F are the fluorescence intensity in the absence and presence of the anionic quencher [Q] respectively. The minor change in K_{SV} values(**Figure-2.J**(C))in the presence of ct-DNA with respect to the free chromophore supports the minor groove binder nature of **27a** to ds-DNA. The displacement assay with Hochest 33258 was monitored at the excitation wavelength 343 nm to see the efficiency of displacement of Hochest 33258 by **27a**.Generally, at low concentrations, small molecule as minor groove binders displaces bounded dye from ds-DNA, and the dynamics can be measured as a considerable decrease in fluorescence emission of Hochest 33258. In the present study, we observed a decrease in fluorescence emission intensity of Hochest 33258, with a displacement constant ($K_{SV} = 3.5 \times 10^3\ M^{-1}$) of the chromophore **27a**, an indication of minor groove-binding. This was further confirmed by the observation that there was negligible change in the fluorescence emission intensity of DNA-bound ethidium bromide (ref. Supporting Information). The CD spectra of 4 μM ct-DNA in the presence and absence of the fluorophore **27a** showed a systematic intensity decrease, keeping the overall spectra the same (**Figure-2.H**(D)).This also supports the predicted minor groove-binding model. The moderate change in DNA melting temperature when **27a** bound to the ds-DNA is in favour of the predicted model (**Figure-2.J**(D)).To observe the intracellular localization of compound **27a**, we stained SiHa cancer cells and visualized them under a confocal microscope and the result was compared with the known

nucleic acid specific dye acridine orange[38]. After 24 hour treatment, the incorporation of **27a** was observed within the nucleus at a lower rate than that of acridine orange (**Figure-2.K**).

2.3 CONCLUTION

In summary, we have explored the detailed behaviour of ketomethyl containing DHPMs in aq. alkaline condition with various scopes and offered a new avenue for synthesizing C6-benzylated DHPMs. The inherent instability of the ketomethyl-containing DHPMs was enhanced by attaching a cyanoethyl group selectively at the *N*3 atom and we have successfully developed a synthetic strategy for accessing a highly conjugated DHPM (fluorophore) by the post-synthesis modification of the Bigineili product. Significantly, we have showed that the synthesized compound **27a** is highly sensitive towards ds-DNA by different photophysical studies. Hence, these types of compounds are useful for developing DNA-based drugs to modulate gene expression, monitor cellular processes involving DNA, visualize and quantify cellular DNA, to monitor the live activities of the nucleus of a cell. Most importantly, we explored the possibility of using of this compound as a cell-imaging agent on the SiHa cancer cell line and the result was compared with the nucleic acid specific dye acridine orange, a popular dye for the identification of live cell nucleus. Although, slightly less cell permeability was observed as compared to acridine orange, but incorporation of it within the cell, along with the particular nucleus target ability of this compound has been established here.

2.4 EXPERIMENTAL SECTION

2.4.1 General information

Solvents and reagents were purchased from Aldrich, Alfa aesar, Merck, SRL, Spectrochem, and Process Chemicals and they were used without furtherpurification. Commercially available (SRL India) calf-thymus DNA (ct-DNA) , Hochest 33258 and Ethidium bromide (EB) were used without purification also. All the reactions were carried out atopen vessel and monitored by TLC (Silica Gel60 F_{254}) and it was observed under UV light (254 nm).Yields refer to the isolated product as mentioned in theexperimental section. All NMR spectra were recorded with Bruker 300 or 400 MHz spectrometers in deuterated solvents ($CDCl_3$). Chemical shifts are reported in parts per million (ppm, δ) relative to tetramethylsilane (TMS) and the solvent resonance was referenced to internal standard $CDCl_3$ (δ 7.28 ppm). All coupling constants (*J*) are absolute values and are expressed in Hz. The descriptions of the signals are reported as follows: s = singlet, d = doublet, dd = doublet of a doublet, t = triplet, m = multiplet, and dt = doublet of a triplet. ^{13}C-NMR spectra were recorded using Bruker Avance III 300 (75 MHz), 400 (100 MHz) spectrometers as solutions in $CDCl_3$ with complete proton decoupling. High-resolutionmass spectra were recorded on ESI-TOF mass spectrometry. LCMS taken using ZORBAXEXT (4.6 × 50 mm, 5μ) column, NH_4OAc (10 mM): CAN:: 90:10 for liquid chromatogram. HPLC was performed on the YL-9000 series.

2.4.2 Representative procedure and spectral data:

Compound **19d** is synthesised by both Methods (A & B) from **17d**, with different yields. Compound **19e**, **19f** are prepared by using Method-A from **17e** and **17f** respectively. Method-B was used for synthesizing compound **19g** and **19h** by the reaction of **17d** with 3-methoxybenzaldehyde and 4-methyl benzaldehyde respectively.

2.4.2.a Method A

Sodium hydroxide (500 mg, 12 mmol) was added to a suspension containing compound **17d** (500 mg, 2.17 mmol) in 25 mL of water at RT, and the mixture was refluxed with constant stirring for 2 hours. After cooling the reaction mixture, the solid product **19d** was collected by filtration, washes with water, dried and collected analytical data without further purification. Yield 35%.

2.4.2.b Method B

Sodium hydroxide (500 mg, 12 mmol) was added to a suspension containing compound **17d** (350 mg, 1.51 mmol), benzaldehyde (192 mg, 1.82 mmol) in 25 mL of water at RT, and the mixture was refluxed with constant stirring for 2 hours. After cooling the reaction mixture, the solid product **19d** was collected by filtration, washes with water, dried and collected analytical data. Yield 88%.

***Analytical and spectroscopic dataof (E)-4-phenyl-6-styryl-3,4-dihydropyrimidin-2(1H)-one* (19d):**

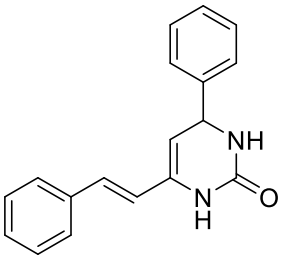

Light yellow solid, m.p. 194°C-195°C, ^{1}H-NMR (400 MHz, DMSO-d_6) δ 8.38 (bs, 1H), 7.43-7.21 (m, 11H), 7.07 (d, J = 16 Hz, 1H), 6.60 (d, J = 16 Hz, 1H), 5.09 (bs, 1H), 5.05 (bs, 1H). ^{13}C-NMR (100 MHz, DMSO-d_6) δ 153.7, 145.4, 137.0, 134.1, 129.1, 129.0, 128.2, 128.0, 127.7, 126.8, 126.6, 122.7, 104.5, 55.5. ESI-TOF MS:Calculated mass for $C_{18}H_{17}N_2O$ $[M+H]^+$ = 277.1341, observed m/z 277.1335

***Analytical and spectroscopic dataof (E)-6-(4-methylstyryl)-4-(p-tolyl)- 3,4-dihydropyrimidin-2(1H)-one* (19e):**

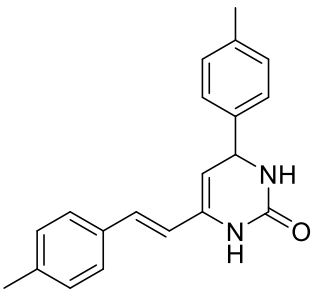

Light yellow solid, yield 28%, m.p. 196°C-198°C, ^{1}H-NMR (300 MHz, $CDCl_3$) δ 7.25-6.95 (m, 8H), 6.87 (s, 1H) 6.61 (d, J = 16 Hz, 1H), 6.44 (d, J = 16 Hz, 1H), 5.22 (s, 2H), 4.91 (s, 1H), 2.34 (s, 6H). ^{13}C-NMR (100 MHz, DMSO-d_6) δ 153.1, 142.1, 137.1, 136.3, 133.7, 133.6, 129.5, 129.2, 128.9, 128.4, 127.3, 126.2, 126.1, 121.3, 103.6, 54.7. ESI-TOF MS: Calculated mass for $C_{20}H_{20}N_2NaO$ $[M+Na]^+$= 327.1473, observed m/z 327.1470

***Analytical and spectroscopic dataof(E)- 4-(2-bromophenyl)-6-(2-bromostyryl)- 3,4-dihydropyrimidin-2(1H)-one* (19f):**

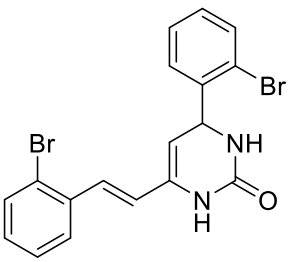

Light yellow solid, yield 41%, m.p. 198°C-200°C, ^{1}H-NMR (300 MHz, DMSO-d_6) δ 8.85 (s, 1H), 7.60-7.17 (m, 10H), 6.55 (d, J = 16 Hz, 1H), 5.39 (s, 1H), 5.17(s, 1H). ^{13}C-NMR (75 MHz, DMSO-d_6) δ 154.2, 142.8, 136.7, 134.2, 133.0, 132.8, 129.3, 129.3, 128.6, 128.3, 127.7, 127.1, 126.87, 125.2, 123.9, 121.4, 102.5, 55.3. ESI-TOF MS: Calculated mass for $C_{18}H_{15}Br_2N_2O$ $[M+H]^+$ = 432.9551, observed m/z 432.9546

***Analytical and spectroscopic dataof(E)- 6-(3-methoxystyryl)-4-phenyl- 3,4-dihydropyrimidin-2(1H)-one* (19g):**

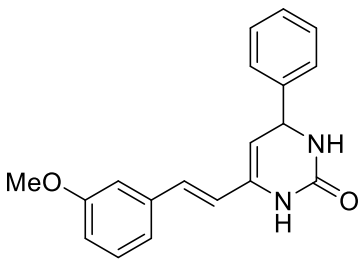

Light yellow solid,yield 74%, m.p. 115°C, ^{1}H-NMR (400 MHz, DMSO-d_6) δ 8.35 (bs, 1H), 7.37-7.20 (m, 8H), 7.03 (d, J = 16 Hz, 1H), 6.98 (m, 1H), 6.81 (d, J = 8 Hz, 1H), 6.62 (d, J = 16 Hz, 1H), 5.09 (bs, 1H), 5.05 (bs, 1H), 3.74 (s, 3H). ^{13}C-NMR (100 MHz, DMSO-d_6) δ 159.5, 153.1, 144.9, 138.0, 133.6, 129.6, 128.4, 127.4, 127.1, 126.1, 122.5, 119.1, 113.5, 111.2, 104.1, 55.0, 54.9. ESI-TOF MS: Calculated mass for $C_{19}H_{19}N_2O_2$ $[M+H]^+$ = 307.1447, observed m/z 307.1441

***Analytical and spectroscopic dataof* (E)- 6-(4-methylstyryl)-4-phenyl- 3,4-dihydropyrimidin-2(1H)-one (19h):**

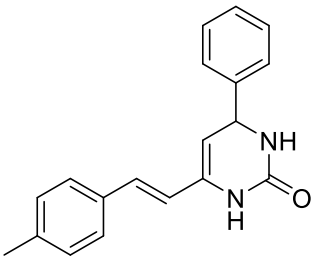

Light yellow solid, yield 57%, m.p. 203°C-205°C, ^{1}H-NMR (400MHz, DMSO-d_6) δ 8.35 (s, 1H), 7.37-7.12 (m, 10H), 7.02 (d, J = 16 Hz, 1H), 6.54 (d, J = 16 Hz, 1H), 5.07 (s, 1H), 5.01 (s, 1H), 2.29 (s, 3H). ^{13}C-NMR (100MHz, DMSO-d_6) δ 153.6, 145.5, 137.6, 134.2, 129.7, 129.0, 127.7, 127.9, 126.8, 126.6, 121.7, 104.0, 55.5, 21.2. ESI-TOF-MS: Calculated mass for $C_{19}H_{18}N_2NaO$ $[M+Na]^+$= 313.1317, observed m/z 313.1317

***Synthesis and analytical data of 3-(5-acetyl-4-methyl-2-oxo-6-phenyl-3,6-dihydropyrimidin-1(2H)-yl) propanenitrile*(26a):**

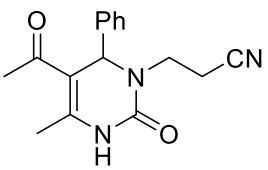

Compound **17d** (200 mg, 0.7902 mmol), acrylonitrile (0.06 mL, 1.5804 mmol) and DBU (0.14 mL, 0.9482 mmol) were taken in a 50 mL round bottom flask in 3 mL DMF at RT. The reaction mixture was stirred at 60 °C for 3 h. After cooling to RT, the reaction mixture was diluted with water followed by work up with ethyl acetate to get analytically pure compound **26a**.White crystal, yield 92%, ^{1}H-NMR (400 MHz, $CDCl_3$) δ 9.08(s, 1H), 7.38–7.32 (m, 5H), 5.50(s, 1H), 3.85-3.78(m, 1H), 3.41-3.34(m, 1H), 2.73-2.65(m, 1H), 2.41-2.34(m, 4H), 2.25 (s, 3H). ^{13}C-NMR (100 MHz, $CDCl_3$) δ194.3, 153.1, 145.2, 140.8, 129.0, 128.5, 127.0, 117.6, 112.3, 61.6, 42.1, 30.8, 19.5, 16.4. ESI-TOF-MS: Calculated mass for $C_{16}H_{17}N_3NaO_2$ $[M+Na]^+$= 306.1218, observed m/z = 306.1314

***Synthesis and analytical data of 3-(5-acetyl-4-methyl-2-oxo-6-(p-tolyl)-3,6-dihydropyrimidin-1(2H)-yl) propanenitrile* (26b):**

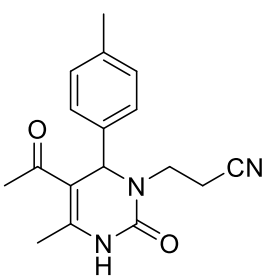

Experimental procedure is same as described for the compound **26a**. White solid, yield 85%, ^{1}H-NMR(300 MHz, $CDCl_3$) δ 8.43(s, 1H), 7.25 (d, J = 8Hz, 2H), 7.16 (d, J = 8 Hz, 2H), 5.45(s, 1H), 3.83-3.74(m, 1H), 3.44-3.35(m, 1H), 2.76-2.65(m, 1H), 2.39–2.24 (m, 7H), 2.23 (s, 3H). ^{13}C-NMR (100 MHz, $CDCl_3$) δ 194.5, 152.9, 144.6, 138.6, 137.8, 129.8, 127.1, 117.7, 112.5, 61.7, 42.2, 30.7, 21.1, 19.7, 16.6. ESI-TOF-MS: Calculated mass for$C_{17}H_{19}N_3NaO_2$ $[M+Na]^+$ = 320.1375, observed m/z = 320.1305

***Synthesis and analytical data of 3-(5-acetyl-6-(3-methoxyphenyl)-4-methyl-2-oxo-3,6-dihydropyrimidin-1(2H)-yl) propanenitrile* (26c):**

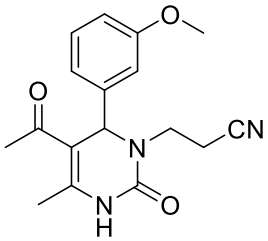

Experimental procedure is same as described for the compound **26a**.White solid, yield 88%, ^{1}H-NMR(300 MHz, $CDCl_3$) δ 8.27(s, 1H), 7.32 – 7.27 (m, 1H), 6.97 – 6.84 (m, 3H), 5.47(s, 1H), 3.84-3.77(m, 4H), 3.45 – 3.35 (m, 1H), 2.78 – 2.67 (m, 1H), 2.43 – 2.31 (m, 4H), 2.26 (s, 3H). ^{13}C-NMR (100 MHz, $CDCl_3$) δ 193.1, 158.8, 151.5, 143.6, 141.2, 128.9, 118.1, 116.4, 112.2, 112.1, 111.1, 60.5, 54.0, 41.1, 28.4, 18.4, 15.3. ESI-TOF MS: Calculated mass for $C_{17}H_{19}N_3NaO_3$ $[M+Na]^+$ = 336.1324, observed m/z = 336.1291

***Synthesis and analytical data of 3-(5-acetyl-4-methyl-6-(4-nitrophenyl)-2-oxo-3,6-dihydropyrimidin-1(2H)-yl)propanenitrile* (26d):**

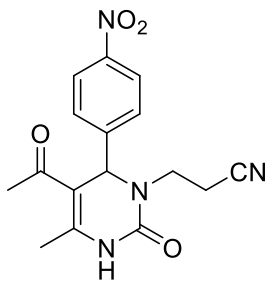

Experimental procedure is same as described for the compound **26a**.Yellow solid; yield 75%; ^{1}H-NMR (300 MHz, $CDCl_3$) δ 8.22 (d, *J* = 12 Hz, 2H), 8.03 (s, 1H), 7.57 (d, *J* = 12 Hz, 2H), 5.72(s, 1H), 4.02 – 3.93(m, 1H), 3.24 – 3.15(m, 1H), 2.81 – 2.70(m, 1H), 2.58 – 2.49(m, 1H), 2.39 (s, 3H), 2.35 (s, 3H).^{13}C-NMR (100 MHz, $CDCl_3$) δ 193.6, 152.7, 147.9, 147.8, 145.5, 127.9, 124.3, 117.3, 112.8, 60.4, 42.4, 31.3, 20.1, 16.8. ESI-TOF MS: Calculated mass for $C_{16}H_{17}N_4O_4$ $[M+H]^+$ = 329.1250, observed m/z = 329.1245

***Procedure for the synthesis of* 27a *and* 28a *(one pot method)*:** A mixture of compound **17d** (200 mg, 0.79 mmol), acrylonitrile (0.06 mL, 1.58 mmol), and DBU (0.14 mL, 0.95 mmol) was taken in a 50 mL round bottom flask in DMF (3 mL). The mixture was heated at 60 °C for 3 h with constant stirring. After complete conversion of **26a** (monitored by TLC), benzaldehyde (0.16 ml, 3.16 mmol) and fresh DBU (120 mg, 0.79 mmol) were added to the same reaction mixture, and the heating was continued for another 10 h at the same temperature. It was then cooled to RT, diluted with water, and extracted by EtOAc. The organic layer was collected, dried, and evaporated to get the crude reaction mixture. The product **27a** (60%) along with **28a** (31%) was obtained by flash chromatography using EtOAc: Hexane (20:80), with 91% overall yield. Similar results were observed when **26a** was separately treated with 2 equivalents of DBU in the presence of 2 equivalents benzaldehyde at 60 °C for 10 h.

***Analytical and spectroscopic dataof3-(5-cinnamoyl-2-oxo-6-phenyl-4-((E)-styryl)-3,6-dihydropyrimidin-1(2H)-yl) propanenitrile* (27a):**

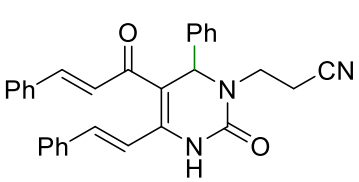

Yellow solid, yield 60%, ^{1}H-NMR (400 MHz, $CDCl_3$) δ 7.49-7.44(m, 9H), 7.40-7.31(m, 9H), 7.18-7.13(m, 2H), 5.63(s, 1H), 3.94-3.87(m, 1H), 3.45-3.38(m, 1H), 2.82-2.74(m, 1H), 2.45-2.38(m, 1H). ^{13}C-NMR

(100 MHz, $CDCl_3$) δ 188.3, 152.6, 142.6, 140.7, 140.5, 134.9, 134.7, 130.4, 129.8, 129.2, 129.1, 128.9, 128.7, 128.2, 127.3, 126.9, 126.1, 119.9, 117.6, 114.5, 62.5, 42.8, 29.7, 16.7. ESI-TOF MS: Calculated mass for $C_{30}H_{25}N_3O_2$ $[M+Na]^+$ =482.1844, observed m/z =481.9262

***Analytical and spectroscopic dataof(E)-3-(2-oxo-6-phenyl-4-styryl-3,6-dihydropyrimidin-1(2H)-yl) propanenitrile*(28a):**

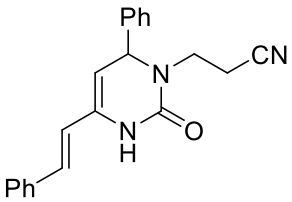

Yellow solid; yield 31%; ^{1}H-NMR (400 MHz, $CDCl_3$) δ 7.44-7.30(m, 11H), 6.82(d, *J*=16 Hz, 1H), 6.41(d, *J*=8Hz, 1H), 5.25(d, *J*=2.4Hz, 1H), 5.02(d, *J*=2.4Hz, 1H), 3.77-3.72(m, 1H), 3.30-3.25(m, 1H), 2.85-2.77(m, 1H), 2.34-2.27(m, 1H). ^{13}C-NMR (100 MHz, $CDCl_3$) δ 153.3, 141.6, 135.9, 132.4, 129.3, 128.8, 128.7, 128.4, 128.2, 127.0, 126.6, 121.2, 118.1, 104.0, 63.1, 42.2, 16.4

2.4.3 DNA-Binding Study

2.4.3.a Materials

Calf thymus DNA (ct-DNA) was purchased from Sigma Aldrich, USA. Ethidium bromide (EB) was purchased from Himedia, India.

Sample Preparation: Stock solution of **27a** (1 mM) was prepared in Ethanol. Calf-thymus DNA (ct-DNA) was suspended in 10 mM Tris-HCl buffer with 1mM EDTA (p^H 7.2) at 4°C for 24 h with occasional mixing by vortex to ensure the formation of a homogeneous solution. To check the purity of the DNA solution, absorbance ratio $A_{260}/A_{280}$was recorded. No further purification was required since the absorbance ratio was between 1.8 and 1.9. Various concentrations of DNA solution were used in different experiments. After determining the concentration of DNA spectrophotometrically using the average molar extinction coefficient value of 6600 $M^{-1}cm^{-1}$ of a single nucleotide at 260 nm, all experiments were done in presence of 10 mM Tris-HCl buffer (P^H 7.2).

2.4.3.b Spectroscopic Methods

Absorption Spectroscopy Method

For the UV-Visible absorption spectra measurements Shimadzu spectrophotometer (model UV-1800, Japan) with 1cm × 1cm quartz cuvette was used. The UV-Visible absorption spectra of **27a** and **27a**-DNA complex were recorded in the wavelength range of 200–400 nm. The experiment was conducted at a defined concentration of **27a** (20 µM) in a fixed volume (3 ml) and quantified by changing the concentration of ct-DNA (0–1 µM).

Fluorescence Spectroscopy Method

Steady-state fluorescence: Fluorescence emission spectra of **27a** were recorded on a Shimadzu spectrofluorometer-5000 (Japan) equipped with a Xenon flash lamp using 1.0 cm quartz cells. Excitation was fixed at 385nm and emission spectra were recorded from 390 nm to 600 nm after setting the widths of both the excitation and the emission slits at 5 nm. The fluorescence titration was carried out by keeping the concentration of **27a** constant (20 µM) and varying the ct-DNA concentration from 0 µM to 2.6 µM.

Time-resolved fluorescence decay measurement: Fluorescence lifetime measurements were conducted on Horiba Jobin Yvon Fluoro Log spectrofluorometer (HORIBA, Les Ulis, France) with the excitation wavelength at 385 nm. Maximum emission wavelength was 475 nm in room temperature. The concentration of **27a** was fixed at 17µM, while ct-DNA concentration varied from 0 µM to 51 µM (**Table-2.C**).

Table-2.C Time-resolved fluorescence study of **27a**

Experiment No.	Concentration of **27a** (µM)	Concentration of DNA (µM)	T_1(ns)	$\chi 2$
1	17	00	2.76	1.01
2	17	17	2.89	1.05
3	17	34	3.00	1.00
4	17	51	3.02	0.99

Comparative binding study with known DNA binders

Displacement assay was done as early reported by several well-known DNA intercalators and groove binders such as Ethidium Bromide (EB) and Hoechst 33258. In the first case i.e; EB displacement assay we have monitored the emission spectra of ct-DNA (50 µM) bound EB (5 µM) in the presence of changing amounts of**27a** (0–60 µM) to assure the binding of **27a** with ct-DNA. After exciting at 471 nm the EB-bound ct-DNA molecule, the corresponding emission spectra were recorded in between the range 500-680 nm (**Figure-2.K**).

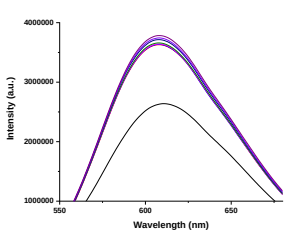

Figure-2.K Ethidium Bromide displacement assay (No such change)

The Hoechst 33258 displacement assay was monitored by excited the Hoechst bound ct-DNA complex at 343 nm, which contains 5µM of Hoechst 33258 and 50µM of ct-DNA. The fluorescence emission spectra were recorded between 350–650 nm by titrating with increasing concentrations of **27a** (0–60 µM). In all the above experiments, the final volume of the reaction mixture was made to 3 ml by adding 10 mM Tris-HCl buffer [For spectra; see the **Figure-2.J** (A)].

Iodide quenching experiments

Iodide quenching experiments were performed in the presence and absence of ct-DNA. Emission spectra were recorded either in the presence or absence of 50 mM ct-DNA in a 3ml reaction mixture which included 20 µM**27a**, 10 mM Tris-HCl (pH 7.2), and varying concentrations of KI between 0–10 mM. Excitation was done at 385 nm and emission spectra were recorded from 390-620 nm.

Melting Point Studies

DNA melting experiments were performed by monitoring the absorption of ct-DNA (4 µM) at 260 nm in the absence and presence of **27a** (1µM) at various temperatures by using a UV-Visible spectrophotometer fitted with a temperature-controlled Peltier. The absorbance was then plotted and normalized as a function of temperature ranging from 30°C to 90°C. The DNA melting temperature (Tm) was determined as the transition midpoint.

2.4.4 Crystallographic Table:

Table 2.D *Crystallographic and structure refinement parameters for 26a*

Emperical formula	$C_{16}H_{17}N_3O_2$
Formula weight	283.32
Crystal system	Monoclinic
space group	P21/c
a/ Å	6.0546(5)
b/Å	25.2587(19)
c/ Å	9.7641(7)
V /Å^3	1431.86 (19)
Z	4
D_c/ mg m^{-3}	1.314
μ /mm^{-1}	0.089
T/K	273
θ range/°	2.708, 27.120
λ (Mo Kα) /Å	0.71073
R indices($I > 2\sigma(I)$)	R_1=0.0847, wR_2=0.1646
R indices (all data)	R_1=0.1226, wR_2=0.1819

Copy of NMR

^{1}H-NMR of 19d

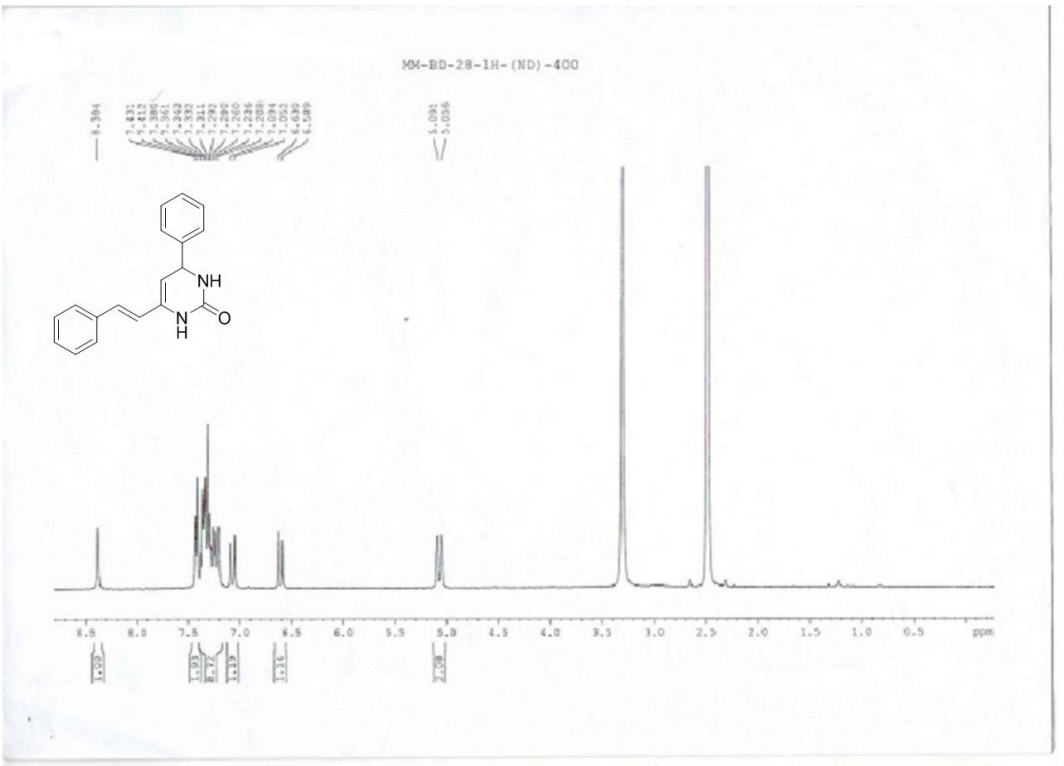

^{13}C-NMR of 19d

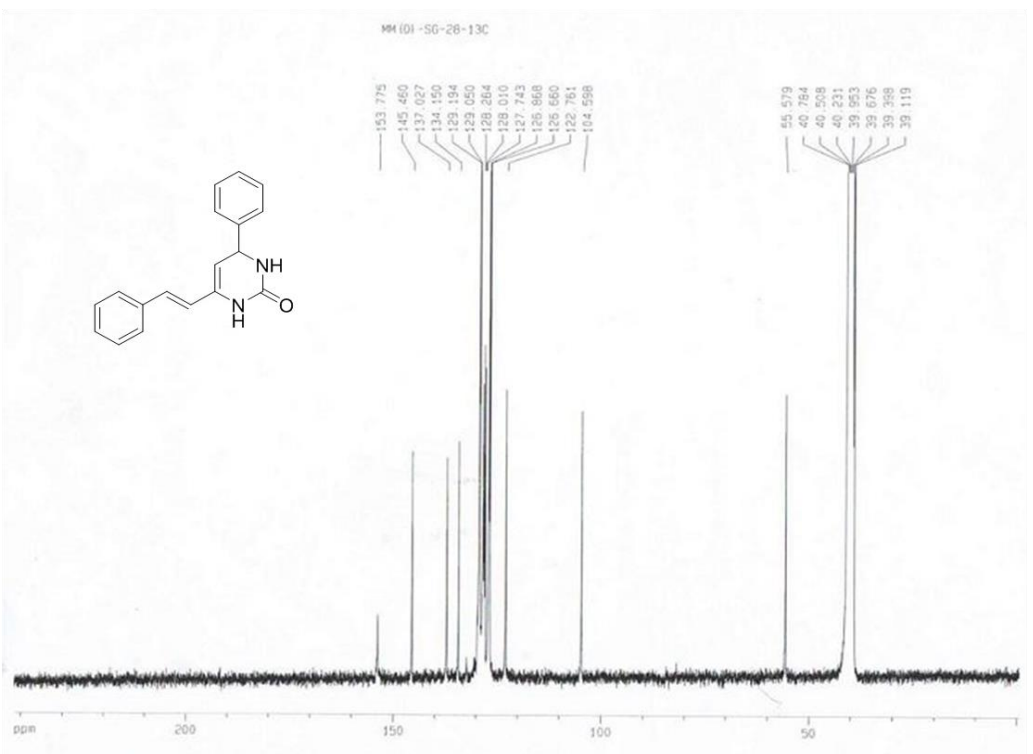

^{1}H-NMR of 19e

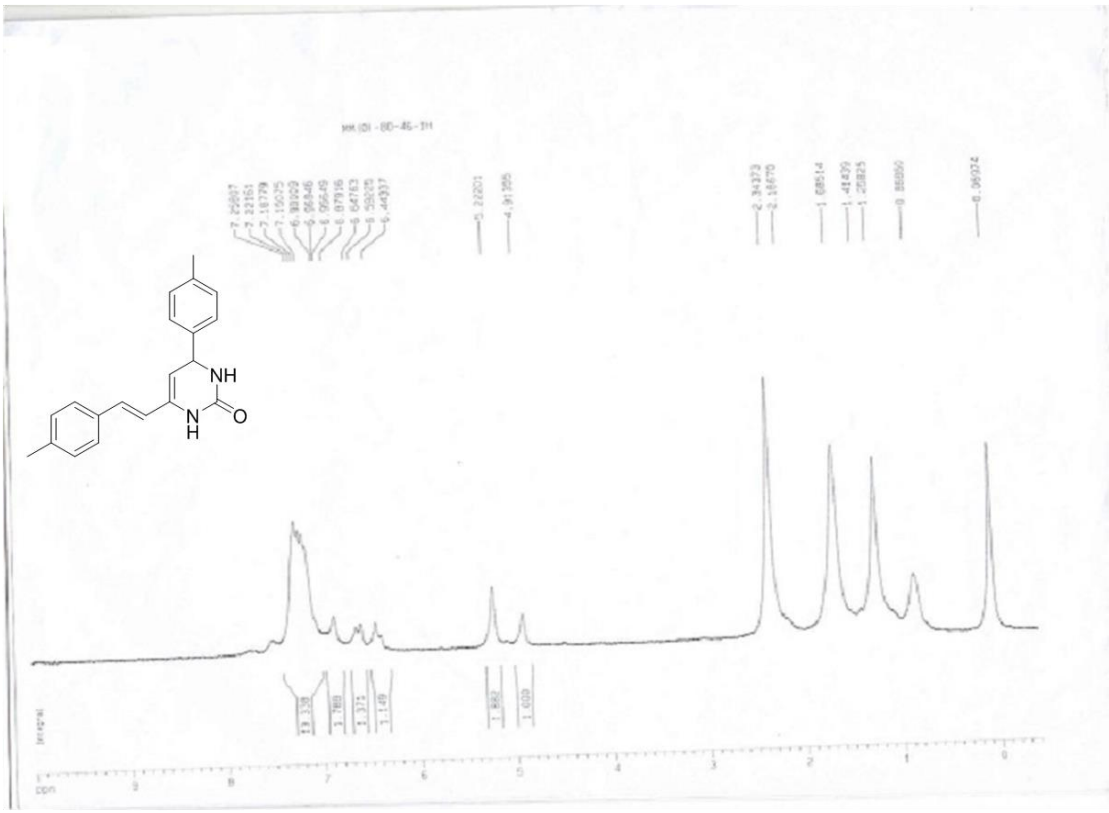

^{13}C-NMR 19e

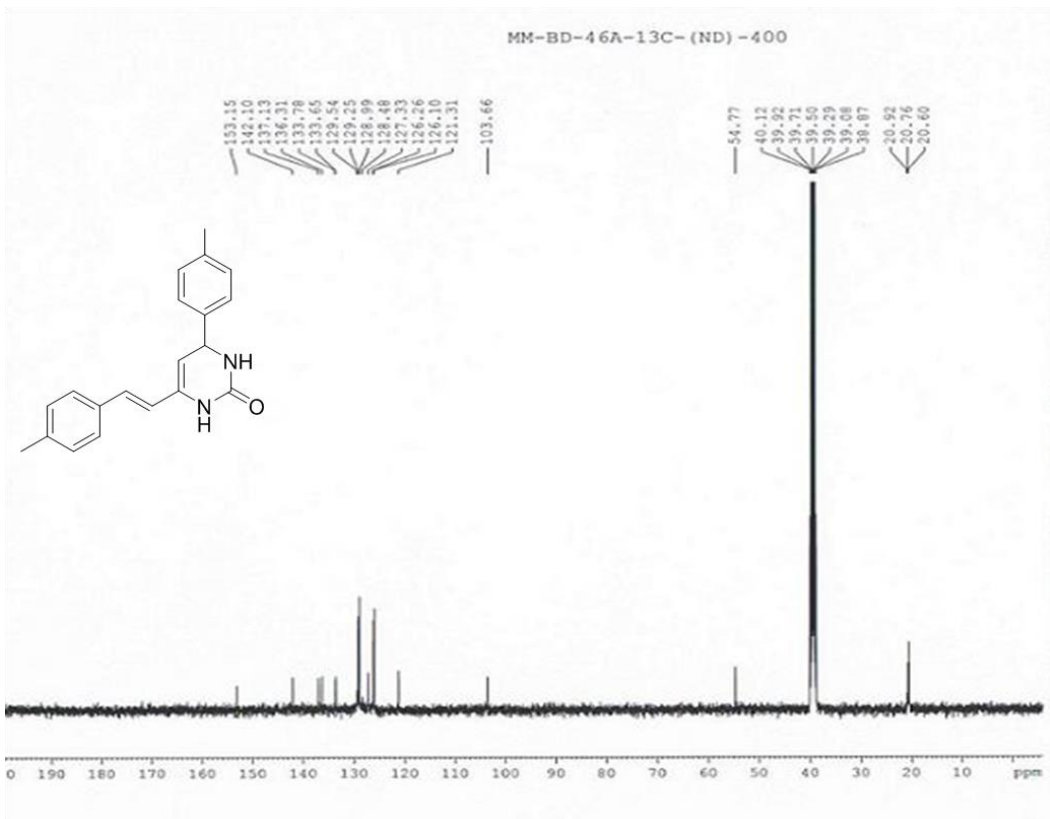

^{1}H-NMR of 19f

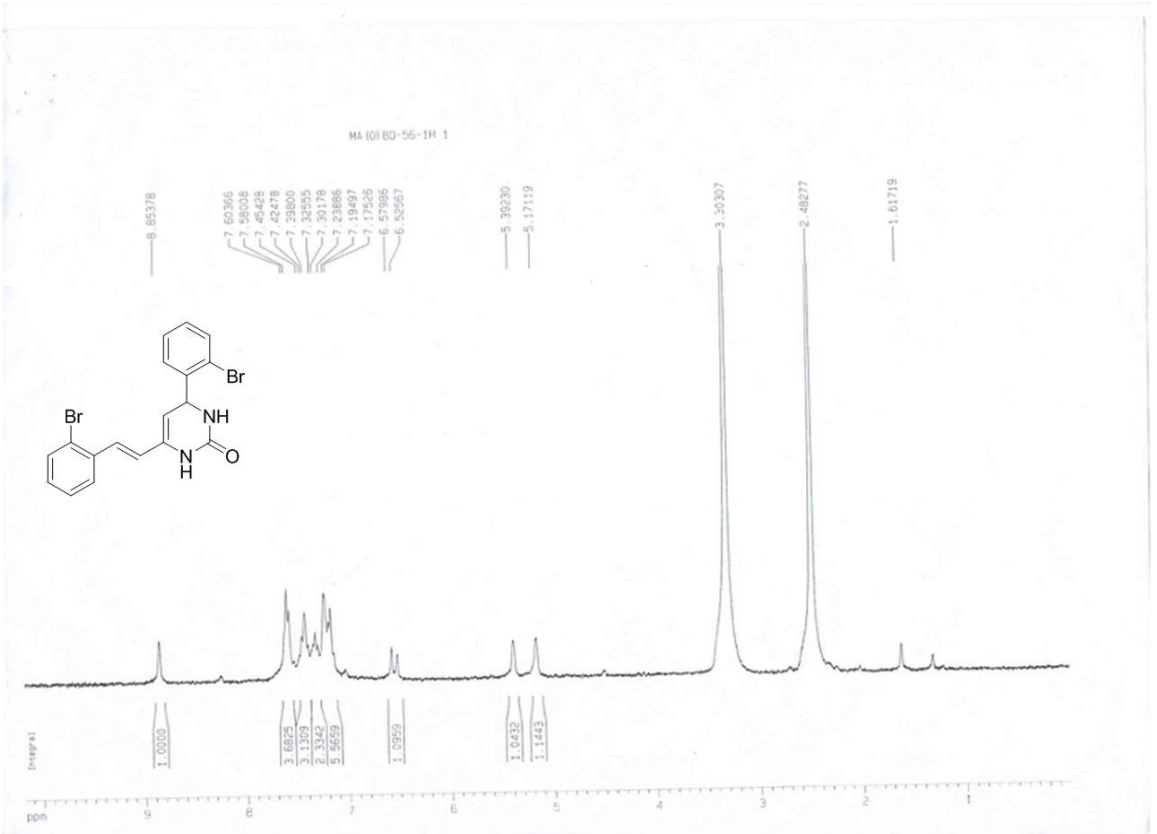

^{13}C-NMR of 19f

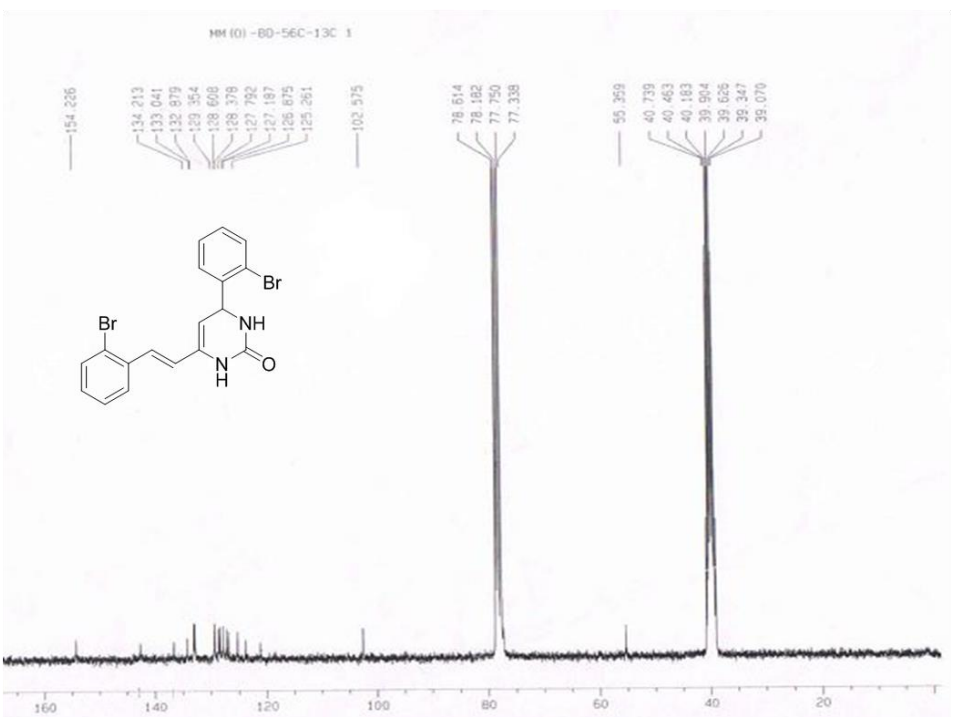

^{1}H-NMR of 19g

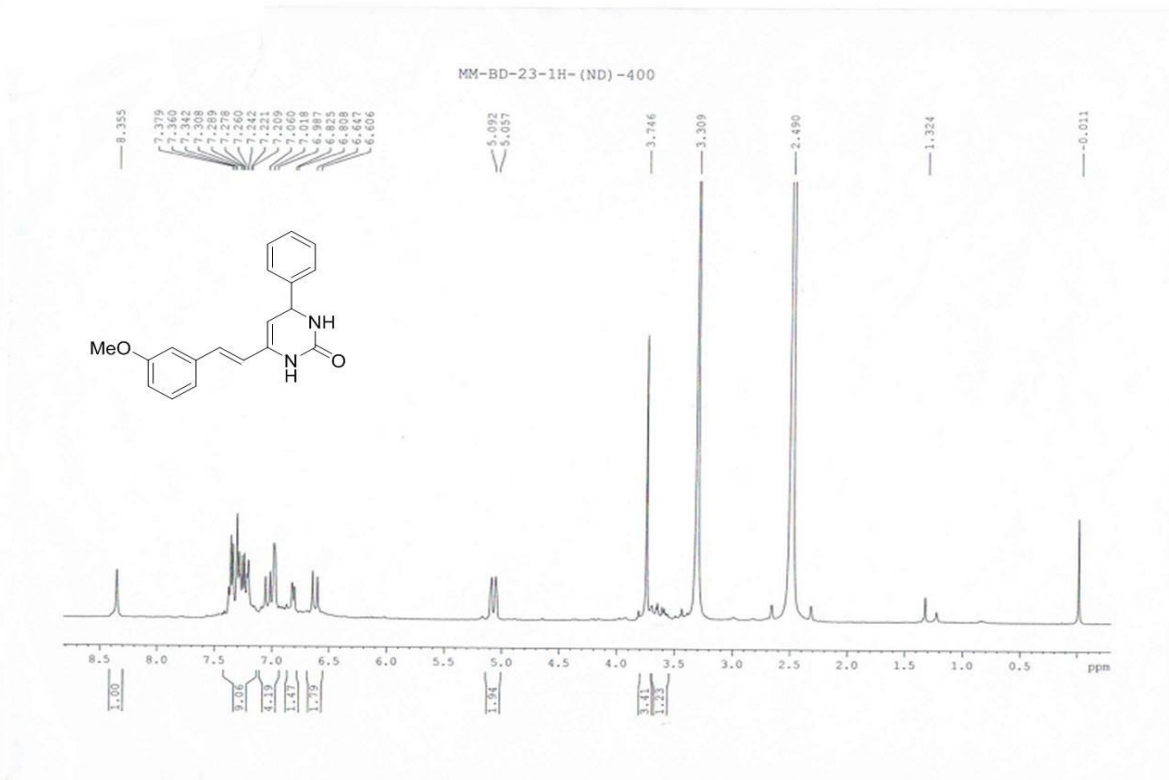

^{13}C-NMR of 19g

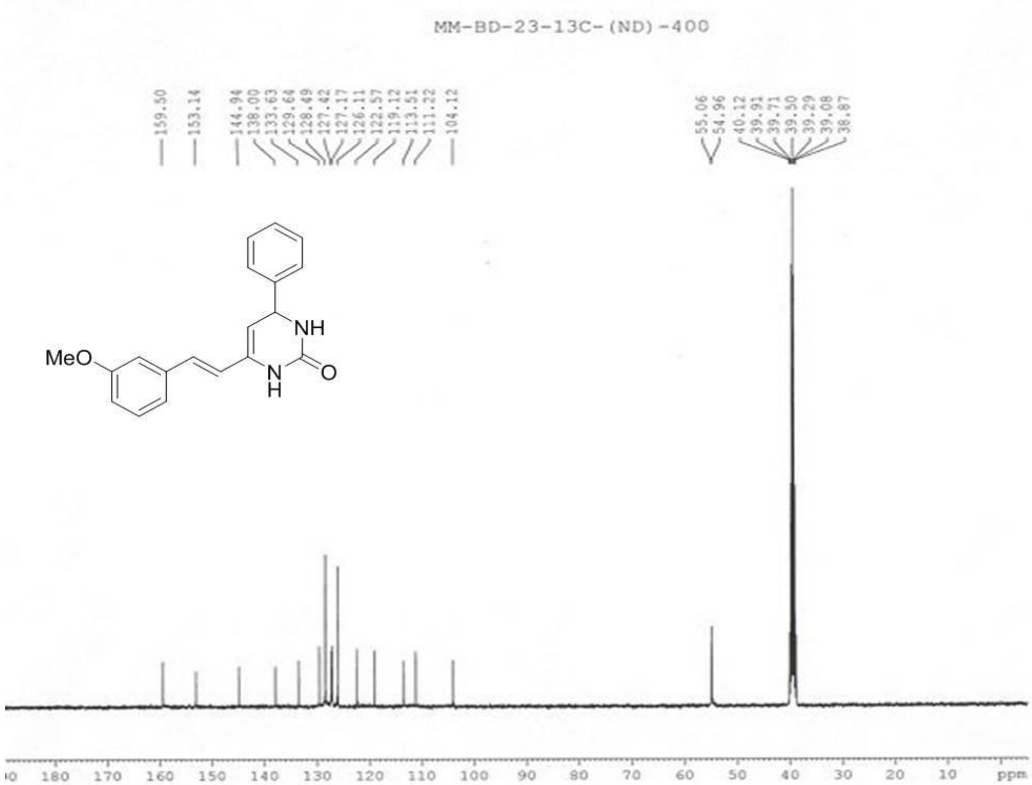

^{1}H-NMR of 19h

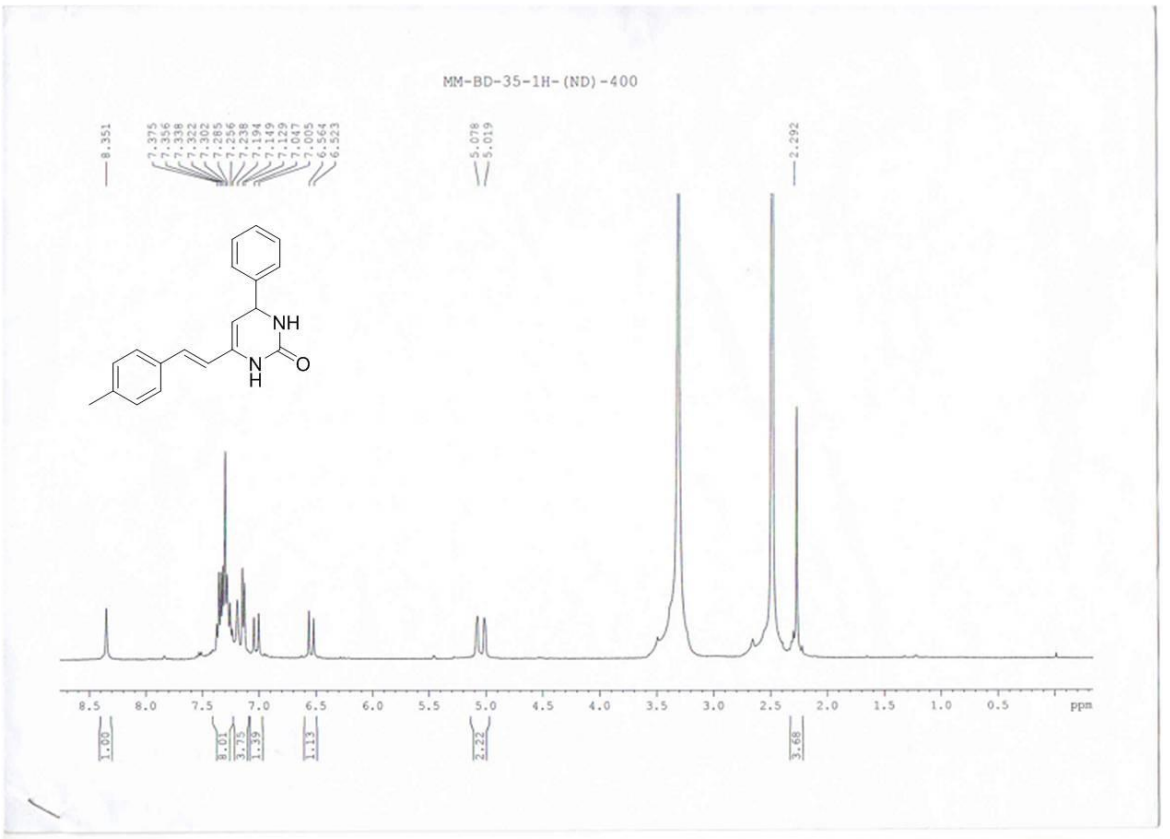

^{13}C-NMR of 19h

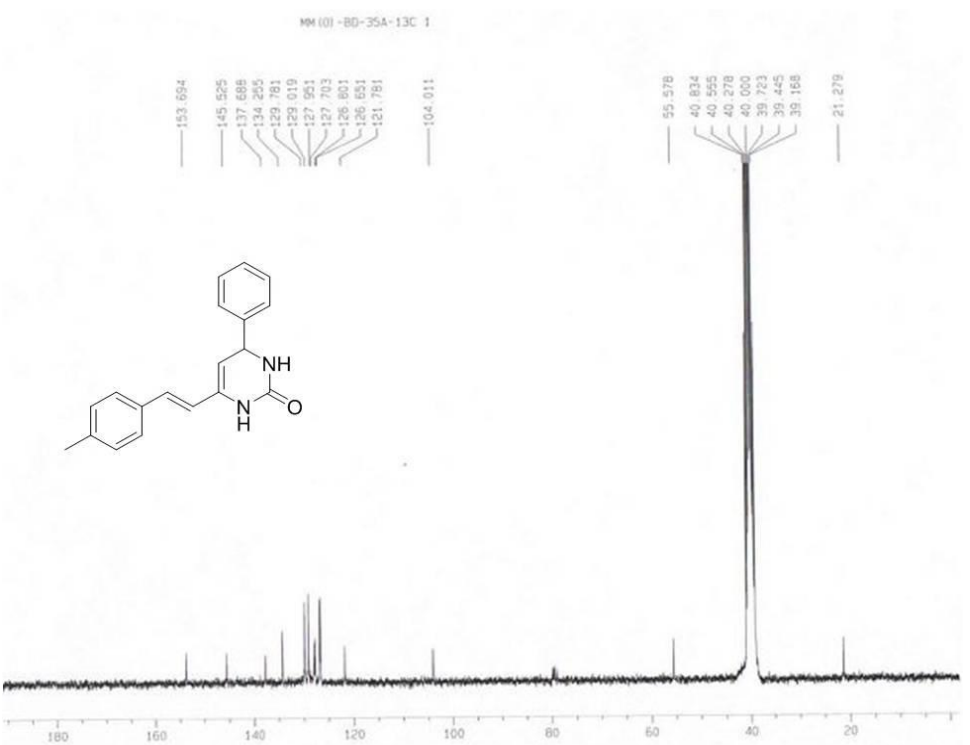

^{1}H-NMR of 26a

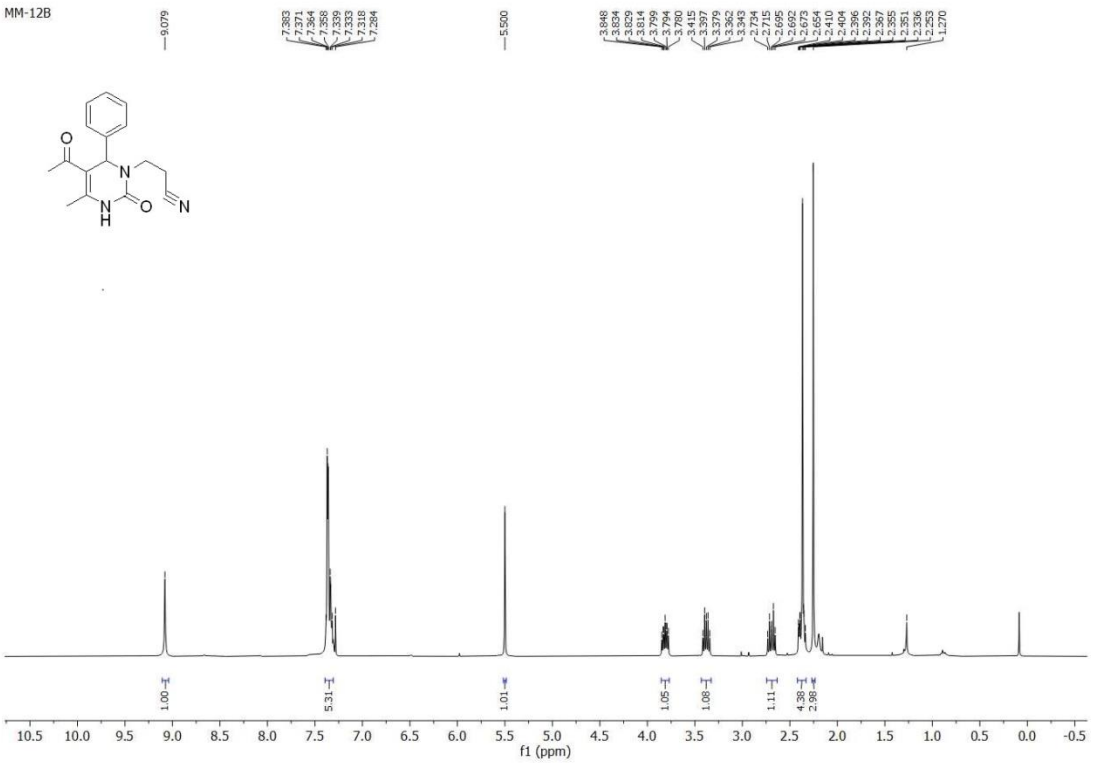

^{13}C-NMR of 26a

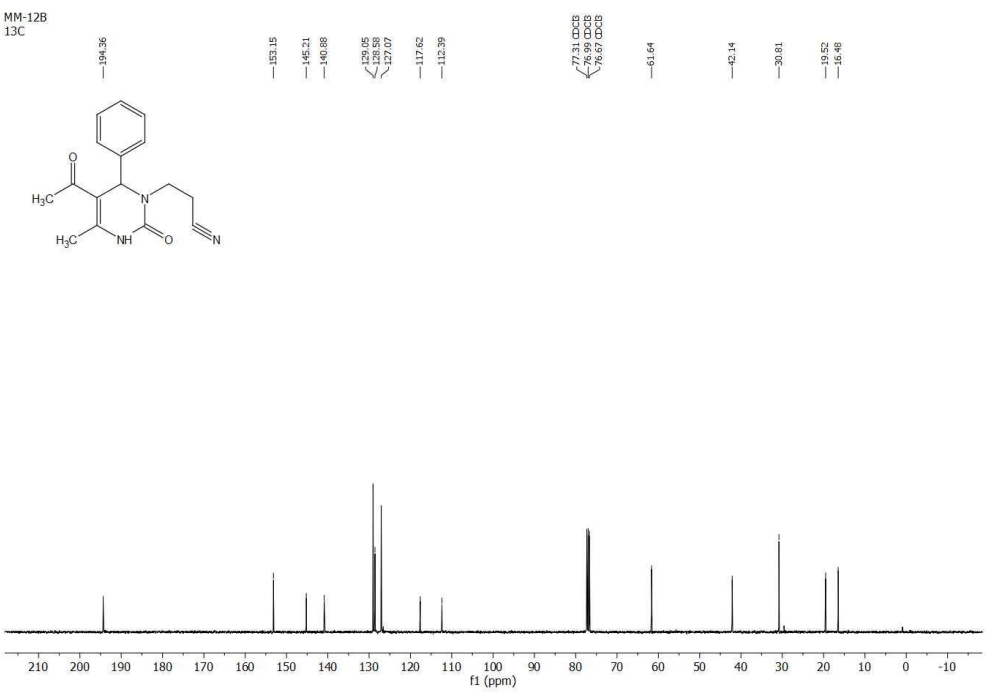

^{1}H-^{1}H-COSY of

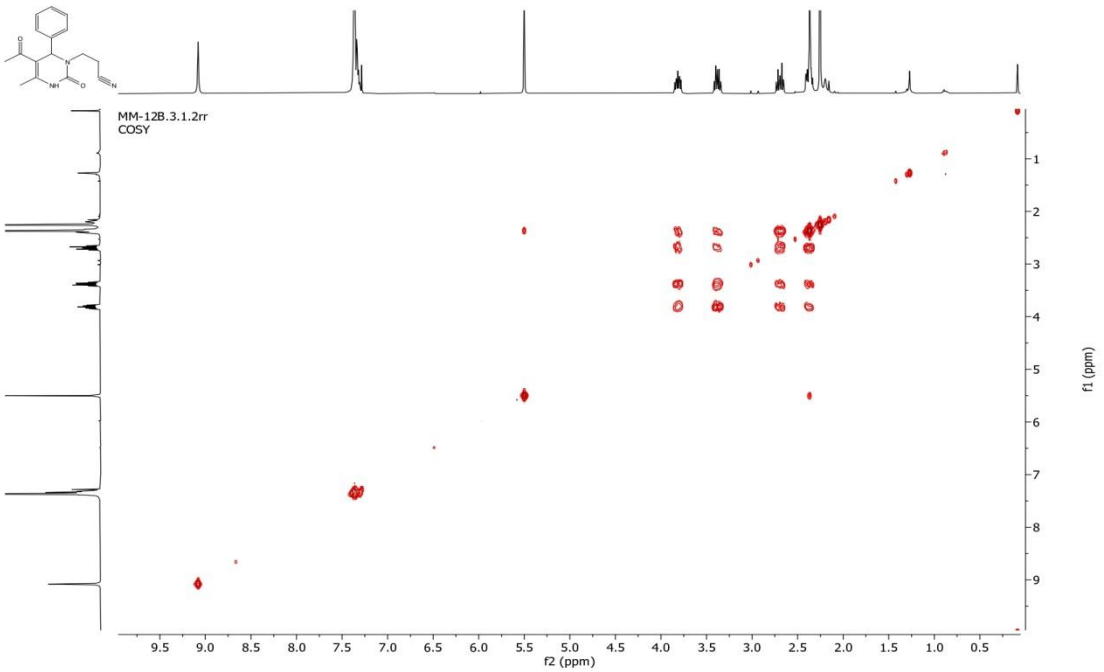

HSQC-of 26a

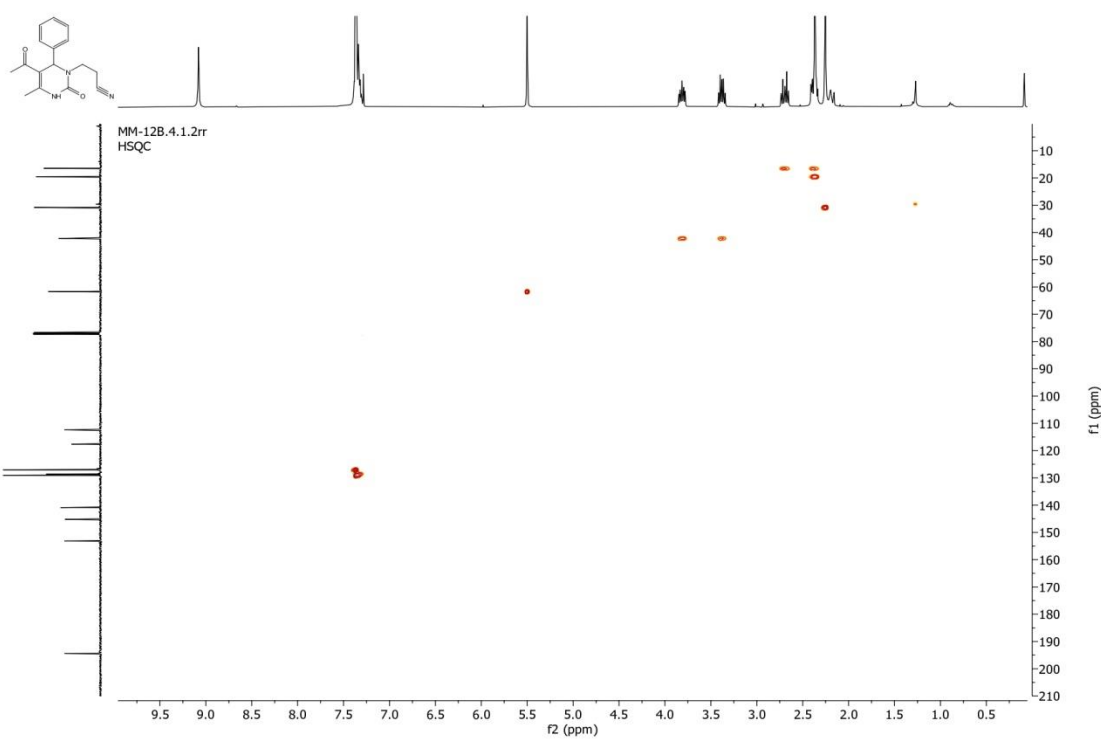

HMBC of 26a

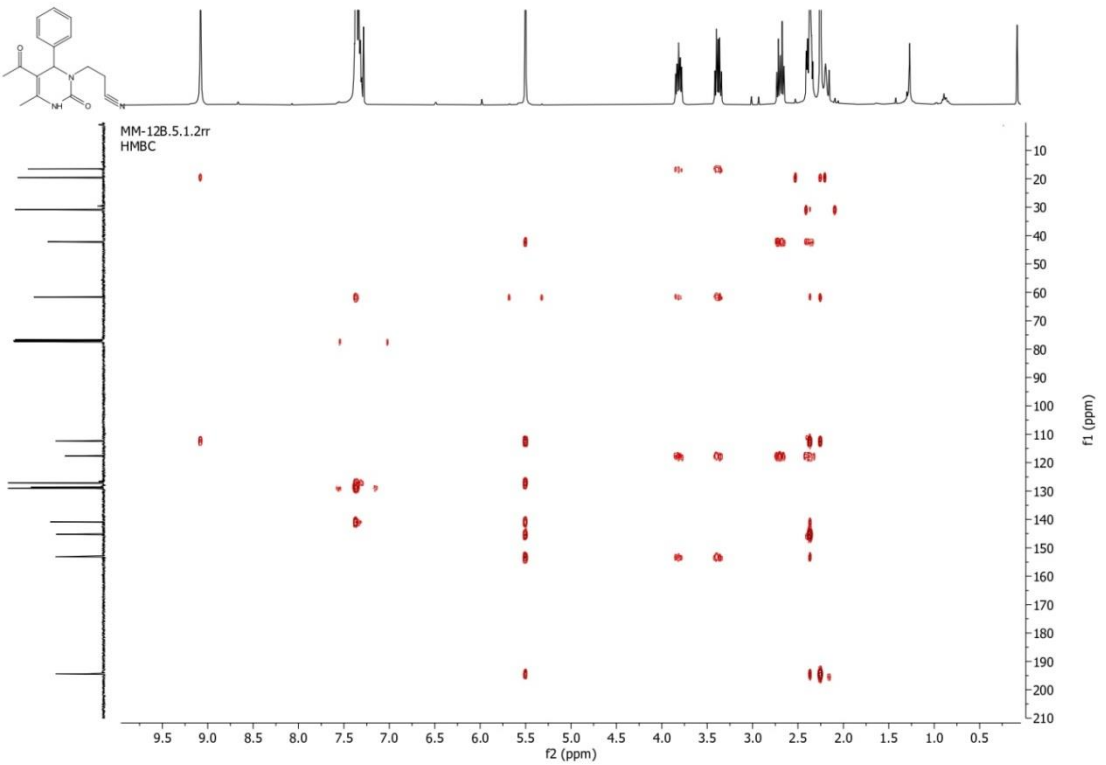

^{1}H-NMR of 26b

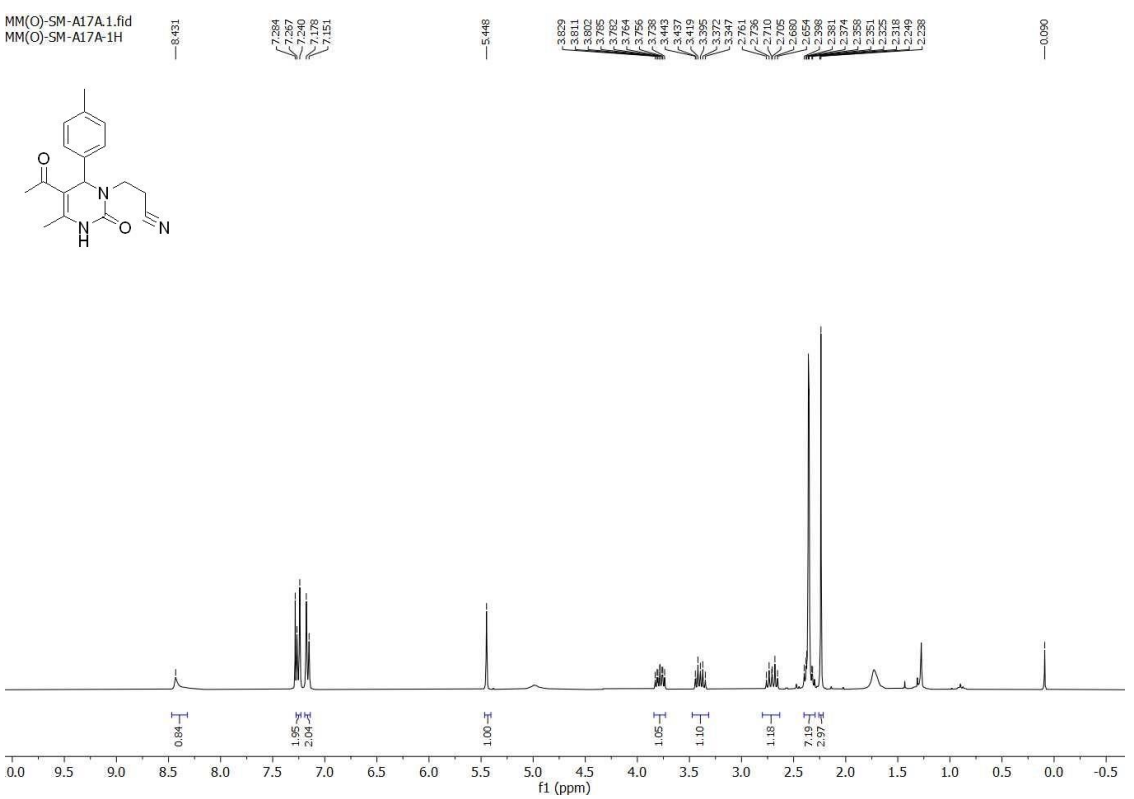

^{13}C-NMR of 26b

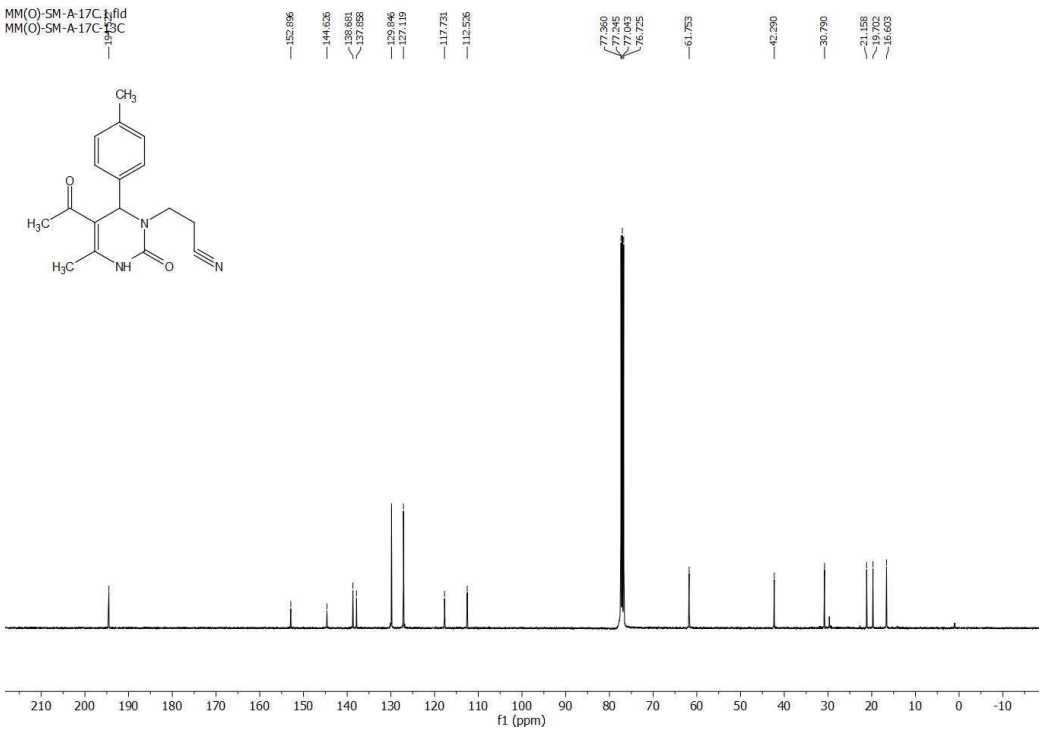

^{1}H-NMR of 26c

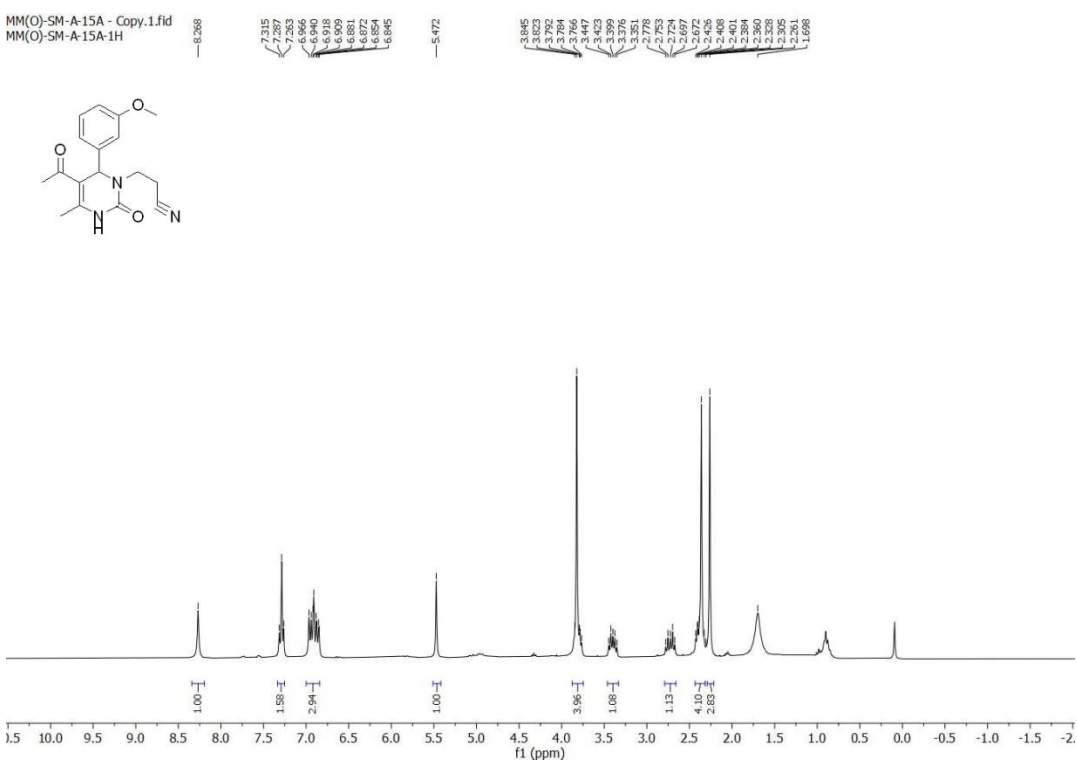

^{13}C-NMR of 26c

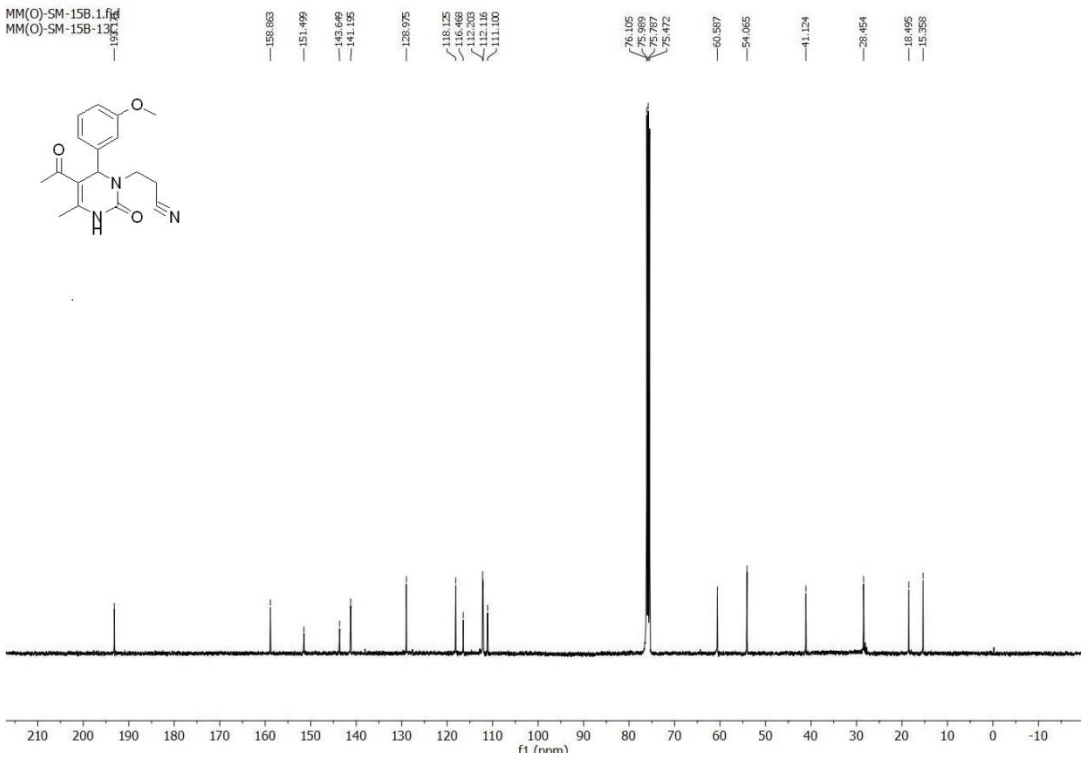

^{1}H-NMR of 26d

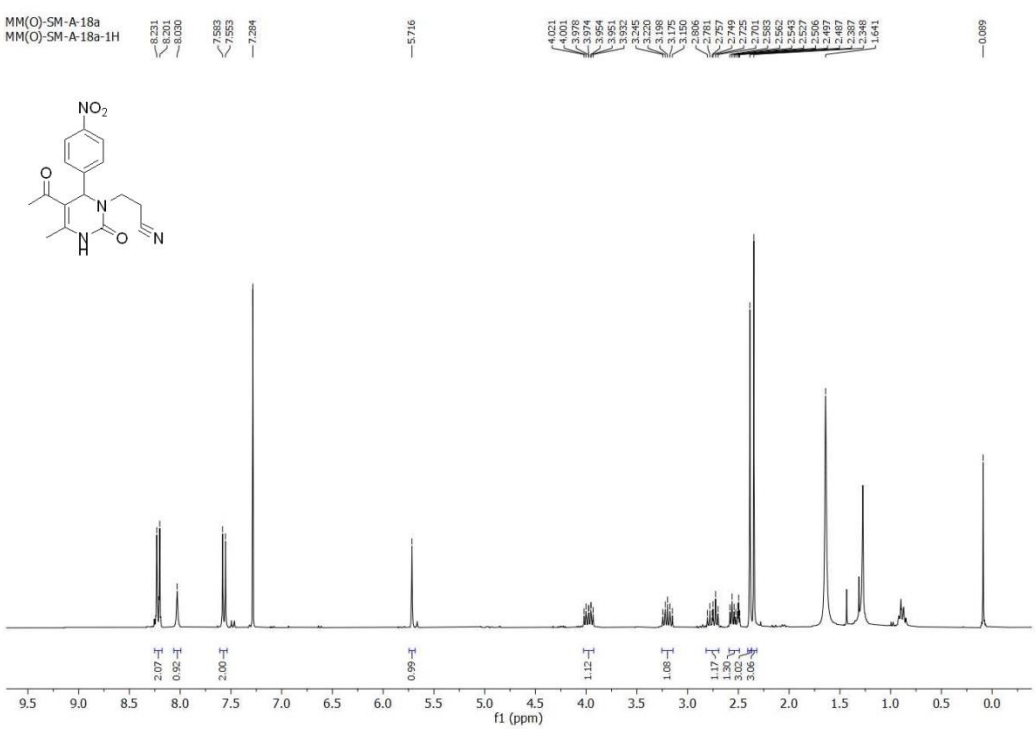

^{13}C-NMR of 26d

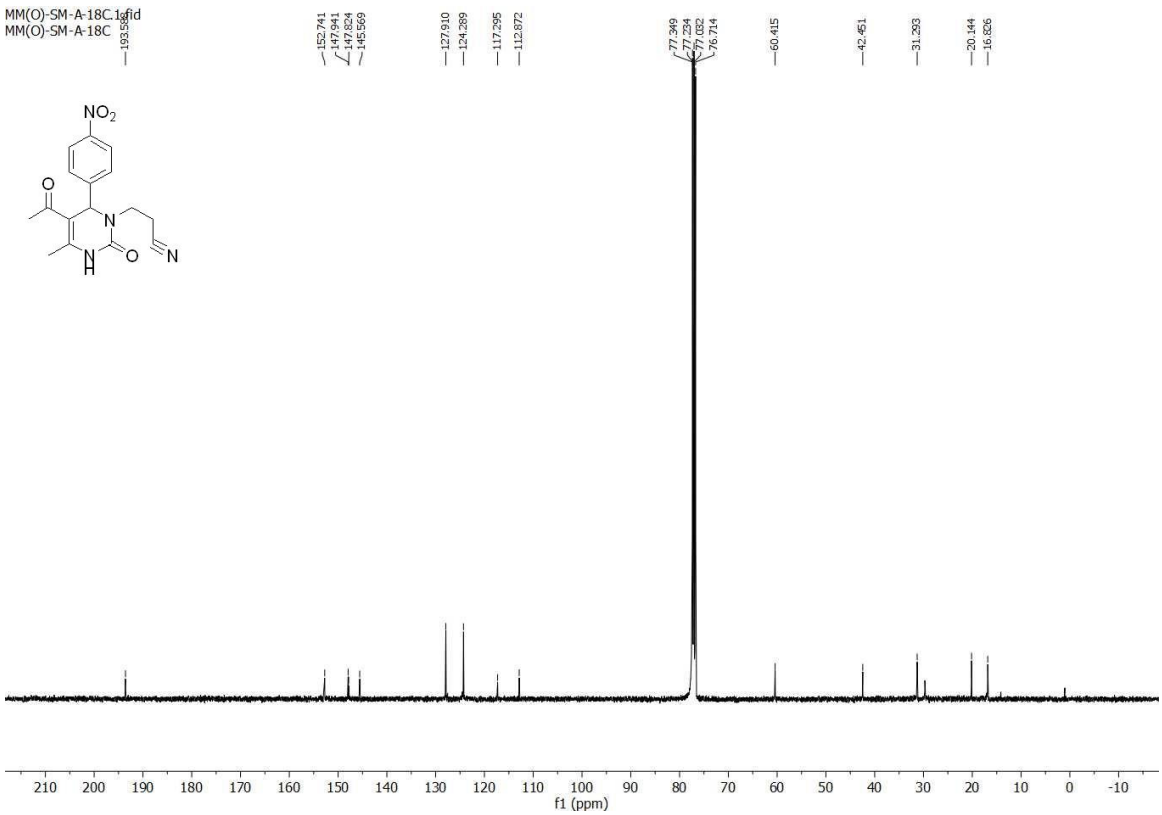

^{1}H-NMR of 28a

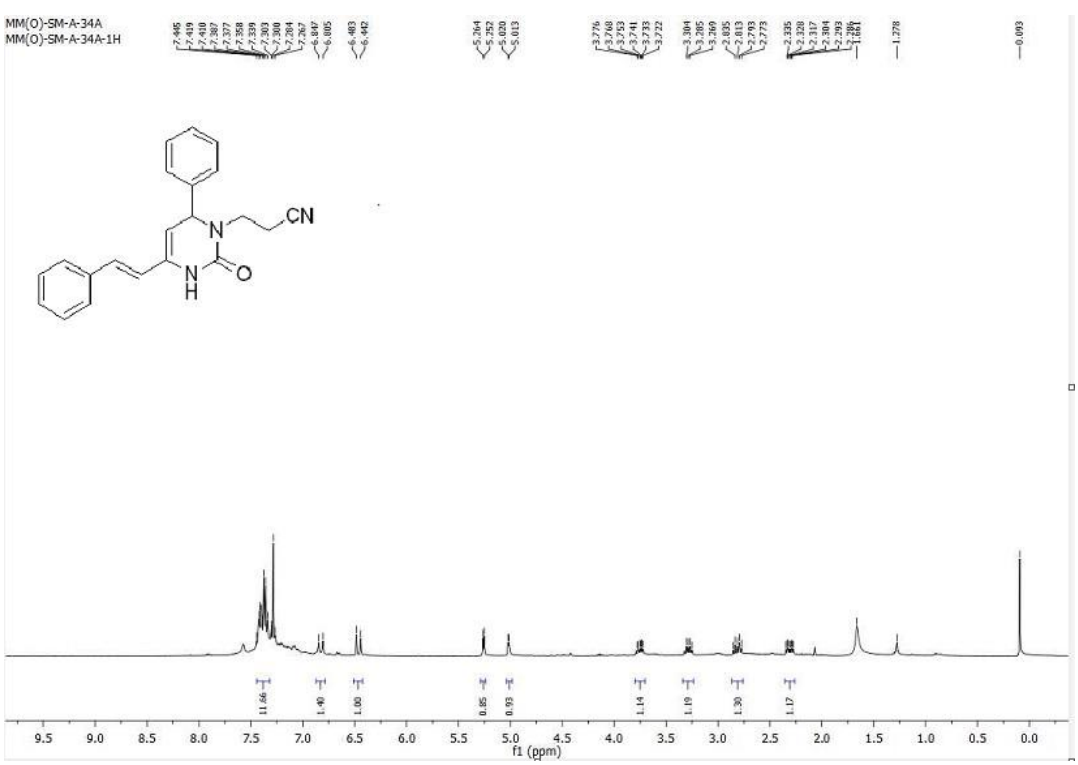

^{13}C-NMR of 28a

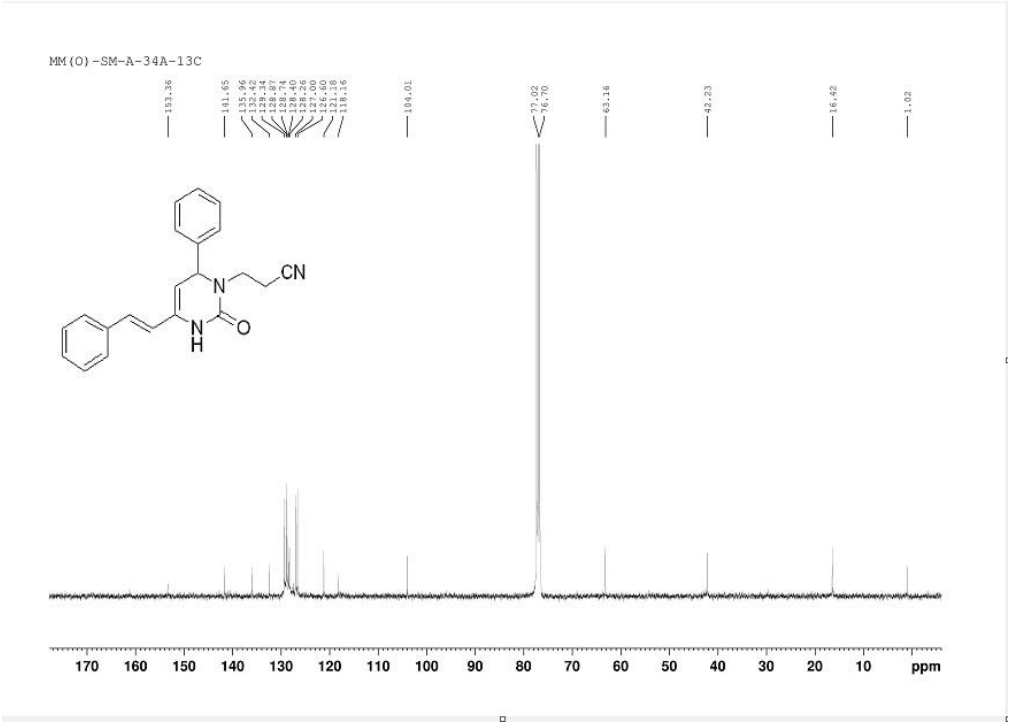

^{1}H-NMR of 27a

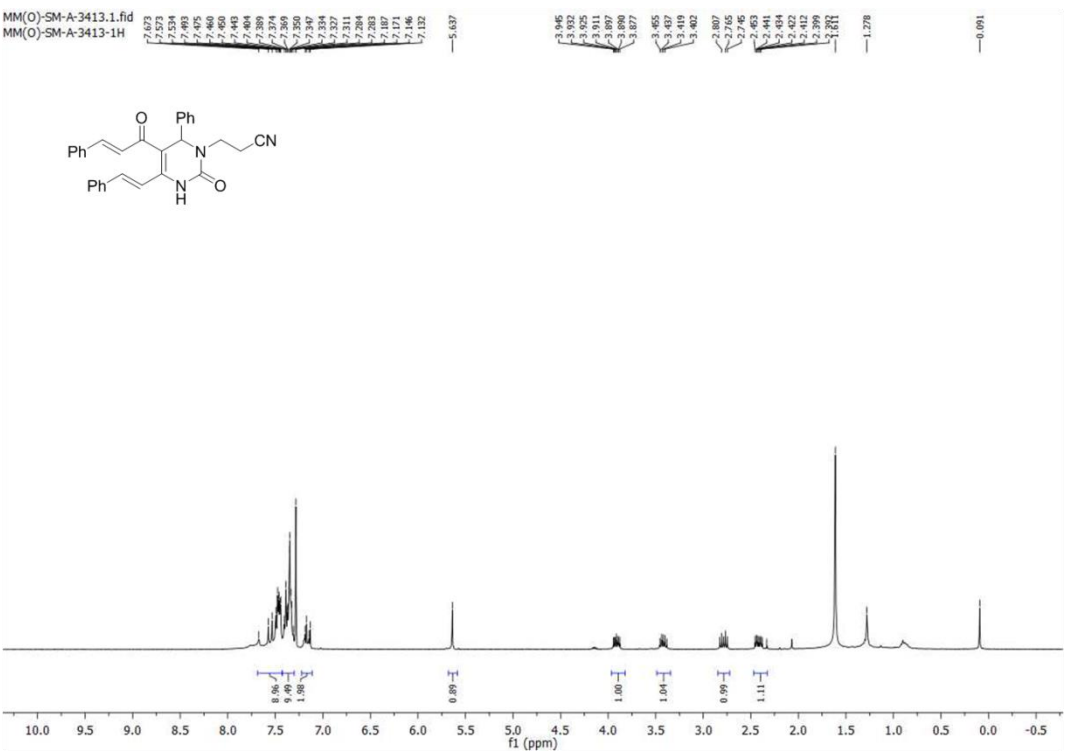

^{13}C-NMR of 27a

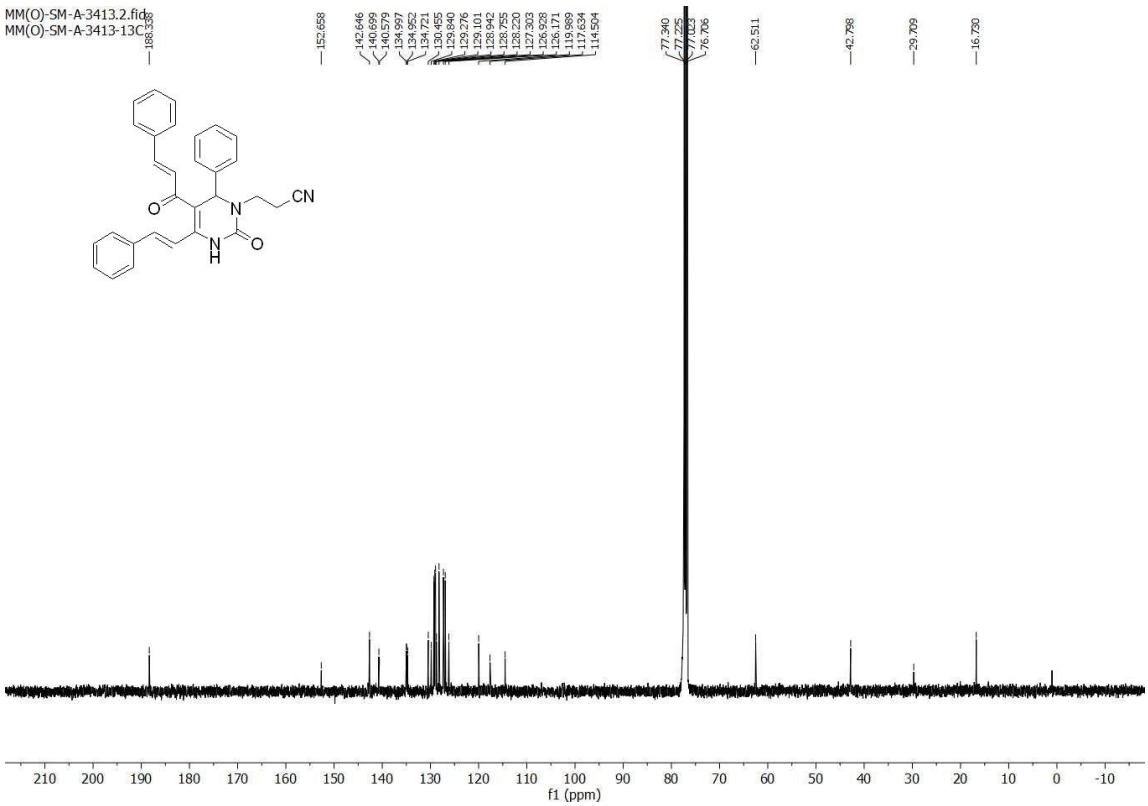

IR-Spectra of 26a

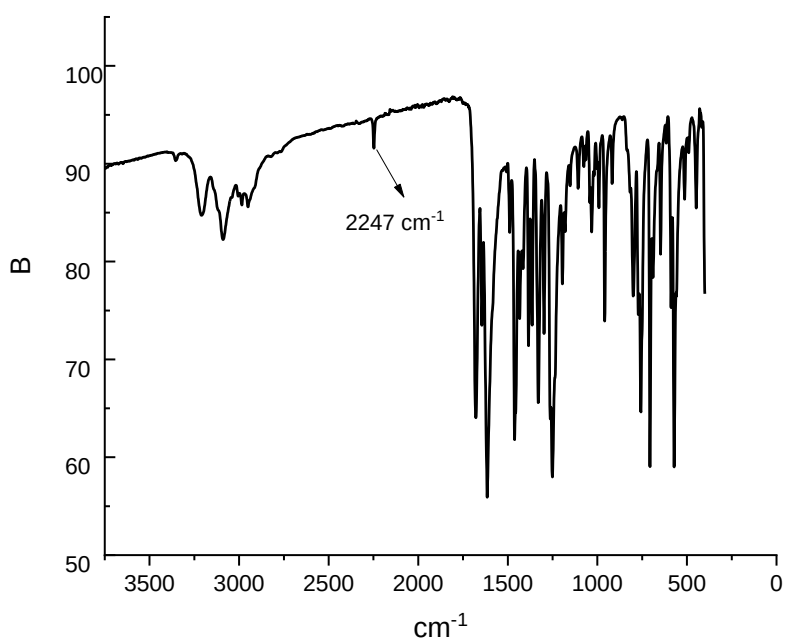

2.5 REFERENCES

[1] S. M. Sondhi, R. N. Goyal, A. M. Lahoti, N. Singh, R. Shukla, R. Raghubir, *Bioorg. Med. Chem.* **2005**, *13*, 3185-3195.

[2] J. G. Maring, H. J. Groen, F. M. Wachters, D. R. Uges, E. G. de Vries, *Pharmacogenomics J.* **2005**, *5*, 226-243.

[3] a)S. Khasimbi, F. Ali, K. Manda, A. Sharma, G. Chauhan, S. Wakode, *Curr. Org. Synth.***2021**, *18*, 270-293; b)R. Kaur, S. Chaudhary, K. Kumar, M. K. Gupta, R. K. Rawal, *Eur. J. Med. Chem.* **2017**, *132*, 108-134.

[4] P. Biginelli, *Ber. Dtsch. Chem. Ges.***1891**,*24*, 1317-1319.

[5] J. M. Matthews, F. Liotta, W. Hageman, R. A. Rivero, L. Westover, M. Yang, J. Xu, K. Demarest, *Bioorg. Med. Chem. Lett.* **2004**, *14*, 1155-1159.

[6] R. Yadlapalli, O. P. Chourasia, R. Perali, *Tetrahedron Lett.* **2012**, *53*, 6725–6728.

[7] A. Shaabani, M. Seyyedhamzeh, A. Maleki, F. Hajishaabanha, *Tetrahedron* **2010**, *66*, 4040-4042.

[8] F. Sánchez-Sancho, M. Escolano, D. Gaviña, A. G. Csáky, M. Sánchez-Roselló, S. Díaz-Oltra, C. del Pozo,*Pharmaceuticals***2022**, *15*, 948.

[9] V. M. Timoshenko, Y. M. Markitanov, Y. G. Shermolovich, *Tetrahedron Lett.* **2011**, *52*, 6619-6622.

[10] U. Rashid, R. Sultana, N. Shaheen, S. F. Hassan, F. Yaqoob, M. J. Ahmad, F. Iftikhar, N. Sultana, S. Asghar, M. Yasinzai, F. L. Ansari, N. A. Qureshi, *Eur. J. Med. Chem.* **2016**, *115*, 230-244.

[11] A. D. Shutalev, A. N. Aksionov, *Mendeleev Commun.* **2005**, *15*, 73-75.

[12] D. Wei, W. D. Wilson, S. Neidle, *J. Am. Chem. Soc.* **2013**, *135*, 1369-1377.

[13] C. H. Leung, D. S. Chan, V. P. Ma, D. L. Ma, *Med. Res. Rev.* **2013**, *33*, 823-846.

[14] J. Portugal, *Biochem. Pharmacol.* **2018**, *155*, 336-345.

[15] K. M. McKinnon, *Cur protoc Immunol.***2018**, *120*, 5.1.1-5.1.11.

[16] C. J. Gomes, M. W. Harman, S. M. Centuori, C. W. Wolgemuth, J. D. Martinez, *Cell Div.* **2018**, *13*, 6.

[17] V. Roukos, G. Pegoraro, T. C. Voss, T. Misteli, *Nat. Protoc.* **2015**, *10*, 334-348.

[18] B. A. D. Neto, J. R. Correa, J. Spencer, *Chem. Eur. J.* **2022**, *28*, e202103262.

[19] A. Ligasová, K. Koberna,*Molecules***2021**, *26*, 5515.

[20] a)S. Neidle, M. Sanderson, **2022**, 191-286; b)K. T. McQuaid, A. Pipier, C. J. Cardin, D. Monchaud, *Nucleic Acids Res.* **2022**, *50*, 12636-12656; c)J. B. Chaires, *Curr. Opin. Struct.*

Biol. **1998**, *8*, 314-320; d)C.-H. Leung, D. S.-H. Chan, V. P.-Y. Ma, D.-L. Ma, *Med. Rec. Rev.***2013**, *33*, 823-846.

[21] A. L. Weis, F. Frolow, *J. Chem. Soc., Perkin Trans.* **1986**, *1*, 83-90.

[22] V. M. Timoshenko, Y. M. Markitanov, Y. G. Shermolovich, *Tetrahedron Lett.* **2011**, *52*, 6619-6622.

[23] S. Cannizzaro, *Justus Liebigs Ann. Chem.***1853**, *88*, 129-130.

[24] H. Kaoukabi, Y. Kabri, C. Curti, M. Taourirte, J. C. Rodriguez-Ubis, R. Snoeck, G. Andrei, P. Vanelle, H. B. Lazrek, *Eur. J. Med. Chem.* **2018**, *155*, 772-781.

[25] E. Safari, A. Maryamabadi, A. Hasaninejad, *RSC Adv.***2017**, *7*, 39502-39511.

[26] A. Sharifi, M. S. Abaee, A. Tavakkoli, M. Mirzaei, *Iran. Chem. Soc.***2008**, *5*, 113-117.

[27] C. O. Kappe, *Acc. Chem. Res.* **2000**, *33*, 879-888.

[28] W.-C. Shieh, S. Dell, O. Repič, *J. Org. Chem.***2002**, *67*, 2188-2191.

[29] N. Ataci, E. Ozcelik, N. Arsu, *Spectrochim. Acta. A Mol. Biomol. Spectrosc.* **2018**, *204*, 281-286.

[30] I. D. Kuntz, Jr., F. P. Gasparro, M. D. Johnston, Jr., R. P. Taylor, *J. Am. Chem. Soc.* **1968**, *90*, 4778-4781.

[31] a)J. Eberhardt, D. Santos-Martins, A. F. Tillack, S. Forli, *J. Chem. Inf. Model.* **2021**, *61*, 3891-3898; b)O. Trott, A. J. Olson, *J. Comput. Chem.* **2010**, *31*, 455-461.

[32] J. O. Trent, G. R. Clark, A. Kumar, W. D. Wilson, D. W. Boykin, J. E. Hall, R. R. Tidwell, B. L. Blagburn, S. Neidle, *J. Med. Chem.* **1996**, *39*, 4554-4562.

[33] L. I. Grossweiner, *J. Photochem. Photobiol. B: Biol.* **2000**, *58*, 175-177.

[34] R. Bera, B. K. Sahoo, K. S. Ghosh, S. Dasgupta, *Int. J. Biol. Macromol.* **2008**, *42*, 14-21.

[35] N. Shahabadi, S. Kashanian, F. Darabi, *DNA Cell Biol.* **2009**, *28*, 589-596.

[36] N. Shahabadi, A. Fatahi,*J. Mol. Struct.***2010**, *970*, 90-95.

[37] C. Schweigert, N. Gaß, H.-A. Wagenknecht, A.-N. Unterreiner, *Chem. Photo.Chem.***2018**, *2*, 12-17.

[38] A. V. Zelenin, in *Fluorescent and Luminescent Probes for Biological Activity (Second Edition)* (Ed.: W. T. Mason), Academic Press, London, **1999**, 117-135.

CHAPTER-3

Studies towards the synthesis of Luotonin/Rutaecarpine alkaloids analogues with applications

3.1 INTRODUCTION

Cancer, a known disease from pre-historic times, has been the most severe and concerning issue in the last five decennary because of increasing levels of carcinogens in the environment.[1] From investigation it was revealed that various types of cancer[2] are the second highest cause of mortality. Among several kinds of used therapeutic drug for the treatment of cancer, quinazolinone based compounds showed promising result. Along with anti-cancer[3] properties, these also show diverse pharmacological activities.[4] Developing cancer therapeutics based on the existing concepts is a complex and challenging process due to the inherent heterogeneity of the disease and drug resistance. Therefore, finding new drugs that selectively target molecular alterations or cancer hallmarks is essential.[5]Two major revolutions have changed the arena of cancer treatment in the past few years: targeting actionable modification in oncogene-driven cancers and immunotherapy. Various challenges are still under way in both fields of cancer therapy. The growing research evidence over the last few decades on the anti-cancer properties of natural quinazolinone and their synthetic derivatives is promising.[6] A handful number of quinazolinone-alkaloids (**Figure-3.A**) such as Luotonin, Rutaecarpine, Evodiamine have been reported in the literature having high pharmacological activities against profuse cell lines.

Luotonin A & B[7], Luotonin E & F[8] were isolated from *Peganum nigellastrum.* The natural and the synthetic analogues of Luotonins are potent inhibitors of the DNA topoisomerase II,[9] besides their other bioactivities.[10] The Rutaecarpine was isolated from *Tetradium Ruticarpum*, exhibit also a wide range of pharmacological activities.Anti-cancer properties of Rutaecarpine was evaluated in different types of cancers such as Prostate Cancer cells, liver cancer,[11] Colorectal Cancer,[12] Cesophageal squamous cell carcinoma,[13] cervical cancer[14]etc. Among the total cancer burden, cervical cancer is the fourth most frequent cancer in women worldwide. Except for anti-cancer activity, Rutaecarpine also shows anti-inflammatory properties through the suppressed COX-2 and COX-1 dependent phases of PGD2 production in BMMC,[15] anti-diabetic properties by preventing vascular aging,[16] inhibition effect from the SARS-CoV-2 infection,[17] anti-fungal activity,[18] etc. On account of the therapeutic importance of Luotonin A, B, E, F and related natural products, the research work towards synthesis and biological study of the natural and synthetic variants became an inevitable topic in medicinal chemistry and allied subjects. [19]

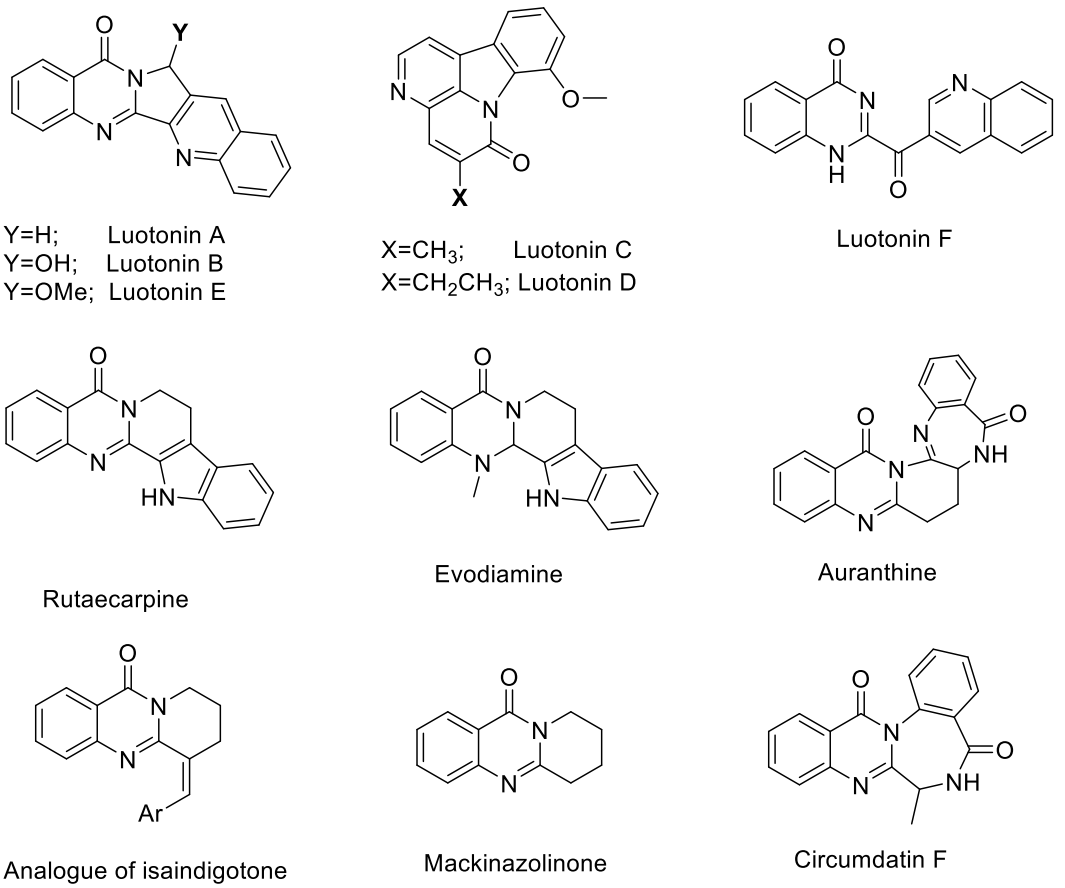

Figure-3.A: Some important Quinazolinone based alkaloids

The available methods for the synthesis of Luotonin and related compounds involve the formation of the ring C and D(**Scheme-3.A**)by the formation of the *C-N* bond 1 with mitsunobu reaction 10% *HCl* in THF,[20] one-pot synthesis by making the ring C and D,[19] formation of the ring B by ammonium persulphate mediated intramolecular formation of *C=N* bond 4[21] (**33a**), Palladium-Catalysed one-pot sequential cyanation followed by cyclization,[22] ammonium persulphate mediated intramolecular *C=N* bond formation, by using a radical cyclization cascade in the presence of Bu_3Sn/AIBN,[23] bifurcated multi-component approaches,[24] visible light-induced intramolecular *C−N* Cross-Coupling intramolecular reductive cyclization of ortho-nitroarenes,[25] (**Scheme-3.A**) etc. Most of these methods used complex starting materials and required multistep for constructing ring C and installing the -Y group in **33a**. The halogenated compounds **32b, 32d** were also used to make the ring C by Pd(II) catalyst[26] or by radical[27] cyclization. Because of the dehalogenation, use of expensive phosphine ligands and extra synthetic steps to install halogen, suffer from low isolated yield. Formation of the *C- C* bond by cross- dehydrogenative coupling (CDC) in substrate **32h** would be a significant advancement as the preparation of *N*-benzyl quinazolinones (**32h**) would be straightforward from easily available starting materials.

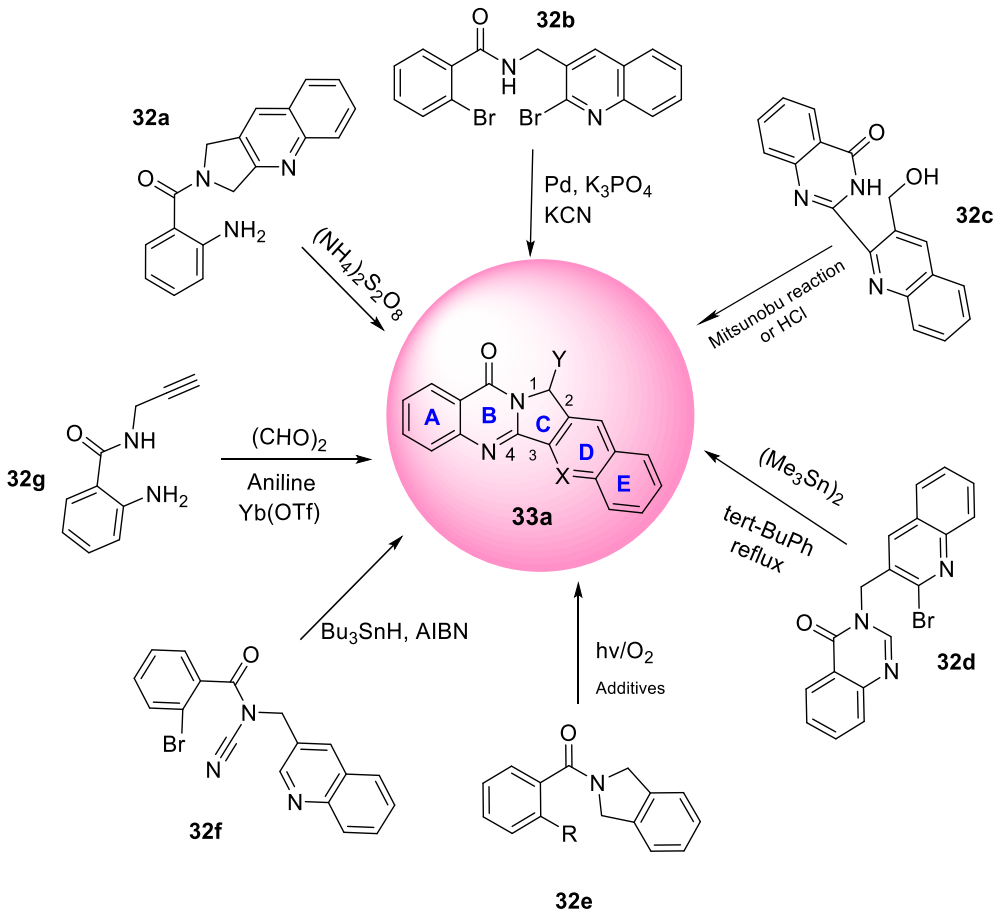

Scheme-3.A Reported methods of synthesis of Luotonin and related compounds

The class of Cross-dehydrogenative coupling (CDC) reaction was unfolded by Chao-Jun Li (McGill U),[28] resulting in the formation of direct *C-C* or *C-N* bond from two unmodified *C-H* bonds for *C-C* bond formation or *C-H* and *N-H* bonds for *C-N* bond formation. The advantage of CDC approach is the direct tandem oxidation of simple *C-H* and *N-H* bonds, which permits the use of simple/ readily available reagents and reduces number of steps towards the formation of the desired product. Although, some difficulties are yet to be overcome e.g; low reactivity of some *C-H* bonds, dimerization, over oxidation etc. The types (CDC) of reaction are used to construct bonds between sp^3-sp^3, sp^3-sp^2, sp^3-sp, sp^2-sp^2, sp^2-sp, and sp-sp carbon atoms, including *C*(sp^3)-*N*. The mechanism and reactivity of these types of coupling reaction are dramatically depends on the substrate. Direct arylation can be achieved with one electron-rich arene (pyridine, amide, carbamate etc) and other electron-deficient arenes. Sanford and Hull have developed a method for Pd-catalyzed oxidative cross-coupling of arenes based on regioselective ligand-directed *C–H* activation.[29] Heterocyclic arenes (**33b)** resulted in a facile, regioselective *C–H* activation to form intermolecular *C-C* bond formation with another aromatic compound.[30] In the absence of a directing ligand, Lu and co-workers[31] obtained Pd-catalyzed *C–H* activation to give cross-coupled products with naphthalene

and anisole in the presence of TFA, giving **33c1** through intermolecular CDC mechanism. Another palladium-catalyzed intermolecular CDC reaction of benzofurans with arenes was achieved by DeBoef and co-workers[32] using oxygen as the terminal oxidant and the co-oxidant heteropolymolybdovanadic acid (HPMV) in acetic acid at 120 °C, the product phenylbenzofuran **33d1** was obtained (**Scheme-3.B**).

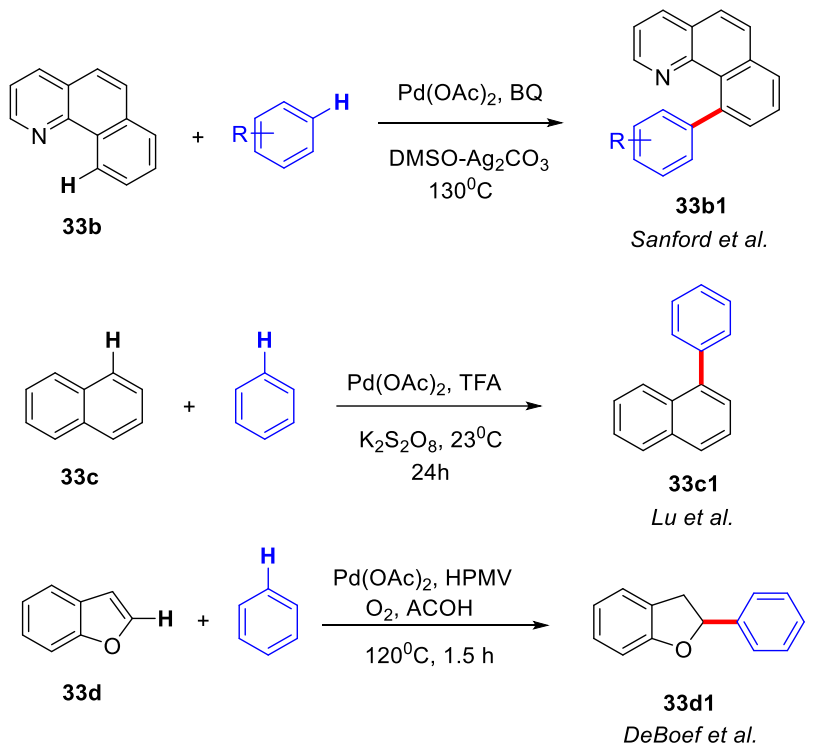

Scheme-3.B Intermolecular cross dehydrogenative coupling

Chen and Xu et al.[33] established a highly efficient palladium-catalyzed and atom-economical intramolecular cross dehydrogenative coupling (CDC) reaction to access coumarin-containing fused polyheterocycles with good to excellent yields. Yang and Ding et al.[34] achieved an efficient palladium-catalyzed intramolecular *C-H* activation CDC reaction for facile construction of diverse coumarins-fused indanone compounds (**33f1**). Along with intermolecular CDC, DeBoef[35]and his co-worker also exhibit Pd-catalyzed intramolecular cross-dehydrogenative coupling product **33g1** from **33g** with microwave heating (**Scheme-3.C**).

Based on the intramolecular CDC reaction,[36] we designed and successfully executed a short, efficient synthetic method for Luotonin/Rutaecarpine analogues. We assumed that the palladium catalyzed one pot, intramolecular CDC reaction of the *N*-benzyl quinazolinone would form ring C along with the formation oxo-functionality –R (**Scheme 3.D**).

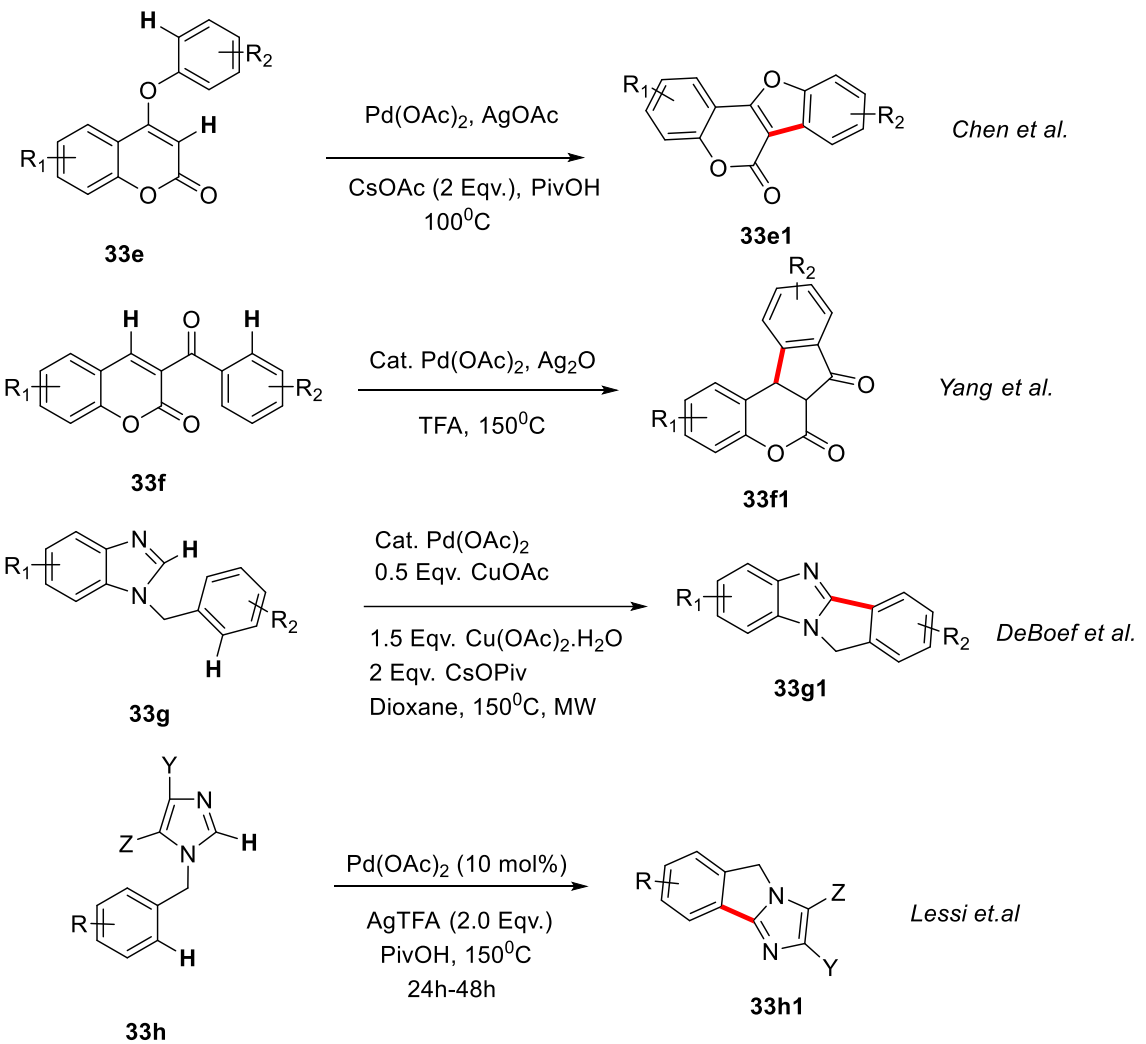

Scheme-3.C Intramolecular dehydrogenative cross coupling

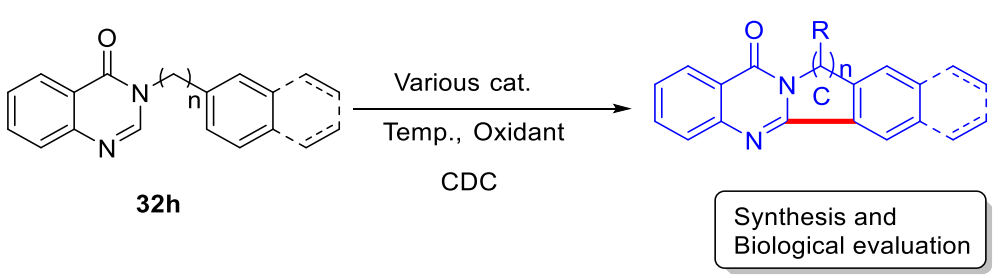

Scheme-3.D Our synthetic strategy

Herein, we established a convenient method for the synthesis of novel Luotonin/Rutaecarpine analogue through palladium catalysed intramolecular cross-dehydrogenative coupling (CDC) and checked the electronic influence of this reaction by varying substrate scopes. The synthetic procedure and spectroscopic data of the starting quinazolinones and corresponding coupling products have been described below. Most importantly, we investigated the novelty of the materials with the study of calf-thymus DNA interaction as a model and finally found an important application of **37d**, one of

the synthesized compounds described in the result and discussion portion of this chapter. We performed a concentration-dependent cell viability assay on the SiHa cell line (human cervical cancer cell line) using the compound **37d** to evaluate anti-cancer properties. The results (cytotoxicity dose calculation) show that the compound may have similar anti-cancer properties with reported Luotonin analogues.[37]

3.2 RESULT AND DISCUSSION:

Our initial study started with the reaction of quinazolin-4(3H)-one (**34a**) and benzyl bromide in the presence of 5 Eqv. K_2CO_3, 10 mol% sodium iodide in acetone under refluxing condition for 24h. Gratifyingly, expected 3-benzylquinazolin-4(3H)-one (**36a**) was isolated in 91% yield (**Scheme-3.E**).The structure of **36a** was characterized by the use of spectroscopic techniques NMR and MS. In ^{1}H NMR spectrum, a characteristic singlet appeared at δ 5.11 ppm for -CH_2 which indicate that the *N*-benzylic/ *O*-benzylic protons position of the expected compound. Because of the ambident nucleophilic nature of compound **34** under the K_2CO_3 condition, the position of *N*-alkylation was precisely confirmed by the single crystal XRD of another same series of compound **36d** (**Figure 3.B**). The α, β-unsaturated carbonyl carbon of amide appeared at δ 161.19 ppm along with all other expected peaks in the ^{13}C NMR spectrum (Experimental section of this chapter) confirmed the structure of **36a**. Also, the peak at *m/z* 259.0834 for the $[M+Na]^+$ ion in HRMS further confirmed the structure of this compound(**36a**).

The required all starting materials 3-benzyl quinazolin-4(*3H*)-ones (**36a–36h**) had been synthesized in good yield by alkylation/benzylation at the *N3* of quinazolinon-4(*3H*)-one in the presence of K_2CO_3 in acetone under refluxing condition, according to above reported protocol[38] (**Scheme 3.E**).The known[39] compound **36k** was synthesized by the alkylation of **34b** with 2-bromomethyl naphthalene under similar conditions. The *N*3-alkylation was extended to synthesize compounds **36i**& **36j**.[40] The structures of all other compounds, **36b**–**36k**, are confirmed by NMR spectroscopy and mass spectrometry. The single crystal XRD of compound **36d** has been shown in **Figure-3.B**. The CIF file of the XRD data of this compound (**36d**) has been submitted to the CCDC centre (CCDC ID 2246052). Having a series of key substrates in hand, we then tried to investigate the optimum reaction condition towards our target synthesis for *C–C* bond formation via catalytic activation.

Inspired by the metal-catalyzed intramolecular CDC developed by Lessi[36] and Srinath,[41] we preliminarily carried out the reaction with the compound **36a** as shown in **Scheme-3.D**, under different catalytic compositions with different oxidants.At preliminary screening, no change of starting material was observed after 48 hours when compound **36a** was treated with 10 mol% of both

$Pd(OAc)_2$ and AgOAc in ethanol at 80°C (**Table-3.A**, Entry 1). However, when we changed the solvent from ethanol to acetic acid, and the temperature raised 120°C, we observed only 10% yield of compound **37a**, and the remaining starting was recovered. It was observed that acetic acid is crucial for the desired conversion. Keeping the reaction medium acetic acid unaltered, we performed the reaction with different compositions of the $Pd(OAc)_2$ and AgOAc and found that 0.2 equivalent $Pd(OAc)_2$ along with 3 equivalent AgOAc gave the best result up to 75% isolated yield (**Table-3.A**, Entry 4). Moreover, AgOAc alone cannot convert **36a** into **37a** under similar conditions (**Table-3.A**, Entry 5).

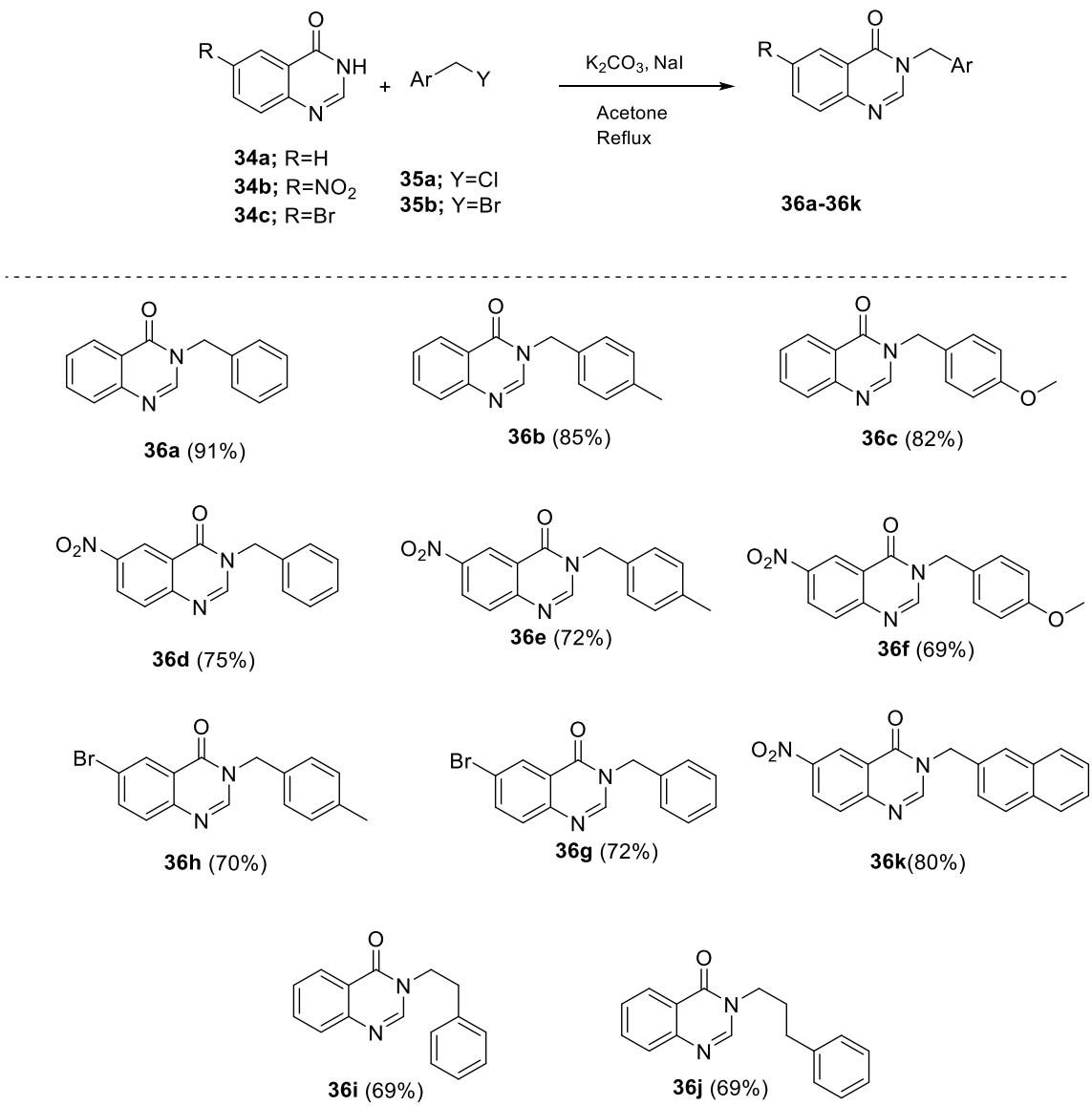

Scheme-3.E Preparation of starting materials

To find an alternative for AgOAc as the oxidizing agent, we have studied the reaction in the presence of different oxidants such as $K_2S_2O_8$, benzoquinone, mCPBA, H_2O_2, ^tBuOOH, $Cu(OAc)_2$, and it appeared that none of these were suitable for the reaction. All of them resulted in the recovery of the

starting compound **36a** (**Table-3.A**, Entry 7–14). The Pivalic acid medium was inappropriate for this study (Entry 6). The structure of compound **37a** is determined unambiguously by NMR and mass spectroscopy. Analysis of the ^{1}H-NMR and ^{13}C-NMR, HSQC, and HMBC data of compound **37a** is shown in **Figure-3.C**. Thus, compound **36a** undergoes one pot, intramolecular CDC, to form a new (sp^2)*C*-*C*(sp^2) bond along with the oxidation of the labile benzylic position and α to the nitrogen *N*-*CH*$_2$-Ar atom to form *N*-*CH*(OAc)$_2$-Ar. Thus, the method is helpful for synthesizing Luotonin analogues from easily accessible starting materials.

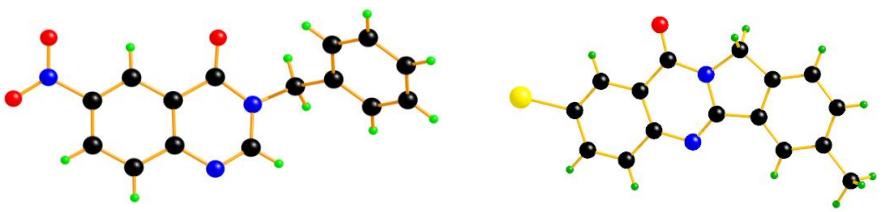

Figure-3.Bsingle crystal XRD structure of **36d**and **38h**

(For the detailed crystal parameters, see the experimental section of this chapter)

Table-3.A Optimization of the reaction condition

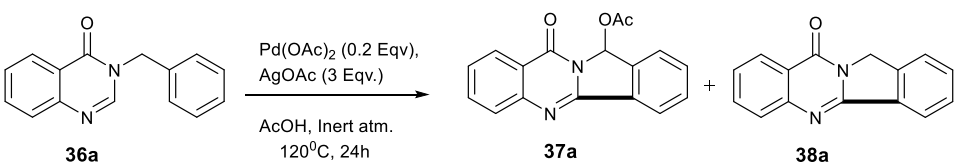

Entry	Catalyst	Additive	Solvent	T (°C)	Time (h)	% Yield (37a :38a)
1	Pd $(OAc)_2$ (0.1 Eqv.)	AgOAc (0.1Eqv.)	EtOH	80	48	SR[a]
2	Pd $(OAc)_2$ (0.1 Eqv.)	AgOAc (0.1Eqv.)	AcOH	120	24	10 :0
3	Pd $(OAc)_2$ (0.1 Eqv.)	AgOAc (1 Eqv.)	AcOH	120	24	25 :0
4	Pd $(OAc)_2$ (0.2 Eqv.)	AgOAc (3 Eqv.)	AcOH	120	24	75 :0
5	–	AgOAc (6 Eqv.)	AcOH	120	24	SR[a]
6	Pd $(OAc)_2$ (0.2 Eqv.)	AgOAc (3 Eqv.)	Pivalic acid	120	24	45 :0
7	Pd $(OAc)_2$ (0.2 Eqv.)	$K_2S_2O_8$ (1Eqv.)	1,4 Dioxane	100	24	SR[k]
8	$Pd_2(dba)_3$ (0.2 Eqv.)	AgOAc (1 Eqv.)	CH_3CN	60	48	SR[k]
9	Pd $(OAc)_2$ (0.2 Eqv.)	Benzoquinone (1 Eqv.)	AcOH	120	24	SR[k]
10	Pd $(OAc)_2$ (0.2 Eqv.)	mCPBA (3 Eqv.)	DCM	40	48	SR[k]
11	Pd $(OAc)_2$ (0.2 Eqv.)	H_2O_2 (2 Eqv.)	AcOH	120	20	SR[k]
12	Pd $(OAc)_2$ (0.2 Eqv.)	^{t}BuOOH(2 Eqv.)	AcOH	120	24	SR[k]
13	Pd $(OAc)_2$ (0.2 Eqv.)	O_2 Gas	Xylene	120	20	SR[k]
14	$Pd(PPh_3)_4$ (0.1Eqv.)	^{t}BuOOH(1.5 Eqv.)	AcOH	120	24	SR[k]

Note: All the reactions are carried out at 100 mg scale under inert atmosphere [k] Starting Recovered

To check the scope of the reaction, we have done the above reaction with various starting materials having electronically different functional groups such as methyl, methoxy, nitro, and bromo at the ring A and D (**Scheme-3.G**) under the optimized condition and the results are shown in **Table-3.B**. It has been observed that the electronic effect of the attached functional group at ring D has less influence, and the outcome of the reactions is almost comparable (**Table-3.B**, Entries 1–3 & 6). However, the course of the reaction depends on the electronic nature of group R_2. The electron-withdrawing group, such as nitro or bromo, resulted in the isolation of the intermediate product **38d**, **38e**, **38g** &**38h** along with the formation of corresponding *O*-acetylated product **37** (**Table-3.B**, Entry 4, 5, 7 &8). NMR spectroscopy and mass spectrometry data were used to confirm the structure of all the synthesized compounds. Particularly, we have assigned some carbons and protons of structure the **37a** from the ^{13}C and HMBC correlation spectra (see the experimental section of this chapter) to confirm the benzylic –OAc group (**Figure-3.C**).

Interestingly, we have noticed that in the presence of cat. $Pd(OAc)_2$, $Cu(OAc)_2$ and the additive K_2CO_3, the outcome of the above reaction was entirely changed. The presence of excess $Cu(OAc)_2$ and K_2CO_3 in the acetic acid solvent at 120°C led to the exclusive formation of compound **39** instead of **37a** (**Scheme-F**). On the other hand, in absence of pd(II), no product was found except starting material.

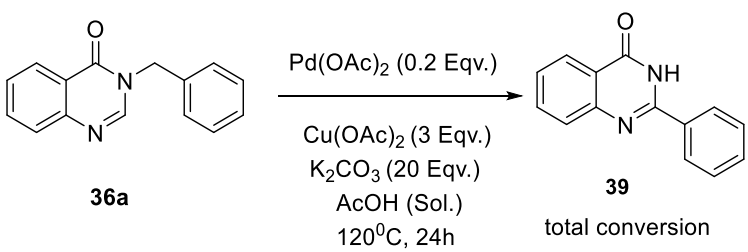

Scheme-F Formation of compound **39**

Having the high crystalline nature of compound **38h**, we have used single crystal XRD along with the NMR and mass to confirm its structure, and the XRD structure has been shown (CCDC ID 2246053) in **Figure-3.B**. Results from the starting **36a**–**36h** (**Table-3.B**) indicate that two distinct chemical transformations are occurring in the presence of $Pd(OAc)_2$/AgOAc, one is the intramolecular catalytic CDC, and another is the *N*-CH_2-oxidation to –*N*-*CH*(OAc)-Ar. The effect of R_2 and R_3 on the *C*-*C* coupling is insignificant, and overall conversions are almost comparable. However, the electronic nature of the R_2 has a critical influence on the–*N*-CH_2-oxidation. Electron withdrawing groups do not favour the -*N*-CH_2-oxidation, so we got the intermediate products **38d**, **38e**, **38g** & **38h**.

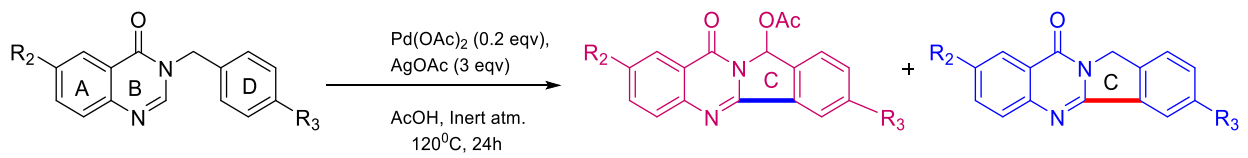

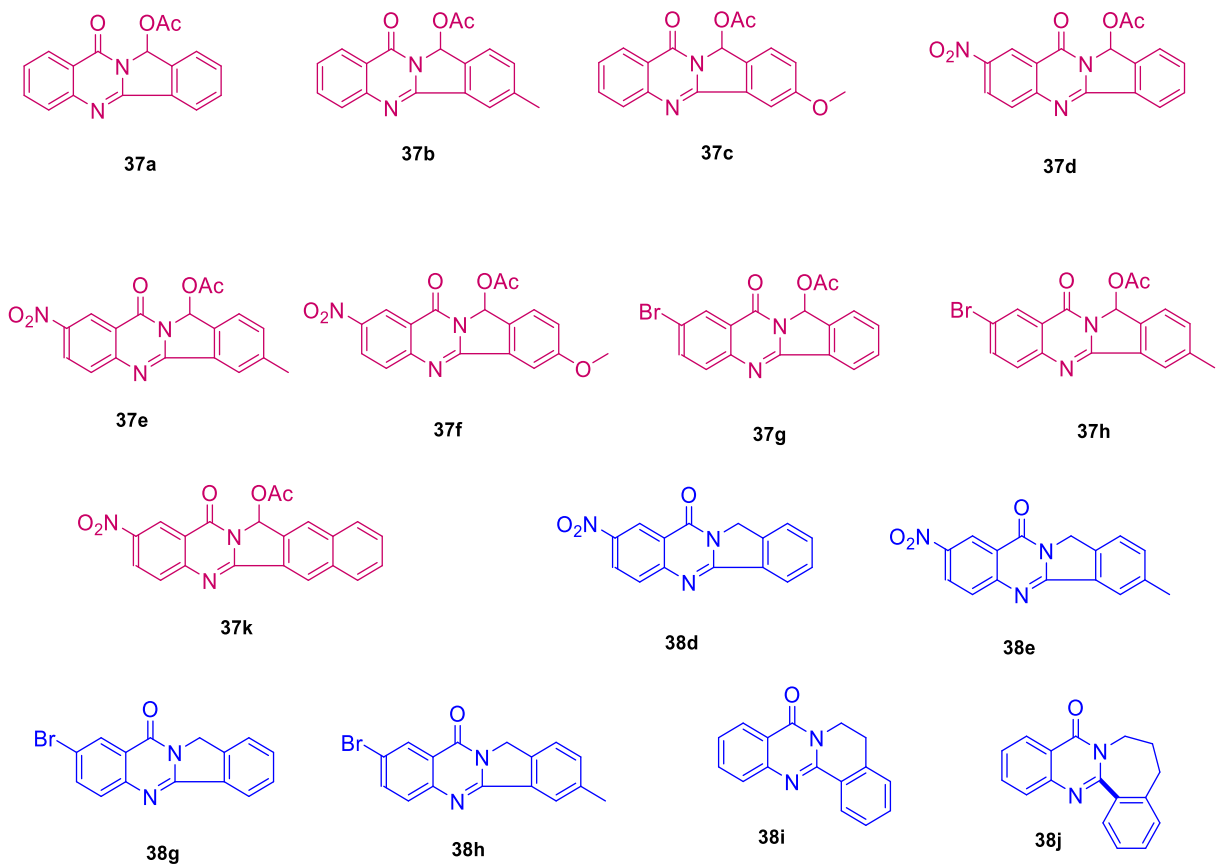

Scheme-3.G Substrate scope study

Table-3.B Result of different substituted products of the reaction **Scheme-3.G**

Entry	Starting	Substituents attached	Product : %yield
1	**36a**	R_2=H R_3=H	**37a**:75 **38a** :0
2	**36b**	R_2=H R_3=Me	**37b**:73 **38b**:0
3	**36c**	R_2=H R_3=OMe	**37c** :80 **38c** :0
4	**36d**	R_2=NO_2 R_3=H	**37d**:50 **38d**:31
5	**36e**	R_2=NO_2 R_3=Me	**37e**:50 **38e** :42
6	**36f**	R_2=NO_2 R_3=OMe	**37f** :60 **38f** :0
7	**36g**	R_2=Br R_3=H	**37g**:0 **38g**:70
8	**36h**	R_2=Br R_3=Me	**37h**:30 **38h**:50

Assignment of selected NMR signals and the HMBC correlations to the structure of **37a**

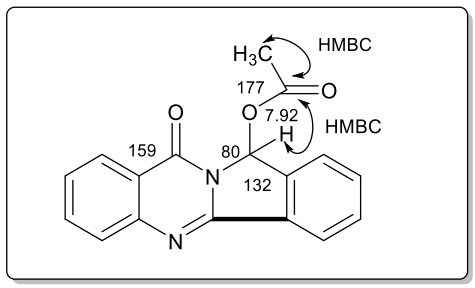

Figure-3.C Structure conformation of **37a**

Moreover, the *N-CH₂-* oxidation depends on the nature of the methylene group. Experimental results from the substrates **36i** and **36j** indicate that the benzylic nature and ring strain facilitates the *N-CH₂-* oxidation (**Scheme-3.H**). We have experimented to find the relative ease of the two transformations, namely CDC and oxidation of *N-CH₂-*, as shown in **Scheme-3.I**. When compound **38e** was treated under the same condition, it converted smoothly to **37e** in a quantitative yield. This result indicates that the dehydrogenation cross-coupling is kinetically more facile than the *N-CH₂-* oxidation under acidic condition. Therefore, the nitro group, being an electron-withdrawing nature, slows down the *N-CH₂-* oxidation, leading to the isolation of the intermediate **38e** from the starting **36e**.

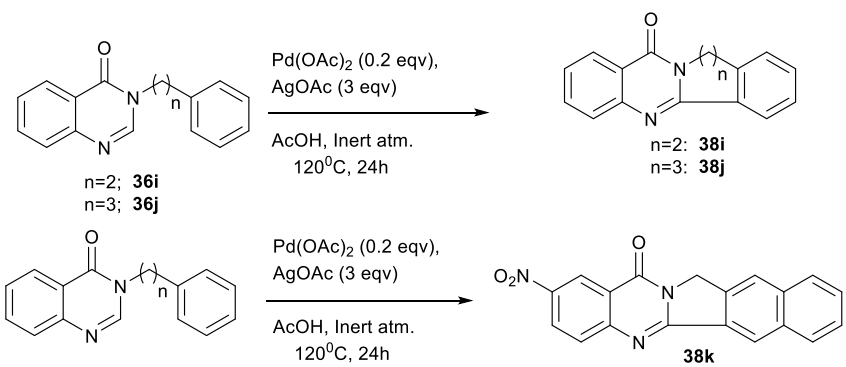

Scheme-3.H Effect of the number of the *-CH₂-* units between nitrogen andaromatic ring

Considering the observed electronic effect of R_2 and R_3 on compounds **36**, the result of the reaction and the study of similar reports, we have proposed a probable mechanism of this transformation in **Scheme-3.J**.

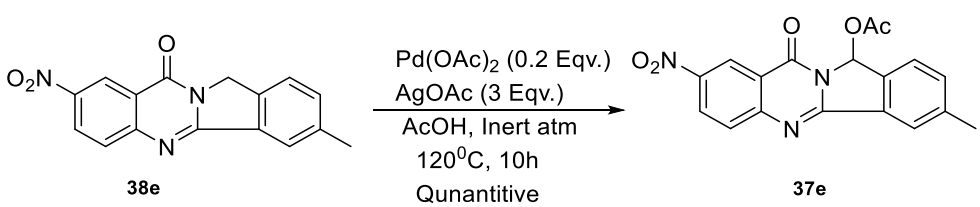

Scheme-3.I Experimental evidence to prove the oxidation sequences

There involves two catalytic cycles: cross-dehydrogenative coupling (CDC) and -*N*-*CH*$_2$-oxidation. The first one is initiated by a directed palladation at the *ortho* position of ring D of **36**, followed by a second step i.e, *C*-*H* activation. Subsequently, reductive elimination leads to product **38**. Product **38** then enters a second the catalytic cycle where the carbonyl-directed acetylation at the -*N*-*CH*$_2$-position occurs to give product **37**.

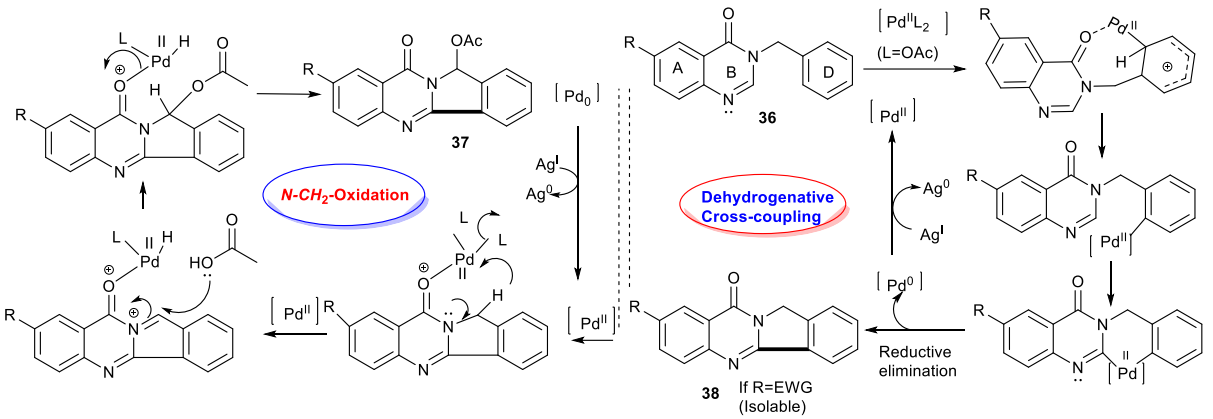

Scheme-3.J Proposed mechanism

In the case of bromo and nitro, the intermediate product generated after the first catalytic cycle was isolated along with the -*N*-*CH*$_2$-oxidation product after the second catalytic cycle. The formation of compound **39** in excess K_2CO_3 is presumably due to the preferred reaction path -*N*-*CH*$_2$-oxidation over the *C*-*C* cross-coupling in the presence of Cu^{II}. Under excess basic conditions, the oxidized product **39a** undergoes structural rearrangement with the release of a unit of HCOOH to convert product **39**, as shown in **Scheme-3.K**.

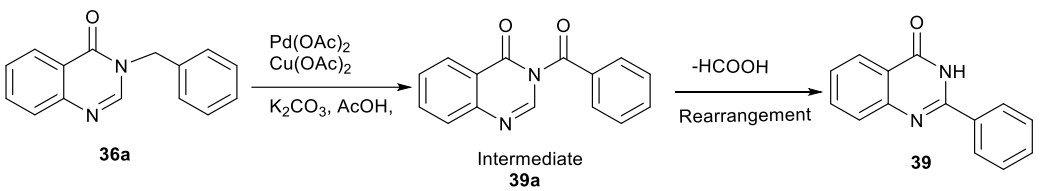

Scheme-3.K Mechanistic explanation for the formation of **39**

3.3 DNA BINDING STUDY TOWARDS DRUG DEVELOPMENT:

Luotonins, having their lower toxicity and higher chemical stability compared with similar alkaloid, campatothecin,[42]have gained considerable interest in the study of biological properties. Sometimes, they afford the novel self-fluorescence properties due to the presence of aromatic heterocyclic rings along with extended conjugation, which facilitates the useful detection of drug-DNA interactions. Notably, the anti-cancer activities of Luotonin A against human breast cancer (MCF–7) and other human cancer have been successfully demonstrated by DNA interaction study[43]. As DNA and proteins is the primary target in the action of anti-cancer drugs, determination of the binding of

molecules to DNA or protein is the basis of discovering the more efficient anti-cancer drug.[43-44]Especially, the drug-DNA interaction analysis is an important tool in pharmacology, for attributing the influence of drug absorption, metabolism, distribution, excretion etc.[45]

3.3.1 Interaction studies on with calf-thymas DNA(ct-DNA)

After successful synthesis and characterize of some new Luotonin analogues compounds, to check the novelty of these molecule, we studied the DNA binding interaction with one of our compound **38h** as it showed a good absorption spectrum with calf-thymus DNA(ct-DNA). The DNA binding mode have been evaluated using absorption (UV-Vis), emission spectral studies (Fluorescence), circular dichroism (CD), melting point measurements etc.

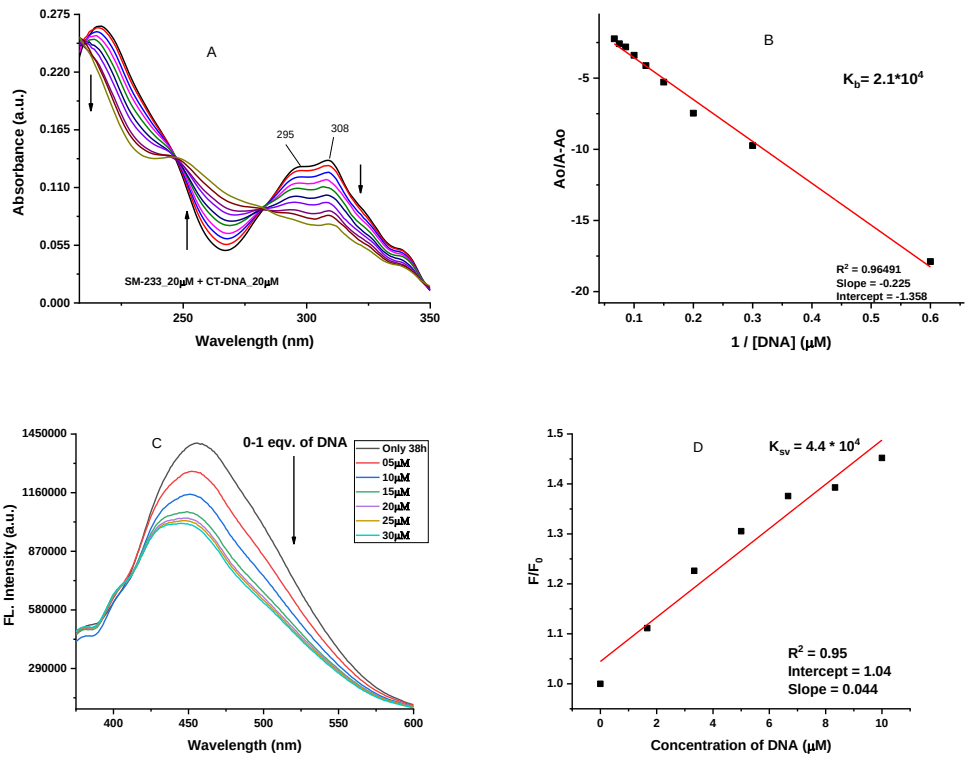

Figure-3.D (A) UV–Vis spectra for **38h** (20 μM) in the absence and presence of ct-DNA. The UV titration was carried out by increasing the concentration of ct-DNA. The arrow direction indicates the change in absorption peak intensity by increasing DNA concentration. (B) Linear plot obtained from A_0 /(A –A_0) vs. 1/[DNA], where A_0 and A are the absorptions in the presence and absence of DNA at 308 nm. Measured K_b = 2.1*10^4 M^{-1}. (C) Fluorescence titration spectra of **38h** (20 μM) in the presence of DNA at a different concentration (0–1 μM), at pH 7.2 in 10 mM Tris–HCl buffer at 25 °C. The first reading (black line) is the Fl spectrum of **38h** in the absence of DNA. The arrow's direction indicates an intensity quenching. (D) The linear plot of F/F$_0$ vs. [DNA]. The emission band at 460 has been used to monitor the change in fluorescence intensity and at the excitation wavelength 308 nm to calculate Kq= 4.4 *10^4 M^{-1}.

The absorption spectral titration study of compound **38h** with ct-DNA is shown in **Figure-3.D**. Upon increasing the addition of DNA to **38h**, a hypochromic shift was observed in the position of maximum absorption peak 308 nm. However, the presence of a clear isosbestic points in the UV-Vis spectra (**Figure-3.D** (A)) revealed that interaction may be present with ct-DNA. In order to quantitatively explore the binding affinity of the compound (**38h**) with DNA, the intrinsic binding constant K_b have been calculated from the Benesi–Hildebrand Equation[46] (see chapter-2). From the linear plot (**Figure-3.D** (B)) i.e, the ratio of intercept to the slope $A_0/(A-A_0)$ vs. 1/[DNA] gave the value of binding constant (K_b= $2.1*10^4$ M^{-1}). As the exact mode of interaction cannot be confirmed merely by this technique, further experiments were carried out to explore the binding mode.

To further elucidate the interaction of **38h** with ct-DNA, the fluorescence titration experiment has also been performed in 10mM Tris-HCl at pH 7.2, showing a broad unstructured peak with maxima around 460 nm (**Figure-3.D** (C)). In addition to ct-DNA, quenching in the fluorescence yield occurred with no detectable shift in the emission peak position. This change in fluorescence spectra establishes the binding interaction of **38h** with ct-DNA. From the classical Stern–Volmer equation (see chapter-2, Eq.(2)), Eq.(6) has obtained:

$$F_0/F = 1 + K_q\,[DNA] \qquad (6)$$

To calculate the quenching constant (K_q), the ratio of peak fluorescence intensity in the presence and absence of ct-DNA (F/F_0) has been plotted as a function of DNA concentration (**Figure-3.D** (D)). The plot indicated that the fluorescent intensity is directly proportional to the DNA concentration. From the slope of the Stren-Volmer plot the calculated moderately higher Kq $4.43*10^4$ established the possibility of intercalation of **38h** with ct-DNA.

From the time-resolved fluorescence spectroscopy (**Figure-3.E** (E)),the average decay lifetime of ct-DNA has been calculated**.** We observed only 0.73 ns (a minor change) enhancement of the half-life ($t_{1/2}$) of the excited state of **38h** between the free and bound state, respectively, in the fluorescence lifetime on increasing concentration of ct-DNA. This value could be regarded as less signified that the interaction between ct-DNA and compound was static. Consequently, the steady-state fluorescence and fluorescence lifetime measurements confirmed that quenching was mainly static caused by ground-state complex formation. The binding nature was also suggested by the effect of iodide on the fluorescence emission quenching of **33h** in the presence and absence of ds-DNA. Iodide is known to promote intersystem crossing (ISC) during a collision with fluorophore molecules. Thus, its quenching nature is dynamic. We measured the quenching constant in the presence and absence of ct-DNA by using the Stern–Volmer equation, $F_0/F = 1 + K_{sv}$ [Q], where F_0 and F are the fluorescence intensity in the absence and presence of the anionic quencher [Q]

respectively. Since earlier experiments suggested the interaction between **38h** and DNA, a relatively similar K_{SV} value was expected in KI quenching studies. With the addition of KI, there is an increase in the ionic strength in the medium, resulting in the release of DNA-bound **38h**. Since the fluorescence intensity of free **38h** is less than **38h**-DNA complex. K_{sv} was calculated with and without DNA for **38h**, which are as follows $5.46*10^4$ $M^{-1}$and $2.84*10^4$ M^{-1} respectively. The significant change in K_{sv} values (**Figure-3.E** (F)) in the presence of ct-DNA with respect to the free chromophore supports the intercalative nature of **38h** to ds-DNA. The significant change in DNA melting temperature, when **38h** bound to the ds-DNA (**Figure-3.E** (H)) is in favour of the intercalation binding mode. The values are shown in **Table-3.F** in the experimental section of this chapter. To obtain further information about the binding of **38h** to DNA, we recorded the CD spectra of ct-DNA with 5.0×10^{-5} mol L^{-1}concentration of **38h** (**Figure-3.E** (G)). A slight change (less prominent) in the CD spectra suggested that, the intercalation is not very persistent.

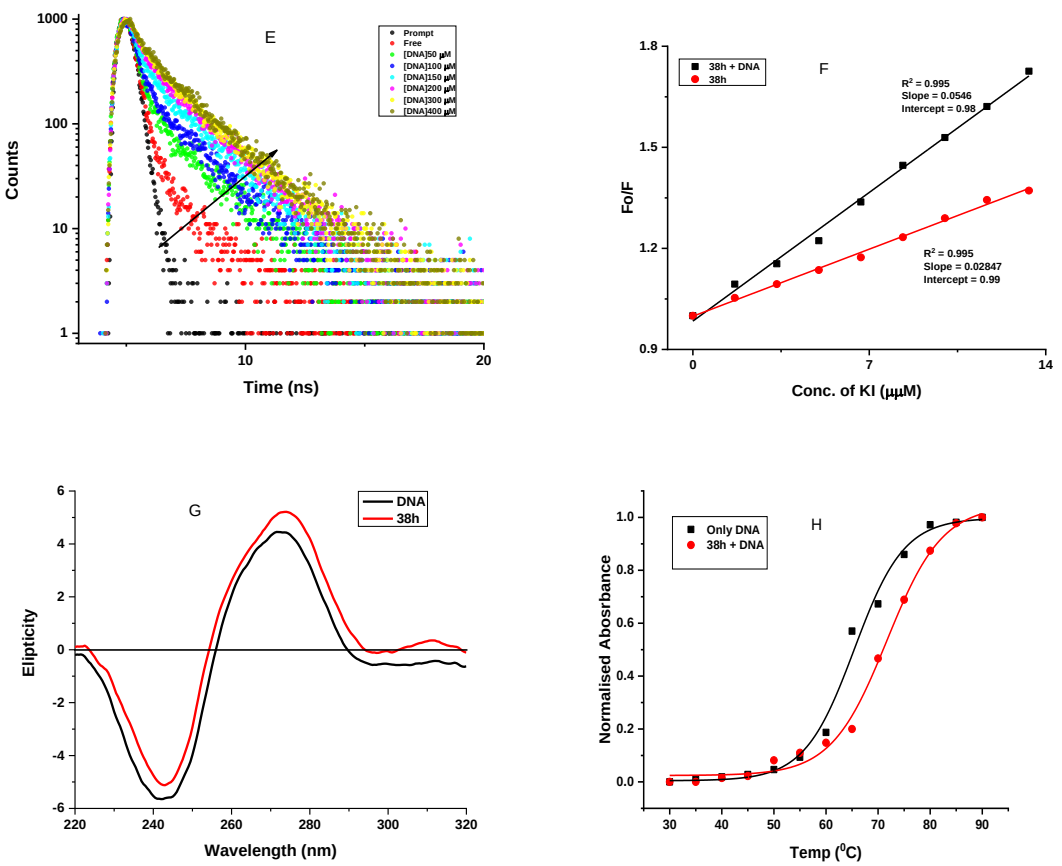

Figure-3.E (E)Time-resolved fluorescence spectra of **38h** at different concentrations of ct-DNA. (F) The relative quenching effect of iodine on fluorescence emission of **38h** in the presence and absence of ct-DNA. (G) CD spectra (black) of ct-DNA in 2 mM Tris–HCl buffer (pH 7.2) and presence of **38h**.(H) DNA melting temperature plot of ct-DNA in 10 mM Tris–HCl buffer (pH 7.2) (black line) and in the presence of compound **38h** (red line).

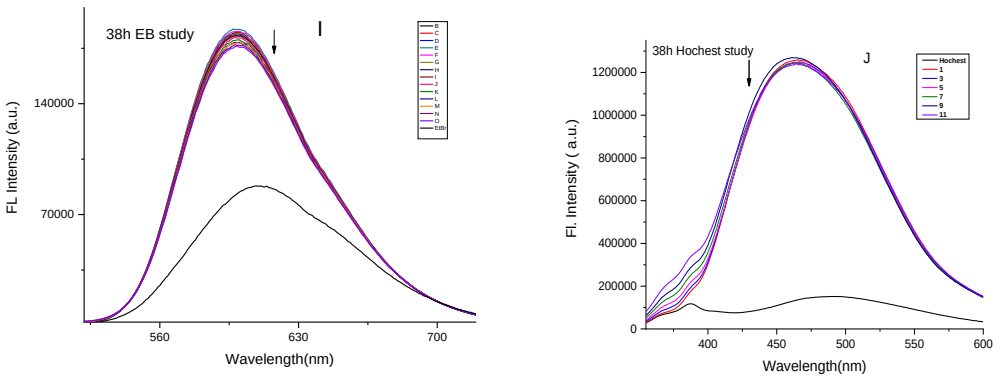

Figure-3.F Comparative study of compound 38h with EB (I) and Hochest 33258(J) dye

The displacement assay with two popular dyes, Ethidium bromide (EB) and Hochest 33258 were monitored at the excitation wavelength 308 nm to see the efficiency of displacement of these dyes by **38h**. EB is a well-known probe that binds to the DNA in an intercalactive fashion and Hoechst 33258 is a well-known groove binder. Hence, these two dyes work as excellent spectral probes to determine the binding mode of drugs with DNA. In the present study, we observed a decrease in fluorescence emission intensity of EB, with the addition of chromophore **38h (Figure-3.F** (I)), an indication of intercalation. On the other hand, there was a negligible change in the fluorescence emission intensity of DNA-bound Hochest 33258 (**Figure-3.F** (J)). This suggested that the compound **38h** moderately replace the EB from ct-DNA, hence it may work as an intercalator with nuclear or cellular DNA. Consequently, we have found the DNA targeting ability of our synthesized compound **38h**, which can be used for the treatment of cancer by DNA cleavage or other.

3.4 BIOLOGICAL STUDY

As we know, all Luotonins[47] have shown promising cytotoxicities towards selected human cancer cell lines, we have tried to check our other series of compound i.e, *N*-benzylic oxidation products (**37**) applicability. Structural modification sometimes used for improving the biological properties. Hence, we carried out a concentration-dependent cell viability assay of one of our compound **37d** having structural similarity with Luotonin-E, to check the cytotoxicity on the SiHa cancer cell line.

3.4.1 Cell viability assay

SiHa cervical cancer cell line, purchased from NCCS Pune, India, was cultured in Dulbecco's modified eagle's medium (DMEM) supplemented with 100 U/ml penicillin, 10% FBS, 100 mg/ml streptomycin, and 50 mM glutamine. Furthermore, cells were harvested using trypsin and seeded in a 96-well cell culture plate for the MTT (3-(4,5-Dimethylthiazol-2-yl)- 2,5-diphenyltetrazolium bromide) assay. Our synthesised compound **37d** was solubilized in cell culture grade DMSO (D8418-100 ML, Sigma Aldrich). Once the cells in 96-well plates were 70% confluent, the

compound was treated in the cells at eight concentrations (0.01, 0.1, 1, 10, 20. 40, 80, 100 μM) at37°C for 48 h (**Figure-3.G**). After 48 h, cells were washed with 1xPBS, and added 100 μL of fresh media in each well along with 10 μL of MTT reagent (5 mg/mL) for another 4 h. After 4 h, the media was again removed and added 100 μL cell culture grade DMSO to dissolve the formazan crystals formed by the reduction of MTT by live cells. The quantity of formed formazan crystal was determined as alterations in absorbance at 570 nm wavelength using an ELISA plate reader (MULTISKAN Sky High, Thermoscientific). The initial screening showed that almost 30% and 93% of cell death occurred at 10 μM and 100 μM concentrations, respectively (**Table-3.G**) (see Experimental section of this chapter)

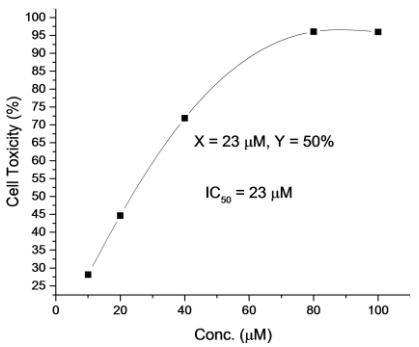

Figure-3.G Plot of toxicity vs. concentration to determine the cytotoxicity dose (IC_{50}) of **37d** in the SiHa cell line by MTT assay.

Therefore, we have further taken three different doses between 10 and 100 μM concentrations (viz. 20 μM, 40 μM, and 80 μM) of this compound (**Figure-3.G**). At 23 μM concentrations of the compound, nearly 50% of cancer cell death occurred. Hence, the 23 μM concentration of the test compound (**37d**) was determined as IC_{50} for the SiHa cell line.

3.4.1.a Chemistry of MTT assay

MTT assay is a colorimetric assay for assessing cell metabolic activity (viability, proliferation and cytotoxicity). This is based on the reduction of the yellow tetrazolium salt namely 3-(4,5-dimethylthiazol-2-yl)-2,5-diphenyltetrazolium bromide (popularly known as MTT) to purple formazan crystals by metabolically active cells enzyme (**Figure-3.H**)[48]. The NADPH-dependent oxidoreductase, present in viable cells, reduces the MTT to formazan[49]. The insoluble formazan crystals are dissolved in solution and the resulting colored solution is quantified by measuring absorbance (500-600 nanometers) using a multi-well spectrophotometer. The amount of the oxidoreductase enzyme, hence the amount of formazan produced, is proportional to the number of viable cells.

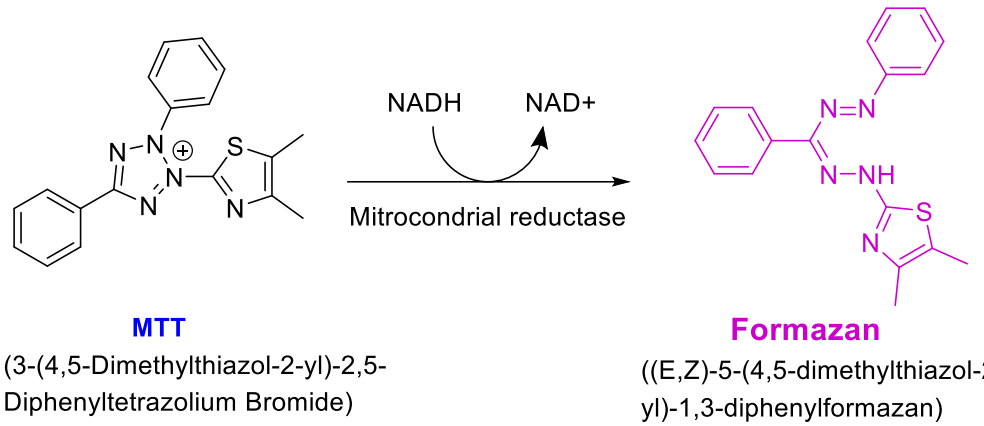

Figure-3.H Metabolism of MTT to a formazan salt by viable cells enzyme

3.5 CONCLUSIONS

We have explored a new synthetic route for Luotonins/ Rutaecarpine analogues compounds and related natural products via a one-pot multistep process. Notably, we observed two distinct chemical transformations: intramolecular dehydrogenative cross-coupling to form a *C-C* bond and functionalization of a *C-H* bond adjacent to a nitrogen atom to *C-OAc*. The combined catalytic system $Pd(OAc)_2$ and excess AgOAc (3 Eqv.) was found to be the most appropriate condition for the said transformations. We observed that the outcome of the reaction is highly dependent on the electronic effect of the group (R_2) attached to the starting materials (**36**) and the P^H of the medium. Based on the experimental observation, a probable mechanism has been proposed.

Therefore, to see the application of our synthesised compound firstly, we saw the DNA target ability with ct-DNA and found slight positive intercalation binding mode of compound **38h**. However, another compound (**37d**) remarkably showed an important biological importance towards application. Significantly, the results of the concentration-dependent cell viability assay study with the compound **37d** on the SiHa carcinoma cell line revealed that it may have anti-cancer property. The observed IC_{50} value was 23 μM, which is a good indication of application. However, a more detailed study is required to prove the anti-cancer properties in this regard, and still under process.

3.6 EXPERIMENTAL SECTION

3.6.1 General information

All NMR (^{1}H, ^{13}C, COSY, HMBC, HSQC) spectra were recorded with Bruker Avance III (300 or 400 MHz) spectrometers in deuterated solvent $CDCl_3$. Chemical shifts are reported in parts per million (ppm, δ) relative to tetramethylsilane (TMS) and the solvent resonance was referenced to internal standard $CDCl_3$ (δ 7.28 ppm). All coupling constants are absolute values and are expressed in Hz. The descriptions of the signals are reported as follows: s = singlet, d = doublet, dd = double of doublet, t = triplet, m = multiplet and dt = doublet of triplets. ^{13}C NMR spectra were recorded using Bruker Avance III 300 (75 MHz), 400 (100 MHz) spectrometers as solutions in $CDCl_3$ with complete proton decoupling. High-resolutionmass spectra were recorded on ESI-TOF mass spectrometry. Solvents, reagents, and chemicals were purchased from Aldrich, Merck, SRL, Spectrochem, and Process Chemicals. Commercially available (SRL India) calf thymus DNA (ct-DNA), Hochest 33258 and Ethidium bromide (EB), Tris buffer were used without purification also. All the reactions were monitored by TLC (Silica Gel60 F_{254}) and it was observed under UV light (254 nm).Yields refer to the isolated product as mentioned in theexperimental section.

3.6.2 Representative procedure and spectral data

Synthesis of compound 36a -36j and 36k:

Synthesis of compound 36a[38]**:**A mixture of 3,4-dihydroquinazolin-4-one(**34a**) (0.5 mmol), sodium iodide (0.05 mmol), potassium carbonate (2.5 mmol), and benzyl bromide (0.5 mmol) in acetone (5 mL) was heated under reflux for 24 h. The resultant mixture was diluted with ethyl acetate (10 mL), washed with brine (10 mL) and organic phase was dried with sodium sulfate. Crude products were purified by column chromatography (hexane/ethyl acetate 8:2) and isolated the pure product **36a**.

The compounds **36b**[38], **36c**[38],**36d**[50], **36e**,**36f**[51], **36g**[52], and **36h**[52]have been synthesized by the same procedure mentioned for **36a** using **34** and appropriate alkyl halide (**35**).

***Synthesis of compound* 36i:** To a solution of 3,4-dihydroquinazolin-4-one (**34a**)(200 mg, 1.36 mmol) in 5mL DMF, at 0°C and under nitrogen atmosphere, was added NaH (60% dispersion in mineral oil, 2 Eqv.) portion-wise. The mixture was stirred at 0°C for 15 min and, then, (2-bromoethyl) benzene (327 mg, 1.64 mmol.) was added dropwise. The mixture was warmed to room temperature and stirred for 20 h. The reaction was quenched with H_2O and the crude mixture extracted with EtOAc. The combined organic layer was washed with water and brine. The organic layer was dried over anhydrous sodium sulfate, filtered and concentrated in vacuo to give the crude material. Purification of the desired compound **36i** was done by column chromatography on silica gel (EtOAc/hexanes). Compound **36j** was prepared by using the same method as mentioned for **36i**,

using **34** and (3-bromopropyl) benzene as starting materials. Analytical data of Compound **36i**[53]and **36j**[40]were exactly comparable with the reported data. 3-benzylquinazolin-4(3H)-one (**36a**).

***Analytical and spectroscopic dataof 3-benzylquinazolin-4(3H)-one* (36a)**

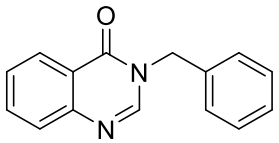

White solid, yield 91%, ^{1}H-NMR (300 MHz, $CDCl_3$) δ 8.24(d, *J*=9Hz, 1H), 8.02(s, 1H), 7.69-7.60(m, 2H), 7.44-7.39(m, 1H), 7.27-7.17(m, 5H), 5.11(s, 2H). ^{13}C-NMR (75 MHz, $CDCl_3$) δ 161.2, 148.1, 146.4, 135.8, 134.4, 129.1 128.4, 128.1, 127.6, 127.5, 127.0, 122.3, 49.7. ESI-TOF MS: Calculated mass for $C_{15}H_{12}N_2NaO$ $[M+Na]^+$=259.0847, observed m/z =259.0834

***Analytical and spectroscopic dataof 3-(4-methylbenzyl)quinazolin-4(3H)-one* (36b)**

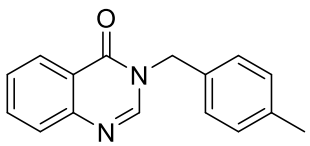

White solid, yield 85%, ^{1}H-NMR (300 MHz, $CDCl_3$) δ 8.36-8.33(d, *J*=1.5Hz, 9Hz, 1H), 8.12(s, 1H), 7.82- 7.70(m, 2H), 7.55-7.50(m, 1H), 7.29-7.26(m, 2H), 7.19-7.16(m, 2H), 5.18(s, 2H), 2.35(s, 3H). ^{13}C-NMR (75 MHz, $CDCl_3$) δ 160.0, 147.0, 145.3, 137.1, 133.2, 131.7, 128.6, 127.0, 126.4, 126.3, 125.8, 121.2, 48.4, 20.1. ESI-TOF MS: Calculated mass for $C_{16}H_{15}N_2O$ $[M+H]^+$=251.1184, observed m/z =251.1193

***Analytical and spectroscopic dataof 3-(4-methoxybenzyl) quinazolin-4(3H)-one* (36c)**

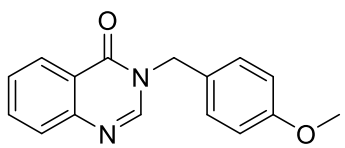

White solid, yield 82%, ^{1}H-NMR (300 MHz, $CDCl_3$) δ 8.75(s, 1H), 8.15(d, *J*=9Hz, 1H), 7.83(t, *J*=9Hz, 1H), 7.70-7.66(m, 1H), 7.54(t, *J*=9Hz, 1H), 7.35(d, *J*=9Hz, 2H), 6.90(d, *J*=9Hz, 2H), 5.13(s, 2H), 3.72(s, 3H). ^{13}C-NMR (75 MHz, DMSO-d_6) δ 160.5, 159.3, 148.3, 134.8, 129.9, 129.3, 127.7, 127.6, 126.5, 122.1, 114.5, 55.6, 48.8. ESI-TOF MS: Calculated mass for $C_{16}H_{14}N_2NaO_2$ $[M+Na]^+$ =289.0953, observed m/z =289.0079

***Analytical and spectroscopic dataof3-benzyl-6-nitroquinazolin-4(3H)-one* (36d)**

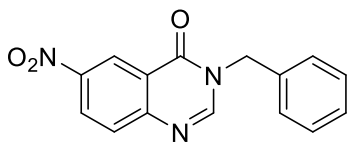

Yellow solid, yield 75%, ^{1}H NMR (300 MHz, $CDCl_3$) δ 9.16(s, 1H), 8.52-8.50(d, *J*=9Hz, 1H), 8.24(s, 1H), 7.82(d, *J*=9Hz, 1H), 7.36-7.35(m, 5H), 5.22(s, 2H). ^{13}C-NMR (75MHz, $CDCl_3$) δ 159.9, 152.0, 149.2, 146.1, 134.9, 129.2, 129.2 128.7, 128.3, 128.2, 123.5, 122.4, 50.0 ESI-TOF MS: Calculated mass for $C_{15}H_{12}N_3O_3$ $[M+H]^+$=282.0879, observed m/z =282.0870

***Analytical and spectroscopic dataof3-(4-methylbenzyl)-6-nitroquinazolin-4(3H)-one*(36e)**

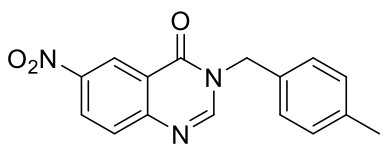

Yellow solid, yield 72%, ^{1}H NMR (300 MHz, $CDCl_3$) δ 9.20(d, *J*=2.7Hz, 1H), 8.56-8.53(dd, *J*=2.7, 9Hz, 1H), 8.24(s, 1H), 7.83(d, *J*=9Hz, 1H), 7.29-7.17(dd, *J*=9Hz, 2.7Hz, 4H), 5.20(s, 2H), 2.36(s, 3H). ^{13}C-NMR (75 MHz, $CDCl_3$) δ 160.1, 152.2, 149.3, 146.2,

138.8, 131.9, 130.0, 129.3, 128.4, 128.4, 123.7, 122.5, 49.9, 21.3. ESI-TOF MS: Calculated mass for $C_{16}H_{14}N_3O_3$ $[M+H]^+$=296.1035, observed m/z =296.1037

***Analytical and spectroscopic dataof3-(4-methoxybenzyl)-6-nitroquinazolin-4(3H)-one*(36f)**

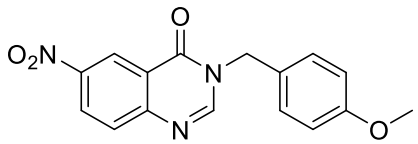

Yellow solid, yield 69%, ^{1}H-NMR (300 MHz, $CDCl_3$) δ 9.17(d, *J*=2.4Hz, 1H), 8.50(dd, *J*=2.4, 9Hz, 1H), 8.23(s, 1H), 7.82(d, *J*=9Hz, 1H), 7.32(d, *J*=9Hz, 2H), 6.89(d, *J*=9Hz, 2H), 5.15(s, 2H), 3.79(s, 3H). ^{13}C-NMR (75 MHz, $CDCl_3$) δ 158.9, 150.9, 148.2, 145.0, 128.8, 128.8, 128.1, 127.3, 125.8, 122.5, 121.4, 113.6, 54.4, 48.7. ESI-TOF MS: Calculated mass for $C_{16}H_{14}N_3O_4$ $[M+H]^+$ =312.0984, observed m/z =312.0995

***Analytical and spectroscopic dataof3-benzyl-6-bromoquinazolin-4(3H)-one* (36g)**

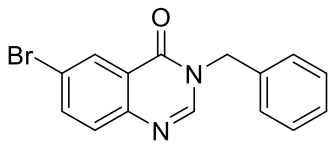

White solid, yield 71%, ^{1}H-NMR (300 MHz, $CDCl_3$) δ 8.38(d, *J*=2.4Hz, 1H), 8.03(s, 1H), 7.75(dd, *J*=2.4, 9Hz, 1H), 7.49(d, *J*=9Hz, 1H), 7.27(s, 5H), 5.12(s, 2H). ^{13}C-NMR (75 MHz, $CDCl_3$) δ 158.9, 145.8, 145.6, 136.5, 134.4, 128.5, 128.3, 128.1, 127.4, 127.0, 122.5, 120.0, 48.7. ESI-TOF MS: Calculated mass for $C_{15}H_{12}BrN_2O$ $[M+H]^+$=315.0133, observed m/z =315.0141

***Analytical and spectroscopic dataof6-bromo-3-(4-methylbenzyl)quinazolin-4(3H)-one*(36h)**

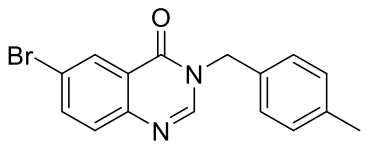

White solid, yield 70%, ^{1}H-NMR (300 MHz, $CDCl_3$) δ 8.44(d, *J*=2.4Hz, 1H), 8.09(s, 1H), 7.82(dd, *J*=2.4, 9Hz, 1H), 7.54(d, J=9Hz, 1H), 7.32-7.14(m, 4H), 5.14(s, 2H), 2.32(s, 3H). ^{13}C-NMR (75 MHz, $CDCl_3$) δ 159.9, 146.9, 146.6, 138.4, 137.5, 132.4, 129.77, 129.5, 129.3, 128.1, 123.6, 120.9, 49.6, 21.1. ESI-TOF MS: Calculated mass for $C_{16}H_{14}BrN_2O$ $[M+H]^+$ =329.0290, observed m/z =331.0265

***Analytical and spectroscopic dataof3-phenethylquinazolin-4(3H)-one*(36i)**

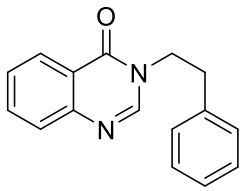

White solid, yield 69%, ^{1}H-NMR (400 MHz, $CDCl_3$) δ 8.33(d, *J*=12Hz, 1H), 7.79-7.68(m, 3H), 7.52(t, *J*=12Hz, 1H), 7.32-7.27(m, 2H), 7.25-7.21(m, 1H), 7.17-7.15(m, 2H), 4.23(t, *J*=8Hz, 2H), 3.11(t, *J*=8Hz, 2H). ^{13}C-NMR (100 MHz, $CDCl_3$) δ 160.9, 147.7, 146.6, 137.4, 134.3, 128.9, 128.9, 127.4, 127.2, 127.1, 126.7, 122.0, 49.0, 35.1. ESI-TOF MS: Calculated mass for $C_{16}H_{15}N_2O$ $[M+H]^+$= 251.1184, observed m/z =251.1642

***Analytical and spectroscopic dataof3-(3-phenylpropyl)quinazolin-4(3H)-one* (36j)**

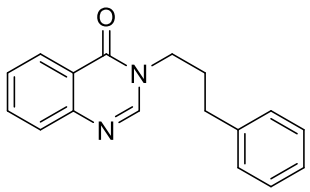

White solid, yield 65%, ^{1}H-NMR (400 MHz, $CDCl_3$) δ 8.31(d, *J*=8Hz, 1H), 7.99(s, 1H), 7.77-7.70(m, 2H), 7.53-7.49(m, 1H), 7.31-7.27(m, 2H), 7.21-7.17(m, 3H), 4.02(t, *J*=8Hz, 2H), 2.73(t, *J*=8Hz, 2H), 2.21-2.13(m, 2H). ^{13}C-NMR (100 MHz, $CDCl_3$) δ 161.0, 147.8, 146.6, 140.3, 134.2,

128.6, 128.3, 127.4, 127.3, 126.7, 126.3, 122.1, 46.7, 32.7, 30.4. ESI-TOF MS: Calculated mass for $C_{17}H_{16}N_2NaO$ $[M+Na]^+$ = 287.1160, observed m/z = 287.1371

***Analytical and spectroscopic dataof3-(naphthalen-2-ylmethyl)-6-nitroquinazolin-4(3H)-one*(36k)**

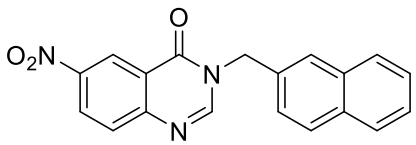

Pale yellow solid, yield 80%, ^{1}H-NMR (300 MHz, $CDCl_3$) δ 9.22(d, *J*=2.7Hz, 1H), 8.56-8.54(dd, *J*=2.7, 9Hz, 1H), 8.33(s, 1H), 7.89-7.83(m, 6H), 7.56-7.46(m, 4H). ^{13}C-NMR (100 MHz, $CDCl_3$) δ 160.0, 152.0, 149.2, 146.1, 133.2, 133.1, 132.2, 129.3, 129.2, 128.4, 127.9, 127.8, 127.6, 126.8, 126.7, 125.4, 123.6, 122.4, 50.2

***Synthesis and spectroscopic data of 5-acetyl-4b,5-dihydroisoindolo[1,2-b]quinazoline-10,12-dione* (37a)**

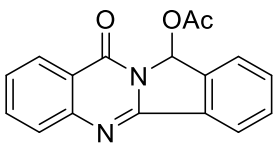

Compound **36a** (100mg, 0.423 mmol) was taken along with $Pd(OAc)_2$ (18.9 mg, 0.084mmol), AgOAc (211.8 mg, 1.26 mmol) in 7ml acetic acid at 120^0C under inert atmosphere. The mixture was refluxed for 24h. After TLC checking the resulting reaction mixture was cooled to room temperature, diluted with EtOAc (100 mL) and filtered through a pad of SiO2/Celite®.The filtrates were collected and concentrated under reduced pressure. The residue was dissolved in EtOAc (50 mL) and washed with saturated $NaHCO_3$ solution and brine (2×50 mL). The organic phase was then dried with Na_2SO_4, filtered, and concentrated under reduced pressure. The crude residue was purified by flash chromatography on silica gel to get purified **37a**. White solid, yield 75%, m.p. 235-237°C, ^{1}H-NMR (300 MHz, $CDCl_3$) δ 8.29-8.26(d, *J*=9Hz, 1H), 8.07-8.04(m, 1H), 7.86(s, 1H), 7.75-7.70(m, 2H), 7.66-7.57(m, 3H), 7.47-7.42(m, 1H), 2.13(s, 3H).^{13}C-NMR (100 MHz, $CDCl_3$) δ 170.0, 159.7, 153.3, 149.0, 139.3, 134.8, 133.0, 132.2, 131.1, 127.9, 127.2, 126.9, 125.0, 123.4, 121.5, 80.2, 20.7.ESI-TOF MS: Calculated mass for $C_{17}H_{13}N_2O_3$$[M+H]^+$ = 293.0926, observed m/z =293.0928

***Synthesis and spectroscopic data of 5-acetyl-3-methyl-4b, 5-dihydroisoindolo[1,2-b]quinazoline-10,12-dione* (37b)**

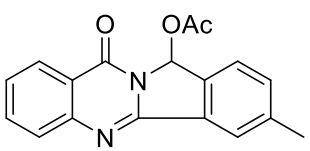

The compound **37b** was synthesized from the compound **36b** using reaction condition mention for **37a**.White solid, yield 73%, m.p. 236-238°C, ^{1}H-NMR (300 MHz, $CDCl_3$) δ 8.36(d, *J*=7.8Hz, 1H), 7.95(s, 1H), 7.89(s, 1H), 7.82-7.80(m, 2H), 7.62-7.59(m, 1H), 7.55-7.46(m, 2H), 2.53(s, 3H), 2.20(s, 3H). ^{13}C-NMR (75 MHz, $CDCl_3$) δ 170.0, 159.7, 153.4, 148.9, 141.7, 136.6, 134.7, 134.0, 132.2, 127.7, 127.1, 126.9, 124.7, 123.6, 121.5, 80.1, 21.5, 20.7. ESI-TOF MS: Calculated mass for $C_{18}H_{15}N_2O_3$ $[M+H]^+$ =307.1083, observed m/z =307.1075

***Synthesis and spectroscopic data of 5-acetyl-3-methoxy-4b,5-dihydroisoindolo[1,2-b]quinazoline-10,12-dione* (37c)**

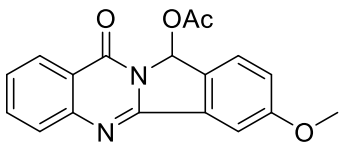

The compound **37c** was synthesized from the compound **36c** using reaction condition mention for **37a**. White solid, yield 80%, m.p. 236-238°C, ^{1}H-NMR (300 MHz, $CDCl_3$) δ 8.32(d, *J*=7.8Hz, 1H), 7.82(s, 1H), 7.79-7.77(m, 2H), 7.59-7.52(m, 2H), 7.53-7.47(m, 1H), 7.17-7.14(dd, *J*=2.4, 8.4Hz, 1H), 3.93(s, 3H), 2.17(s, 3H). ^{13}C-NMR (75 MHz, $CDCl_3$) δ 170.1, 162.2, 159.5, 153.3, 148.9, 134.7, 133.7, 131.5, 127.7, 127.2, 126.9, 126.0, 121.6, 121.1, 106.1, 80.0, 55.9, 20.7. ESI-TOF MS: Calculated mass for $C_{18}H_{15}N_2O_4$ $[M+H]^+$ =323.1032, observed m/z =323.1032

***Synthesis and spectroscopic data of 5-acetyl-8-nitro-4b,5-dihydroisoindolo[1,2-b]quinazoline-10,12-dione*(37d)**

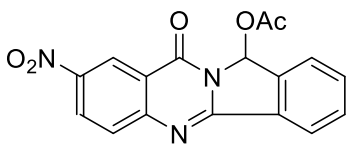

The compound **37d** was isolated from the compound **36d** using reaction condition mention for **37a**. White solid, yield 50%, m.p. 235-237°C, ^{1}H-NMR (300 MHz, $CDCl_3$) δ 9.22-9.21(m, 1H), 8.62-8.58(dd, *J*=2.4Hz,9Hz, 1H), 8.19- 8.16(m, 1H), 7.96-7.93(m, 2H), 7.75-7.70(m, 3H), 2.23(s, 3H). ^{13}C-NMR (75 MHz, $CDCl_3$) δ 169.7, 158.3, 156.2, 153.3, 145.9, 139.7, 134.1, 131.4, 131.4, 129.2, 128.8, 125.1, 124.0, 123.4, 121.8, 80.2, 20.6. ESI-TOF MS: Calculated mass for $C_{17}H_{12}N_3O_5$ $[M+H]^+$ =338.0777, observed m/z =338.0781

***Synthesis and spectroscopic data of 8-nitroisoindolo[1,2-b]quinazolin-10(12H)-one* (38d)**

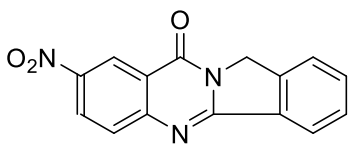

The compound **38d** was isolated from the compound 5d using reaction condition mention for **37a**. White solid, yield 31%, m.p. 228-230°C, ^{1}H-NMR (300 MHz, $CDCl_3$) δ 9.28(d, *J*=2.7Hz, 1H), 8.62-8.59 (dd, *J*=2.7Hz, 2.7Hz, 1H), 8.26(d, *J*=9Hz, 1H), 7.96(d, *J*=9Hz, 1H), 7.79-7.63(m, 3H), 5.25(s, 2H). ^{13}C-NMR (100 MHz, $CDCl_3$) δ 159.5, 158.0, 153.8, 145.3, 140.1, 133.5, 132.0, 129.3, 128.8, 128.4, 124.2, 123.7, 123.3, 120.7, 50.1

***Synthesis and spectroscopic data of 5-acetyl-3-methyl-8-nitro-4b,5-dihydroisoindolo[1,2-b]quinazoline-10,12-dione*(37e)**

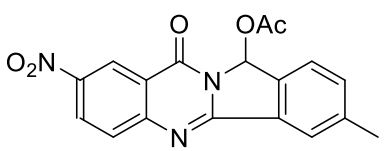

The compound **37e** was isolated from the reaction mixture of **36e** using reaction condition mention for **37a**. Off white solid, yield 50%, m.p. 238-240°C, ^{1}H-NMR (300 MHz, $CDCl_3$) δ 9.20(s, 1H), 8.60-8.57(m, 1H), 7.97-7.90(m, 3H), 7.64-7.53(m, 2H), 2.55(s, 3H), 2.21(s, 3H). ^{13}C-NMR (75 MHz, $CDCl_3$) δ 169.7, 158.4, 156.4, 153.4, 145.7, 142.1, 136.9, 135.2, 131.4, 129.15, 128.8, 124.8, 124.2,

123.4, 121.8, 80.2, 21.6, 20.6. ESI-TOF MS: Calculated mass for $C_{18}H_{14}N_3O_5$ $[M+H]^+$ = 352.0933, observed m/z =352.2543

***Synthesis and spectroscopic data of 3-methyl-8-nitroisoindolo[1,2-b]quinazolin-10(12H)-one* (38e)**

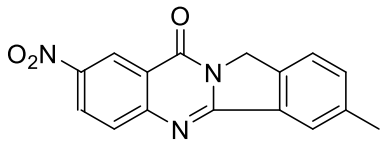

The compound **38e** was isolated from the reaction mixture of **36e** using reaction condition mention for **37a**. White solid, yield 42%, m.p. 226-228°C, ^{1}H-NMR (300 MHz, $CDCl_3$) δ 9.25(s, 1H), 9.58(d, *J*=9Hz, 1H), 8.03(s, 1H), 7.93(d, *J*=9Hz, 1H), 7.57(s, 2H), 5.18(s, 2H), 2.55(s, 3H). ^{13}C-NMR (75 MHz, $CDCl_3$) δ 159.5, 158.1, 153.9, 145.2, 139.6, 137.4, 134.7, 132.1, 128.7, 128.3, 124.2, 123.3,123.3, 120.6, 49.9, 21.4. ESI-TOF MS: Calculated mass for $C_{16}H_{12}N_3O_3$ $[M+H]^+$=294.0879, observed m/z =294.0370

***Synthesis and spectroscopic data of 5-acetyl-3-methoxy-8-nitro-4b, 5-dihydroisoindolo[1,Z 2-b]quinazoline-10,12-dione*(37f)**

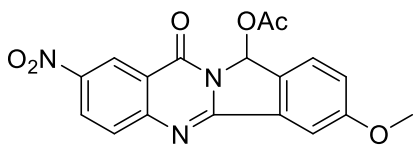

The compound **37f** was synthesized from the compound **36f** using reaction condition mention for **37a**. Off white solid, yield 60%, m.p. 237-239°C, ^{1}H-NMR (300 MHz, $CDCl_3$) δ 9.22(d, *J*=2.7Hz, 1H), 8.61- 8.58 (dd, *J*=2.7, 9Hz, 1H), 7.95-7.87 (m, 2H), 7.67-7.64 (d, *J*=9Hz, 1H), 7.62-7.61 (d, *J*=2.7 Hz, 1H), 7.26 (S, 1H), 3.99(s, 3H), 2.21(s, 3H). ^{13}C-NMR (75 MHz, $CDCl_3$) δ 169.9, 162.4, 158.2, 156.3, 153.2, 145.8, 132.9, 131.9, 129.1, 128.8, 126.2, 123.4, 122.1, 121.9, 106.7, 80.1, 56.0, 20.7. ESI-TOF MS: Calculated mass for $C_{18}H_{14}N_3O_6$ $[M+H]^+$ =368.0883, observed m/z =368.0881

***Synthesis and spectroscopic data of 8-bromoisoindolo[1,2-b]quinazolin-10(12H)-one* (38g)**

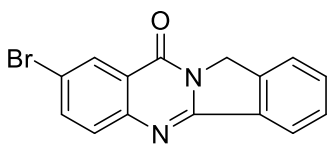

The compound **38g** was synthesized from the compound **36g** using reaction condition mention for **37a**. White solid, yield 70%, m.p. 225-227°C, ^{1}H-NMR (400 MHz, $CDCl_3$) δ 8.54(d, *J*=2.4Hz, 1H), 8.20(d, *J*=8Hz, 1H), 7.90-7.88(dd, *J*=2.4, 8Hz, 1H), 7.74-7.61(m, 4H), 5.19(s, 2H). ^{13}C-NMR (100 MHz, $CDCl_3$) δ 159.5, 155.4, 148.4, 139.6, 137.5, 132.6, 132.5, 129.2, 129.1, 129.1, 123.7, 123.6, 122.0, 119.8, 49.9. ESI-TOF MS: Calculated mass for $C_{15}H_{10}BrN_2O$ $[M+H]^+$ =312.9977, observed m/z =312.9096

***Synthesis and spectroscopic data of5-acetyl-8-bromo-3-methyl-4b,5-dihydroisoindolo[1,2-b]quinazoline-10,12-dione* (37h)**

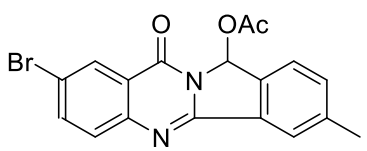

The compound **37h** was isolated from the reaction mixture of **36h** using reaction condition mention for **37a**. White solid, yield 30%, m.p. 234-236°C, ^{1}H-NMR (300 MHz, $CDCl_3$) δ 8.47(s, 1H), 7.93-7.87(m, 3H), 7.68(d, *J*=9Hz, 1H), 7.61(d, *J*=9Hz, 1H), 7.48(d, *J*=9Hz, 1H),

2.53(s, 3H), 2.20(s, 3H). ^{13}C-NMR (75 MHz, $CDCl_3$) δ 169.9, 158.5, 153.7, 147.9, 141.8, 137.8, 136.6, 134.3, 131.9, 129.5, 129.4, 124.7, 123.6, 122.9, 120.6, 80.1, 21.5, 20.7. ESI-TOF MS: Calculated mass for $C_{18}H_{14}BrN_2O_3$ $[M+H]^+$ =385.0188, observed m/z =384.9339

***Synthesis and spectroscopic data of 5-acetyl-2-nitro-5,5a-dihydrobenzo[5,6]isoindolo[1,2-b]quinazoline-12,14-dione* (37k)**

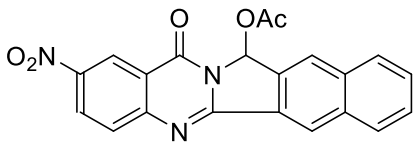

The compound **37k** was synthesized from the compound **36k** using reaction condition mention for **37a**. White solid, yield 70%, m.p. 242-244°C, ^{1}H-NMR (300 MHz, $CDCl_3$) δ 9.59(d, *J*=6Hz, 1H), 9.24(d, *J*=2.7Hz, 1H), 8.64-8.62(dd, *J*=2.7, 9Hz, 1H), 8.21(d, *J*=9Hz,1H), 8.09-8.03(m, 3H), 7.88-7.83(m, 1H), 7.78-7.72(m, 2H), 2.26(s, 3H). ^{13}C-NMR (100 MHz, $CDCl_3$) δ 169.8, 158.3, 153.5, 145.8, 140.1, 135.4, 134.7, 129.5, 129.3, 128.9, 128.7, 128.2, 125.9, 124.9, 123.3, 121.4, 120.6, 79.8, 29.7. ESI-TOF MS: Calculated mass for $C_{21}H_{13}N_3NaO_5$ $[M+Na]^+$ = 410.0753, observed m/z 410.0746

***Synthesis and spectroscopic data of 8-bromo-3-methylisoindolo[1,2-b]quinazolin-10(12H)-one* (38h)**

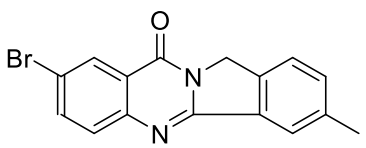

The compound **38h** was isolated from the reaction mixture of **36h** using reaction condition mention for **37a**. White solid, yield 50%, m.p. 229-231°C, ^{1}H-NMR (400 MHz, $CDCl_3$) δ 8.51(d, *J*=2.4Hz, 1H), 8.02(s, 1H), 7.88-7.86(dd, *J*=2.4, 12Hz, 1H), 7.72(d, *J*=8Hz, 1H), 7.55-7.47(m, 2H), 5.13(s, 2H), 2.53(s, 3H). ^{13}C-NMR (100 MHz, $CDCl_3$) δ 159.4, 155.5, 148.1, 139.3, 137.4, 136.9, 133.8, 132.3, 129.1, 128.9, 123.8, 123.2, 121.9, 119.8, 49.8, 21.4. ESI-TOF MS: Calculated mass for $C_{16}H_{12}BrN_2O$ $[M+H]^+$ =327.0133, observed m/z =327.0119

***Synthesis and spectroscopic data of 5, 6-dihydro-8H-isoquinolino[1,2-b]quinazolin-8-one* (38i)**

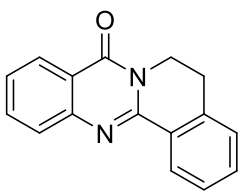

The compound **38i** was synthesised from the compound **36i** using reaction condition mention for **37a**. White solid, yield 75%, m.p. 226-228°C, ^{1}H-NMR (400 MHz, $CDCl_3$) δ 8.57(d, *J*=8Hz, 1H), 8.35- 8.33(dd, *J*=2, 8Hz, 1H), 7.90-7.83(m, 1H), 7.79(t, *J*=8Hz, 1H), 7.547.46(m, 3H), 7.32(d, *J*=8Hz, 1H), 4.45(t, *J*=8Hz, 2H), 3.14(t, *J*=8Hz, 2H). ^{13}C-NMR (100 MHz, $CDCl_3$) δ 161.5, 149.6, 147.1, 137.1, 134.4, 132.0, 129.0, 128.3, 127.7, 127.5, 127.2, 126.9, 126.7, 120.5, 39.6, 27.4. ESI-TOF MS: Calculated mass for $C_{16}H_{13}N_2O$ $[M+H]^+$ =249.1028, observed m/z =249.1020

***Synthesis and spectroscopic data of 7-dihydrobenzo[3,4] azepino[2,1-b]quinazolin-9(5H)-one* (38j)**

The compound **38j** was synthesised from the compound **36j** using reaction condition mention for **37a**. White solid, yield 80%, m.p. 223-225°C, ^{1}H-NMR (300 MHz, $CDCl_3$) δ 8.36 (d, *J*=7.8Hz, 1H),

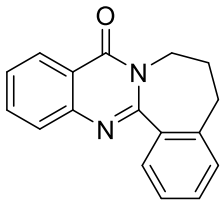

7.91- 7.89(dd, *J*=6Hz, 1H), 7.83-7.77(m, 2H), 7.57-7.44(m, 3H), 7.29-7.27(m, 1H), 4.14(s, 2H), 2.79(t, *J*=6Hz, 2H) 2.27(s, 2H). ^{13}C-NMR (75 MHz, $CDCl_3$) δ 161.6, 156.5, 147.7, 138.0, 134.8, 134.3, 131.3, 129.0, 128.6, 127.5, 127.5, 126.9, 126.8, 120.4, 41.5, 29.7, 28.8. ESI-TOF MS: Calculated mass for $C_{17}H_{15}N_2O$ $[M+H]^+$ =263.1184, observed m/z =263.1183

3.6.3 Crystallographic Table:

Table-3.C ***Crystallographic data and structural refinement parameters for*** **36d**

Empirical Formula	$C_{15}H_{11}N_3O_3$
Formula weight	281.27
Crystal system	Triclinic
Space group	p-1
a/Å	6.2723(2)
b/Å	9.1749(3)
c/Å	11.8955(3)
α/°	69.5440(10)
β/°	88.4680(10)
γ/°	75.2740(10)
V/mm^3	618.86(3)
Z	2
Dc/g cm^{-3}	1.509
μ/mm^{-1}	0.901
F_{000}	292
Θ range/°	5.331, 64.928
Reflections collected	13900
Unique reflections	2020
reflections *I>2σ(I)*	1976
R_{int}	0.0452
goodness-of-fit (F^2)	1.125
R_1 (I>2σ(I)) [a1]	0.0449
wR_2 (I>2σ(I)) [a1]	0.1247

Δρ min /max /e Å^3	-0.85, 0.48

[a1]$R_1 = \Sigma \left| \left| F_o \right| - \left| F_c \right| \right| / \Sigma \left| F_o \right|$, $wR_2 = [\Sigma (w (F_o^2 - F_c^2)^2) / \Sigma w (F_o^2)^2]^{1/2}$

Table-3.D ***Crystallographic data and structural refinement parameters for*** **38h**

Empirical formula	$C_{16}H_{11}BrN_2O$
formula weight	327.18
crystal system	Monoclinic
space group	C 2/m
a/ Å	15.53(13)
b/Å	6.80(6)
c/ Å	13.81(11)
α/°	90
β/°	108.905(3)
γ/°	90
V/ nm^3	1.3814(2)
Z	2
D_c/ g cm^{-3}	1.636
μ /mm^{-1}	2.980
F_{000}	688
θ range/°	2.7, 27.1
reflections collected	25121
unique reflections	1716
reflections $I > 2\sigma(I)$	1276
R_{int}	0.098

goodness-of-fit (F^2)	1.07
R_1 ($I > 2\sigma(I)$) [b1]	0.0664
$wR_2(I > 2\sigma(I))$ [b1]	0.1884
$\Delta\rho$ min / max /e Å^3	-0.85, 0.48

[b1] $R_1 = \Sigma \left| \left| F_o \right| - \left| F_c \right| \right| / \Sigma \left| F_o \right|$, $wR_2 = [\Sigma (w (F_o^2 - F_c^2)^2) / \Sigma w (F_o^2)^2]^{1/2}$

3.6.4 Photophysical study:

Absorption Spectroscopic Method

For the UV-Visible absorption spectra measurements Shimadzu spectrophotometer (model UV-1800, Japan) with 1cm × 1cm quartz cuvette was used. For the absorption spectral titration with ct-DNA was performed in Tris-HCl buffer solution (10 mM, pH 7.2). The spectrum of ct-DNA in the Tris buffer show bands at 260 and 280nm with absorbance ratio of 1.8-1.9:1, which was an indication of DNA was sufficiently pure[54]. The conc. of ct-DNA is calculated at 260 nm by using the molar extinction coefficient value of 6600 $M^{-1}cm^{-1}$[55]. The UV-Visible absorption spectra of **38h** and **38h**-DNA complex were recorded in the wavelength range of 200–400 nm. The experiment was conducted at a defined concentration of **38h** (20 µM) in a fixed volume (3 ml) and quantified by changing the concentration of ct-DNA (0–1 µM).

Fluorescence Spectroscopic Method

Steady-state fluorescence: Fluorescence emission spectra of **38h** were recorded on a Shimadzu spectrofluorometer-5000 (Japan) equipped with a Xenon flash lamp using 1.0 cm quartz cells. Excitation was fixed at 308 nm and emission spectra were recorded from 313 nm to 600 nm after setting the widths of both the excitation and the emission slits at 5 nm. The fluorescence titration was carried out by keeping the concentration of **38h** (20 µM) constant and varying the ct-DNA concentration from 0 µM to 2 µM.

Time-resolved fluorescence decay measurement: Fluorescence lifetime measurements were conducted on Horiba Jobin Yvon Fluoro Log spectrofluorometer (HORIBA, Les Ulis, France) with the excitation wavelength at 308 nm. The concentration of **38h** was fixed, while ct-DNA concentration varied from 0 µM to 300 µM. All decay values were analyzed by bi-exponential iterative fitting, the quality of which was assessed by χ^2 values and residuals to obtain the mean fluorescence lifetime (τ_{av}). The fitting parameters are listed in **Table-3.E**. The average fluorescence

lifetime of **38h** was acquired by the following relation: $\tau_{avg}=A_1\tau_1+A_2\tau_2$ where τ_1 and τ_2 are decay times, and A_1 and A_2 are pre-exponential factors.

Table-3.E Time-resolved fluorescence study of **38h**

	τ_1	A_1	τ_2	A_2	τ_{av} (ns)	χ^2
Free	0.296	88.11	1.54	11.89	0.44	1.02
50 µM	0.318	58.58	2.00	41.42	1.014	1.007
100 µM	0.347	57.36	2.01	42.64	1.056	1.17
150 µM	0.35	41.19	2.02	58.81	1.33	1.14
200 µM	0.418	41.48	2.07	58.52	1.38	1.04
250 µM	0.473	31.54	2.08	68.54	1.57	1.10
300 µM	0.591	17.50	2.11	82.50	1.84	1.12

Comparative binding study with known DNA binders

Displacement assay was done as early reported by several well-known DNA intercalators and groove binders such as Ethidium Bromide (EB) and Hoechst 33258. In the first case i.e; EB displacement assay we have monitored the emission spectra of ct-DNA (50 µM) bound EB (5 µM) in the presence of changing amounts of **38h** (0–60 µM) to assure the binding of **38h** with ct-DNA. After exciting at 471 nm the EB-bound ct-DNA molecule, the corresponding emission spectra were recorded in between the range 500-680 nm [For spectra; see the **Figure 3.F** (I)].

The Hoechst 33258 displacement assay was monitored by excited the Hoechst bound ct-DNA complex at 343 nm, which contains 5 µM of Hoechst 33258 and 50 µM of ct-DNA. The fluorescence emission spectra were recorded between 350–650 nm by titrating with increasing concentrations of **38h** (0–60 µM). In all the above experiments, the final volume of the reaction mixture was made to 3 ml by adding 10 mM Tris-HCl buffer [For spectra; see the **Figure 3.F** (J)].

Iodide quenching experiments

Iodide quenching experiments were performed in the presence and absence of ct-DNA. Emission spectra were recorded either in the presence or absence of 50mM ct-DNA in a 3ml reaction mixture which included 20µM **38h**, 10 mM Tris-HCl (pH 7.2), and varying concentrations of KI between 0–10 mM. Excitation was done at 385 nm and emission spectra were recorded from 390-620 nm [For spectra; see the **Figure 3.E** (F)].

DNA Melting Study

DNA melting experiments were performed by monitoring the absorption of ct-DNA (4 µM) at 260 nm in the absence and presence of **38h** (1µM) at various temperatures by using a UV-Vis

spectrophotometer fitted with a temperature-controlled Peltier. The absorbance was then plotted and normalized as a function of temperature ranging from 30°C to 90°C. The DNA melting temperature (Tm) was determined as the transition midpoint [For spectra: see the **Figure 3.E** (H)].

Table-3.F DNA melting temperature (Tm) in presence and absence of ligand

Ligand (^{0}C)	Tm of only DNA (°C)	Tm of DNA with Ligand (°C)	Difference(°C)
38h	65.4	70.92	5.5

3.6.5 Result of Cell viability assay:

SiHa cervical cancer cell line, purchased in 2022 from NCCS Pune, India, was cultured in Dulbecco's modified eagle's medium (DMEM) supplemented with 100 U/ml penicillin, 10% FBS, 100 mg/ml streptomycin, and 50mM glutamine. Cells were harvested using trypsin and seeded in a 96-well cell culture plate for the MTT assay. All tests were accomplished in triplicate. The cell toxicity (%) was calculated using the following formula: Cell Toxicity (%)=100-[(OD of treated well/ OD of untreated well)×100]. The cell toxicity experiment was performed thrice and the average OD value of each concentration was used to calculate cell toxicity.

Table-3.G Cell toxicity measurement by OD values

Conc. Of **38h** →	**100µM**	**10µM**	**1µM**	**0.1µM**	**0.01µM**	**0µM**
OD Value →	0.117	1.56	1.758	1.856	1.923	2.036
	0.104	1.279	1.798	1.945	1.977	2.009
	0.113	1.377	1.903	1.833	1.943	2.054
Avg.OD Value →	0.111333	1.405333	1.819667	1.878	1.947667	2.033
Cell viability (%) →	5.476308	69.12609	89.50648	92.3758	95.80259	100
Cell toxicity →	94.52369	30.87391	10.49352	7.624201	4.197409	0

Copy of NMR

^{1}H-NMR of 37a

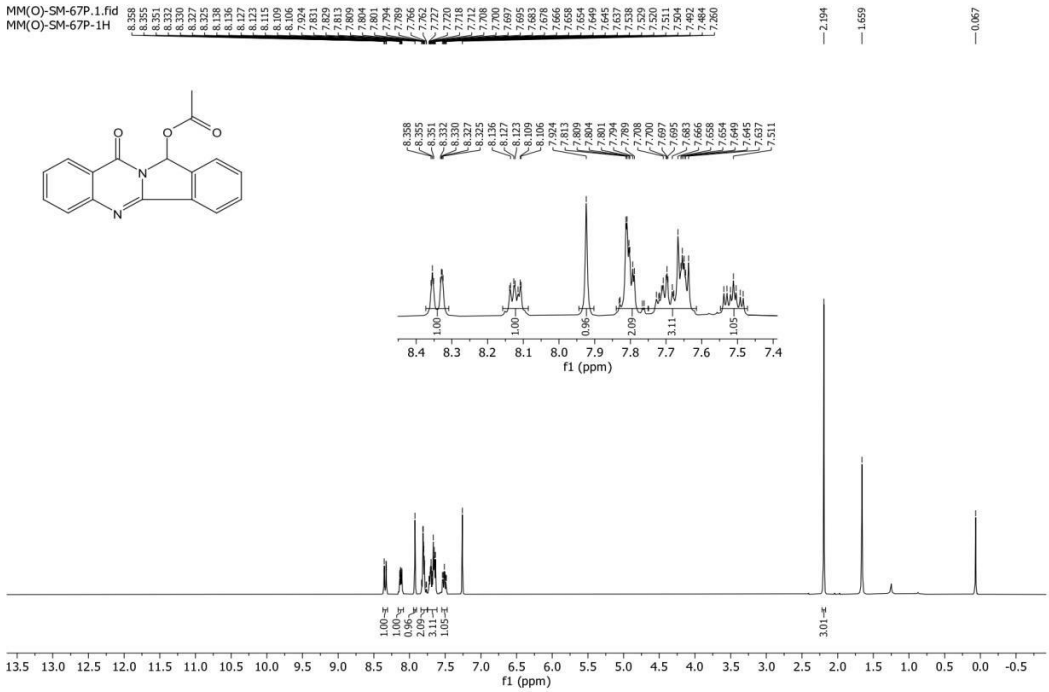

^{13}C-NMR of 37a

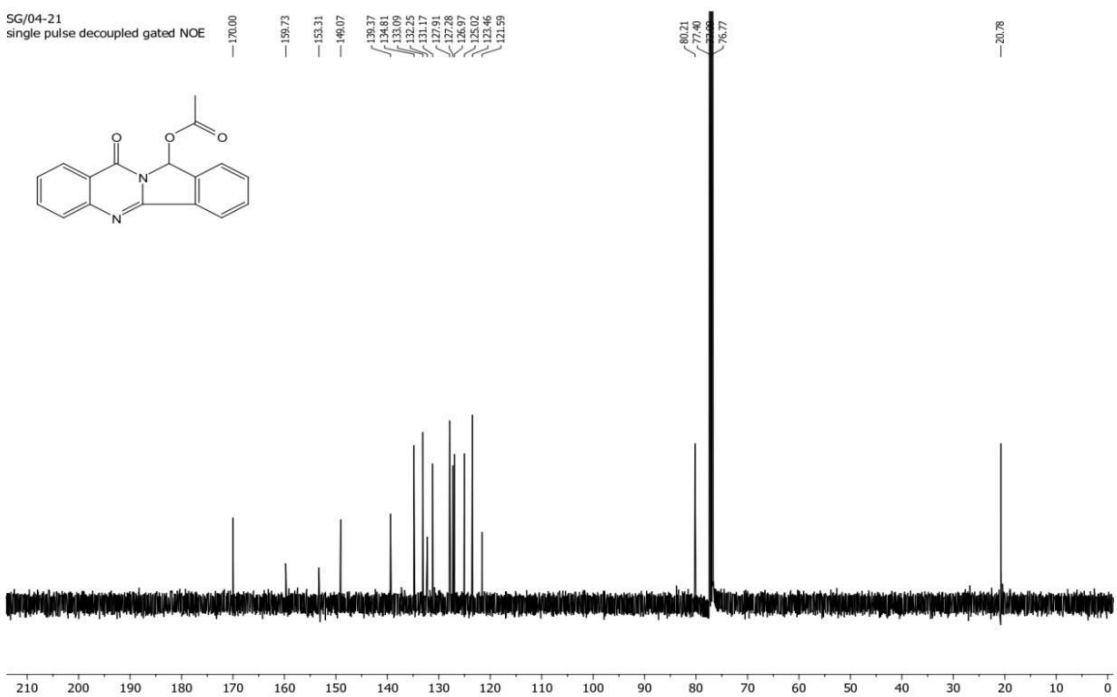

DEPT-90 NMR of 37a

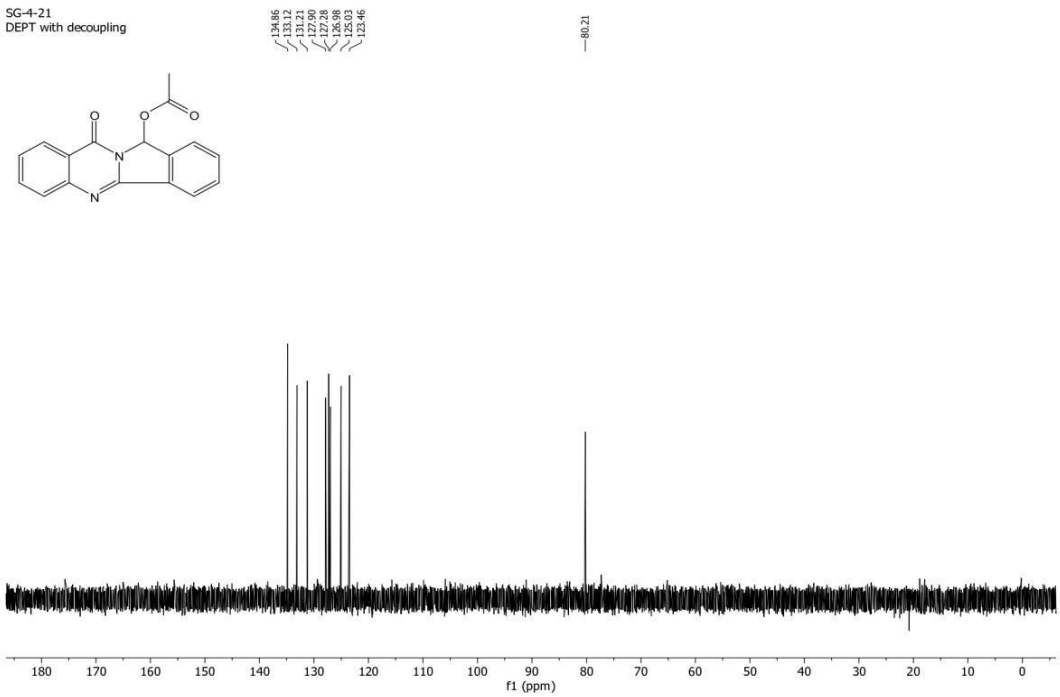

DEPT-135 NMR of 37a

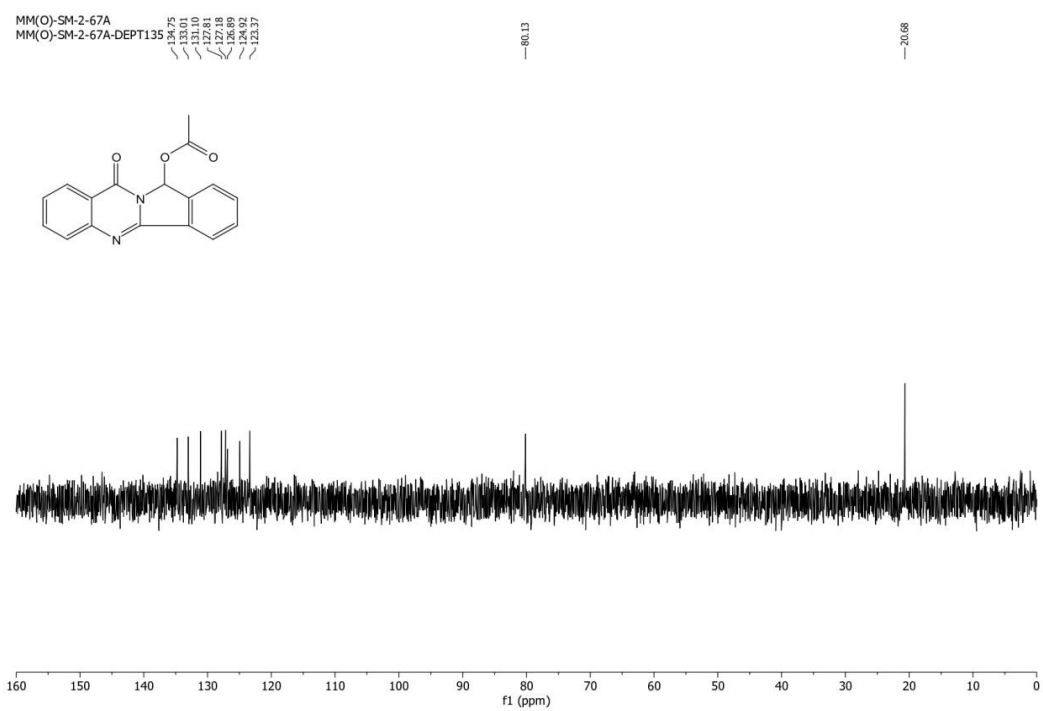

^{1}H-^{1}H-COSY NMR 37a

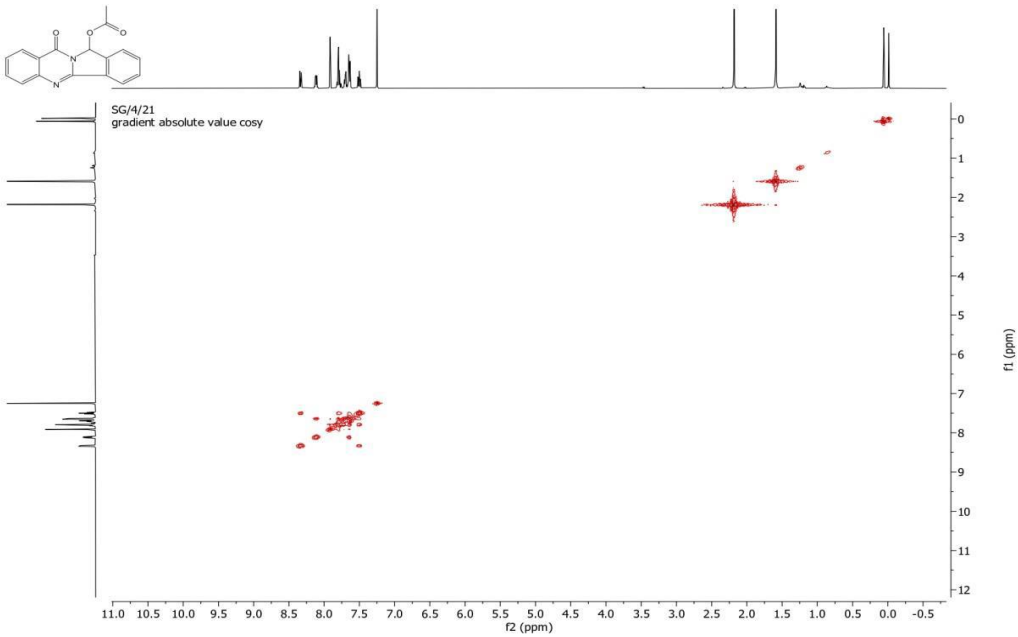

HMBC NMR of 37a

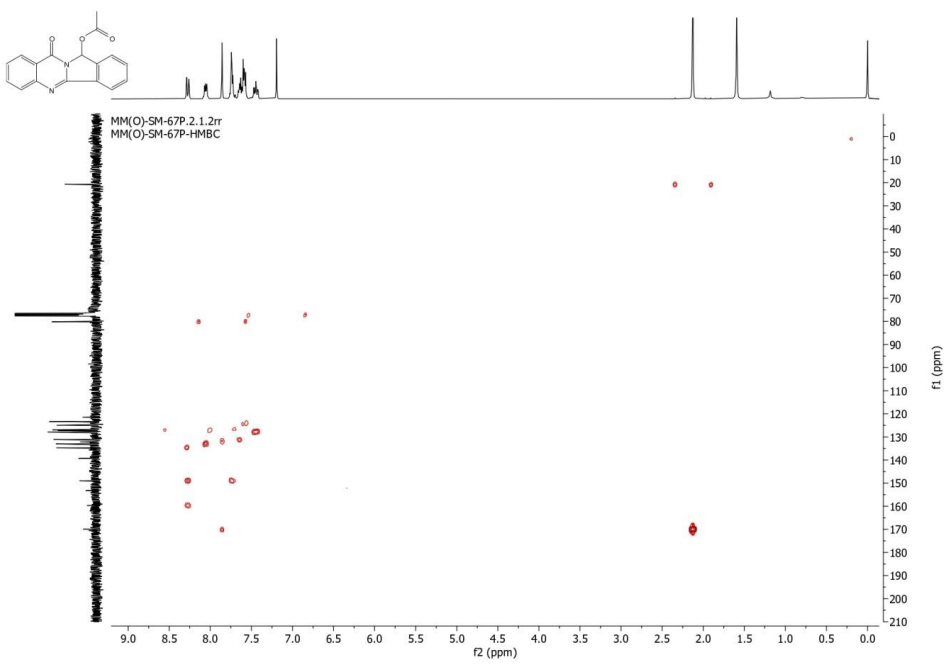

HSQC-NMR of 37a

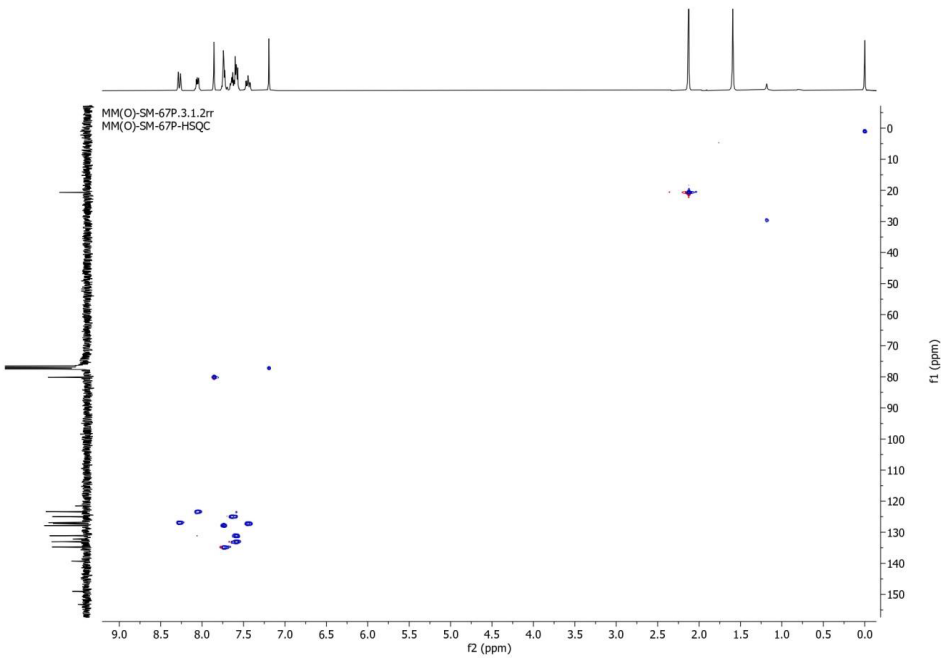

^{1}H-NMR of 37b

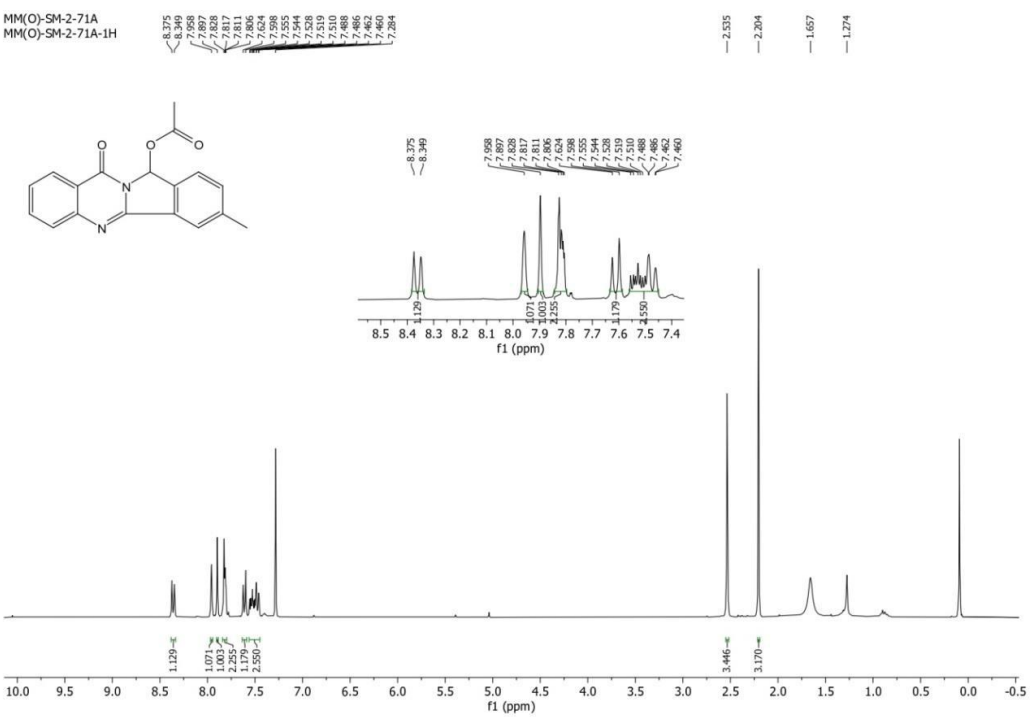

^{13}C-NMR of 37b

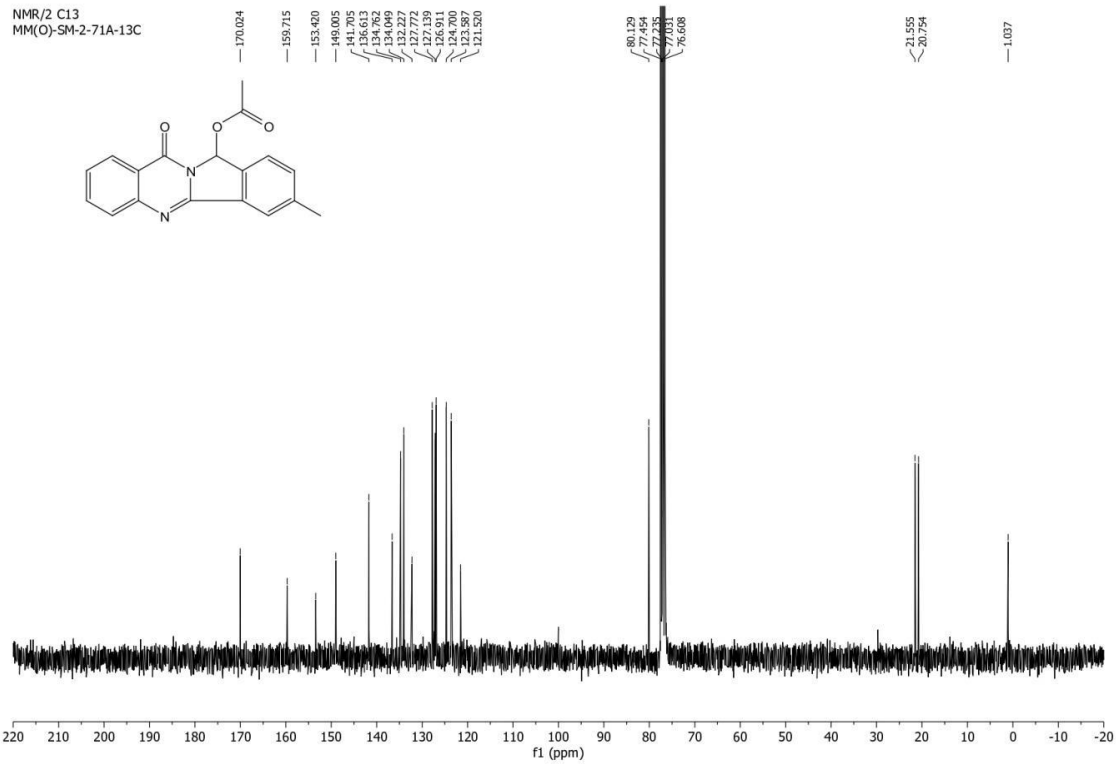

^{1}H-NMR of 37c

^{13}C-NMR of 37c

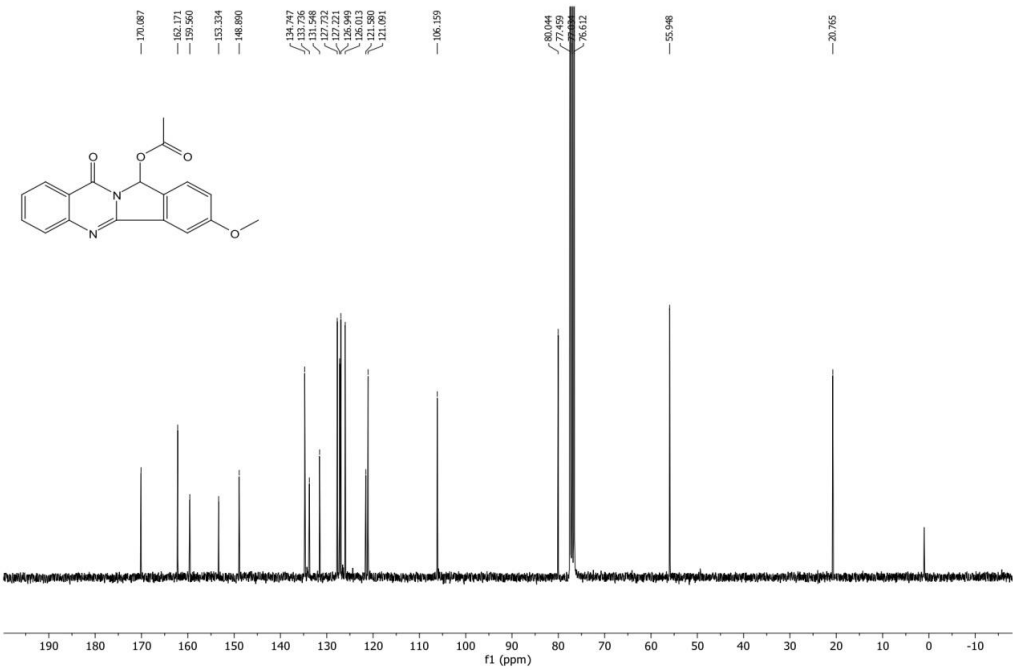

^{1}H-NMR of 37d

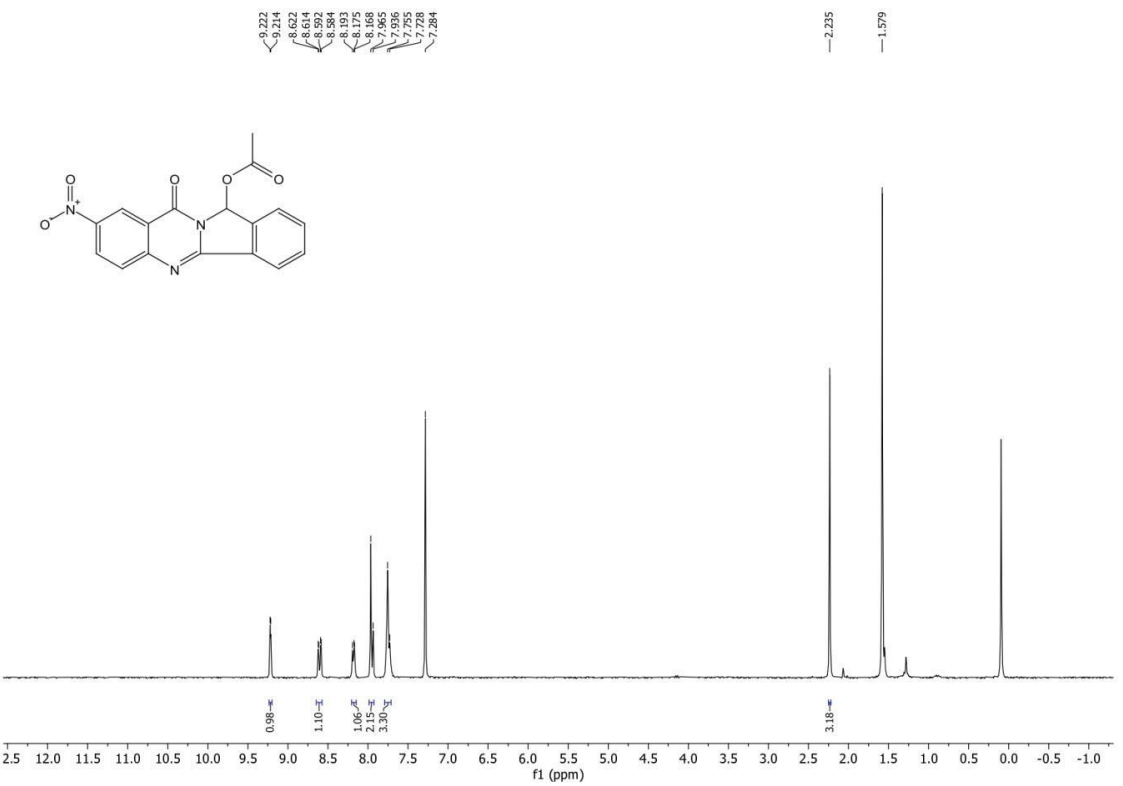

^{13}C-NMR of 37d

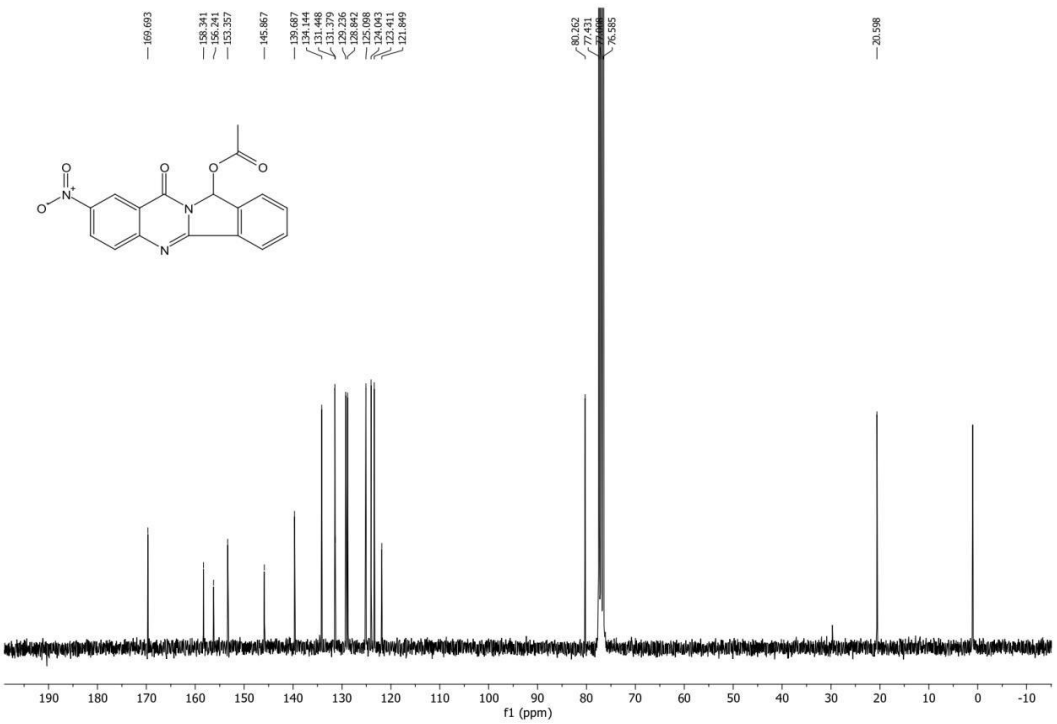

^{1}H-NMR of 37e

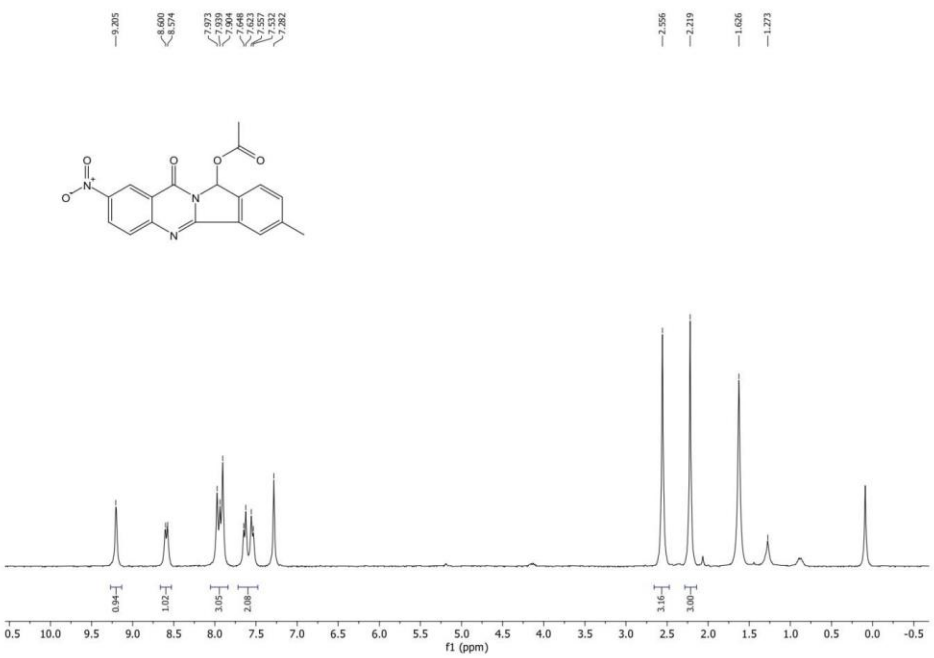

^{13}C-NMR of 37e

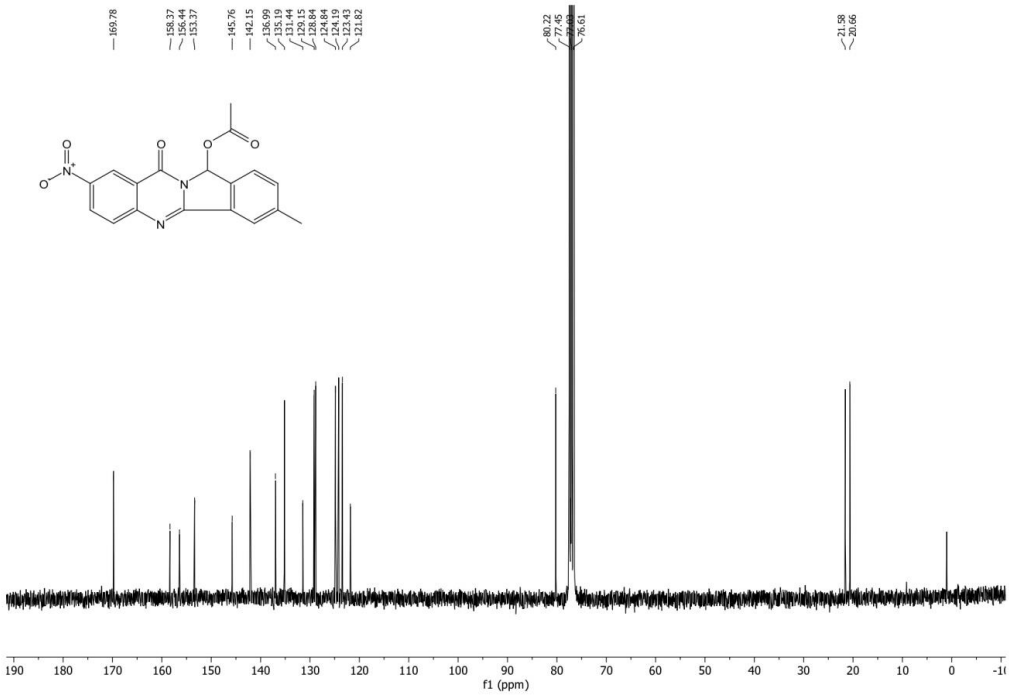

^{1}H-NMR of 37f

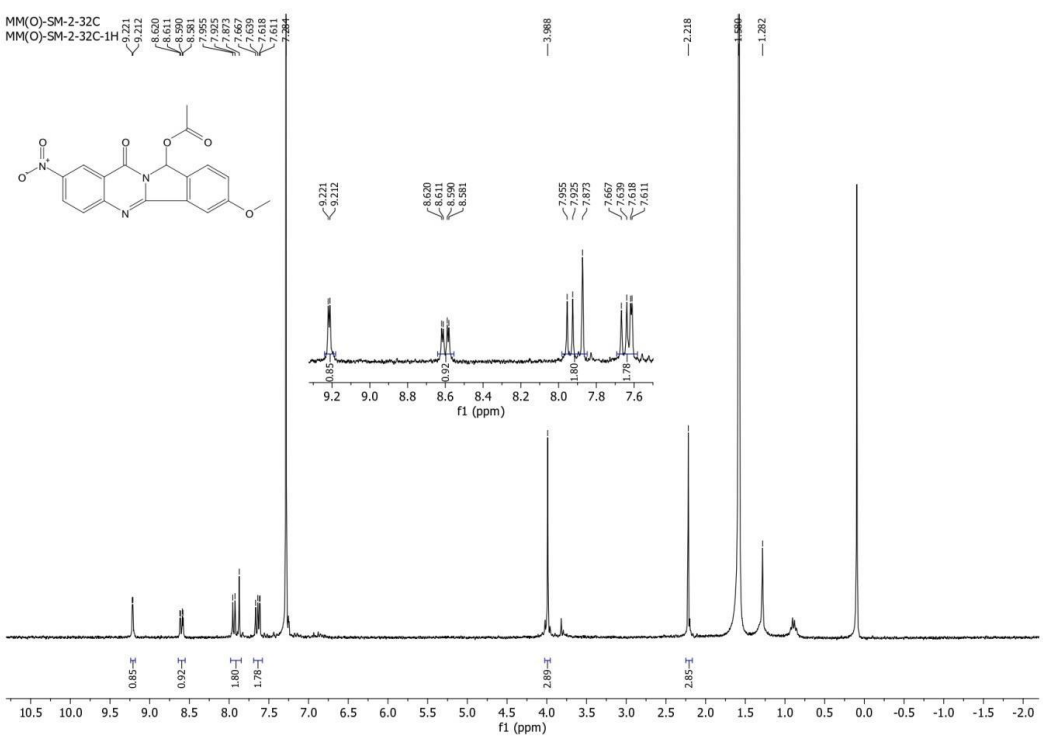

^{13}C-NMR of 37f

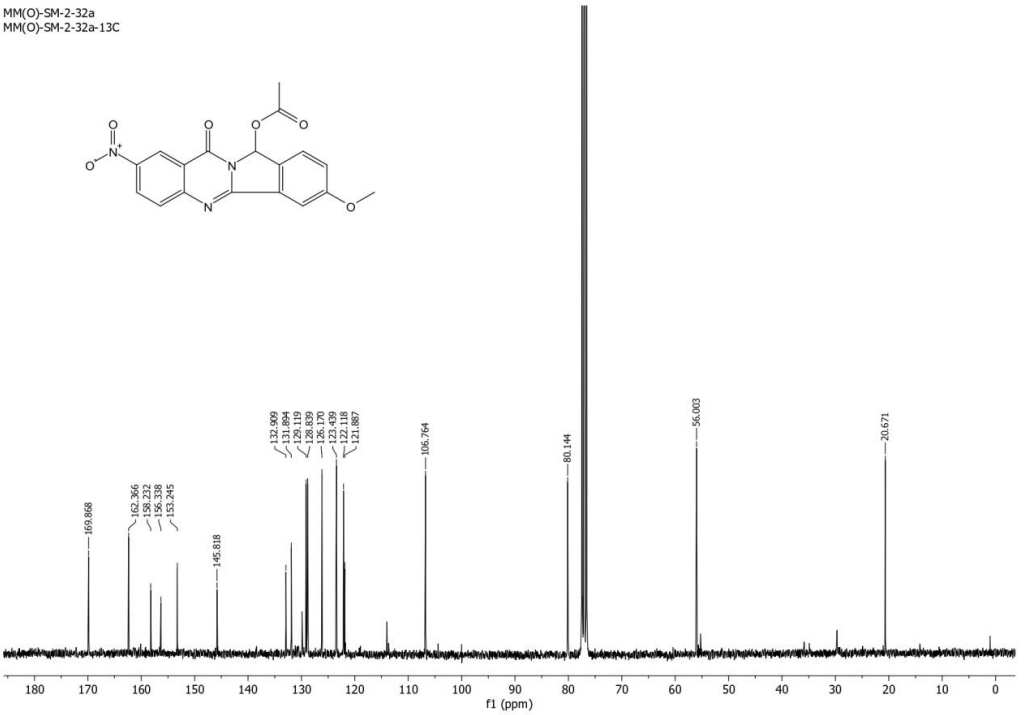

^{1}H-NMR of 37h

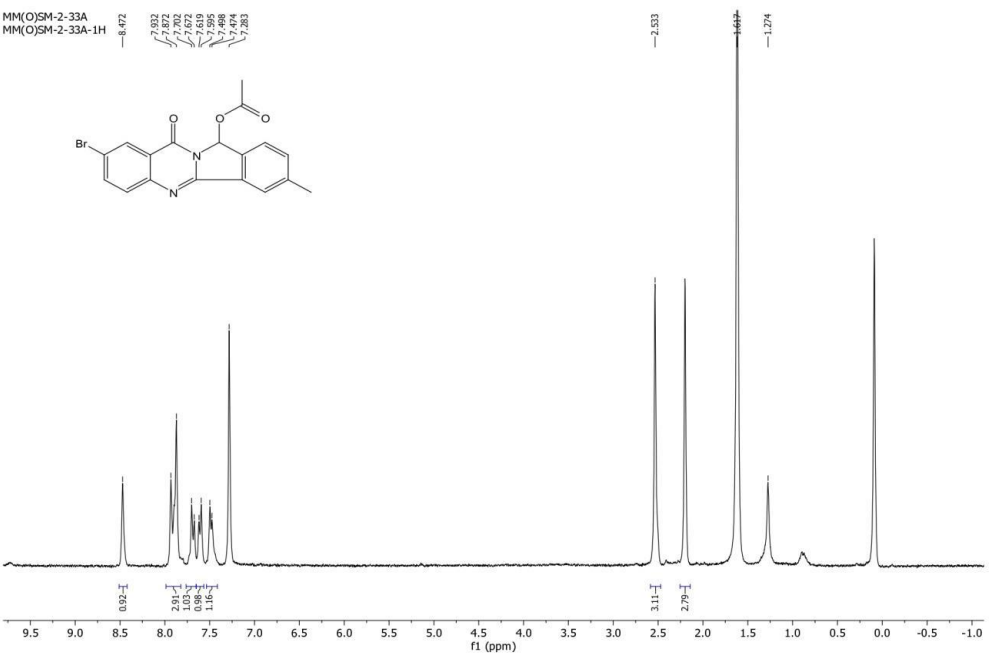

^{13}C-NMR of 37h

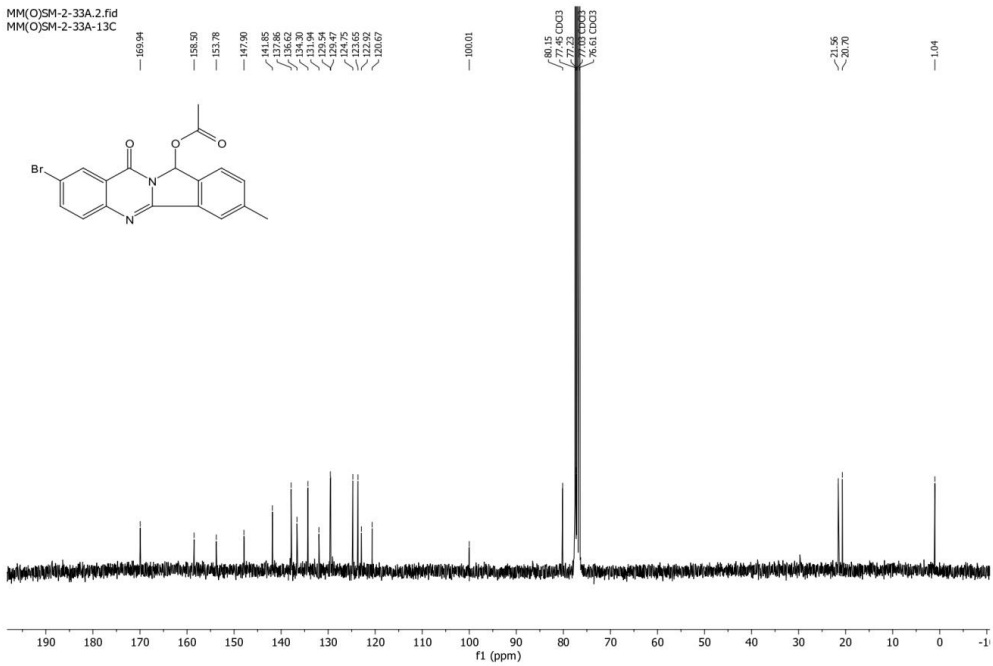

^{1}H-NMR of 37k

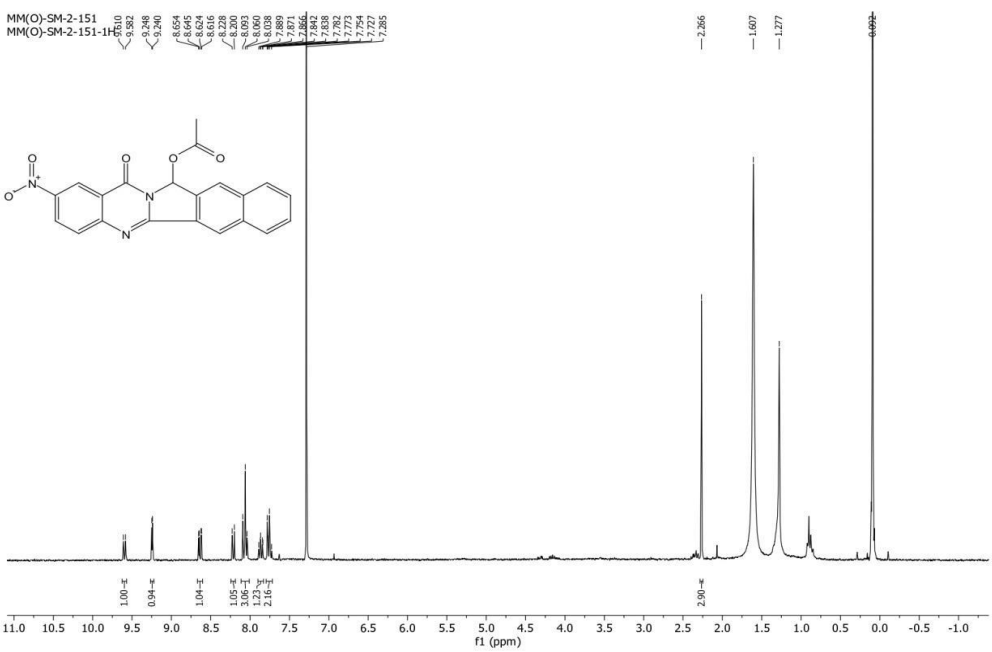

^{13}C-NMR of 37k

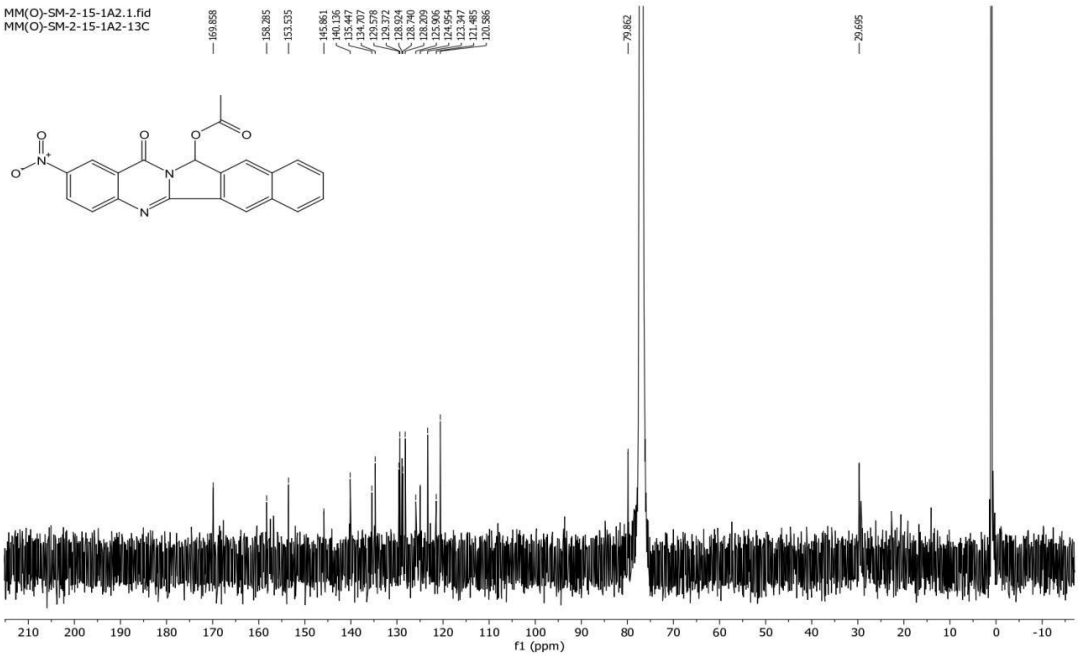

^{1}H-NMR of 38d

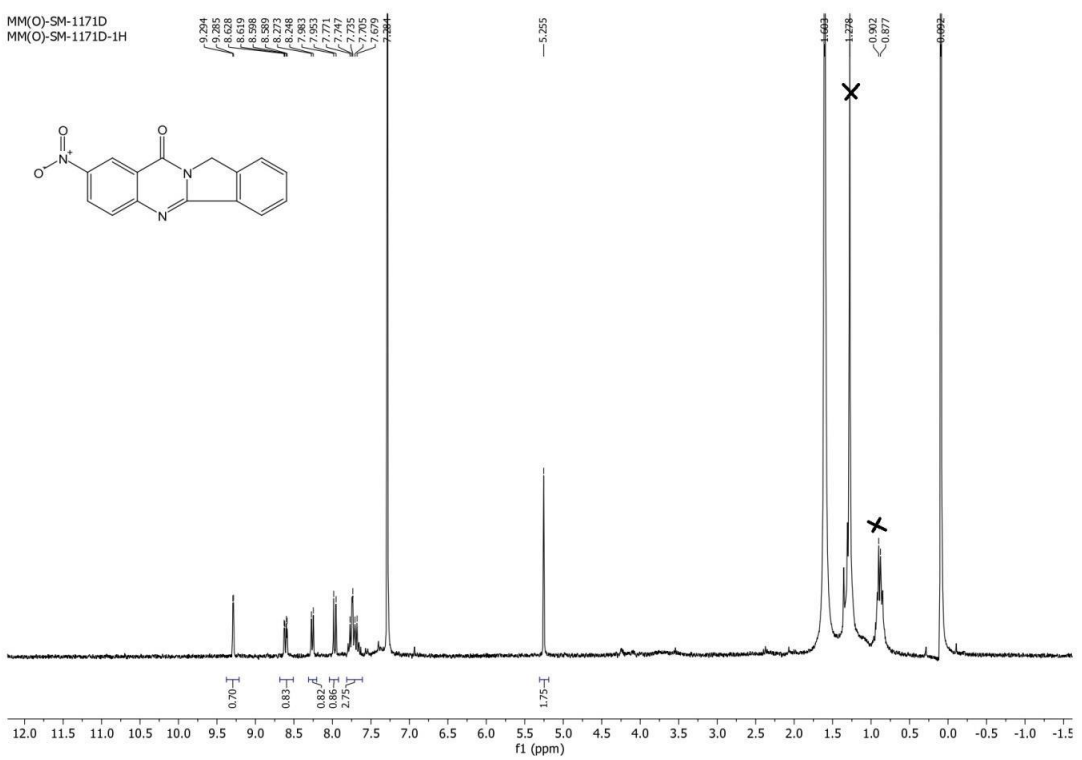

^{13}C-NMR of 38d

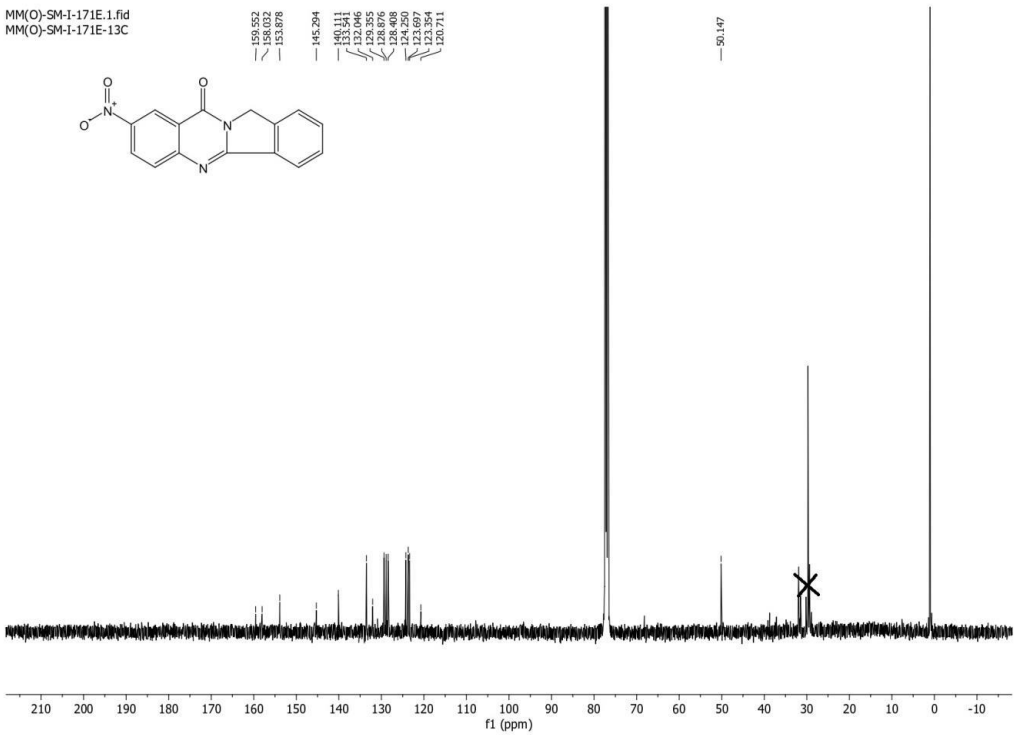

^{1}H-NMR 38e

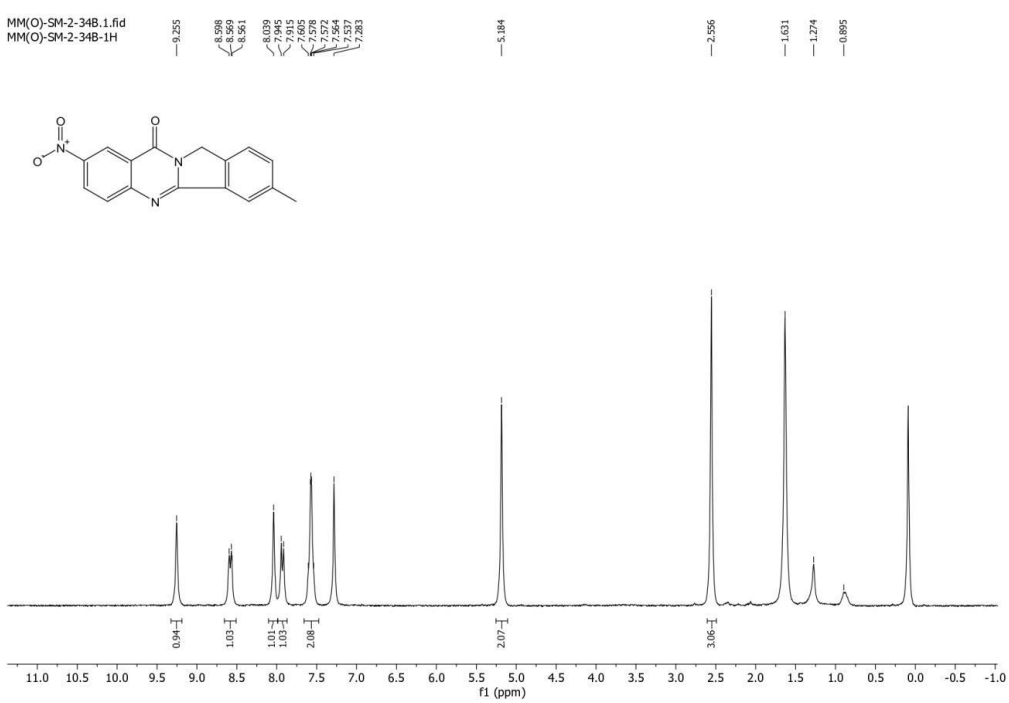

^{13}C-NMR 38e

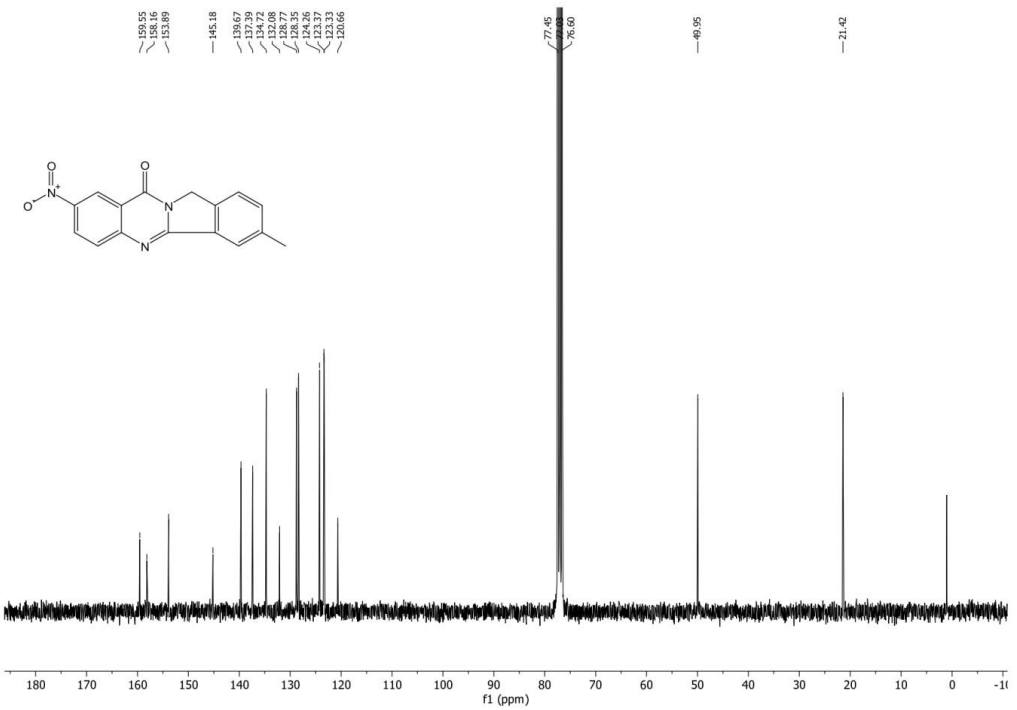

^{1}H-NMR of 38g

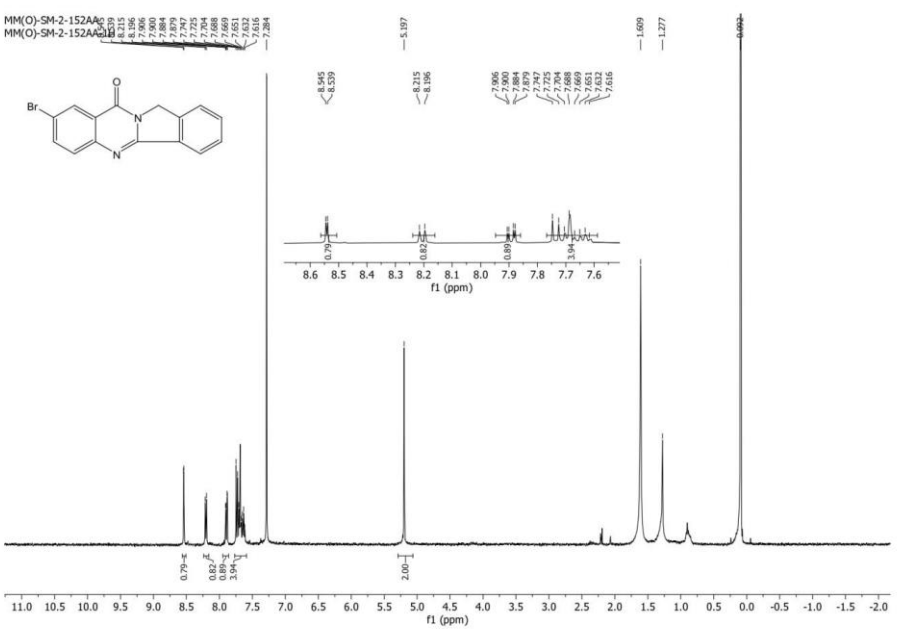

^{13}C-NMR of 38g

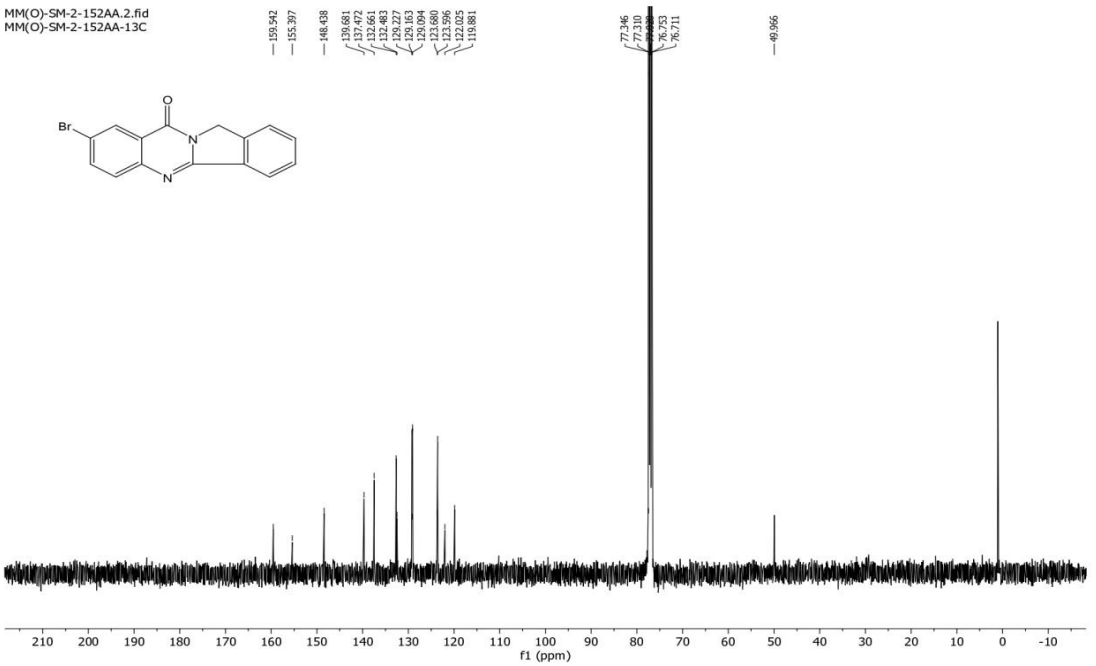

^{1}H-NMR of 38h

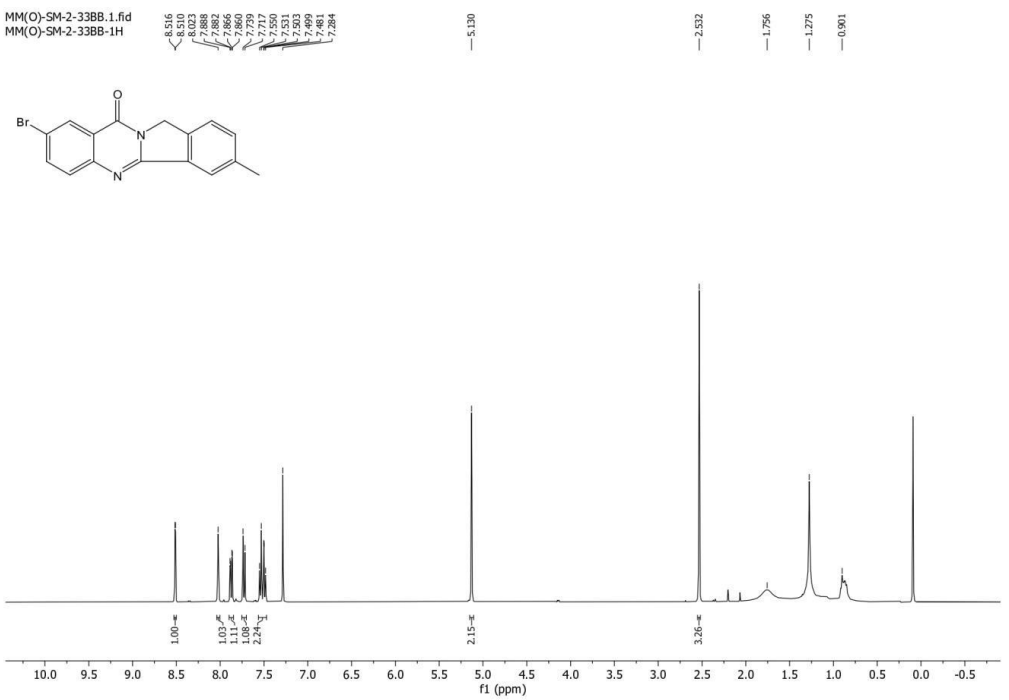

^{13}C-NMR 38h

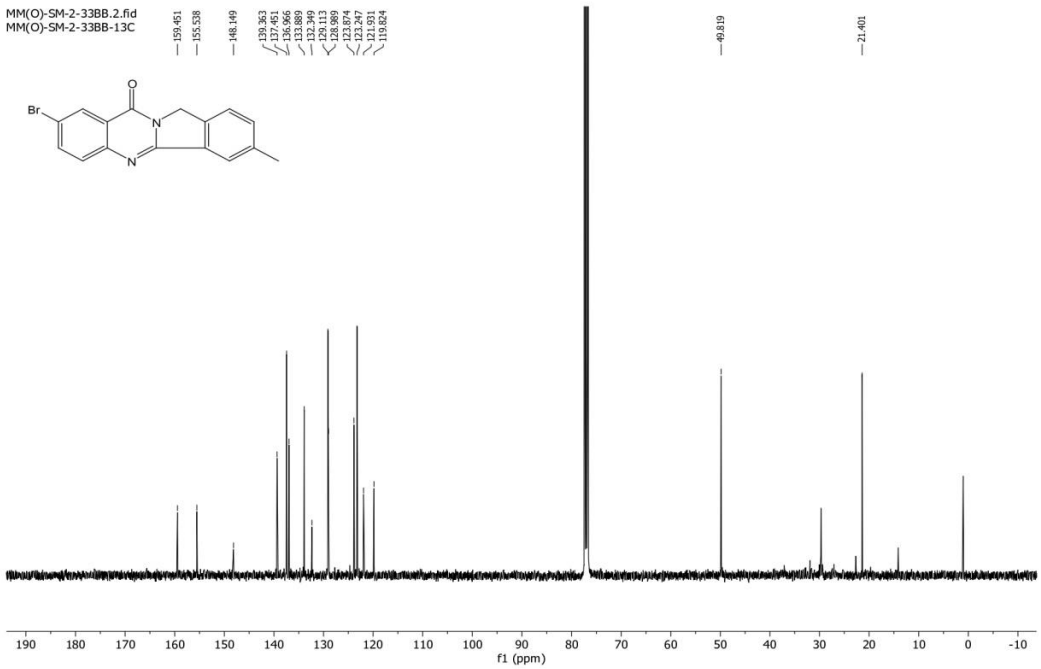

^{1}H-NMR of 38i

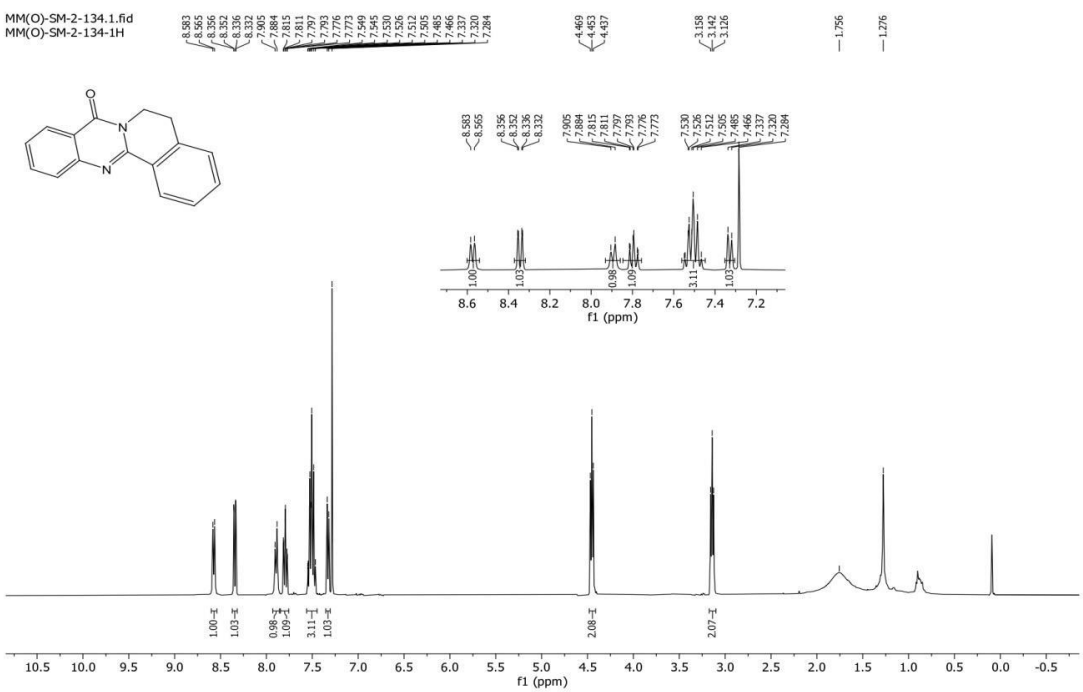

^{13}C-NMR of 38i

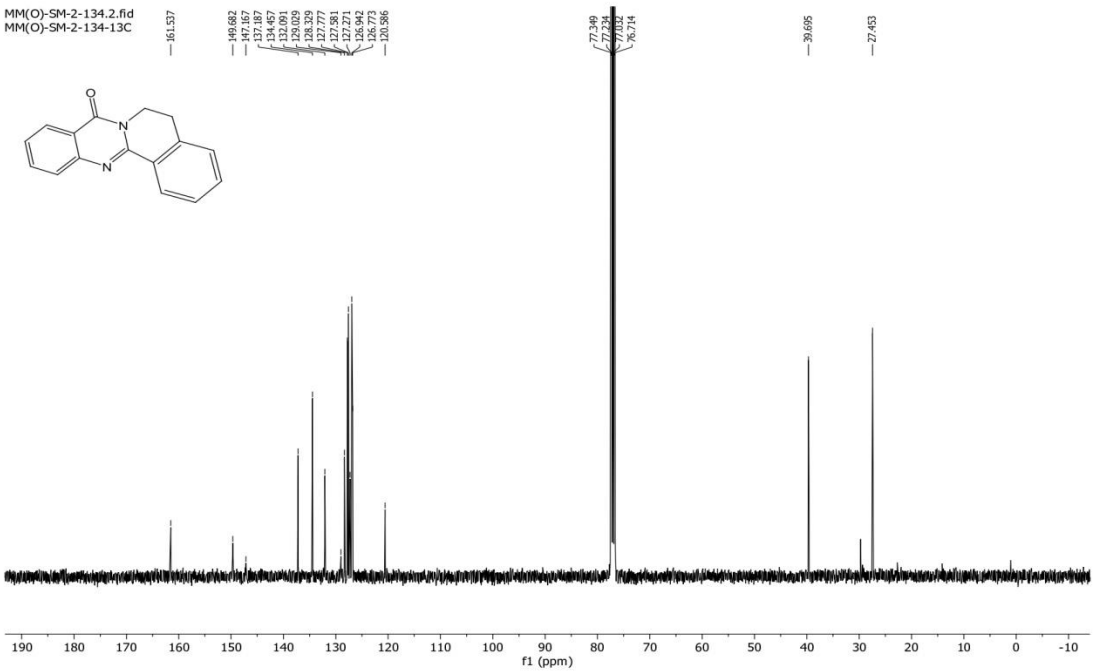

^{1}H-NMR of 38j

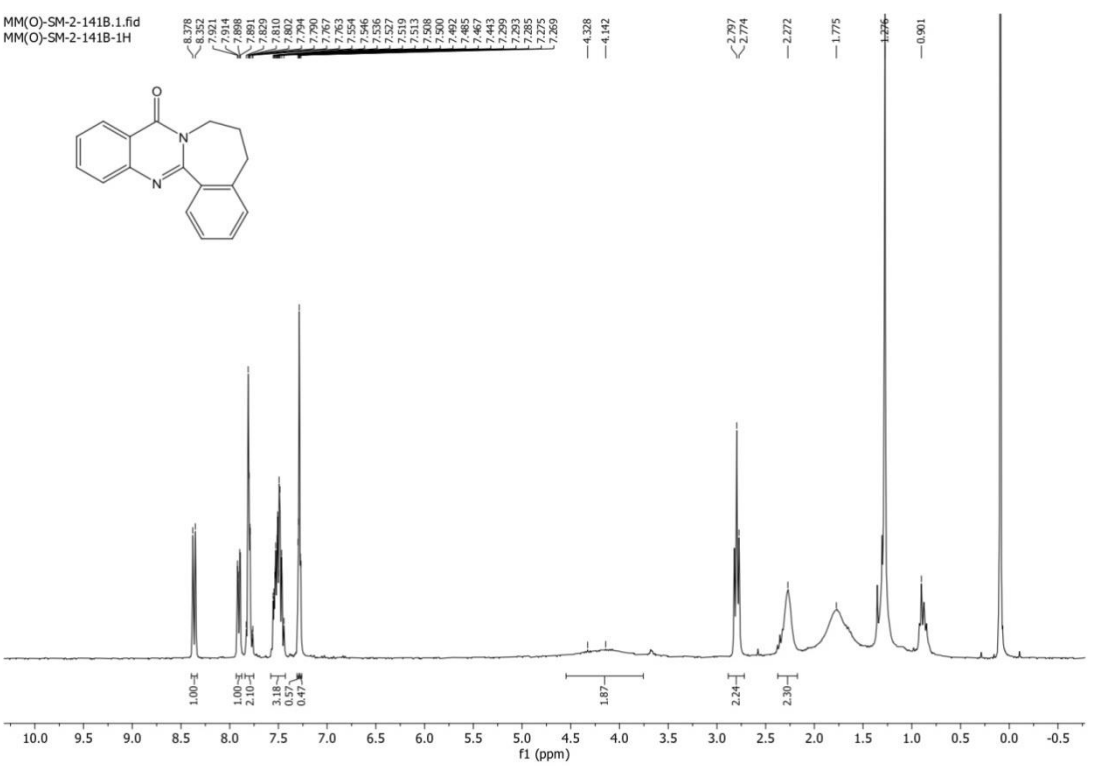

^{13}C-NMR of 38j

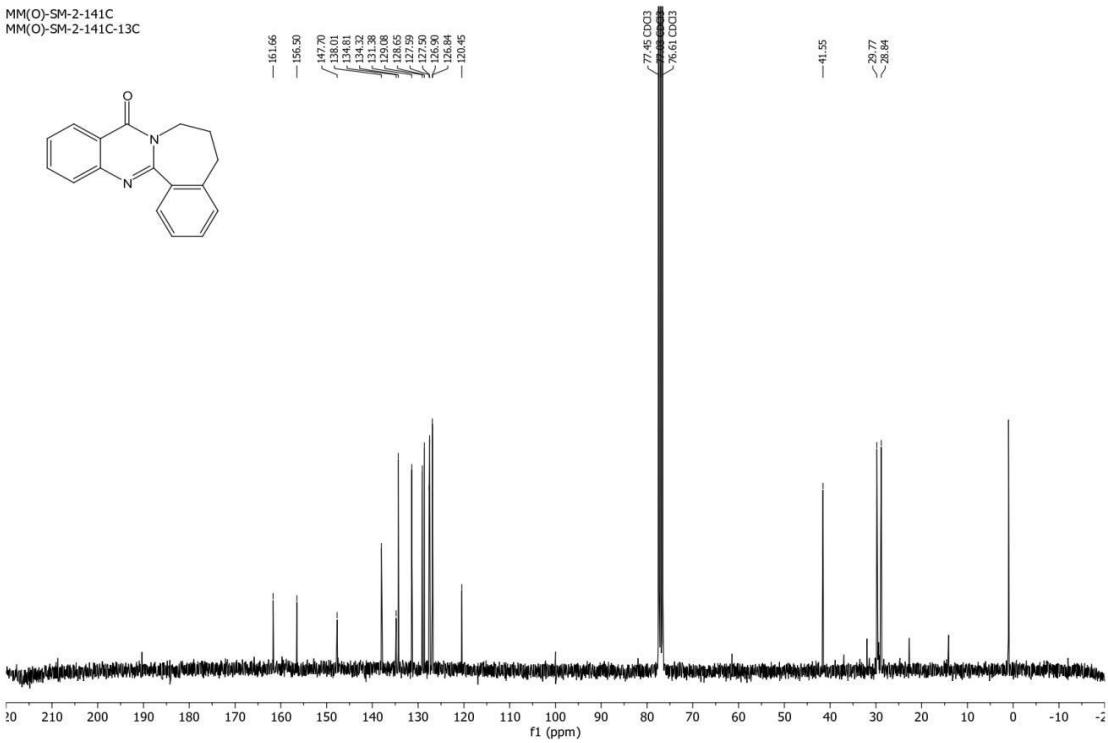

3.7 REFERENCES

[1] F. Pishgar, H. Ebrahimi, S. Saeedi Moghaddam, C. Fitzmaurice, E. Amini, *J. Urol.* **2018**, *199*, 1224-1232.

[2] F. Bray, A. Jemal, N. Grey, J. Ferlay, D. Forman, *Lancet Oncol.* **2012**, *13*, 790-801.

[3] Shagufta, I. Ahmad, *Med. Chem. Comm.***2017**, *8*, 871-885.

[4] a)M. F. Zayed, in *ChemEngineering, Vol. 6*, **2022**; b)A. Dutta, D. Sarma, *Tuberculosis (Edinb)* **2020**, *124*, 101986; c)E. Honkanen, A. Pippuri, P. Kairisalo, P. Nore, H. Karppanen, I. Paakkari, *J. Med. Chem.* **1983**, *26*, 1433-1438; d)N. Sepehri, A. Iraji, A. Yavari, M. S. Asgari, S. Zamani, S. Hosseini, S. Bahadorikhalili, S. Pirhadi, B. Larijani, M. Khoshneviszadeh, H. Hamedifar, M. Mahdavi, M. Khoshneviszadeh, *Bioorg. Med. Chem.* **2021**, *36*, 116044; e)F. Taayoshi, A. Iraji, A. Moazzam, M. Soleimani, M. Asadi, K. Pedrood, M. Akbari, H. Salehabadi, B. Larijani, N. Adibpour, M. Mahdavi, *BMC Chem.***2022**, *16*, 35; f)M. M. Khalifa, H. M. Sakr, A. Ibrahim, A. M. Mansour, R. R. Ayyad, *J. Mol. Struct.* **2022**, *1250*, 131768; g)M. Sohrabi, M. Nazari Montazer, S. M. Farid, N. Tanideh, M. Dianatpour, A. Moazzam, K. Zomorodian, S. Yazdanpanah, M. Asadi, S. Hosseini, M. Biglar, B. Larijani, M. Amanlou, M. Barazandeh Tehrani, A. Iraji, M. Mahdavi, *Sci. Rep.* **2022**, *12*, 2003.

[5] J. Zugazagoitia, C. Guedes, S. Ponce, I. Ferrer, S. Molina-Pinelo, L. Paz-Ares, *Clin. Ther.* **2016**, *38*, 1551-1566.

[6] H. Zhang, Y. Gao, G. Fu, J. Liu, Q. Jiao, *Eur. J. Med. Chem.* **2023**, *247*, 115041.

[7] Z.-Z. Ma, Y. Hano, T. Nomura, Y.-J. Chen, *Heterocycles* **1997**, *46*, 541-546.

[8] Z.-Z. Ma, Y. Hano, T. Nomura, Y.-J. Chen,*Heterocycles***1999**, *8*, 1883-1889.

[9] Z. Ma, Y. Hano, T. Nomura, Y. Chen, *Bioorg. Med. Chem. Lett.* **2004**, *14*, 1193-1196.

[10] G.-Z. Yang, J. Zhang, J.-W. Peng, Z.-J. Zhang, W.-B. Zhao, R.-X. Wang, K.-Y. Ma, J.-C. Li, Y.-Q. Liu, Z.-M. Zhao, X.-F. Shang, *Eur. J. Med. Chem.* **2020**, *194*, 112253.

[11] M.-J. Don, D. F. Lewis, S.-Y. Wang, M.-W. Tsai, Y.-F. J. B. Ueng, **2003**, *13*, 2535-2538.

[12] W. S. Byun, E. S. Bae, W. K. Kim, S. K. Lee, *J. nat. prod.***2022**, *85*, 1407-1418.

[13] D. F. Lewis, B. G. Lake, S. G. George, M. Dickins, P. J. Eddershaw, M. H. Tarbit, A. P. Beresford, P. S. Goldfarb, F. P. Guengerich, *Toxicology* **1999**, *139*, 53-79.

[14] U. Kojalo, A. Tisler, K. Parna, A. Kivite-Urtane, J. Zodzika, M. Stankunas, N. Baltzer, M. Nygard, A. Uuskula, *BMC Public Health* **2023**, *23*, 660.

[15] T. C. Moon, M. Murakami, I. Kudo, K. H. Son, H. P. Kim, S. S. Kang, H. W. Chang, *Inflammation research : official journal of the European Histamine Research Society ... [et al.]* **1999**, *48*, 621-625.

[16] W. Peng, *Global Strategy***2022**.

[17] S. P. John, A. Singh, J. Sun, M. J. Pierre, L. Alsalih, C. Lipsey, Z. Traore, S. Balcom-Luker, C. J. Bradfield, J. Song, T. E. Markowitz, M. Smelkinson, M. Ferrer, I. D. C. Fraser, *Cell rep.***2022**, *41*, 111441.

[18] Y. Feng, Y. Lu, J. Li, H. Zhang, Z. Li, H. Feng, X. Deng, D. Liu, T. Shi, W. Jiang, Y. He, J. Zhang, Z. Wang, *Eur. J. med. chem.***2022**, *227*, 113888.

[19] M.-C. Tseng, Y.-W. Chu, H.-P. Tsai, C.-M. Lin, J. Hwang, Y.-H. Chu, *Org. Lett.* **2011**, *13*, 920-923.

[20] S. M. Roopan, F.-R. N. Khan, J. S. Jin, *Chem. Pap.***2011**, *65*, 345-351.

[21] L. Xie, C. Lu, D. Jing, X. Ou, K. Zheng, *Eur JOC***2019**, *2019*, 3649-3653.

[22] Y. Ju, F. Liu, C. Li, *Org. Lett.* **2009**, *11*, 3582-3585.

[23] A. Beaume, C. Courillon, E. Derat, M. Malacria, *Chem. Eur. J.***2008**, *14*, 1238-1252.

[24] R. Xu, Z. Wang, Q. Zheng, P. Patil, A. Dömling, *J. Org. Chem.***2022**, *87*, 13023-13033.

[25] C. Lu, Z. Su, D. Jing, S. Jin, L. Xie, L. Li, K. Zheng, *Org. Lett.* **2019**, *21*, 1438-1443.

[26] T. Harayama, A. Hori, G. Serban, Y. Morikami, T. Matsumoto, H. Abe, Y. Takeuchi, *Tetrahedron* **2004**, *60*, 10645-10649.

[27] W. R. Bowman, M. R. J. Elsegood, T. Stein, G. W. Weaver, *Org. Biomol. Chem.* **2007**, *5*, 103-113.

[28] C.-J. Li, *Acc. Chem. Res.* **2009**, *42*, 335-344.

[29] K. L. Hull, M. S. Sanford, *J. Am. Chem. Soc.* **2007**, *129*, 11904-11905.

[30] T. W. Lyons, M. S. Sanford, *Chem. Rev.* **2010**, *110*, 1147-1169.

[31] R. Li, L. Jiang, W. Lu, *Organometallics* **2006**, *25*, 5973-5975.

[32] T. A. Dwight, N. R. Rue, D. Charyk, R. Josselyn, B. DeBoef, *Org. Lett.* **2007**, *9*, 3137-3139.

[33] C. Cheng, W.-W. Chen, B. Xu, M.-H. Xu, *Org. Chem. Front.***2016**, *3*, 1111-1115.

[34] T. Yang, X. Ding, X. Zhan, Y. Weng,*Asian J. Org. Chem.* **2020**, *9*, 1765-1768.

[35] K. C. Pereira, A. L. Porter, B. DeBoef, *Tetrahedron Lett.* **2014**, *55*, 1729-1732.

[36] M. Lessi, A. Lucci, A. Cuzzola, F. Bellina,*Eur. J. Org. Chem.***2020**, *2020*, 796-802.

[37] A. Cagir, S. H. Jones, R. Gao, B. M. Eisenhauer, S. M. Hecht, *J. Am. Chem. Soc.* **2003**, *125*, 13628-13629.

[38] P. Bhandu, H. Verma, M. Singh, M. Kumar, G. Narendra, S. Choudhary, P. K. Singh, O. Silakari, *J. Mol. Struct.* **2022**, *1270*, 133825.

[39] J. Luo, J. Wan, L. Wu, L. Yang, T. Wang, *J. Org. Chem.***2022**, *87*, 9864-9874.

[40] S. Li, J. Ren, C. Ding, Y. Wang, C. Ma,*J. Org. Chem.***2021**, *86*, 16848-16857.

[41] R. Srinath, A. Manna, S. Shee, V. B. Pathi, S. Ghosh, K. Khamaru, N. C. Maiti, B. Banerji, *Org. Lett.* **2021**, *23*, 9365-9370.

[42] a)K. Nacro, C. C. Zha, P. R. Guzzo, R. Jason Herr, D. Peace, T. D. Friedrich, *Bioorg. Med. Chem.* **2007**, *15*, 4237-4246; b)A. Cagir, B. M. Eisenhauer, R. Gao, S. J. Thomas, S. M. Hecht, *Bioorg. Med. Chem.* **2004**, *12*, 6287-6299; c)A. Cagir, S. H. Jones, B. M. Eisenhauer, R. Gao, S. M. Hecht, *Bioorg. Med. Chem. Lett.* **2004**, *14*, 2051-2054.

[43] R. Palchaudhuri, P. J. Hergenrother, *Curr. Opin. Biotechnol.* **2007**, *18*, 497-503.

[44] L. B. Hendry, V. B. Mahesh, E. D. Bransome, Jr., D. E. Ewing, *Mutat. Res.* **2007**, *623*, 53-71.

[45] M. Sirajuddin, S. Ali, A. Badshah, *J. Photochem. Photobiol. B* **2013**, *124*, 1-19.

[46] I. D. Kuntz, Jr., F. P. Gasparro, M. D. Johnston, Jr., R. P. Taylor, *J. Am. Chem. Soc.* **1968**, *90*, 4778-4781.

[47] J. L. Liang, H. C. Cha, Y. Jahng, *Molecules* **2011**, *16*, 4861-4883.

[48] aY. Maehara, H. Anai, R. Tamada, K. Sugimachi, *Eur. J. Cancer Clin. Oncol.* **1987**, *23*, 273-276; bD. T. Vistica, P. Skehan, D. Scudiero, A. Monks, A. Pittman, M. R. Boyd, *Cancer Res.* **1991**, *51*, 2515-2520.

[49] M. V. Berridge, A. S. Tan, *Arch. Biochem. Biophys.* **1993**, *303*, 474-482.

[50] F.-R. Alexandre, A. Berecibar, R. Wrigglesworth, T. Besson, *Tetrahedron Lett.* **2003**, *44*, 4455-4458.

[51] A. Testard, C. Logé, B. Léger, J.-M. Robert, O. Lozach, M. Blairvacq, L. Meijer, V. Thiéry, T. Besson, *Bioorg. Med. Chem. Lett.* **2006**, *16*, 3419-3423.

[52] E. Sheikhi, M. Adib, R. Yazzaf, M. Jahani, M. Ghavidel, *Synlett.***2018**, *29*, 2046-2050.

[53] N. Adhikary, S. Mandal, A. Jana, A. Pramanik, *Results Chem.***2021**, *4*, 100270.

[54] J. A. Glasel, *BioTechniques* **1995**, *18*, 62-63.

[55] N. Shahabadi, S. Kashanian, F. Darabi, *Eur. J. Med. Chem.* **2010**, *45*, 4239-4245.

LIST OF PUBLICATIONS

1. Mohabul A.Mondal, **Sudipta Mondal**, Abdul A. Khan, Mechanistic study and one-pot synthesis of Isoindole -fused Quinazolin(4)-ones, *J. Chem. Sci*. **2020**,*132,* 63. DOI: https://doi.org/10.1007/s12039-020-01768-3
2. **Sudipta Mondal**, Mohabul A.Mondal, Synthesis of 3,4-dihydropyrimidin-2(1H)-one via Retro-Biginelli reaction, *J. Heterocycl.Chem*. **2020**, 57, 4175–4180. DOI: https://doi.org/10.1002/jhet.4124
3. Mohabul A. Mondal, **Sudipta Mondal**, Abdul A. Khan, Synthesis of Functionalized Quinazolinones via Acid-Catalyzed Redox Neutral Reaction, *Chemistry Select* **2021**, *6*, 1– 5. DOI: https://doi.org/10.1002/slct.202102976
4. **Sudipta Mondal**, Rwitabrita Panda, Soumya Das, Farhin Sultana, Sankhadeep Dutta, Mohabul A. Mondal, Synthesis and ct-DNA Binding Study of a Donor-π-Acceptor Dihydropyrimidinone Fluorophor, *J. Mol. Struct*. **2023**, *1285*, 135438. DOI: https://doi.org/10.1016/j.molstruc.2023.135438
5. **Sudipta Mondal**, Farhin Sultana, Dr. Sankhadeep Dutta, Mohabul A. Mondal, Synthesis of Luotonin and Rutaecarpine Analogues by One- Pot Intramolecular Dehydrogenative Cross-Coupling and Benzylic C-H Oxidation, and In Vitro Cytotoxicity Assay, *Chemistry Select*, **2023**, *8*, e202300980. DOI: https://doi.org/10.1002/slct.202300980
6. Arunava Misra, **Sudipta Mondal,** Mohabul A. Mondal, Synthesis of 11H-Benzo[b]Fluoren-11-One via an Unprecedented Cascade Reaction of *O*-Phthaladehyde, *Polycycl. Aromat. Compd.* **2023**, 1-8. DOI: https://doi.org/10.1080/10406638.2023.2270124

PUBLICATIONS ABSTRACT

J. Chem. Sci. (2020)132:63
https://doi.org/10.1007/s12039-020-01768-3

REGULAR ARTICLE

A mechanistic insight into the acid catalyzed, one-pot synthesis of isoindole-fused quinazolin 4-ones

MOHABUL A MONDAL*, SUDIPTA MONDAL and ABDUL A KHAN
Department of Chemistry, Jadavpur University, Kolkata 700 032, West Bengal, India
E-mail: mohabula.mondal@jadavpuruniversity.in

MS received 20 June 2019; revised 22 November 2019; accepted 2 January 2020

Abstract. One-pot synthesis of isoindole fused quinazolin 4-ones *via* intramolecular 1,3 hydride transfer in the presence of acid catalyst has been described. Substrate scope and mechanistic insights were investigated. Substituents on the amide side have a negligible influence on the key step and therefore the method have wide scope for accessing various bicyclic core structure.

JOURNAL OF HETEROCYCLIC CHEMISTRY

ARTICLE | Full Access

Synthesis of 3,4-dihydropyrimidin-2(1*H*)-one via Retro-Biginelli reaction

Sudipta Mondal, Mohabul A. Mondal

First published: 13 August 2020 | https://doi.org/10.1002/jhet.4124 | Citations: 3

Funding information: Jadavpur University, Kolkata; SERB New Delhi

SECTIONS PDF TOOLS SHARE

Abstract

Hydrolytic behavior of 5-acetyl-6-methyl-4-phenyl-3,4-dihydropyrimidin-2(1H)-one under alkaline condition has been explored. Mechanistic details are established by LCMS and HPLC. Evidence suggested that the deacetylative benzylidenation proceeds through the retro-Biginelli reaction. The scope of the retro-Biginelli reaction has been explored by the synthesis of substituted DHPs.

ChemistrySelect

Chemistry Europe
European Chemical Societies Publishing

Communication | Full Access

Synthesis of Functionalized Quinazolinones via Acid-Catalyzed Redox Neutral Reaction

Dr. Mohabul A. Mondal, Sudipta Mondal, Dr. Abdul A. Khan

First published: 10 November 2021 | https://doi.org/10.1002/slct.202102976 | Citations: 1

Graphical Abstract

A facile 1,5 hydride shift was observed in a one-pot synthesis of functionalized quinazolinones from anthranilamide and glutaraldehyde under a mild acidic condition at ambient temperature. The hydride is being transferred from a dihydroquinazolinone moiety to a distal imine functional group. Suggested a hydride transfer mechanism based on experimental evidence. The influence of steric and electronic effects, and length of the dialdehyde towards the hydride transfer reaction, was studied.

ChemistrySelect

Chemistry Europe
European Chemical Societies Publishing

Research Article | Full Access

Synthesis of Luotonin and Rutaecarpine Analogues by One-Pot Intramolecular Dehydrogenative Cross-Coupling and Benzylic C–H Oxidation, and In Vitro Cytotoxicity Assay

Sudipta Mondal, Farhin Sultana, Dr. Sankhadeep Dutta, Dr. Mohabul A. Mondal

First published: 04 July 2023 | https://doi.org/10.1002/slct.202300980

Graphical Abstract

We designed and explored a new route for synthesizing Luotonin and Rutaecarpine analoges by a one-pot multi-step reaction catalysed by palladium metal. All the new compounds are characterized by NMR Mass and Single crystal XRD. The result of the cell viability study of one of the synthesized compounds with SiHa carcinoma cell is promising.

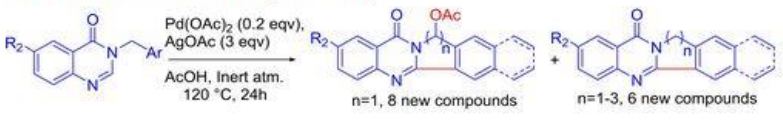

Journal of Molecular Structure 1285 (2023) 135438

Contents lists available at ScienceDirect

Journal of Molecular Structure

journal homepage: www.elsevier.com/locate/molstr

Synthesis and ct-DNA binding study of a donor-π-acceptor dihydropyrimidinone fluorophore

Sudipta Mondal[a], Rwitabrita Panda[a], Soumya Das[a], Farhin Sultana[b], Sankhadeep Dutta[b], Mohabul A. Mondal[a,*]

[a] Department of Chemistry, Jadavpur University, Kolkata 700032, India
[b] Department of Oncogene Regulation, Chittaranjan National Cancer Institute, 37 S. P. Mukherjee Road, Kolkata 700 026, India

ARTICLE INFO

Article history:
Received 20 November 2022
Revised 23 March 2023
Accepted 25 March 2023

Keywords:
Dihydropyrimidinone
DNA binding study
Photophysical study
Molecular docking study
AZA Michael addition

ABSTRACT

We have described the synthesis of a Donor-π-Acceptor dihydropyrimidinone (DHP) fluorophore via functional group modification of dihydropyrimidinone, commonly known as Biginelli product, to probe ds-DNA. The intermediates including the target compounds was characterized by NMR, mass, and XRD. The inherent fluorescence of the synthesized DHP is very weak. However, in the presence of ds-DNA, the fluorescence emission intensity enhances up to 5 times. The type of interactions of the DHP with ds-DNA was investigated thoroughly by spectroscopic methods. The combined result of Gaussian calculation and the time-resolved fluorescence spectroscopy suggested the formation of an effective charge transfer of Donor-π-Acceptor system. The results of the iodide quenching effect and displacement assay with Hoechst and Ethidium bromide indicated a minor groove binding mechanism. A theoretical model has been constructed by using the AutoDoc Vina package to visualize different types of non-bonded interaction of the DHP with other heteroatomic units in the narrow and shallow cut of the minor groove of ds-DNA. We observed the incorporation of **3a** within the cell and the targeting of the nucleus by using a confocal microscope.

POLYCYCLIC AROMATIC COMPOUNDS
https://doi.org/10.1080/10406638.2023.2270124

Taylor & Francis
Taylor & Francis Group

Check for updates

Synthesis of 11*H*-Benzo[b]Fluoren-11-One via an Unprecedented Cascade Reaction of *O*-Phthaladehyde

Arunava Misra, Sudipta Mondal, and Mohabul A. Mondal

Department of Chemistry, Jadavpur University, Kolkata, India

ABSTRACT

Developing multicomponent reactions in a cascade manner is a long-standing interest to chemists to access valuable organic materials more economically. Herein, we described a simple, economically viable method for synthesizing 11H-benzo[*b*]fluoren-11-one, a dual-state organic fluorophore, starting from ortho phthalaldehyde (OPA) in DMSO solvent. Simple and rapid product isolation, high atom economy, short reaction time, and scalability are the attractive features of the method. During the optimization of the reaction condition, we observed that DMSO, DMF, and acetone served one carbon to form the said compound besides their role as solvents. A plausible mechanism has been proposed based on the evidence obtained from LCMS analysis of the incomplete reaction mixture.

ARTICLE HISTORY
Received 5 July 2023
Accepted 29 September 2023

KEYWORDS
Ortho phthalaldehyde; benzo fluorenone; mechanistic study; tandem aldol condensation

POSTER PRESENTATION IN CONFERENCE

Title: "A Mechanistic Insight into the Acid Catalyzed, One-Pot Synthesis of Isoindole-Fused Quinazolin 4-ones"

Department of chemistry, ***2020****, Jadavpur University, Kolkata*

LIST OF SEMINAR ATTENDED

1. National seminar on ***" CHEMICAL SCIENCE: TODAY AND TOMORROW (CSTT-2019)"*** *at* Jadavpur University, Kolkata

2. National seminar on ***" Emerging Trends in chemical Science(January 07,2020)"*** , Jadavpur University, Kolkata